8-2019

Synthesis, Characterization and Biological Evaluation of Novel (S,E)-11-[2-(Arylmethylene) Hydrazono] Pyrrolo [2,1-c] [1,4] Benzodiazepine Derivatives

David Mingle
East Tennessee State University

Synthesis, Characterization and Biological Evaluation of Novel (*S,E*)-11-[2-(Arylmethylene) Hydrazono] Pyrrolo [2,1-c] [1,4] Benzodiazepine Derivatives

---

A thesis

presented to

the faculty of the Department of Chemistry

East Tennessee State University

In partial fulfilment

of the requirements for the degree

Master of Science in Chemistry

---

by

David Mingle

August 2019

Dr. Abbas G. Shilabin, Chair

Dr. Marina Roginskaya

Dr. Aleksey Vasiliev

Keywords: Pyrrolobenzodiazepine (PBD), L-proline, isatoic anhydride, Lawesson's reagent, cytotoxicity, cancer cell lines, non-β-lactam β-lactamase inhibitors, cannabinoid

ABSTRACT

Synthesis, Characterization and Biological Evaluation of Novel (*S,E*)-11-[2-(Arylmethylene) Hydrazono] Pyrrolo [2,1-c] [1,4] Benzodiazepine Derivatives

by

David Mingle

Pyrrolo [2,1-c] [1,4] benzodiazepine (PBD) is a class of natural products obtained from various actinomycetes which have both anti-tumor and antibiotic activities and can bind to specific sequences of DNA. PBD-dilactam was initially produced using isatoic anhydride and (L)-proline which was then converted to the PBD-thiolactam using Lawesson's reagent. Reaction of thiolactam with hydrazine in ethanol afforded PBD-11-hydrazinyl. Condensation of 11-hydrazinyl PBD with aldehydes possessing various substitutions was performed to obtain (*S,E*)-11-[2-(arylmethylene) hydrazono] pyrrolo [2,1-c] [1,4] benzodiazepine derivatives. ^{1}HNMR, ^{13}C-NMR, DEPT, IR, GC-MS and X-ray crystallography were used for the characterization. Inhibition activity of the products were carried out using TEM-1, AmpC and P99 β-lactamases. A minimal inhibition growth of 25% was observed for one of the selected PBDs on cancer cell line. A promising result was observed on preliminary cannabinoid binding activity test on one of the compounds.

DEDICATION

I dedicate this work to Father-Mother God for its ever-unfolding love and grace. Also, to my grandmother Mary-Ahima Mingle for motivating me to carry on this work. It has been amazing the kind of help I received from my family especially uncle Daniel Mingle, Mavis and Jerry Ogwezi, Michelle Mingle, David Mingle, my parents and the entire Mingle family in Ghana. Thanks for believing in me.

ACKNOWLEDGEMENTS

I acknowledge God as my guiding light and my strength throughout my study. My advisor, Dr. Abbas G. Shilabin has been of great help throughout this research work. His guidance and leadership have been awesome. I appreciate Dr. Marina Roginskaya and Dr. Aleksey Vasiliev for serving as committee members. Also Dr. Eagle was very helpful with the X-ray crystallography and Dr. Reza Mohseni also assisted with instrumentation for this research work. Enzyme kinetics was done with the help of Mr. Noah Lyon.

I am also grateful to the faculty members of the Department of Chemistry, ETSU. I also want to thank Mr. Kofi Amissah for his guidance and support. My final gratitude also goes to my research group members, Garreth Johnson, Chimdi Kalu and all my friends for their attention and support.

TABLE OF CONTENTS

LIST OF TABLES

Table Page

LIST OF FIGURES

Figure Page

LIST OF SCHEMES

Scheme Page

LIST OF ABBREVATIONS

µL	Microliter
anhyd	Anhydrous
Boc_2O	Di-tert-butyl dicarbonate
DMSO	Dimethyl sulfoxide
DNA	Deoxyribonucleic acid
FT-IR	Fourier Transform Infra-Red
GC/MS	Gas Chromatography Mass Spectrometer
h	hours
K_2CO_3	Potassium carbonate
KBr	Potassium bromide
Min	minutes
mL	milliliter
mmol	millimoles
MOPS	(3-(*N*-morpholino) propanesulfonic acid)
nM	nanomolar
NCF	Nitrocefin
NMR	Nuclear Magnetic Resonance

ORTEP	Oak Ridge Thermal Ellipsoid Plot Program
PBDs	Pyrrolo[2,1-c] [1,4] benzodiazepines
PBP	Penicillin-binding protein
rt	Room temperature
TLC	Thin Layer Chromatography
UV/Vis	Ultraviolet/Visible spectrophotometer
v/v	Volume to Volume

CHAPTER 1

INTRODUCTION

Natural Products

There is an abundance of organic compounds provided by nature which we call natural products. There are two types of metabolites obtained from natural products which are primary and secondary. Primary metabolites are directly involved in growth and metabolism examples include carbohydrates, proteins, and lipids. Secondary metabolites are not directly involved in the growth and development of organic compounds.[1] Alkaloids are one of the largest groups of organic compounds that have cyclic structure and nitrogen atom in its core structure. They have a wide range of properties some of which include a defense mechanism (chemical) against microbes and herbivores that includes sheep, cow, and elephant. Alkaloids are used as medications because of their pharmacological effects. Morphine, caffeine, nicotine, and quinine are some examples of alkaloids that have medicinal properties. Many alkaloids contain other functional groups that give them the ability to interact with biological targets of interest.[1,2]

Pyrrolo[2,1-c] [1,4] benzodiazepines

In 1960, *Streptomyces* species were found to contain Pyrrolo[2,1-c] [1,4] benzodiazepines (PBDs). PBDs were first isolated and synthesized from *Streptomyces refuineus*, and this was done in the laboratory by Leimgruber *et al*.[3] After the isolation of anthramycin (**12**, Figure 1) from cultures of *Streptomyces*.[4] The three isomers of pyrrolo[2,1c] [1,4]benzodiazepines (Figure 1) have been thoroughly studied and the other important PBDs isolated from *Streptomyces* species are tomaymycin, sibiromycin, neothramycins and DC-81.[5]

Their mechanism of action depends on the right-handed helical conformation because of their (S)-configuration at C-11a found from an X-ray crystal structure analysis of anthramycin (**12**)[6] which facilitates the molecules to fit in the minor groove of DNA selectivity at the 51-purine-G-purine sequences, by alkylating the C2 amino group of guanine.[7]

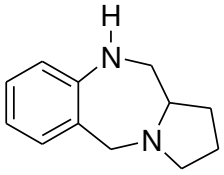

9

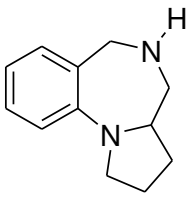

10

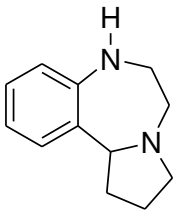

11

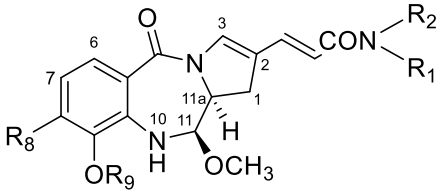

12 Anthramycin (R_8=CH_3, R_9=R_1=R_2=H)

13 Mazethramycin (R_8=R_1=CH_3, R_9=R_2=H)

14 Porothramycin (R_8=H, R_9=R_1=R_2=CH_3)

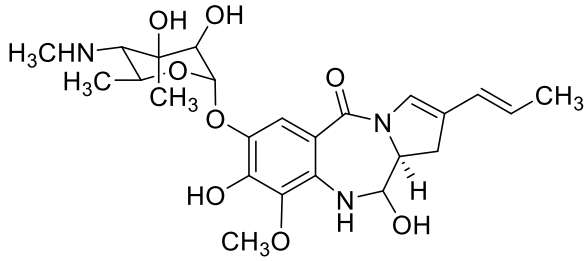

15 Sibiromycin

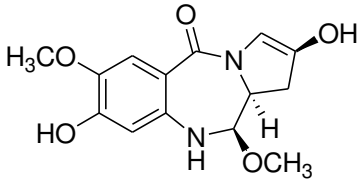

16 Chicamycin A

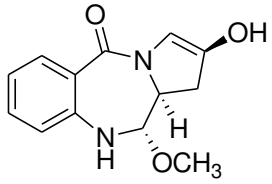

17 Abbeymycin

Figure 1. Structure of the three pyrrolo [1,4] benzodiazepine isomers **9**–**11** and the derivatives **12-17**

Of all the natural products, anthramycin was very promising because it was active against a wide range of cancers. Despite the fact of having low hematological toxicity, the clinical use of anthramycin is restrained because of dose-limiting damage to the heart muscles.[8] The undesired side effects of the naturally occurring PBDs have led to an increase in research on the synthesis of analogs. Two examples that have been tested in *vivo* against various human xenografts are SG2042 and SG2738 which have the C10-C11 imine structure, but no noticeable DNA damages have been identified yet. Also, the structure activity relationship (SAR) studies have shown that the correlation of the primary position C8 of DC-81 with the moieties of DNA intercalators or pyrrole and imidazole polyamide analogs of distamycin and neotropsin have produced PBD conjugates having pharmacophoric heads with enhanced *in vitro* DNA binding affinity and cytotoxic efficacy.[9] An important discovery of PBD antitumor agents was the PBD dimers which were made to create cross-links in the DNA by forming the guanine bases at the end of each molecule. The assessment of antitumor activity of PBD is controlled by *in vitro* cytotoxicity against tumor cells lines and DNA foot printing assay. DNA thermal denaturing experiments are used to measure DNA- binding affinity and find the sequence selectivity of these compounds.[10,11]

The general features of pyrrolo [2,1-c] [1,4] benzodiazepines in this research include an aromatic or non-aromatic pyrrole ring and two carbonyl group on the diazepine ring which is at position 5 and 11 on the PBD. These compounds are called “dilactams.” In the past five years, three novels [2,1-c] PBD synthesis have been reported in this division of compounds: (Section “Reductive cyclisation of N-(2-azidobenzoyl)pyrrolidine-2-carboxaldehydes”), (section “cyclisation of N-(2-azidobenzoyl)pyrrolidine-2-carboxaldehydes”) but new compounds [2,1-c] PBD scaffolds in their structure have been synthesized as effective anti-cancer agent.[11]

Cancer

What is Cancer?

After cardiovascular disease, cancer is the second major cause of death in the world. It has been estimated that about half of the men and one-third of the women are likely to develop cancer at a point in their life. [12] The human body contains millions of cells that are constantly growing and dividing in a regular plan, but these cells are likely to grow uncontrollably leading to cancer. Cancer cells have the propensity to proliferate and spread in every part of the human body. Not all tumorous cells spread relentlessly in the body, most are not malignant. Normal cells can control their growth and when they decline in their activity, they are able to destroy themselves. Lymphoma cancer can be detected when one is vulnerable to aldehydes and formaldehyde. Sometimes a solid growth of the tumor can occur which could be because of lack of oxygen in the tissues. Trying to single out a specific cause of cancer is difficult, but there may be risk factors which increase the chance of one getting cancer. Exposure to ultraviolet radiation and some lifestyles which include a poor diet, tobacco, alcohol and obesity are some of the contributing factors that can cause cancer. Additionally, lack of physical exercise contributes to about 5% of cancer cases. This can also be attributed to people inheriting damaged DNA. The latest research from at NCI reveals that people who are exposed to solvent, grease, and oils have a higher risk of getting cancer. If cancer is identified at its early stages, it could be treated, and the patient will have a good chance of surviving for many years. [12,13]

History and Major Cancer Types

From 460-370 BC, Hippocrates explained cancer which originates from the Greek word "Karkinos" as an abnormal mass of tissue. The oldest case of cancer recorded was breast cancer which happened in Egypt around 1500 BC. At that time there was no treatment.[12,13]

Major Cancer Types

There are three major types of cancer which include:

- Carcinomas
- Lymphomas
- Sarcomas

Carcinomas. So far, 85% of carcinoma cases have been diagnosed and these develop in the epithelial cells. There are four sub-types which include:

Adenocarcinoma (example Lung cancer)

Squamous cell carcinomas (example oral cancer)

Transitional cell carcinomas (example bladder cancer)

Basal cell carcinomas (example skin cancer)

Lung cancer. The main role of the lungs is breathing, and when we take in air, it spreads to the bronchi tubes. There are two types of lung cancer namely Non-small lung cancer and small cell lung cancer which can combine to form metastatic cancer.[13] Some of the causes of lung cancer are attributed to cigarette smoking. Also, alcohol intake and tobacco use can cause lung cancer. People who are exposed to air pollution and high level of arsenic are susceptible to this

type of cancer. This type of cancer is mostly seen in the aged group and less common in people below 40 years.[14] It is difficult for the symptoms to show at an early stage, however, others like chest pain, breathing problems and loss of weight becomes evident as cancer progresses.[15]

Oral cancer. This is a type of squamous carcinoma cell cancer which is enclosed in the epithelial neoplasm of the oral cavity.[16] Oral cancer can affect the gums and the floor of the mouth. Also, the salivary gland tumor is a part of oral cancer. Some of the causes of this cancer are attributed to lack of oral hygiene, smoking, and an intake of alcohol. Also, the use of immune-suppressant drugs during filling of the teeth can also cause this type of cancer. Some of the symptoms of this kind of cancer include mouth sores, mouth ulcers, difficulty in speaking, and some cracks in the edge of the mouth.[13,17]

Bladder cancer. This is often located at the bladder areas occupying the central part of the lower belly. Potential causes of this type of cancer are frequent exposure to arsenic and those who also drive trucks. Some chemical agents can cause this type of cancer. Symptoms of this type of cancer include weight loss, fatigue, blood seen during urination, and abdominal pains.[18,19]

Skin cancer. This is one of the most common cancers widely known. Each year this type of cancer is diagnosed in far more than 1 million people in the USA. There are two types of this cancer, namely non-melanoma and melanoma.[20,21] The commonly seen ones are the nonmelanoma which is less dangerous than melanoma. Some of the causes of skin cancer are exposure to ultraviolet light exposure, high amount of X-ray, exposure to toxic chemicals like arsenic. Also, working in the mining and plastic industry raises the risk of getting this type of cancer. Common symptoms of this type of cancer include the skin becoming red and scales begin to appear. Itching and ulcers develop as well as bleeding and tanning.[13,22]

Lymphomas. This is the type of cancer in the lymph cells of the immune system. People who are diagnosed with lymphoma have their lymph nodes gradually develop lumps over a period.[23]

Sarcomas. This is a type of cancer is found in the mesoderm tissue. Tumors are found in fat, bone, muscle, and hematopoietic tissue. Soft tissue sarcomas exist in the form of malignant fibrous histiocytoma.[24,25]

This type of cancer can be found in patients that are treated with radiation therapy. Also, those who work at places using chemicals such as arsenic and phenoxyacetic acid are at risk of this type of this cancer. Chemicals in herbicides can also cause sarcomas.[26] Major symptoms are found all over the body. It is accompanied by pain in nerves and muscles. Bleeding may occur in the tumor.[27]

Sources of Cancer

This is study looked at sources of cancer in two divisions: Chemical and Environmental sources.

Chemical sources. Data from the NCI has concluded that 30% of cancer deaths is associated with smoking in the USA. Out of this, lung cancer contributes to 87% cases recorded.[28] Avoiding smoking can tremendously reduce the risk of cancer.

Exposure to asbestos, which contains silicon and oxygen molecular structures, is linked to this source of cancer. There are two major types of asbestos minerals, namely serpentine asbestos, and amphibole asbestos. Genetics is also a factor in cancer growth and cancer development. History of cancer in one's family, such as breast cancer, means extra cautions must be taken.

Genetic cancer is likely to pass mutated genes onto the next generation. The fact that a person in someone's family has cancer does not mean they will also automatically get it. However, there is a probability of them also developing cancer. Working out for about 30-40 minutes a day, can lower the chance of some cancers. From statistics, obesity is a major cause of cancer. Routine exercise can prevent colon, breast, lung, and prostate cancer.[13,29]

Environmental Sources. The environment plays an important role in influencing some types of cancers. Skin cancer is attributed to exposure of ultraviolet rays of the sun. Tanning and skin burn are ways of damaging the cells. This can be prevented by using sunscreen when one is exposed to the sun's intense rays. Also, having unprotected sex makes one vulnerable to Human Papilloma virus (HPV). HPV is an assortment of more than 100 viruses that can contribute to raising the chance of cancer associated with anal, vulvar, cervical, and vagina. More studies are being conducted on HPV's function in the growth and development of other cancers.[13,15,29]

Treatments of Cancer

There are three types of cancer treatment which includes surgery, chemotherapy, and radiation therapy. Surgical treatment involves taking out tumors by removing lesions of the tumors. This process lessens the cancerous cells but cannot absolutely eliminate. It minimizes the cancer but may develop again. Alternative ways employed in eliminating cancer include, ultrasonography, open surgical and Biopsy exploration.

Chemotherapy is the process of using anti-cancer drugs to kill cancerous cells.[15,30] Using tamoxifen, skin cancer appears normal after treatment.[31] Radiation therapy is the process of killing cancer cells using X-rays, gamma rays and charged particles. Some cancer cells can be

treated with the combination of all the three treatments. A good example is head and neck squamous cell cancer.[32,33]

Anti-Cancer Activity of PBD-Derivatives

Anti-cancer activity of compounds from literature [34] carried out in selected cancer cell including cervix, lung, colon, oral and ovarian using sulforhoda- mine B (SRB) method. The compounds showed $GI_{50} \leq 10^{-5}$ M, implying that they were active on the cell lines tested. All the conjugates showed good anti-cancer activity. The good GI_{50} values ranging from less than 0.1 to 2.81 µM while the positive control also showed a GI_{50} range of 0.10-7.25 µM. Every conjugate synthesized showed significant anticancer activity against hormone-dependent (estrogen receptor positive) MCF-7 cell line having GI_{50} values ranging from less 0.1 to 0.17 µM, C_2-monofluoro-PBD estradiol conjugates, gave a slightly better anticancer activity compared to the E_2-PBD conjugates. It was discovered that the addition of the piperazine and triazole moieties in the alkane linker spacer between the estradiol and PBD subunits enhanced the anticancer activity. Also, PBD conjugates with propyloxy spacers showed a slightly more activity compared to the pentyloxy spacers.[34]

Anti-cancer activities of PBD compounds synthesized from literature [35] showed cytotoxicity towards cancer cells. Single dose *invitro* studies on NCI-60 cancer cell lines at a concentration of 10 µM performed at NCI showed that, (S,Z)-11-(propylimino)-1,2,3,10,11,11a-hexahydro-5H-benzo[e]pyrrolo[1,2-a] [1,4]diazepin-5-one (**18**) and 3-phenyl-1-propyl-1,12,13,14,14a,14b-hexahydro-2H,10H-benzo[e]pyrimido[2,1- c] pyrrolo[1,2-a][1,4]diazepine-2,4,10(3H)-trione(**19**) had inhibition on cell lines SNB-75 (CNS) (22.3%) and NCI-H522 (NSCL) (22.2%),

respectively. Maximum inhibition activity was exhibited by compound (S)-3-phenyl-1,12,13,14,14a,14b-hexahydro-2H,10H-benzo[e]pyrimido[2,1-c] pyrrolo[1,2-a] [1,4] diazepine-2,4,10(3H)-trione (**20**) on the renal UO-31 cell line with a 28.5% growth inhibition. (S)-11,12,13,13a-tetrahydro-9H-benzo[e]pyrrolo[1,2-a] [1,2,4] triazolo[3,4-c] [1,4] diazepine-3,9(2H)-dione (**21**) showed growth inhibition in both the HOP-62 and NCI-H522 cell lines at 22.68% and 23.68%, respectively.

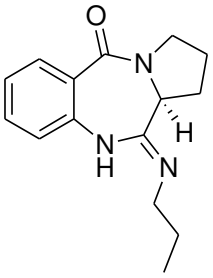

18

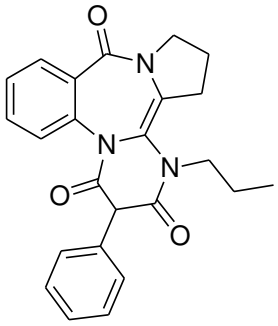

19

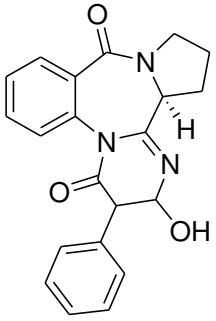

20

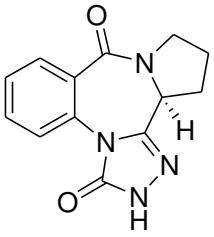

21

Figure 2: Anti-cancer activity of some PBD derivatives[35]

History of Antibiotics

Since the discovery of penicillin by Fleming in 1928, β-lactam antibiotics have been widely used for the treatment of bacterial infection. A lot of β-lactam drugs which are still used today came from natural product organisms like penicillin, cephalosporin, and other β-lactam based antibiotics. [36] Over time, bacteria have developed resistance to the β-lactams because the drugs produced had the same mode of action which was inhibition of the bacterial cell wall formation by forming a stable covalent bond with the active site of serine residue of penicillin-binding proteins. High molecular weight penicillin-binding proteins and low molecular weight penicillin-binding proteins are the two classes of penicillin-binding proteins. The β-lactams were targeted at the high molecular weight penicillin-binding proteins, which was very essential for bacteria existence. [37] The clinical use of β-lactam antibiotics in the present age (Figure **3**) include cefotaxime, monobactams e.g. aztreonam, and carbapenems. Classes of antibiotics have a similar structural character, that is the four-membered β-lactam ring which is reactive. Microorganisms are the fountain of chemical derivatives of most penicillin and cephalosporins.[38]

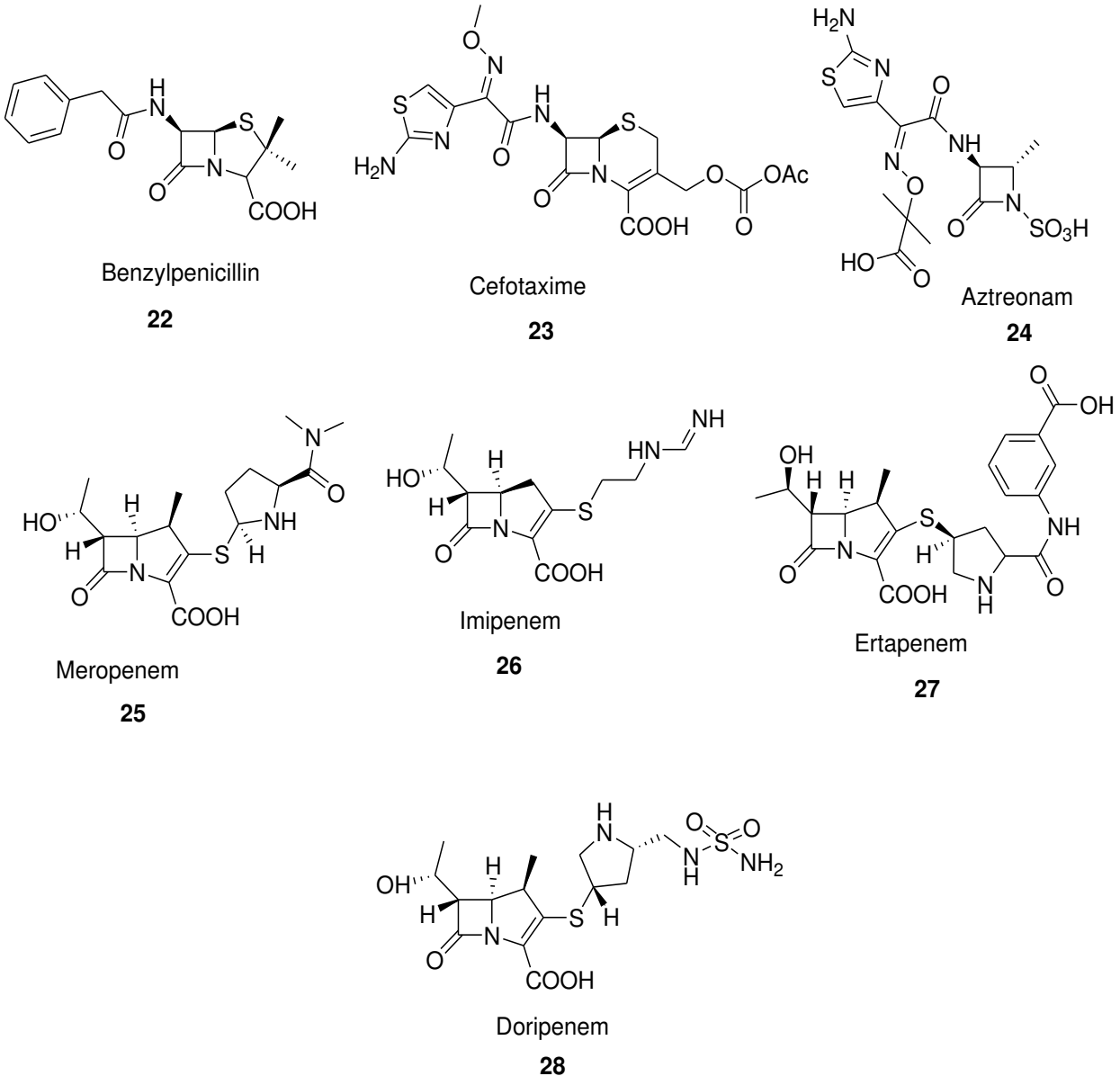

Figure 3: Examples of the first generation of β-lactam antibiotics [39]

Mechanism of β-lactam Resistance

β-lactamase breaks a bond in the β-lactam ring of the penicillin to render the molecule ineffective. Bacteria with the enzyme β-lactamase may be able to resist the effect of penicillin

and other β-lactam antibiotics. The penicilloic acid form will not be able to deactivate the cell wall of the bacteria. The resistance of bacteria to β-lactams and other antibacterial agents is a serious concern and there is a need to research and look for new and effective ways to address this problem. Bacteria have a lot of resistant-mechanisms against β-lactam antibiotics in many forms.[4,40] The most widely used mechanism of resistance in gram-negative bacteria is the production of β-lactamases that cleave β-lactam ring by means of hydrolysis. Rapid resistance over a broad range of bacteria is possible by the transfer of plasmid-encoded β-lactamases.[41] One vital mechanism employed by gram-positive bacteria (e.g. methicillin-resistant *S. aureus* (MRSA)) for its resistance is the formation of low-affinity PBPs that are involved in breaking down the transpeptidase reaction. The main factor that enhances the resistance of microorganisms to β-lactam antibiotics is due to mutation. Because of that, PBPs has low-affinity to β-lactams. Typically, PBPs of class B (homologous to *Escherichia coli* PBP3) are mostly affected by this mechanism because they are primary targets of β-lactam in these microorganisms.[42] Some microorganisms such as *S. pneumoniae* PBP2X, *Neisseria gonorrhoeae* PBP2 have been found to contain mutations.[43] Also, resistance to β-lactams can occur by gene transfer which can be horizontal, for example, the resistance in *Streptococci* is by the transformation which is considered natural.[44]

Movement of β-lactams through the outer membrane is enabled by Outer membrane proteins (OMPs). When the rate of OMPs declines, a decrease in the concentration of antibiotics at the periplasm is detected and an increase in MIC-values.[45,46] In gram-negative bacteria, efflux pumps can reduce the effective concentration of β-lactam antibiotics in the periplasm. β-lactams

is then transported outside the cells by the outer membrane by the outward flow pumps in bacteria.[46]

The alarming rate of β-lactam resistance has urged the advancement of a lot of strategies to fight this issue. The abuse of antibiotics is the main factor contributing to the increase in this trend. The drive of pharmaceutical industries to continue research in quest of antibiotic resistance has reduced drastically in the last 23 years. Inactivators and "suicide inhibitors" of class-A β-lactamases have been used for some time now. These β-lactamases inhibitors are clavulanic acid, tazobactam, and sulbactam (Figure **4**), they are great reactive four-membered β-lactam ring. When the β-lactamase inhibitors are used in combination with β-lactam antibiotics such as amoxicillin/clavulanate, ampicillin/sulbactam, piperacillin/tazobactam, they significantly lower the MICs of the β-lactam antibiotics against varieties of bacteria. As these combination drugs are used over a period, they encounter resistance from the proliferation of inhibitor of β-lactamases. The drawbacks of these molecules are that they are hydrolyzed by β-lactamases. Hence, their performance is increased when combined with a β-lactamase inhibitor. Non-β-lactam inhibitors of PBPs have shown to be preferred substitute for the resistance of β-lactamase than β-lactam due to their distinctive properties. This makes it impossible for β-lactamases to identify them as substrates. Researchers have worked hard in the last three decades to find non-β-lactam inhibitors that can substitute β-lactams. NXL104 has been the only non-β-lactam β-lactamase inhibitor that has been studied in clinical trials to date.[7,40,47] The examples below show when the parent structure of traditional β-lactam has converted to new molecules which have important activities against resistant pathogens that are of medicinal value. Significant activity on PBP2a of

a methicillin-resistant *S. aureus* has been observed by the action of non-traditional β-lactams which include 1,3-bridged 2-azetideiones.[48–50]

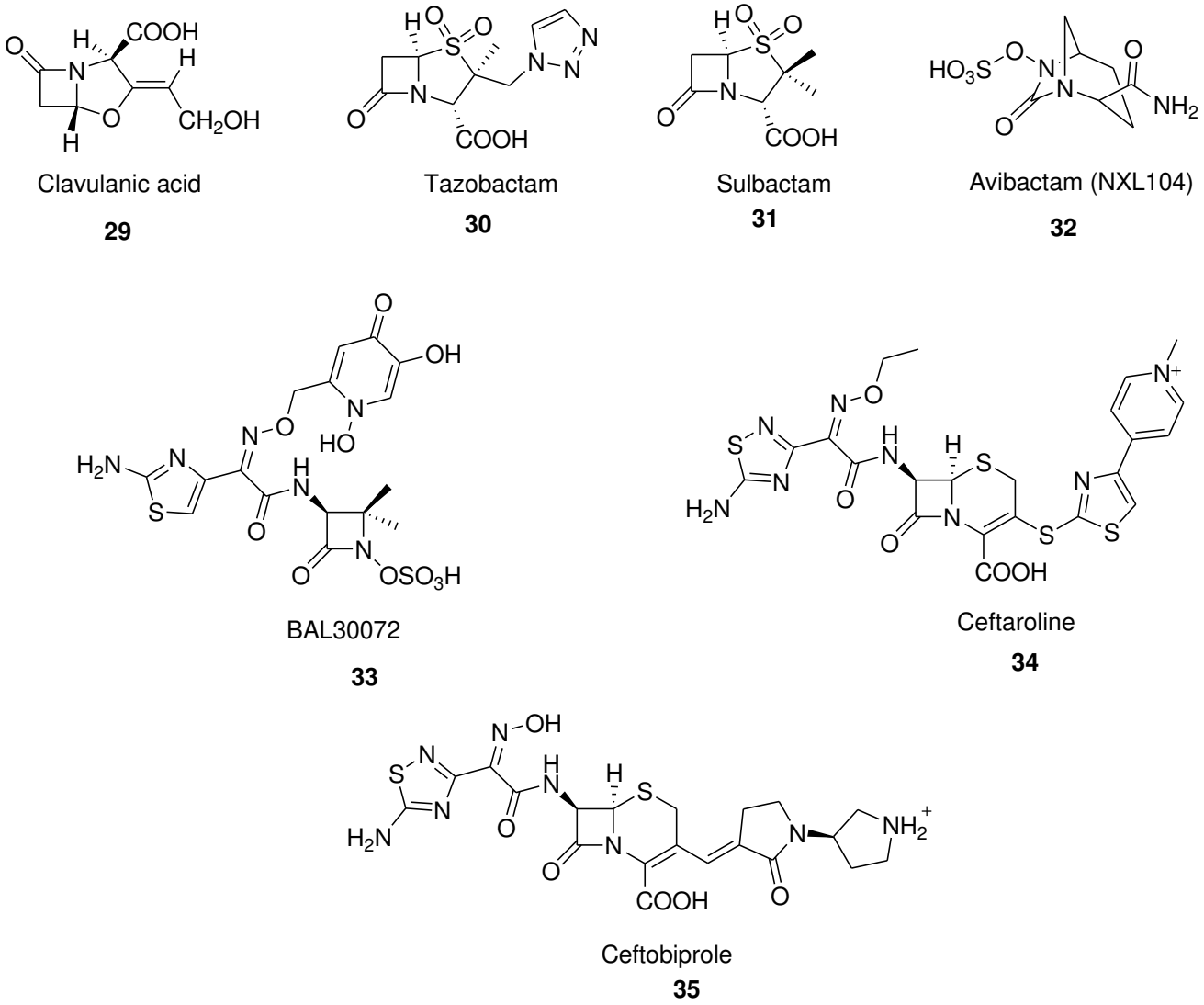

Figure 4: β-lactam based β-lactamase inhibitors and examples of new β-lactam antibiotics.[5,51–53]

β-Lactamases

β-lactamase enzyme was first isolated from Bacillus *Escherichia coli* and described as B. coli "penicillinase". [54] As at that time β-lactamase was not of clinical significance because penicillin was only used to treat staphylococcal and streptococcal infections. Scientists were unsuccessful to separate the β-lactamase enzyme from Gram-positive organisms. [54–56] Successful isolation of β-lactamase was done by Kirby et al. from *Staphylococcus aureus* and he observed that it could be a possible major clinical problem as these enzymes are likely to be the major causes of resistance in bacteria throughout the world. [57]

More than 850 β-lactamases have been identified and it has also been considered that active recombination, high mutation frequency, and replication rates have been the bedrock for bacteria to adjust to new β-lactams by the production of these β-lactamases.[58]

Classification of β-lactamase

β-lactamase enzymes are classified into two main groups these include:

1. Classes A to D, using Amber classification focusing on the sequence of amino acid homology, and

2. Group 1 to 4 using Bush-Jacoby-Medeiros classification focusing on substrate and inhibitor scheme.[58,59]

Classes A, C, and D serine-β-lactamase have some equivalence in their structure which gives them the ability to cleave β-lactams by hydrolysis. However, class B β-lactamases are metallo-β-

lactamases (MBLs) and they have a Zn^{2+} ion linked to His/Cys/Asp residues in the active site.[60,61]

The type classification structure used in this literature review is Amber.

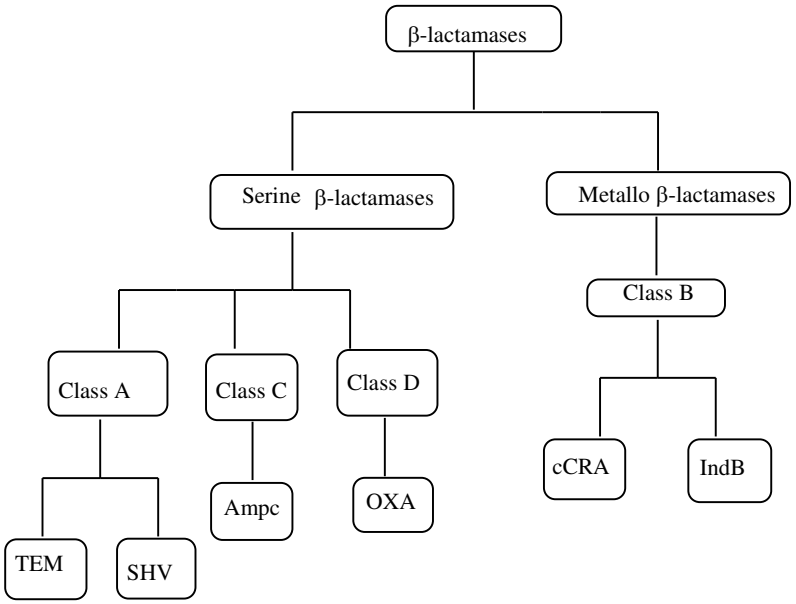

Figure 5: Classes of β-lactamases

Class A Serine β-lactamase. A lot of class A enzymes are easy target to β-lactamase inhibitors that are accessible on the market which includes clavulanate, But *K. pneumoniae* carbapenemase (KPC) is exempted to this category as they are unaffected to clavulanate.[62]

Class A Extended-spectrum β-lactamases (ESBLs). They can chemically breakdown by hydrolysis of the oxyimino-cephalosporins, monobactam, and carbapenems. This category of lactamase activity can be restricted by clavulanate.[63]

Class A Serine carbapenemases β-lactamases. This class comprises of non-metallo carbapenemase of class A (NMC-A), IMI, SME, and KPC. They can cleave the first generation β-lactams by hydrolysis examples of such include carbapenems, penicillin, and aztreonam cephalosporins. This category of β-lactamases have been studied and noticed to be predominant in *K. pneumoniae, Serratia marcescens,* and *Enterobacter cloacae*, but they are an easy target to clavulanate [64]

Class B Metallo-β-lactamases. This class of β-lactamases relies on Zn^{+2} and they cleave β-lactam antibiotics by hydrolysis. But the mechanism used is not similar compared to the of rest other β-lactamases. They can cleave β-lactams using hydrolysis and are also able to withstand activities from penicillin, cephalosporins and carbapenems,.[56,65]

Class C Serine cephalosporinases. Serine cephalosporinases of class C contain the *bla* genes of the bacterial chromosomes. Organisms that have this β-lactamase are can mostly withstand the action of penicillin, β-lactam β-lactamase inhibitor combinations, and cephalosporins. But AmpC enzymes, as an example of this category of serine β-lactamases, are known to be restricted by their mode of action with aztreonam, oxacillin, and cloxacillin.[60,65]

Class D Serine Oxacillinases. Initially, they were referred as "oxacillinases" because they can breakdown oxacillin at a faster rate of 50% compared the slow pace cleavage of oxacillin by classes A and C. They are able to withstand the activities of carbapenems, cephalosporins, and penicillins.[66]

Non-β-lactam Lactamase Inhibitors

Non-β-lactam based PBP inhibitors have been found to withstand β-lactamase hydrolysis which has caught the attention of many and more emphasis has been put on the exploration of non-β-lactam derivatives. NXL104 (avibactam) (Figure **4**) is a non-β-lactam that can prevent the activity of serine β-lactamases. When avibactam is used together with broad-spectrum cephalosporins and aztreonam, it is active against Gram-negative infections (including Klebsiella). Avibactam is the maiden β-lactamase inhibitor to undergo clinical trials.[67–69]

Classification of non β-lactam based PBP inhibitors are identified in three groups:

1. Transition state analogs

2. Substrate analogs and

3. Non-covalent inhibitors

1. Transition State Analog. These inhibitors have been recognized to be useful protease inhibitors and serine β-lactamases.[70–72] Transition state analog inhibitors like boronic acid, carbonyl compounds, and phosphonates have been classified as effective inhibitors of PBPs. LMW-PBPs have binding affinity to boronic acid.[36,73] Reversible and covalent bonds with serine proteases have been associated with boronic compounds which prevent these enzymes by adopting tetrahedral intermediates of the reaction.[74,75] Phosphonates are good inhibitors of serine proteases which have their clinical ability narrowed because of they are unable to stay longer in aqueous solution and affected by phosphodiesterases.[70,76]

2. Substrate Analogs. Acylation of the effective serine PBP makes them act as suicide substrates. Also,[81] lactivicins (LTV) and Bicyclic pyrazolidinones and they have demonstrated some clinical significance related to PBP inhibitors and antibacterial activities.[77–79]

3. Non-covalent Inhibitors. They bind firmly to the active site of PBPs using other means apart from acylation, which makes them very potent inhibitors. They do not need the undesirable changes in the active site of PBP2a of MRSA that is needed for acylation.[80,81] Examples of non-covalent inhibitors are aminothiadiazole, inhibitors of class C β-lactamases, and ortho-phenoxyldiphenylurea derivatives, anthranilic acids, naphthalene sulfonamides, cyclic peptides, Cibacron Blue and Erie Yellow, and quinolones. Inhibitors of PBPs that are classified as Noncovalent of *E. coli* and *B. subtilis* have been discovered on 4-Quinolones .[82–88]

The Endocannabinoid System

The endocannabinoid system is comprised of endogenous cannabinoids (endocannabinoids), cannabinoid receptors and the synthetic and degrading enzymes involved in the synthesis and the breakdown of endocannabinoids.[89–91] They are called endocannabinoids because they were first recognized to activate the same receptors as cannabinoids, which is the principal psychoactive ingredient of cannabis. Endocannabinoid that was identified first was arachidonoyl ethanolamide. 2-arachidonoyl glycerol (2-AG) was the second endocannabinoid identified. Synthesis, cellular transport and breaking down of endocannabinoids are processes that are strictly regulated.[90,92] Endocannabinoids differ from other neuromodulators in that they are not produced in advance and stored in vesicles but rather, their precursors remain in cell membranes and are cleaved by specialized enzymes. This can also be termed as they are

produced when there is a need for them.[93–95] The psychoactive properties of Δ^9-tetrahydrocannabinol (THC), which is the main psychoactive ingredient of cannabis became a point of interest with the identification of cannabinoid receptors. A lot of various experiments suggested the probable existence of specific protein receptors for Δ^9-THC, but Howlett et al.[90] gave definitive confirmation for a cannabinoid receptor. The outcome of their work was that cannabinoids activated a G protein-coupled receptor (GPCR) inhibited adenylyl cyclase. They also developed an assay for receptor binding activity and found out that this receptor was present in some brain regions at high levels. GPCRs that are expressed in greater quantity includes cannabinoid receptor cannabinoid receptors. Initial autoradiographic studies showed that cannabinoid binding sites are the highest in the brain regions because of cannabis.[90,96,97]

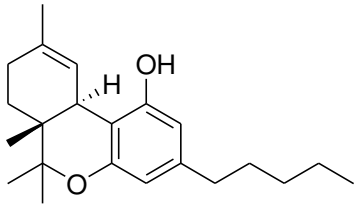

Figure 6: Structure of Δ^9-tetrahydrocannabinol (THC)

The mammalian tissue has two types of cannabinoid receptors. They are CB_1 receptors, which was cloned in 1990,[98] and CB_2 receptors, cloned in 1993.[99] Anandamide acts as a partial cannabinoid agonist receptor with higher CB_1 than CB_2 affinity.[100] Anandamide and 2-arachidonoyl glycerol may both serve as neurotransmitters or neuromodulators. Endocannabinoids uses the reverse synapse for signal transduction. [101] Expression of CB_1 receptors are seen in the central nervous system and in some peripheral tissues. Examples include but not limited to the heart, kidney and the lungs. CB_2 receptors are found principally in the immune cells, especially B-cells and natural killer cells.[102] CB_1 receptors can also found on

pain pathways in the brain and spinal cord and they are also likely to be found at the peripheral ends of primary afferent neurons.[103]

Signaling of Cannabinoid Receptors and Modulation Release of Chemical Messengers

CB_1 and CB_2 receptors primarily send signals through the inhibitory G proteins G_i and G_o. When the inhibitory G protein activation is triggered by CB_1 receptors adenylyl cyclase is inhibited. This causes mitogen-activated protein kinases to be activated, leading to the shutting down of some voltage-gated calcium channels and finally activating of G protein-linked within adjusting potassium channels. CB_2 receptors have almost the same effects when stimulated, except that the regulation of ion channels by CB_2 receptors is more fluctuating. Suppression of neuronal excitation by CB_1 receptors prevents neurotransmission. Considerable evidence clearly shows that endocannabinoids perform an important role in several forms of brain plasticity. There are two types of plasticity; namely short-term and long-term. [89,90,104] Endocannabinoids are produced in a short time but their effects last longer. More studies analyzing the effects of endocannabinoid have much emphasis on neurotransmission however, there is proof of functions associated with somatic CB_1 receptors, which when activated hyperpolarizes neurons.[105,106]

The main property of CB_1 and CB_2 is to be able to control the release of chemical messengers by natural or induced means. Neurotransmitters are release from both central and peripheral neurons are inhibited by the presynaptic CB_1 receptors and cytokine released are also hindered or facilitated when CB_2 receptors on immune cells are activated. Currently, cannabinoid-receptor regulated effects on cytokine release have recently been explained. When CB_1 receptors are activated during pre-synapse, it leads to inhibition of chemical messengers from some areas of the brain and peripheral neurons. *In vivo* or *in vitro* activity have been

conducted on some compounds like dopamine, acetylcholine, and D-aspartate and the outcome has confirmed the release of neurotransmitters.

Some research findings also shows that when CB_1 receptor is activated: (a) They can increase the natural firing of neurons in the pars reticulata of rat substantia nigra and does not affect the effects of neurons to iontophoretically applied GABA (b) can limit the occurrence but not the amplitude of miniature IPSCs that were assumed to be stimulated by natural neuronal release of single GABAergic synaptic vesicles (c) has no substantial decline in effect on neuronal firing rates or inside currents stimulated by internal dispensation of GABA.[107,108]

Justification of Research

The interaction between PBD and DNA is studied using the DNA helical structure. The double-helical DNA structure contains two parts: major and minor grooves. The major groove is wide in space compared to the minor groove which makes it possible for molecules like protein to interact with it. Molecules that are small and usually less than 1000 Da can bind to the minor groove. The difference in the size of the grooves is because the sugar-phosphate backbone is not evenly spaced. Major and minor grooves have a specific arrangement pattern in which each base have hydrogen bond donors and acceptors. Selective drug uses the size, spacing and the difference between donor and acceptor groups for potential drug interaction.

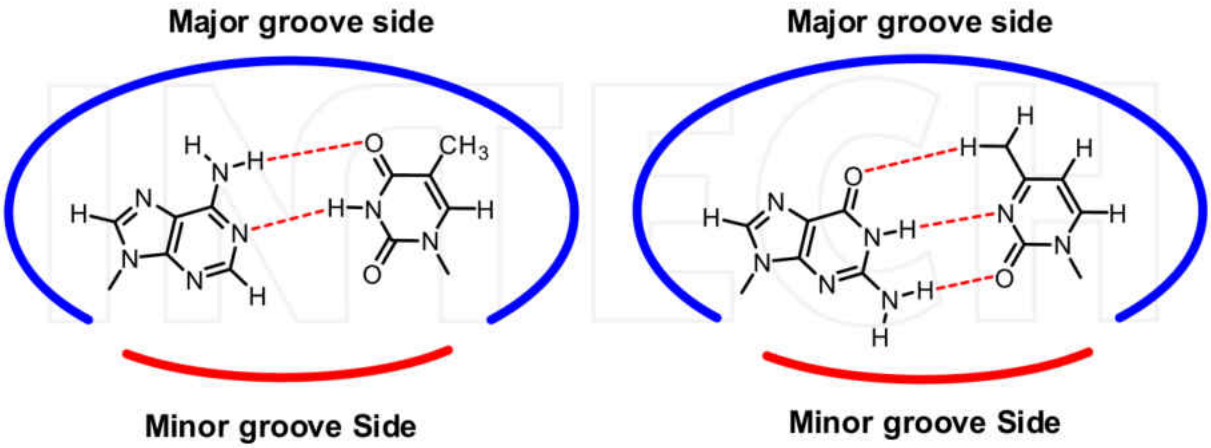

Figure 7: Hydrogen bonding between adenosine/thymine (left) and guanosine/cytosine (right) base pairs of DNAs.[109]

The configuration of PBD at carbon C-11a gives the molecule a right-handed twist. The right-handed twist fits well to the B-form of the DNA giving it the ability to interfere with the processing of the DNA forming adduct in the minor groove. Synthetic PBD with R-configuration has no DNA binding activity and *in vitro* cytotoxicity. The minor groove is mostly unoccupied and likely to be exposed for small molecules to be attacked. PBD have electrophilic carbon at C-11 position and this with the right-handed twist of the molecule allows PBD to alkylate the nucleophilic NH_2 group of the guanine in the minor groove of the DNA. PBD can form covalent bonds guanine base of the DNA to obstruct the activity of biological processes. The structure-activity relationship (SAR) on cytotoxicity and anti-tumor activities of PBD has not been fully understood.[110]

The main goal for further advances in research of PBDs as potential non-β-lactam lactamase inhibitors was because the active regions of characteristic β-lactam β-lactamase inhibitors are

tantamount to the PBD core structure whiles maintaining the same active sites of a regular non-β-lactam β-lactamase inhibitor. (**Scheme 1**). PBDs can act as suicide inhibitors against Serine β-lactamase. Clavulanic acid, which is one of the first β-lactam β-lactamase inhibitors, is a suicide inhibitor and its mode of action is shown in (**Scheme 2**).

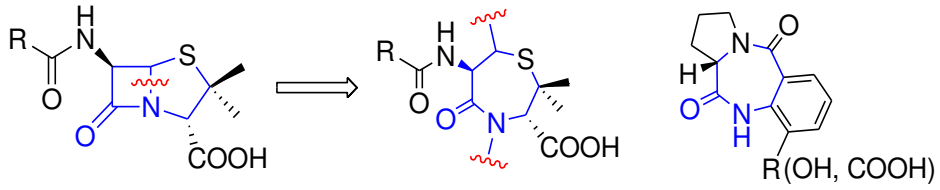

Scheme 1: Fragment-based relationship connecting β-lactam β-lactamase inhibitors and PBDs

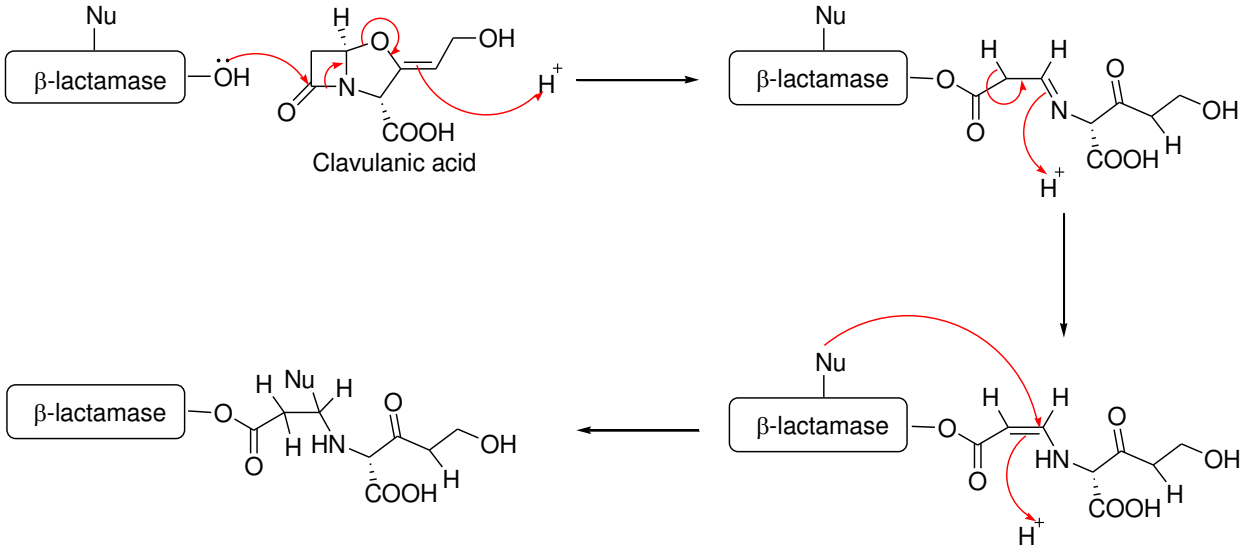

Scheme 2: Mechanism of action of β-lactam β-lactamase inhibitors (suicide inhibitors) (Adapted from http://wizard.pharm.wayne.edu/medchem/betalactam.html).

Exploring the cannabinoid receptor with PBD is to enable us to understand the structure-activity relationship of receptor binding sites. Understanding the SAR of cannabinoid binding receptor will help in finding new substances of therapeutic effect. The principal active ingredients in *Cannabis sativa* which is Tetrahydrocannabinol (THC) has some structural similarities to PBD derivatives.

Alkyl groups with a short chain on THC lowers the efficacy to bind to the cannabinoid receptor. Also, when the number of carbon atoms are increased, the potency of the ligand to bind to the cannabinoid receptor is increased. Compounds with ring-opening that includes pyran only shows small extent of affinity towards CB_1/CB_2 cannabinoid receptors.

THC analogs without phenolic hydroxyl groups may show some substantial changes in their pharmacological abilities. It was noted that THC derivatives that experienced etherification or elimination of the phenol group exhibited good affinity for CB_2.[111]

THC have 19 carbons in its structure with a molecular weight of 314.5g/mol, in this research, PBD derivatives have 19-23 carbons in their structure and with a molecular weight of 318g/mol to 403 g/mol. Structural modifications of PBD derivatives in this research has been enhanced to determine a potential cannabinoid receptor binding activity.

Specific Aims

Novel synthesis and structure-activity relationship (SAR) of lead compounds were fundamental to this research. Enzyme kinetic inhibition was conducted on the PBD derivatives using lactamases TEM-1, P99 and AmpC to determine the percentage of inhibition. To

determine the compounds synthesizes as potential anti-cancer agents, NCI determined the percentage of inhibition of the PBD derivatives on 60 cancer cell lines. Other Biological activity of the PBD derivatives including preliminary cannabinoid binding activity was conducted on one of the compounds.

CHAPTER 2

RESULTS AND DISCUSSION

Synthesis of Pyrrolo[2,1-c] [1,4] Benzodiazepine (PBD) Derivatives

Novel derivatives of PBD Synthesis was done using starting material from the primary structure of natural product obtained from *Isatis indigotica*[3].

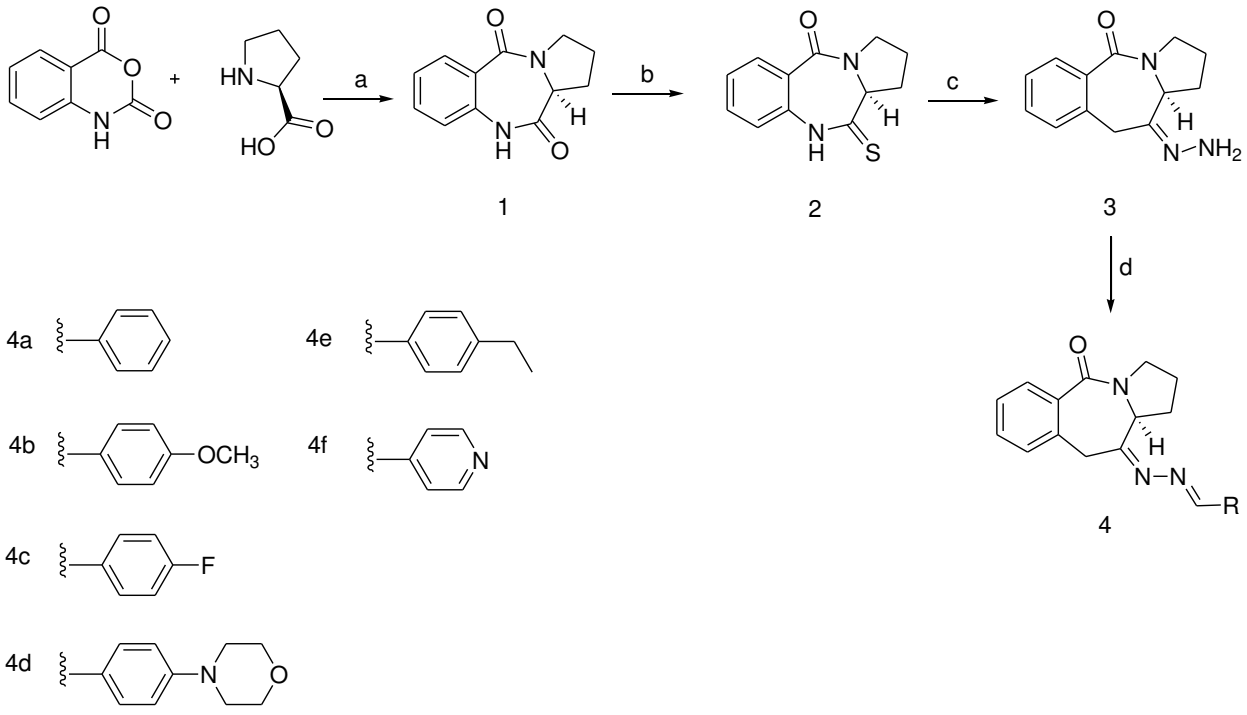

Scheme 3: Reagents and conditions of compound **4(a-f)** (a) DMF, 155 ºC, 5 h; (b) Lawesson's reagent, THF, rt, 15 h; (c) $N_2H_4.H_2O$ (98%), EtOH(abs.), rt, 15 h; (d) Aldehydes, MeOH (anhyd.), rt, 15 h.

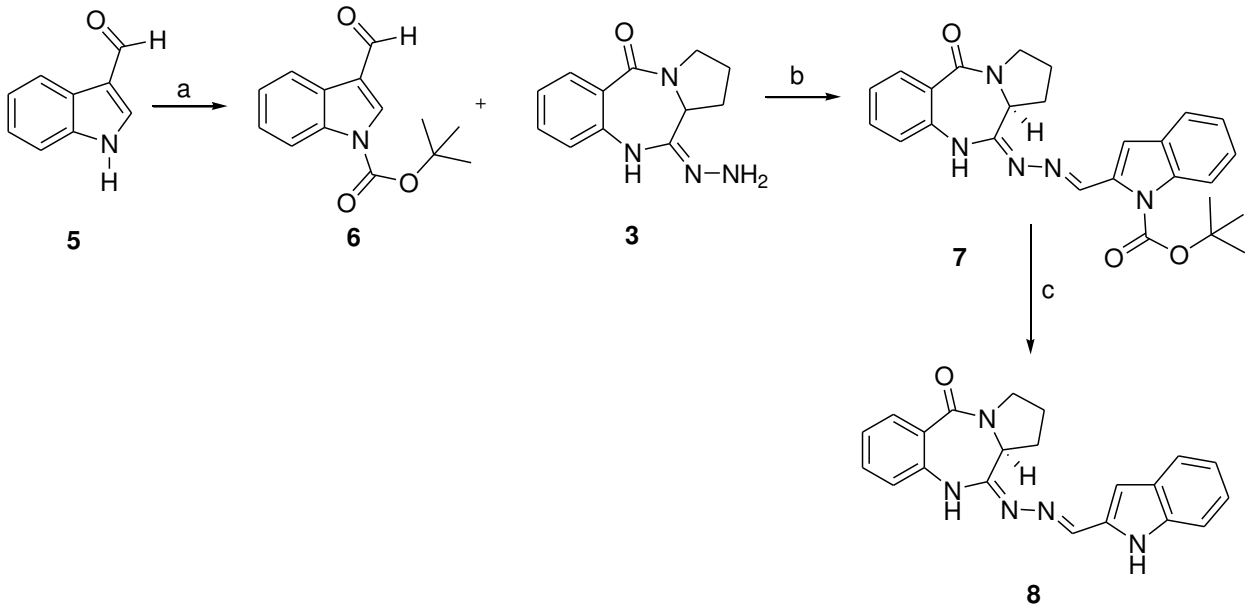

Scheme 4: Reagents and conditions of compound **8** (a) DMAP, DCM, Boc_2O, rt, 15 h; (b) MeOH (anhyd.), rt, 15 h. (c) K_2CO_3, MeOH/H_2O, reflux 30 min.

(*S,E*)-11-hydrazono-1,2,3,10,11,11a-hexahydro-5H-benzo[e]pyrrolo[1,2-a] [1,4] diazepin-5-one (**3**)

Synthesis of compound **1** was done using procedures literature[112–114]cyclocondensation of equimolar of isatoic anhydride with (L)-proline in DMF for 5 hours. Recrystallization from acetone/DMF (v/v 10:1) gave 82% yield, ^{1}H NMR in DMSO-d6 displayed 12 signals; a singlet for the N-H group at 10.51 ppm, two each of doublet-doublet and doublet-doublet-doublet for the aromatic protons between 7.79-7.11 ppm, a doublet for the 11aH between 4.10-4.12 ppm, and six multiplets for the three CH_2 groups on the pyrrolidine ring between 1.78-3.59 ppm (refer to spectra in **Appendix A1, A2 and A3**) three signals were predicted but more splitting of the

individual multiplets gave a total of six multiplets from the pyrrolidine ring. The individual peaks were integrated to give relatively 1:1:1:1 ratio for the aromatic protons and 1 for the 11aH doublet peak. ^{13}C NMR also produced 12 peaks. Secondary and tertiary amide carbons were observed at 171.315 and 165.090 ppm C=O respectively. Six of the aromatic carbons were found between 121.832-136.957 ppm and the C11a which is the stereocenter gave a peak at 56.772 ppm. The following peaks 47.435, 26.338, 23.638 ppm were three CH_2 groups on the pyrrolidine ring (refer to spectrum in **Appendix A4**). ^{13}C-DEPT 135 analysis validated the number of methylene CH and methine C-H groups in the structure. The spectrum showed 3 negative signals in the negative phase for the three CH_2 groups on the pyrrolidine ring and 5 signals for the methane groups all in the positive phase; 4 aromatic C-H groups and a C11a signal. But, quaternary carbons were not seen in the spectrum (refer to spectrum **in Appendix 5**). Gas Chromatographic Mass Spectrometry analysis of **1** in chloroform showed molecular ion peak at *m/z* = 216.0 amu and a base peak at *m/z* = 70.0 amu. IR analysis gave peaks at 3218 cm^{-1}, 2975 cm^{-1} and 1619 cm^{-1} for the secondary amide, C-H and the C=O stretching sequentially (refer to spectrum in **Appendix A7**).

Monothionation of compound **1** with 2,4-bis-(4-methyoxyphenyl)-1,3-dithia-2,4-diphosphetane-2,4-disulfide (Lawesson's reagent) in THF at room temperature for 28 hours[112–114] produced compound **2** a yellow solid in good yield (**Scheme 3**). ^{1}H NMR, ^{13}C NMR and ^{13}C-DEPT 135 spectra in DMSO-d6 gave signals identical to compound **1** except that the ^{13}C NMR spectrum gave distinctive peaks at 202.568 ppm for C=S and 164.746 for ppm C=O of the tertiary amide that was not the same as compound **1** (refer to spectra in **Appendix B1, B2, and B3**). IR analysis gave stretching peaks at 3450 cm^{-1}, 2969 cm^{-1} and 1619 cm^{-1} for the N-H, C-H

and the C=O for amide respectively (refer to spectrum in **Appendix B7**). GC/MS analysis of compound **2** in chloroform produced molecular ion peak at *m/z* = 232.0 amu and a base peak at *m/z* = 70.0 amu.

Synthesis of compound **3** was done using procedures from literature[115] by stirring a mixture of compound **2** and hydrazine monohydrate (98%) in absolute ethanol at room temperature for 15 hours. Evaporation of the solvent was done in a vacuum and the residue was taken up in water. The precipitate was dried and washed with diethyl ether to afford compound **3** as an off-white solid. Compound **3** was then used as starting material for the synthesis of novel compounds from 4a to 4g in good yields (**Scheme 3**). ^{1}H NMR of compound **3** in $CDCl_3$ gave two doublet and two triplet and peaks for the aromatic protons between 6.82-7.86 ppm. A singlet peak for the N-H group at 7.29 ppm, another singlet for the 11aH at 4.22 ppm and six multiplets for the three CH_2 groups on the pyrrolidine ring between 1.93-3.70 ppm (refer to spectra at **Appendix C1 and C3**). ^{13}C NMR gave 12 proposed peaks with the peculiar peaks at 166.207 ppm for C=O and 152.152 ppm for C-N ppm. The 6 aromatic carbon peaks were found between 119.744-137.768 ppm and the C11a peak showed at 55.495 ppm. The three CH_2 groups on the pyrrolidine ring also produced peaks at 23.401, 26.093 and 47.328 ppm (refer to spectrum at **Appendix C4**). IR analysis showed peaks at 3261 cm^{-1}, 2871-2948 cm^{-1} and 1631 cm^{-1} for the N-H, C-H and the C=O stretching respectively (refer to spectrum in **Appendix C5**).

General method for synthesis of (S, E)-11-[2-(arylmethylene) hydrazono] Pyrrolo [2,1-c] [1,4] Benzodiazepine (**4a-f**)

Synthesis of compounds (4a-g) was done by reacting compound (**3)** in anhydrous methanol using modification of procedures [116] with different aldehyde and stirred at room temperature.

(*S,E*)-11-[2-(phenyl methylene) hydrazono] Pyrrolo [2,1-c] [1,4] Benzodiazepine(**4a**)

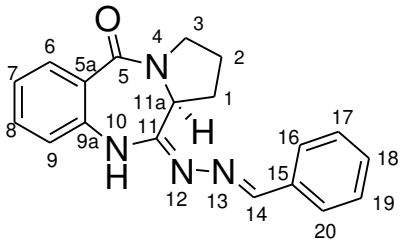

The general procedure was followed, and benzaldehyde used for the reaction. Extraction was done with chloroform/isopropanol after the reaction was completed. The organic layer was dried over anhydrous sodium sulfate and the solvent was then removed in vacuum, washed with diethyl ether to afford an off-white solid of compound **4a**. The final product was purified from isopropanol to yield colorless needle shape crystals. ^{1}H NMR of **4a** in $CDCl_3$ gave two doublet, two singlet and one triplet peak for the aromatic protons between 6.98-7.97 ppm. A doublet peak for N-H, N=C-H group between 8.53-8.48 ppm. A doublet for the 11aH between 4.37-4.38 ppm and a double doublet for N-CH_2 between 3.65-3.83 ppm on the pyrrolidine ring. A singlet and a multiplet were recorded for the two CH_2 groups on the pyrrolidine ring between 2.02-3.02 ppm (refer to spectra in **Appendix D1, D2, and D3**). ^{13}C NMR gave 17 proposed peaks with the peculiar peaks at 166.06 ppm for C=O, 157.82 ppm and 157.62 ppm for the two C=N ppm. Instead of 12 aromatic carbon peaks, 10 carbon peaks were found between 120.77-136.80 ppm

because two of them were symmetric carbons. And the C11a peak showed at 55.52 ppm. The three CH_2 groups on the pyrrolidine ring also produced peaks at 47.42, 26.15 and 23.56 ppm (refer to spectrum in **Appendix D4 and D5**). In ^{13}C DEPT-135 all quaternary carbons disappeared and N=CH appeared on the positive phase at 157.83 ppm. 7 aromatic carbons were found on the positive phase between 120.77-132.47 ppm and C-11a showed on the positive phase at 55.52 ppm. All the CH_2 on the pyrrolidine ring 47.39, 26.16 and 23.43 ppm appeared on the negative phase (refer to spectrum in **Appendix D6**). IR analysis showed peaks at 3351 cm^{-1}, 2981 and 2879 cm^{-1}, and 1627 cm^{-1} for the N-H, C-H and the C=O stretching respectively (refer to spectrum at **Appendix D7**). UV-Vis absorption of the compound in methanol was at 223 and 319 nm (refer to spectrum at **Appendix D8**). GC/MS analysis of the compound in acetone produced molecular ion peak at *m/z* = 318.0 amu and a base peak at *m/z* = 241.0 amu (refer to spectrum at **Appendix D9**).

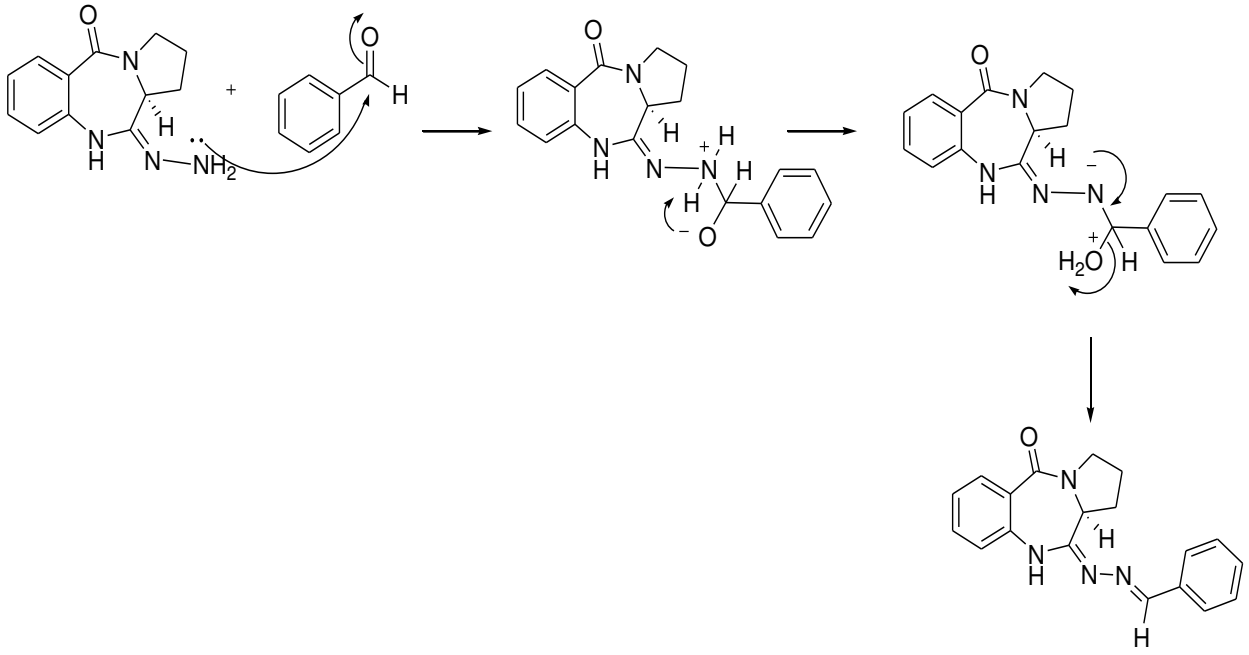

Scheme 5: Proposed mechanism for compound **4a**

(*S,E*)-11-[2-(4-Methoxyphenyl) Methylene Hydrazono] Pyrrolo [2,1-c] [1,4] Benzodiazepine(**4b**)

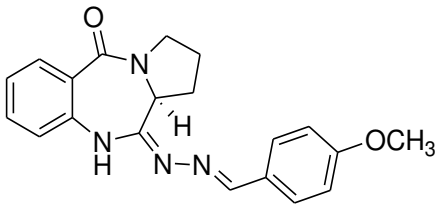

The general procedure was followed, and 4-methoxybenzaldehyde was used and the reaction was stirred for 6 hours. The solution was filtered and washed with diethyl ether to afford a light-yellow solid of compound **4b**. The final product was purified using crystallization from isopropanol to yield colorless needle shape crystals. ^{1}H NMR of **4b** in $CDCl_3$ gave two doublet, two triplet and a multiplet peak for the aromatic protons between 6.92-7.96 ppm. A two-singlet peak for N-H and N=C-H group at 8.52-8.42 ppm respectively. A doublet for the 11aH between 4.36-4.38 ppm and a multiplet for N-CH_2 and CH_3 between 3.69-4.38 ppm on the pyrrolidine ring. A two multiplet was recorded for the two CH_2 groups on the pyrrolidine ring between 1.88-3.01 ppm (refer to spectra at **Appendix E1, E2, and E3**). ^{13}C NMR gave 17 proposed peaks with peaks at 166.11 for C=O, 161.83 C-O, 157.38 and 156.98 ppm for the two C=N ppm. 9 carbon peaks were found between 114.29-136.97 ppm. And the C-11a and CH_3 peak showed at 55.50 ppm. The three CH_2 groups on the pyrrolidine ring also produced peaks at 47.40, 26.14 and 23.55 ppm (refer to spectrum at **Appendix E4**). In ^{13}C DEPT-135 all quaternary carbons disappeared and N=CH appeared on the positive phase at 157.21 ppm. 6 aromatic carbons were found on the positive phase between 114.28-132.47 ppm and C-11a and CH_3 showed on the positive phase at 55.49 ppm. All the CH_2 on the pyrrolidine ring 47.31, 26.10 and 23.57 ppm appeared on the negative phase (refer to spectrum at **Appendix E5**). IR analysis showed peaks at 3259 cm^{-1}, 2956 and 2854 cm^{-1}, and 1627 cm^{-1} for the N-H, C-H and the C=O stretching

respectively (refer to spectrum at **Appendix E6**). UV-Vis absorption of the compound in methanol was at 221 nm and 325 nm (refer to spectrum at **Appendix E7**). GC/MS analysis of the compound in acetone produced molecular ion peak at *m/z* = 348.0 amu and a base peak at *m/z* = 241.0 amu (refer to spectrum at **Appendix E8**).

Figure 8: Spongy crystals of compound 4b from isopropanol

(*S,E*)-11-[2-(4-Fluorophenyl) Methylene Hydrazono] Pyrrolo [2,1-c] [1,4] Benzodiazepine(**4c**)

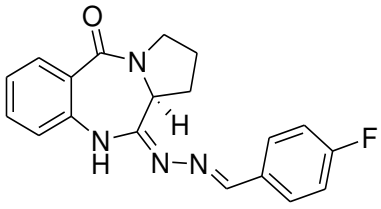

The general procedure was followed, and 4-flurobenzaldehyde was used and the reaction was stirred for 4 hours followed by quenching with distilled water and filtered to give a white solid of compound **4c**. The final product was purified using crystallization from hexane/acetone to yield white cube shape crystals. ^{1}H NMR of **4c** in $CDCl_3$ gave two double, two triplet and peak for the aromatic protons between 6.98-7.97 ppm. A doublet peak for N-H and N=C-H were

found between 8.48-8.45 ppm. A doublet for the 11aH between 4.37- 4.39 ppm and a multiplet for N-CH_2 between 3.67-3.81 ppm on the pyrrolidine ring. A two multiplet was recorded for the two CH_2 groups on the pyrrolidine ring between 2.00-3.01 ppm (refer to spectra in **Appendix F1, F2, and F3**). ^{13}C NMR gave 16 proposed peaks with peaks at 166.03 for C=O, 157.65 and 156.52 ppm for the two C=N ppm. 9 carbon peaks were found between 115.94-136.74 ppm. And the C-11a peak showed at 55.50 ppm. The three CH_2 groups on the pyrrolidine ring also produced peaks at 47.42, 26.14 and 23.55 ppm (refer to spectrum in **Appendix F4 and F5**). In ^{13}C DEPT-135 all quaternary carbons disappeared and N=CH appeared on the positive phase at 156.52ppm. 7 aromatic carbons were found on the positive phase between 115.94-132.50 ppm and C-11a and CH_3 peaks showed on the positive phase at 55.50 ppm. All the CH_2 on the pyrrolidine ring 47.42, 26.19 and 23.55 ppm appeared on the negative phase (refer to spectrum in **Appendix F6**). IR analysis showed peaks at 3261 cm^{-1}, 2950 and 2877 cm^{-1}, and 1627 cm^{-1} for the (N-H), (C-H) and the C=O stretching respectively (refer to spectrum in **Appendix F7**). UV-Vis absorption of the compound in methanol was at 222 nm, 236 nm and 313 nm (refer to spectrum in **Appendix F8**). GC/MS analysis of the compound in acetone produced molecular ion peak at m/z = 336.0 amu and a base peak at m/z = 241.0 amu (refer to spectrum in **Appendix F9**).

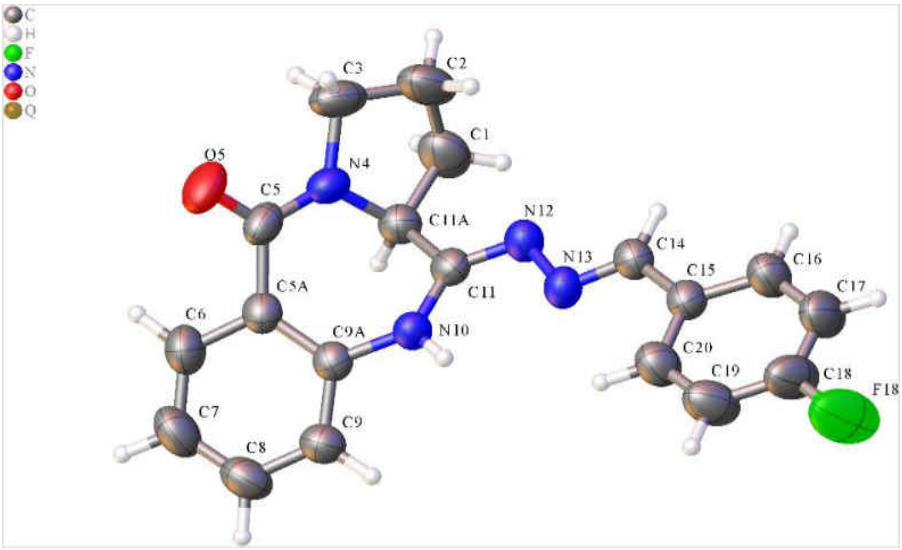

Figure 9: X-ray diffraction ORTEP analysis of compound **4c**

Figure 10: Crystals of compound **4c** from hexane/acetone

(*S,E*)-11-[2-4-(4-Formylphenyl) Morpholine Methylene Hydrazono] Pyrrolo [2,1-c] [1,4] Benzodiazepine(**4d**)

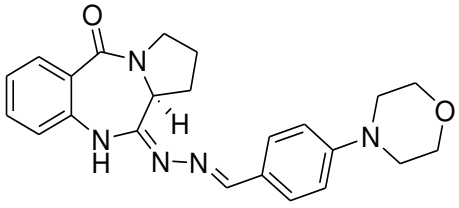

The general procedure was followed, and 4-(4-formylphenyl) morpholine was used and the reaction was stirred overnight under nitrogen gas. Flash column chromatography using hexane/acetone (v/v 1:1) was used and the solvent was evaporated in vacuum. Crystallization of the compound was done using pentane to afford a yellow rod shape crystal of compound **4d**. ^{1}H NMR of **4d** in $CDCl_3$ gave four doublet and, two triplet peaks representing for the aromatic 8 protons between 6.98-7.97 ppm. A two-singlet peak for N-H and N=C-H group at 8.40-8.52 ppm respectively. A doublet for the 11aH between 4.37-4.38 ppm and a multiplet for N-CH_2 and O-CH_2 between 3.68-3.86 ppm on the pyrrolidine and morpholine ring came together respectively representing 6 protons. A singlet was observed for N-CH_2 on the morpholine representing 4 protons. A singlet and a multiplet were observed for the two CH_2 groups on the pyrrolidine ring between 1.99-3.01 ppm (refer to spectra in **Appendix G1, G2, and G3**). ^{13}C NMR gave 19 expected peaks with peaks at 166.14 ppm for C=O, 157.59 ppm and 156.65 ppm for the two C=N ppm. 152.65 was observed for C-N which connects the phenylene and the morpholine ring. 9 carbon peaks were found between 114.68-137.04 ppm. C-O on the morpholine peak was observed at 66.79 ppm while the C-11a peak showed at 55.50 ppm. C-N on the morpholine was observed at 48.22 ppm while the three CH_2 groups on the pyrrolidine ring also produced peaks at 47.40 ppm, 26.14 ppm, and 23.55 ppm (refer to spectrum in **Appendix G4 and G5**). In ^{13}C DEPT-135 all quaternary carbons disappeared and N=CH appeared on the positive phase at 157.59 ppm. 6 aromatic carbons were found on the positive phase between 114.67-132.44 ppm. CH_2-O on the morpholine ring appeared on the negative phase at 66.8 ppm and C-11a and peak showed on the positive phase at 55.50 ppm. CH_2-N on the morpholine ring appeared on the negative phase. All the CH_2 on the pyrrolidine ring 47.40 ppm, 26.14ppm and 23.56 ppm appeared on the negative phase (refer to spectrum in **Appendix G6**). IR analysis showed peaks at

3259 cm^{-1}, 2955 cm^{-1} and 2854 cm^{-1}, and 1619 cm^{-1} for the N-H, C-H and the C=O stretching respectively (refer to spectrum at **Appendix G7**). UV-Vis absorption of the compound in methanol was at 235 nm and 350 nm. GC/MS analysis of the compound in acetone produced molecular ion peak at *m/z* = 403.0 amu and a base peak at *m/z* = 207.0 amu (refer to spectrum at **Appendix G8**).

Figure 11: Crystals of compound **4d** from pentane

(*S,E*)-11-[2-(4-Ethylphenyl) Methylene Hydrazono] Pyrrolo [2,1-c] [1,4] Benzodiazepine(**4e**)

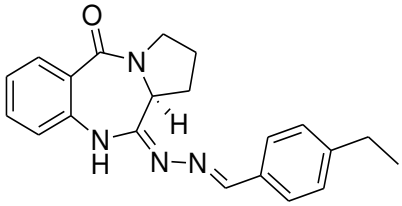

The general procedure was followed, and 4-ethylbenzaldehyde was used and stirred overnight under nitrogen and evaporation of the solvent was done in a vacuum. Crystallization of the compound was done using pentane to give a yellow solid rod shape crystal of compound **4e**. ^1H NMR of **4e** in $CDCl_3$ gave a double doublet, two doublet and three triplet peaks for the

aromatic protons between 6.98-7.98 ppm. A doublet peak for the N-H, N=C-H group between 8.53-8.48 ppm. A doublet for the 11aH between 4.37-4.38 ppm and a multiplet for N-CH_2 between 3.64-3.84 ppm on the pyrrolidine ring. A multiplet was recorded for one proton on the pyrrolidine ring between 2.98-2.99 ppm. A quartet was recorded for CH_2 between 2.66-2.72 ppm and a multiplet was recorded for the CH_2 groups on the pyrrolidine ring between 1.99-2.15 ppm. CH_3 was between 1.24-1.27 ppm. (refer to spectra in **Appendix H1, H2, and H3**). ^{13}C NMR gave 19 expected peaks with the characteristic peaks at 166.11ppm for C=O, 157.86 ppm and 157.31 ppm for the two C=N ppm. Instead of 12 aromatic carbon peaks, 10 carbon peaks were found between 120.76 ppm-147.59 ppm respectively because two of them were symmetric carbons. And the C11a peak showed at 55.53 ppm. The three CH_2 groups on the pyrrolidine ring also produced peaks at 47.43 ppm, 26.15 ppm and 23.56 ppm whiles CH_2 and CH_3 of ethene attached to the phenyl was observed at 29.03 ppm and 15.50 ppm respectively (refer to spectrum at **Appendix H4 and H5**). In DEPT-135 all quaternary carbons disappeared and N=CH appeared on the positive phase at 157.86ppm. 6 aromatic carbons were found on the positive phase between 120.77 ppm-132.49 ppm and C-11a showed on the positive phase at 55.53 ppm. All the CH_2 on the pyrrolidine ring 47.44 ppm, 29.04 ppm, 26.16 ppm, and 23.57 ppm appeared on the negative phase whiles CH_3 of ethene appeared on the positive phase (refer to spectrum at **Appendix H6**). IR analysis showed peaks at 3343 cm^{-1}, 2966 cm^{-1}, 2873 cm^{-1}, and 1627 cm^{-1} for the N-H, C-H and the C=O stretching respectively (refer to spectrum at **Appendix H7**). UV-Vis absorption of the compound in methanol was at 224 nm and 322 nm. GC/MS analysis of the compound in acetone produced molecular ion peak at m/z = 346.0 amu and a base peak at m/z = 241.0 amu (refer to spectrum at **Appendix H8**).

(S,E)-11-[2-(4-Pyridine) Methylene Hydrazono] Pyrrolo [2,1-c] [1,4] Benzodiazepine(**4f**)

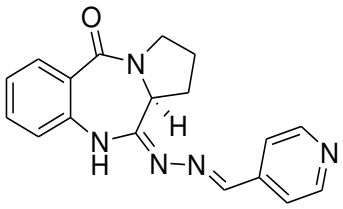

The general procedure was followed, and 4-pyridine carboxaldehyde was used and the reaction stirred for 4 hours under nitrogen. The reaction was quenched with 20mL distilled water and filtered. Crystallization of the compound was done using pentane to afford a yellow crystal solid of compound **4f**. ^{1}H NMR of **4f** in $CDCl_3$ gave four doublet and two triplet peaks for the aromatic protons between 7.01-7.98 ppm and two N=CH on the pyridine was found between 8.68-8.69 ppm. A doublet peak for N-H and N=C-H group at 8.50-8.44 ppm respectively. A doublet for the 11aH between 4.37- 4.39 ppm and a multiplet for N-CH_2 between 3.67-3.84 ppm on the pyrrolidine ring. A two multiplet was recorded for the two CH_2 groups on the pyrrolidine ring between 1.88-2.98 ppm (refer to spectra in **Appendix I1, I2, and I3**). ^{13}C NMR gave 16 expected peaks with characteristic peaks at 165.86 ppm for C=O, 158.86 and 155.39 ppm for the two C=N ppm. 9 carbon peaks were found between 120.93-150.54 ppm on the aromatic regions. And the C-11a peak showed at 55.52 ppm. The three CH_2 groups on the pyrrolidine ring also produced peaks at 47.43 ppm, 26.15 ppm, and 23.55 ppm (refer to spectrum in **Appendix I4**). In DEPT-135 all quaternary carbons disappeared and N=CH appeared on the positive phase at 155.39 ppm. 6 aromatic carbons were found on the positive phase between 120.94 -150.54 ppm and C-11a showed on the positive phase at 55.51 ppm. All the CH_2 on the pyrrolidine ring 47.44 ppm, 26.15 ppm and 23.55 ppm appeared on the negative phase (refer to spectrum at **Appendix I5**). IR analysis showed peaks at 3343 cm^{-1}, 2966 cm^{-1} and 2873 cm^{-1}, and 1625 cm^{-1} for the N-

H, C-H and the C=O stretching respectively (refer to spectrum at **Appendix I6**). UV-Vis absorption of the compound in methanol was at 223 nm and 334 nm (refer to spectrum at **Appendix I7**). GC/MS analysis of the compound in acetone produced molecular ion peak at *m/z* = 319.0 amu and a base peak at *m/z* = 241.0 amu (refer to spectrum at **Appendix I8**).

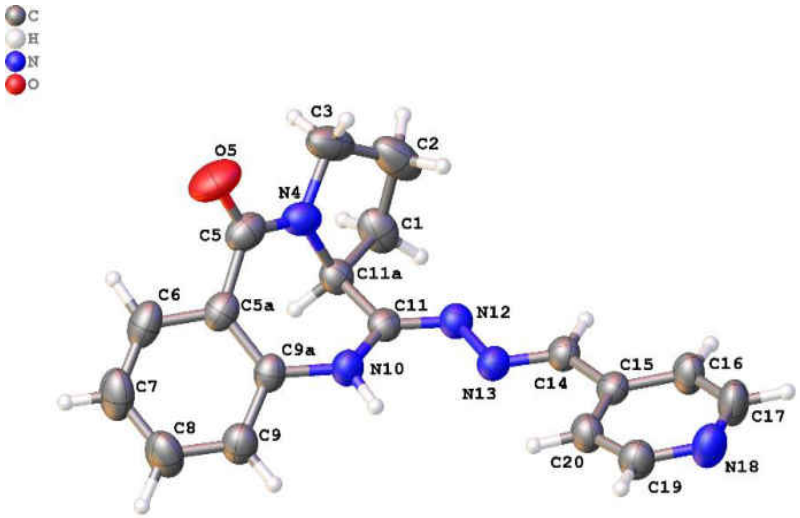

Figure 12: X-ray diffraction ORTEP analysis of compound **4f**

Figure 13: Crystals of compound **4f** from pentane

Protection of Indole-3-Carboxaldehyde to *ter*t-Butyl 3-Formyl-1H-Indole-1-Carboxylate (**6**)

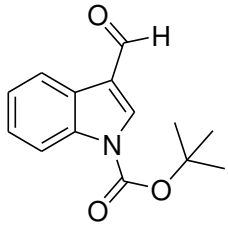

Indole-3-carboxaldehyde was dissolved in DCM and reacted with 4-dimethylaminopyridine (DMAP) at 0° C. Di-tert-butyl dicarbonate solution in THF was added slowly and in dropwise using an addition funnel and was warmed at room temperature for 6 hours. The reaction mixture was then quenched with 50 mL of water and the organic layer was separated. The organic layer was washed with 5% HCl and saturated NaCl. It was then dried ($MgSO_4$), filtered and concentrated in a vacuum. The crude solid was purified by dissolving it in DCM followed by precipitation by adding hexanes and filtered with a fritted funnel. The filtered residue was washed with hexanes and dried in a vacuum to give compound **5** [117]. ^{1}H NMR of compound **5** in $CDCl_3$ gave a singlet for HC=O at 10.01 ppm, aromatic protons produced two doublet a singlet and a multiplet from 7.36-8.29 ppm and tert-butyl group CH_3 produced 9 protons at 1.69 ppm (refer to spectrum in **Appendix J1, J2, and J3**). ^{13}C NMR gave 11 peaks with characteristic peaks at C=O 185.93, COO 148.86 ppm. Aromatic carbons were found between 115.26 ppm to 136.67 ppm. 85 ppm was recorded for C-O and CH_3 appeared at 28.16 ppm (refer to spectrum in **Appendix J4**).

(*S,E*)-11- [2-(*Tert*-butyl 3-formyl-1H-Indole-1-Carboxylate) Methylene Hydrazono] Pyrrolo [2,1-c] [1,4] Benzodiazepine(**7**)

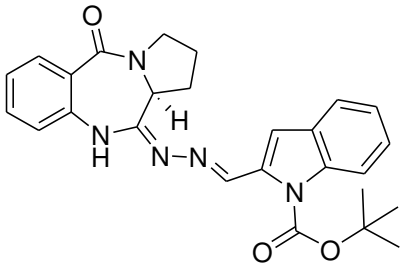

The general procedure was followed, and *tert*-butyl 3-formyl-1H-indole-1-carboxylate was used, and the reaction stirred overnight under nitrogen. Flash column chromatography with (1:1 v/v) hexane/acetone was used, and the solvent was evaporated in vacuum followed by solidification the compound in pentane to afford a yellow solid of compound **7.** ^{1}H NMR of compound **7** in $CDCl_3$ gave two doublets, a double doublet a triplet, a multiplet and a singlet peaks representing for the aromatic 9 protons between 6.99 ppm-8.26 ppm. A two-singlet peaks for N-H and N=C-H group at 8.64 ppm and 8.47 ppm respectively. A double doublet for the 11aH between 4.40 ppm-4.41 ppm and a multiplet for N-CH_2 between 3.69 ppm-3.83 ppm on the pyrrolidine ring. A multiplet was observed for N-CH_2 on the pyrrolidine ring another multiplet was observed for the two CH_2 groups on the pyrrolidine ring between 2.01 ppm-2.16 ppm. A *tert*-butyl group occurred at 1.69 ppm as singlet (refer to spectra in **Appendix K1, K2, and K3**). ^{13}C NMR gave 24 expected peaks with peaks at 166.12 ppm and 156.57ppm for C=O, 152.30 ppm and 149.29 ppm for the two C=N ppm. 14 carbon peaks were found between 115.45 ppm-136.97 ppm for the aromatic carbons. C-O carbon peak was observed at 84.89 ppm while the C-11a peak showed at 55.54 ppm while the three CH_2 groups on the pyrrolidine ring also produced peaks at 47.46 ppm, 26.18 ppm, and 23.55 ppm. Also, *tert*-butyl group occurred at

28.25 ppm (refer to spectrum in **Appendix K4 and K5**). In ^{13}C DEPT-135 all quaternary carbons disappeared and N=CH appeared on the positive phase at 152.33 ppm. 8 aromatic carbons were found instead of 9 on the positive phase between 114.67 ppm-132.44 ppm. This was because one of the carbons were the same. C-11a peak showed on the positive phase at 55.54 ppm. All the CH_2 on the pyrrolidine ring 47.47 ppm, 26.18 ppm, and 23.56 ppm appeared on the negative phase whiles tert-butyl group appeared on the positive phase (refer to spectrum in **Appendix K6**). IR analysis showed peaks at 3353 cm^{-1}, 2977 cm^{-1}, and 2879 cm^{-1}, and 1627 cm^{-1} for the N-H, C-H and the C=O stretching respectively (refer to spectrum in **Appendix K7**). UV-Vis absorption of the compound in methanol was at 235 nm and 350 nm. GC/MS analysis of the compound in acetone produced molecular ion peak at *m/z* = 457.0 amu and a base peak at *m/z* = 391.0 amu (refer to spectrum in **Appendix K8**).

(*S,E*)-11- [2-(Indole) Methylene Hydrazono] Pyrrolo [2,1-c] [1,4] Benzodiazepine(**8**)

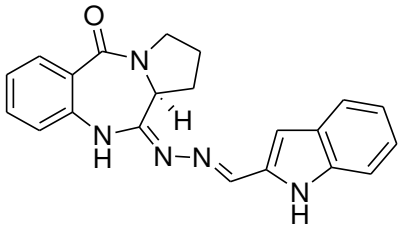

Procedures from[118,119] was used with some modifications (*tert*-butyl 3-formyl-1H-indole-1-carboxylate) methylene hydrazono PBD was reacted with potassium carbonate in a 20 mL mixture of $MeOH/H_2O$ and reflux for 30 minutes. The mixture was cooled down and washed with ether to afford white solid of compound **8.** ^1H NMR of compound **8** in C_2D_6OS gave two doublets, a double doublet a triplet, a multiplet and a singlet peaks representing for the aromatic

9 protons between 7.14 ppm-8.34 ppm. A two-singlet peaks for N-H and N=C-H group at 8.97 ppm and 8.67 ppm respectively. A double doublet for the 11aH between 4.45 ppm-4.57 ppm and a multiplet for N-CH_2 between 3.54 ppm-3.63 ppm on the pyrrolidine ring. A multiplet was observed for the two CH_2 groups on the pyrrolidine ring between 1.94 ppm-2.03 ppm (refer to spectra in **Appendix L1, L2, and L3**). ^{13}C NMR gave 18 peaks with peaks at 166.63 ppm for C=O, 154.66 pm and 153.92 ppm for the two C=N ppm. 11 carbon peaks were found between 112.65 ppm-138.13 ppm for the aromatic carbons because three of the aromatic carbons were symmetric. C-11a peak showed at 55.56 ppm while the three CH_2 groups on the pyrrolidine ring also produced peaks at 47.44, 26.30, and 23.66 ppm. (refer to spectrum in **Appendix L4 and L5**). In ^{13}C DEPT-135 all quaternary carbons disappeared and N=CH appeared on the positive phase at 153.93 ppm. 7 aromatic carbons were found on the positive phase between 121.17 ppm-132.62 ppm. C-11a peak showed on the positive phase at 55.56 ppm. All the CH_2 on the pyrrolidine ring 47.44 ppm, 26.30 ppm and 23.66 ppm appeared on the negative phase (refer to spectrum in **Appendix L6**). IR analysis showed peaks at 3504 cm^{-1}, 2917 and 2850 cm^{-1}, and 1617 cm^{-1} for the N-H, C-H and the C=O stretching respectively (refer to spectrum in **Appendix L7**). UV-Vis absorption of the compound in methanol was at 221 nm and 331 nm. GC/MS analysis of the compound in acetone produced molecular ion peak at *m/z* = 357.0 amu and a base peak at *m/z* = 207.0am u (refer to spectrum in **Appendix L8**).

Biological Activity

Cancer Inhibition Activity

PBD compound derivatives were determined for cytotoxicity on cancer cell lines. Using a single dose application, four of the compounds were evaluated on NCI-60 cell lines at the National Cancer Institute (refer to table **1**). Screening of the compound was done at a concentration of 10 μM.

In leukemia, cancer cell line K-562 had 11.05% inhibition on compound **4b**. Less than 10% was observed for the rest of the compounds. Non- small cell lung cancer showed 16.41% inhibition on cell line HOP-92 for compound **4c** and compound **4b** also showed 13.44% inhibition. Colon cell line recorded less than 5% for all the compounds tested. Cell line SNB-75 for CNS showed 20.93% and 24.99 % inhibition for compound **4a** and **4b** respectively. Melanoma cell line MALME-3M recorded 12.16% inhibition for compound **4a** and cell line UACC-62 recorded 8.29% inhibition for compound **4b**. In ovarian cell line OVCAR-4, 10.62% inhibition were recorded for both compound **4a** and **4b**. Renal cell line 786-0 and UO-31, 15.43% and 16.16% was recorded for compound **4b** respectively. In prostate cell line PC-3, 8.72% and 6.65% inhibition were recorded for compound **4b** and **4c** respectively. Breast cancer cell line T-47D recorded 11.88% and 15.8% respectively.

Table 1: In vitro cytotoxicity data of PBD derivatives on NCI-60 cell lines

		Growth Percent of PBD derivatives			
Cancer	Cell line	Compound **4a**	Compound **4b**	Compound **4c**	Compound **4e**
Leukemia	K-562	91.38	88.94	94.41	103.68
	RPMI-8226	98.54	96.69	98.39	106.83
Non-Small Cell Lung	EKVX	95.49	91.13	97.21	106.24
	HOP-92	87.32	86.56	83.59	100.70
Colon	HCT-116	99.81	98.39	98.52	99.62
	SW-620	101.30	95.62	100.37	100.07
CNS	SNB-75	79.07	75.01	86.94	95.58
	U251	94.54	96.24	91.89	101.33
Melanoma	MALME-3M	87.84	93.34	107.58	95.32
	UACC-62	92.37	91.71	93.09	93.33
Ovarian	OVCAR-4	89.38	89.38	94.03	104.98
	OVCAR-8	96.70	100.02	99.97	103.33
Renal	786-0	88.76	84.57	85.06	98.59
	UO-31	87.62	83.84	85.13	87.32
Prostate	PC-3	95.35	91.28	93.35	99.95
	DU-145	102.92	100.11	100.34	106.30
Breast	MCF7	90.30	98.06	93.87	98.55
	T-47D	89.32	88.12	84.20	101.60

Enzyme Inhibition Kinetics

Enzyme inhibition kinetics was done to determine the percentage inhibition and residual activity of the enzymes TEM-1, AmpC, and P99 lactamase was carried out in 20 mM MOPS buffer. 3µL (final concentration = 0.25, 0.2 and 0.20 nM for TEM-1, AmpC and P99 respectively) of enzymes was used for the assay.

Table 2: Residual activity (%) and percent inhibition of TEM-1

Compound	Initial Rate $V_\circ \pm$ SD (ΔA, s^{-1}) × 10^{-3}	Initial Rate +Inhibitor $V_i \pm$ SD (ΔA, s^{-1}) × 10^{-3}	Residual Activity (%)	Inhibition (%)
4a	5.074 ±0.029	1.010±0.023	80.4	19.6
4b	5.074 ±0.029	6.532±0.018	100	0
4c	5.074 ±0.029	0.535±0.019	89.8	10.2
4d	5.074 ±0.029	2.531±0.017	50.2	49.8
4e	5.074 ±0.029	6.032±0.015	100	0
4f	5.074 ±0.029	1.512±2.214	89.0	21.0
8	5.074 ±0.029	6.232±0.017	100	0

Final concentration and volume of enzyme (TEM-1) = 3 µL (0.45 nM),

Substrate (NCF) = 10 uL (100 µM),

0.1 % BSA in MOPS buffer = 562 µL (0.02 mM, pH – 7.5),

Inhibitor (in 3% acetone) = 20 µL (500 µM)

Table 3: Residual activity (%) and percent inhibition of AmpC

Compound	Initial Rate $V_\circ \pm SD$ ($\Delta A, s^{-1}$) × 10^{-3}	Initial Rate +Inhibitor $V_i \pm SD$ ($\Delta A, s^{-1}$) × 10^{-3}	Residual Activity (%)	Inhibition (%)
4a	8.718±0.018	8.526±0.212	95.56	4.44
4c	8.718±0.018	7.824±0.128	88.45	11.55
4d	8.718±0.018	9.394±0.024	100	0

Final concentration and volume of enzyme (AmpC) = 3 µL (0.45 nM),

Substrate (NCF) = 10 uL (100 µM),

0.1 % BSA in MOPS buffer = 562 µL (0.02 mM, pH – 7.5),

Inhibitor (in 3% acetone) = 20 µL (500 µM)

Table 4: Residual activity (%) and percent inhibition of P99

Compound	Initial Rate $V_\circ \pm SD$ ($\Delta A, s^{-1}$) × 10^{-3}	Initial Rate +Inhibitor $V_i \pm SD$ ($\Delta A, s^{-1}$) × 10^{-3}	Residual Activity (%)	Inhibition (%)
4d	5.184±0.025	4.824±0.028	92.03	7.97

Final concentration and volume of enzyme (p99) = 3 µL (0.45 nM),

Substrate (NCF) = 10 uL (100 µM),

0.1 % BSA in MOPS buffer = 562 µL (0.02 mM, pH – 7.5),

Inhibitor (in 3% acetone) = 20 µL (500 µM)

The results of the inhibition studies conducted on TEM-1 shows that compound **4d** had the highest inhibition of 49.8% followed by compound **4f** and **4a** at 20.99% and 19.6% respectively. Compound **4c** recorded 10% inhibition and no inhibition was recorded for compound **4b**, **4e,** and **4g**. No inhibition was recorded for compound **4b**, **4e** and **8** because they did not produce a supernatant solution when the enzyme was added. The other results from lactamase AmpC also showed that compound **4c** had the highest inhibition of 11.55% but there was no inhibition recorded for compound **4d**. On lactamases p99, compound 4d only showed 7.97% inhibition. In summary, only compound **4d** was a selective inhibitor of the lactamase TEM-1.

Cannabinoid Binding Activity

Preliminary cannabinoid binding activity was conducted on compound **4a** and it was found out that the compound had 46.8% binding affinity to cannabinoid receptor 1 and 77.4% binding activity to cannabinoid receptor 2. However, a comprehensive binding activity of the compound will be evaluated with the rest of the compounds in the future.

CHAPTER 3

EXPERIMENTAL SECTION

Materials and General Methods

L-proline, isatoic anhydride and other chemicals were purchased and used without further purification unless otherwise stated.

^{1}H NMR, ^{13}C NMR, GC-MS, IR spectroscopy and X-ray crystallography were used for the characterization of the synthesized compounds. All the NMR spectra were executed with JEOL-NMR Eclipse-400 MHz spectrophotometer and the coupling constants value (J) was recorded in Hz. The patterns of splitting resonance were presented as singlet (s), doublet (d), triplet (t), and multiplet (m). Shimadzu 1R Prestige-21 FT-IR was used for all IR spectra. The melting point of the compounds was done using Cambridge Melt-Temp apparatus. Fragments of the compounds produced molecular ion and was performed with Shimadzu GC-MS 2010 device. Thin layer chromatography and column chromatography were used to purify the compounds. X-ray crystallography was also used for the crystal structure determination of the compounds produced. Agilent Technology UV- Vis was used to determine the compounds that absorb UV radiation.

Experimental Procedures

(S)-1,2,3,11aTtetrahydro-5H-Benzo[e]Pyrrolo[1,2-a][1,4]Diazepine-5,11(10H)-dione (**1**)

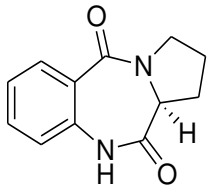

Dilactam **1** was synthesized using formally reported methods with some alterations. Isotaic anhydride (10.0 g, 61.34 mmol) and L-proline (7.06 g, 61.34 mmol) was reacted using N,N-dimethylformamide (50 mL) and the reaction mixture was heated to about 155 ˚C for 5 h. The solvent was then removed in vacuo after cooling was done at room temperature and the residue was finally taken up in water. A solid of white color with gray was obtained after drying. Recrystallization was done using acetone/DMF (v/v 10:1) which gave 10.87 g of pure compound **1** as off-white crystals. Yield: 83.0 %; m.p: 223-225 ^{o}C; $[\alpha]_D^{25}$ = + 512 ^{o} (*c* 0.5, MeOH); ^{1}H-NMR (400 MHz, DMSO-d_6): δ = 1.76-1.95 (m, 3H), 3.42-3.48 (m, 1H), 3.56-3.61 (m, 1H), 4.10 (d, *J* = 8 Hz, 1H), 7.12 (dd, *J* = 12, 4 Hz, 1H), 7.20-7.24 (m, 1H), 7.49-7.51 (m, 1H), 7.82 (dd, *J* = 12, 8Hz, 1H), 10.51 (s, 1H); ^{13}C-NMR (100 MHz, DMSO-d_6): δ = 23.6, 26.3, 47.4, 56.8 (C-11a), 121.8, 124.4, 127.1, 130.8, 132.6, 136.9, 165.0 (CO), 171.3 (CO); UV λ_{max} (MeOH): 222, 231, 235 nm. IR (KBr); 3218 (N-H), 2969 (C=O), 2879, 1693 (C=O), 1619 (C=O), 1479, 1444, 1413, 1285, 1259, 1162, 757, 700. GC-MS (70 eV) *m/z* (%): 216 (10) [M^+], 119 (14), 92 (20), 70 (100), 64 (10).

(*S*)-11-Thioxo-1,2,3,10,11,11a-Hexahydro-5H-Benzo[e]Pyrrolo[1,2-a][1,4]Diazepin-5-one (**2**)

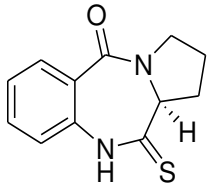

A mixture of **1** (33.35 g, 154 mmol) and Lawesson's reagent (31.11 g, 77 mmoL) in THF (350 mL) was stirred over night at room temperature. The solvent was then evaporated in vacuo to produce a solid yellow residue which was washed with toluene and further washed with cold toluene to give 20.2 g of pure compound **2** as yellow solid.[36] Yield 84.0 %; m.p: 272-274 ^{o}C ; $[\alpha]_D^{25}$ = + 762 ^{o} (*c* 0.5, $CHCl_3$); ^{1}H-NMR (400 MHz, DMSO-d_6): δ = 1.76-2.00 (m, 1H), 1.98-2.09 (m, 2H), 2.88 (d, *J* = 5.9 Hz, 1H), 3.31-3.51 (m, 3H), 3.56-3.61 (m, 1H), 4.28 (d, *J* = 6.2 Hz, 1H), 7.29 (d, *J* = 8.1 Hz, 1H), 7.33-7.37 (m, 1H), 7.58 (t, *J* = 7.7 Hz, 1H), 7.83 (dd, *J* = 7.7, 1.5 Hz, 1H); ^{13}C-NMR (100 MHz, DMSO-d_6): δ = 23.39, 26.12, 47.30, 55.53 (C-11a), 119.88, 122.84, 125.30, 131.34, 132.45, 137.92, 166.24 (CO). UV λ_{max} (MeOH): 209, 212, 231 nm. IR (KBr): 3456 (N-H), 2969 (C-H), 1739, 1619 (C=O), 1479, 1367, 1216, 759. GC/MS (70 eV) *m/z* (%): 232 (7) [M+], 108 (6), 70 (100), 68 (6).

(*S,E*)-11-hydrazono-1,2,3,10,11,11a-hexahydro-5H-benzo[e]Pyrrolo[1,2-a][1,4]Diazepin-5-one (**3**)

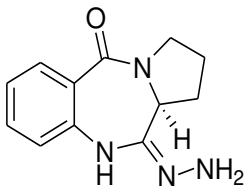

Compound **2** (23.2g, 100 mmoL) was reacted with 98% hydrazine monohydrate (15.0 g, 14.6 mmoL) in ethanol (300 mL) and stirred for 15 h at room temperature. Water was added to the residue to obtain the product after the solvent was evaporated in vacuum. The precipitate was then dried and washed with diethyl ether to give 18.34 g of compound **3** as off-white solid.[37] Yield: 80.0 %; m.p. : 178-180 °C; $[\alpha]_D^{25}$ = + 552 ° (*c* 0.5, MeOH); ^{1}H-NMR (400 MHz, $CDCl_3$): δ = 1.931−2.13 (m, 4H), 2.72 (s, 1H), 3.61−3.70 (m, 2H), 4.2 (s, 1H), 6.83 (d, *J* = 8 Hz, 1H), 7.05 (t, *J* = 7.3 Hz, 1H), 7.31 (t, *J* = 15.4 Hz, 2H), 7.86 (d, *J* = 7.7 Hz, 1H); ^{13}C-NMR (100 MHz, $CDCl_3$): δ = 23.4, 26.1, 47.3, 55.5 (C-11a), 119.7, 123.0, 125.4, 131.5, 132.5, 137.8, 152.2, 166.2 (CO). UV λ_{max} (MeOH): 219, 266, 311 nm. IR (KBr): 3261(N-H), 2948 (C-H), 2877, 1710, 1631 (C=O), 1471, 1394, 1251, 1201, 1160, 757, 703, 597. GC/MS (70 eV) *m/z* (%): 232 (7) [M+], 108 (6), 70 (100), 68 (6).

General method for synthesis of *(S,E)*-11-[2-(Arylmethylene)Hydrazono] Pyrrolo [2,1-c] [1,4] Benzodiazepine (**4a-f**)

To a solution of compound **3** (690 mg, 3 mmoL) in anhydrous methanol (20 mL) was added aldehyde (10 mmoL). 3A° molecular sieves (2.0 g) was also added and stirred at room temperature. Various modifications were used to obtain compound (**4a**-**f**).

(*S,E*)-11-[2-(Phenylmethylene) Hydrazono] Pyrrolo [2,1-c] [1,4] Benzodiazepine (4a)

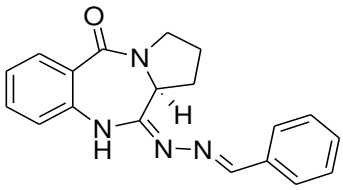

Benzaldehyde (1.02 mL, 10 mmoL) was added and stirred overnight. Extraction was done with chloroform/isopropanol in ratio (2:1) using (3×20 mL). Anhydrous sodium sulfate was used to absorb excess moisture in the organic layer. The solvent was then removed in vacuo and wash with diethyl ether, filtered and dried to afford an off-white solid of compound **4a**. The final product was purified using crystallization from isopropanol to yield colorless needle shape crystals. Yield 497 mg (72%); mp 198-200 °C; $[\alpha]_D^{25}$ = + 50 ° (*c* 0.5, $CHCl_3$): ^{1}H-NMR (500 MHz, $CDCl_3$): δ =2.02-2.07 (m, 3H), 3.00 (d, *J* = 11.4 Hz, 1H), 3.68-3.83 (m, 2H), 4.38 (d, *J* = 6.2 Hz, 1H), 6.99 (d, *J* = 8 Hz, 1H), 7.17 (t, *J* = 15 Hz, 1H), 7.43 (s, 4H), 7.79 (s, 2H), 7.96 (d, *J* = 8Hz, 1H), 8.48 (s, 1H), 8.53 (s, 1H); ^{13}C-NMR (100 MHz, $CDCl_3$): δ = 23.56, 26.15, 47.42, 55.52 (C-11a), 120.77, 123.86, 126.44, 128.22, 128.85, 130.86, 131.49, 132.48, 134.57, 136.80, 157.63, 157.83, 166.06 (CO). UV λ_{max} (MeOH): 223, 319 nm. IR (KBr): 3351, 2981, 2879, 2370, 1963, 1710, 1627 (C=O), 1471, 1400, 1295, 1097, 964, 831, 757, 692, 630. GC/MS (70 eV) *m/z* (%): 318 (25) [M+], 241 (100), 172 (9), 145 (16), 119 (13), 90 (10), 70 (13)

(*S,E*)-11-[2-(4-Methoxyphenyl) Methylene Hydrazono] Pyrrolo [2,1-c] [1,4] Benzodiazepine(**4b**)

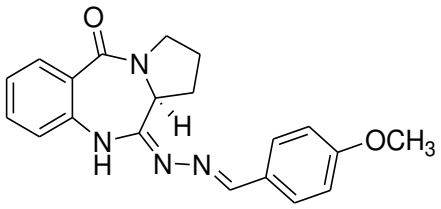

4-Methoxybenzaldehyde (1.22 mL, 10 mmoL) was used and the reaction was stirred for 6 hours. The solution was filtered and wash with diethyl ether to afford a light yellow solid 469.2 mg of compound **4b**. The final product was purified using crystallization from isopropanol to yield colorless needle shape crystals. Yield 68%; mp 212-214 °C. $[\alpha]_D^{25}$ = + 40 ° (*c* 0.5, $CHCl_3$): ^{1}H-NMR (400 MHz, $CDCl_3$): δ =1.88-2.130 (m, 3H), 2.99-3.0 (m, 1H), 3.69-3.84 (m, 5H), 4.37 (d, *J* = 8 Hz, 1H), 6.98 (q, *J* = 19.76, 18.7 Hz, 3H), 7.15 (t, *J* = 15.5 Hz, 1H), 7.42 (t, *J* = 15.4 Hz, 1H), 7.73 (d, *J* = 8 Hz, 2H), 7.95 (d, *J* = 4 Hz, 1H), 8.42 (s, 1H), 8.52 (s, 1H); ^{13}C-NMR (100 MHz, $CDCl_3$): δ = 23.55, 26.11, 47.40, 55.028 (C-11a, CH_3), 114.29, 120.72, 123.67, 126.34, 127.32, 129.84, 131.46, 132.45, 136.96, 156.98, 157.38, 161.83, 166.11 (CO). UV λ_{max} (MeOH): 221, 325 nm. IR (KBr): 3259, 2958, 2854, 2350, 1706, 1619 (C=O), 1517, 1469, 1394, 1224, 1120, 927, 827, 759, 700. GC/MS (70 eV) *m/z* (%): 348 (65) [M+], 241 (100), 160 (8), 145 (10), 119 (23), 90 (10), 70 (15).

(*S,E*)-11-[2-(4-Fluorophenyl) Methylene Hydrazono] Pyrrolo [2,1-c] [1,4] Benzodiazepine(**4c**)

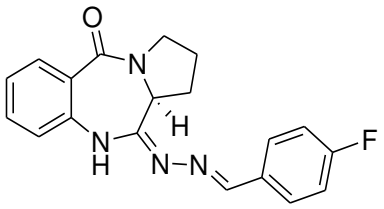

4-Flurobenzaldehyde (1.22 mL, 10 mmoL) was used and the reaction was stirred for 4 hours followed by quenching with 20 mL distilled water and filtered to give a white solid 505.8 mg of compound **4c**. The final product was purified using crystallization from hexane/acetone to yield yellow rod shape crystals. Yield 73.3%; mp 205-207 ^{o}C $[\alpha]_D^{25}$ = + 30 ^{o} (*c* 0.5, $CHCl_3$): ^{1}H-NMR (400 MHz, $CDCl_3$): δ =2.00-2.13 (m, 3H), 2.96-3.0 (m, 1H), 3.68-3.81 (m, 2H), 4.38 (d, *J* = 5.9 Hz, 1H), 7.00 (d, *J* = 4 Hz, 1H), 7.01-7.19 (m, 3H), 7.42 (t, *J* = 15.4 Hz, 1H), 7.78 (t, *J* = 9.9 Hz, 2H), 7.96 (d, *J* = 8 Hz, 1H), 8.45 (s, 1H,) 8.49 (s, 1H); ^{13}C-NMR (100 MHz, $CDCl_3$): δ = 23.55, 26.14, 47.42, 55.50 (C-11a), 115.94, 116.17, 120.76, 123.91, 126.46, 130.05, 130.14, 131.50, 132.49, 136.74, 156.52, 157.65, 161.83, 166.04 ((C=O). UV λ_{max} (MeOH): 222, 236, 313 nm. IR (KBr): 2348, 1710, 1625 (C=O), 1508, 1471, 1396, 1270, 1226, 1155, 833, 755, 700, 520. GC-MS (70 eV) *m/z* (%): 336 (44) [M+], 241 (100), 172 (9), 145 (19), 119 (19), 90 (10), 70 (13)

(*S,E*)-11-[2-4-(4-Formylphenyl) Morpholine Methylene Hydrazono] Pyrrolo [2,1-c] [1,4] Benzodiazepine(**4d**)

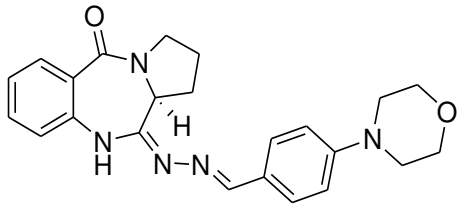

4-(4-Formylphenyl) morpholine (1.91g, 10 mmoL) was used and the reaction was stirred overnight under nitrogen gas. Flash column chromatography using hexane/acetone (v/v) 1:1 was used and the solvent was evaporated in vacuo. Crystallization of the compound was done using pentane to afford a yellow rod shape crystal 358.8 mg of compound **4d**. Yield 52.0%; mp ;198-200 °C; C $[\alpha]_D^{25}$ = + 46 ° (*c* 0.5, $CHCl_3$):^{1}H-NMR (400 MHz, $CDCl_3$): δ =1.73-2.16 (m, 3H), 2.97-3.01 (m, 1H), 3.25 (s, 4H), 3.68-3.86 (m, 6H), 4.38 (d, *J* = 5.8 Hz, 1H), 6.91 (d, *J* = 8.8 Hz, 2H), 6.98 (d, *J* = 8 Hz, 1H), 7.16 (t, *J* = 16.1 Hz, 1H), 7.42 (t, *J* = 15.4 Hz, 1H), 7.7 (d, *J* = 8.8 Hz, 2H), 7.96 (d, *J* = 8 Hz, 1H), 8.40 (s, 1H), 8.52 (s, 1H); ^{13}C-NMR (100 MHz, $CDCl_3$): δ = 23.55, 26.14, 47.40, 48.21, 55.50 (C-11a), 66.79, 114.68, 120.68, 123.60, 125.59, 126.31, 129.62, 131.47, 132.43, 137.04, 152.95, 156.65, 157.59, 166.14 (C=O). UV λ_{max} (MeOH): 235, 350 nm. IR (KBr): 3259, 2956, 2854, 2350, 1706, 1619 (C=O), 1517, 1469, 1394, 1224, 1120, 927, 827, 759.82, 700. GC-MS (70 eV) *m/z* (%): 403 (1) [M+], 355 (8), 327 (9), 281 (49), 253 (20), 207 (100), 119 (16), 133 (12), 96 (13), 73 (20), 44 (50)

(*S,E*)-11-[2-(4-Ethylphenyl) Methylene Hydrazono] Pyrrolo [2,1-c] [1,4] Benzodiazepine(**4e**)

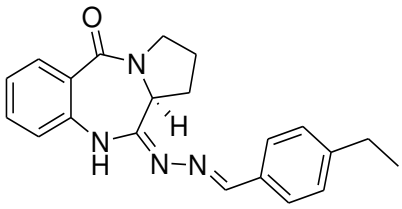

4-Ethylbenzaldehyde (1.37 mL, 10 mmoL) was used and stirred overnight under nitrogen and evaporation of the solvent was done in vacuo. Crystallization of the compound was done using pentane to give a yellow solid rod shape crystal of 499.6 mg of compound **4e**. Yield 72.4%; mp; 168-170 °C; C $[\alpha]_D^{25}$ = + 54 ° (*c* 0.5, $CHCl_3$): ^{1}H-NMR (400 MHz, $CDCl_3$): δ =1.26 (t, *J* = 15 Hz, 4H), 2.02-2.15 (m, 3H), 2.66-2.72 (m, 2H), 2.98-2.99 (m, 1H), 3.64-3.84 (m, 2H), 4.38 (d, *J* = 5.6 Hz, 1H), 7.00 (d, *J* = 4 Hz, 1H), 7.17 (t, *J* = 16.1 Hz, 1H), 7.26 (d, *J* = 8.6 Hz, 1H), 7.43 (t, *J* = 15.4 Hz, 1H), 7.71 (d, *J* = 8 Hz, 2H), 7.97 (d, *J* = 9.5 Hz, 1H), 8.46 (s, 1H), 8.52(s,1H); ^{13}C-NMR (100 MHz, $CDCl_3$): δ = 15.50, 23.56, 26.15, 29.03, 47.43, 55.52 (C-11a), 120.73, 126.38 , 128.31, 128.42, 131.47, 132.09, 132.48, 136.89, 147.59, 157.31, 157.68, 166.10 (C=O). UV λ_{max} (MeOH): 224, 322. IR (KBr): 3733, 3598, 3343, 3261, 2966, 2873, 2360, 2341, 1625 (C=O), 1469, 1396, 1270, 1160, 970, 831, 752, 669. GC-MS (70 eV) *m/z* (%): 403 (1) [M+], 346(32), 241 (100), 207 (9), 172 (8), 145 (14), 119 (12), 90 (8), 70 (11), 44 (4)

(*S,E*)-11-[2-(4-Pyridine) Methylene Hydrazono] Pyrrolo [2,1-c] [1,4] Benzodiazepine(**4f**)

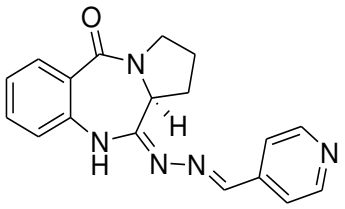

4-pyridine carboxaldehyde (0.95 mL, 10 mmoL) was used and the reaction stirred for 4 hours under nitrogen. The reaction was quench with 20 mL distilled water and filtered. Crystallization of the compound was done using pentane to afford a yellow crystal solid 436.8 mg of compound **4f**. Yield 63.3% mp; 242-244 ºC; C $[\alpha]_D^{25}$ = + 56 º (*c* 0.5, $CHCl_3$): ^{1}H-NMR (400 MHz, $CDCl_3$): δ =1.88-2.10 (m, 3H), 2.98 (d, *J* = 5.1 Hz, 1H), 3.67-3.84 (m, 2H), 4.39 (d, *J* = 5.8 Hz, 1H), 7.02 (d, *J* = 4 Hz, 1H), 7.2 (t, *J* = 15 Hz, 1H), 7.45 (t, *J* = 15.4 Hz, 1H), 7.63 (d, *J* = 4Hz, 2H), 7.97 (d, *J* = 8Hz, 1H), 8.43 (s, 1H), 8.5 (s, 1H), 8.67 (d, *J* = 4 Hz, 2H); ^{13}C-NMR (100 MHz, $CDCl_3$): δ = 23.55, 26.15, 47.43, 55.52 (C-11a), 120.92, 121.82, 124.32, 126.67, 131.53, 132.55, 136.33, 141.65, 150.54, 155.39, 158.86, 165.86 (C=O). UV λ_{max} (MeOH): 223, 334 nm. IR (KBr): 3276, 2977, 2879, 2360, 2341, 1625 (C=O), 1585, 1400, 1220, 1097, 991, 755, 530. GC-MS (70 eV) *m/z* (%): 319 (14) [M+], 281(4), 241 (100), 207 (9), 172 (11), 145 (16), 119 (12), 90 (11), 70 (15), 44 (4).

Protection of the Indole-3-Carboxaldehyde to *Tert*-Butyl 3-Formyl-1H-Indole-1-Carboxylate (**6**)

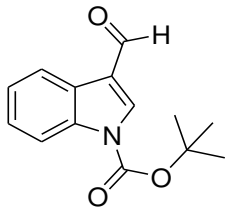

Indole-3-carboxaldehyde (0.44 g, 3 mmoL) in 50 mL of DCM was reacted with 4-dimethylaminopyridine (DMAP) (122 mg, 1 mmoL) at 0˚C (ice-bath). Di-tert-butyl dicarbonate (1.0M in THF) solution (2.76 mL, 12 mmoL) was added slowly and in drop wise using an addition funnel. It was then allowed to warm at room temperature for 6 hours. The reaction mixture was then quenched with 50 mL of water and the organic layer was separated. The organic layer was washed with 5% HCl (2.0 × 30 mL) and saturated NaCl (50 mL), dried ($MgSO_4$), filtered and concentrated in a vacuum. The crude solid was purified by dissolving it in DCM (10 mL) followed by precipitation by adding hexanes (30 mL) and filtered with fritted funnel. The filtered residue was be washed with hexanes and dried in a vacuum to give 0.34 g of *ter*t-butyl 3-formyl-1H-indole-1-carboxylate. Yield: 78.07 %; ^{1}H-NMR (400 MHz, $CDCl_3$): δ = 1.7 (s, 9H), 7.34-7.42 (m, 2H), 8.14 (d, *J* = 4 Hz, 1H), 8.23 (s, 1H), 8.29 (d, *J* = 4 Hz, 1H), 10.1 (s, 1H); ^{13}C-NMR (100 MHz, $CDCl_3$): δ = 28.17, 85.76, 115.26, 121.60, 122.21, 124.69, 126.17, 136.02, 136.67, 148.86 (C=O), 185.94. UV λ_{max} (MeOH): 215, 239, 288 nm.

(*S,E*)-11- [2-(*Tert*-Butyl 3-Formyl-1H-Indole-1-Carboxylate) Methylene Hydrazono] Pyrrolo [2,1-c] [1,4] Benzodiazepine(**7**)

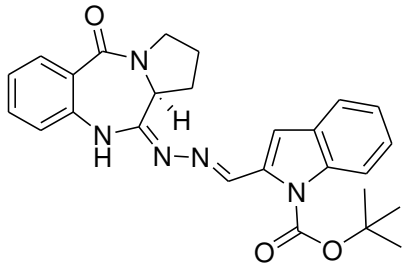

Tert-butyl 3-formyl-1H-indole-1-carboxylate (2.46 g, 10 mmoL) was used and the reaction stirred overnight under nitrogen. Flash column chromatography using hexane/acetone (v/v) 1:1 was used and the solvent was evaporated in vacuo followed by solidification the compound in pentane to afford a yellow solid 517.5 mg of compound **7**. Yield 75.0% mp; 253-255 ^{o}C; C $[\alpha]_D^{25}$ = + 32 ^{o} (*c* 0.5, $CHCl_3$): ^{1}H-NMR (400 MHz, $CDCl_3$): δ =1.53-1.75 (s, 9H), 2.0-2.16 (m, 4H), 3.0-3.03 (m, 1H), 3.58-3.83 (m, 2H), 4.43 (d, *J* = 5.4 Hz, 1H), 7.0 (d, *J* = 8 Hz, 1H), 7.20 (t, *J* = 8 Hz, 1H), 7.36-7.52 (m, 3H), 7.96 (t, *J* = 15.4 Hz, 2H), 8.26 (d, *J* = 1.4 Hz, 1H), 8.47 (s, 1H), 8.64 (s, 1H). ^{13}C-NMR (100 MHz, $CDCl_3$): δ = 23.55, 26.18, 28.25 47.46, 55.54 (C-11a), 84.89, 115.45, 117.24, 121.07, 122.34, 123.74, 125.17, 125.60, 126.35, 127.45, 131.23, 132.53, 136.24, 136.97, 149.29, 152.30, 156.57, 166.13 (C=O). UV λ_{max} (MeOH): 211, 323 nm. IR (KBr): 3353, 2977, 2879, 2360, 2341, 1735, 1627 (C=O), 1540, 1469, 1365, 1321, 1234, 1155, 1093, 754, 669, 597. GC-MS (70 eV) *m/z* (%): 457 (1) [M+], 406 (78), 391 (100), 313 (23), 281(29), 253 (14), 235 (16), 207 (57), 191 (12), 105 (53), 91 (13), 73 (12), 44 (25).

(*S,E*)-11- [2-(Indole) Methylene Hydrazono] Pyrrolo [2,1-c] [1,4] Benzodiazepine(**8**)

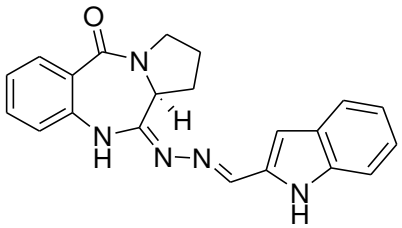

(*Tert*-butyl 3-formyl-1H-indole-1-carboxylate) methylene hydrazono PBD (460 mg, 1 mmoL) was reacted with potassium carbonate (979 mg, 7.1 mmoL) in a 20 mL mixture of MeOH/H_2O and reflux for 30 minutes. The mixture was cooled down and washed with ether to afford 802. 8 mg white solid of compound **8.** Yield 75.0% mp; 242-243 ^{o}C; C $[\alpha]_D^{25}$ = + 56 ^{o} (*c* 0.5, $CHCl_3$): ^{1}H-NMR (400 MHz, $CDCl_3$): δ =1.94-2.03 (m, 3H), 2.85 (d, *J* = 6.1 Hz, 1H), 3.54-3.63 (m, 2H), 4.46 (d, *J* = 4 Hz, 1H), 7.16-7.18 (m, 3H), 7.36-7.38 (m, 3H), 7.76 (d, *J* = 1.8 Hz, 2H), 7.96 (s, 1H), 8.34 (d, *J* = 17.2 Hz, 1H), 8.97 (s, 1H); ^{13}C-NMR (100 MHz, $CDCl_3$): δ = 23.66, 26.30, 47.44, 55.56 (C-11a), 112.65, 121.17, 122.40, 122.74, 123.01, 123.19, 131.02, 132.61, 137.97, 138.12, 153.92, 154.66, 165.63 (C=O). UV λ_{max} (MeOH): 221, 331 nm. IR (KBr): 3504, 2917, 2850, 2337, 1751, 1617 (C=O), 1371, 1240, 1052, 877, 746, 608. GC-MS (70 eV) *m/z* (%): 357 (2) [M+], 355 (6), 327 (9), 281 (52), 253 (18), 249 (7), 207 (100), 191 (15), 177 (5), 133 (11), 119 (5), 96 (13), 73 (19), 44 (46).

CHAPTER 4

CONCLUSIONS AND FUTURE WORK

Conclusions

In the research, seven novel compounds were synthesized from dialactam **1** a as biological active molecule. The PBD derivatives synthesized were: (*S,E*)-11-[2-(phenylmethylene)hydrazono] pyrrolo [2,1-c] [1,4] benzodiazepine, (*S,E*)-11-[2-(4-methoxyphenyl) methylene hydrazono] pyrrolo [2,1-c] [1,4] benzodiazepine, (*S,E*)-11-[2-(4-fluorophenyl) methylene hydrazono] pyrrolo [2,1-c] [1,4] benzodiazepine, (*S,E*)-11-[2-4-(4-formylphenyl)morpholine methylene hydrazono] pyrrolo [2,1-c] [1,4] benzodiazepine, (*S,E*)-11-[2-(4-ethylphenyl) methylene hydrazono] pyrrolo [2,1-c] [1,4] benzodiazepine, (*S,E*)-11-[2-(4-pyridine) methylene hydrazono] pyrrolo [2,1-c] [1,4] benzodiazepine and (*S,E*)-11- [2-(indole) methylene hydrazono] pyrrolo [2,1-c] [1,4] benzodiazepine.

The highest inhibition growth for cancer cell was observed for CNS on cell line SNB-75 with compound **4b** at 25.0% followed by compound **4a** at 20.90%. Low inhibition was observed for the rest of the compounds on the cancer cells which was less than 20%. Results from the enzyme kinetics showed that compound **4d** has a good inhibition on TEM-1 at 49.8%. This shows that compound **4d** has the best potentials of being non-β-lactam β-lactamase inhibitor on TEM-1 of the serine lactamase class A. This is because it had a better interaction with the active site residue of the enzyme. There was no significant inhibition on the AmpC lactamase that was tested on the compounds also a specific test of compound **4d** on lactamase P99 did not also show any significant inhibition. The poor inhibitory activities of other PBD derivatives could have been because of poor solubility of the compounds in the solvent that was used. Another reason

for the poor enzyme inhibition result could also be attributed to the bulkiness of the PBD derivatives so the active site of the enzyme was unavailable for better interaction with the ligand.

The cannabinoid receptors CB_1 and CB_2 are have become a vital subject for research in a variety of neurological and immunological processes. With CB_1 expressing predominately in the brain and peripheral neurons, and CB_2 expressing in the immune cells, preliminary results of cannabinoid binding activity showed that compound **4a** showed high selective binding to CB_2 at 77.4% than CB1 at 46.8%. however, to determine whether to the binding of the ligand to the receptor is agonist or antagonist is in the pipeline. This could be a promising ligand for the cannabinoid receptor in the future.

Future Work

We will focus on evaluating the cannabinoid binding receptor activity for the rest of the compounds synthesized. Compound **4a** had a good binding affinity to CB_2, which could be due to an activating group attached to PBD hydrazone, which had a better interaction with G-couple proteins of the cannabinoid receptor. It will be interesting to know how the other derivatives of the PBD which has deactivating, and bulky groups will interact with cannabinoid receptors to establish structure-activity relationship. We will also focus on introducing functional groups on the PBD rings to improve the solubility of the PBD analogs for better interactions with the enzymes. Other substituents that are biologically active including thiophene will be added to PBD hydrazone.

REFERENCES

(1) Pettersson, B. *Synthetic Studies towards 7-and 8-Membered N-Heterocycles, Particularly 1, 4-Pyrrolobenzodiazepines: Total Synthesis of Fuligocandin A and B*; Inst för biovetenskaper och näringslära/Dept of Biosciences and Nutrition, 2011.

(2) Khatoon, S. A Novel Histological Approach for Identification of Alkaloid Bearing Plants. *Int. J. Bot.* **2017**, *13*, 28–36.

(3) Brazhnikova, M. G.; Konstantinova, N. V; Mesentsev, A. S. Sibiromycin: Isolation and Characterization. *J. Antibiot. (Tokyo).* **1972**, *25* (11), 668–673.

(4) Leimgruber, W.; Stefanović, V.; Schenker, F.; Karr, A.; Berger, J. Isolation and Characterization of Anthramycin, a New Antitumor Antibiotic. *J. Am. Chem. Soc.* **1965**, *87* (24), 5791–5793.

(5) Thurston, D. E. Advances in the Study of Pyrrolo [2, 1-c][1, 4] Benzodiazepine (PBD) Antitumour Antibiotics. In *Molecular aspects of anticancer drug-DNA interactions*; Springer, 1993; pp 54–88.

(6) Arora, S. K. Structural Investigations of Mode of Action of Drugs. II. Molecular Structure of Anthramycin Methyl Ether Monohydrate. *Acta Crystallogr. Sect. B Struct. Crystallogr. Cryst. Chem.* **1979**, *35* (12), 2945–2948.

(7) Hurley, L. H.; Reck, T.; Thurston, D. E.; Langley, D. R.; Holden, K. G.; Hertzberg, R. P.; Hoover, J. R. E.; Gallagher Jr, G.; Faucette, L. F. Pyrrolo [1, 4] Benzodiazepine Antitumor Antibiotics: Relationship of DNA Alkylation and Sequence Specificity to the Biological Activity of Natural and Synthetic Compounds. *Chem. Res. Toxicol.* **1988**, *1* (5), 258–268.

(8) Fotso, S.; Zabriskie, T. M.; Proteau, P. J.; Flatt, P. M.; Santosa, D. A.; Sulastri; Mahmud,

T. Limazepines A− F, Pyrrolo [1, 4] Benzodiazepine Antibiotics from an Indonesian Micrococcus Sp. *J. Nat. Prod.* **2009**, *72* (4), 690–695.

(9) Hu, W.-P.; Yu, H.-S.; Sung, P.-J.; Tsai, F.-Y.; Shen, Y.-K.; Chang, L.-S.; Wang, J.-J. DC-81-Indole Conjugate Agent Induces Mitochondria Mediated Apoptosis in Human Melanoma A375 Cells. *Chem. Res. Toxicol.* **2007**, *20* (6), 905–912.

(10) Varvounis, G. An Update on the Synthesis of Pyrrolo [1, 4] Benzodiazepines. *Molecules* **2016**, *21* (2), 154.

(11) Kamal, A.; Reddy, D. R.; Reddy, M. K.; Balakishan, G.; Shaik, T. B.; Chourasia, M.; Sastry, G. N. Remarkable Enhancement in the DNA-Binding Ability of C2-Fluoro Substituted Pyrrolo [2, 1-c][1, 4] Benzodiazepines and Their Anticancer Potential. *Bioorg. Med. Chem.* **2009**, *17* (4), 1557–1572.

(12) Sudhakar, A. History of Cancer, Ancient and Modern Treatment Methods. *J. Cancer Sci. Ther.* **2009**, *1* (2), 1.

(13) Pudata, V.; v, S. V. A Short Note on Cancer. *J. Carcinog. Mutagen.* **2012**, *02* (04), 2–7. https://doi.org/10.4172/2157-2518.1000128.

(14) Marijani, R.; Abonyo, O. B. CTP: Phosphocholine Cytidyltransferase Alpha (CCTα) SiRNA Induce Cell Death of Lung Cancer Cells. *Pharm. Anal. Acta2* **2011**.

(15) Khan, D. R. The Use of Nanocarriers for Drug Delivery in Cancer Therapy. *J Cancer Sci Ther* **2010**, *2* (3), 58–62.

(16) Miyazaki, Y.; Kikuchi, K.; González-Alva, P.; Inoue, H.; Noguchi, Y.; Tsuchiya, H.; Hayashi, J.; Shin, K.; Ochiai, K.; Kusama, K. Association of Butyric Acid Produced by Periodontopathic Bacteria with Progression of Oral Cancer. *J Cancer Sci Ther* **2010**, *2* (2), 26–32.

(17) Goel, S.; Khorate, M.; Nahar, P.; Ahmed, J. Cheilitis Granulomatosa-An Uncommon Clinicopathological Entity: A Case Report. *J Cancer Sci Ther* **2010**, *2* (4), 86–88.

(18) Hsieh, C.-L.; Wang, H.-E.; Ker, Y.-B.; Peng, C.-C.; Chen, K.-C.; Peng, R. Y. GC/MS Determination of N-Butyl-N-(3-Carboxypropyl) Nitrosamine (BCPN) in Bladder Cancers: The Skewed Molecular Interaction Caused Retention Time Shift. *J Anal Bioanal Tech.* **2011**, *2* (1).

(19) Bassett, J. C.; Gore, J. L.; Chi, A. C.; Kwan, L.; McCarthy, W.; Chamie, K.; Saigal, C. S. Impact of a Bladder Cancer Diagnosis on Smoking Behavior. *J Clin Oncol* **2012**, *30* (15), 1871–1878.

(20) Pusztaszeri, M.; Soccal, P. M.; Mach, N.; Pache, J.; Mc Kee, T. Cytopathological Diagnosis of Non Small Cell Lung Cancer: Recent Advances Including Rapid on-Site Evaluation, Novel Endoscopic Techniques and Molecular Tests. *J Pulm. Respir. Med S* **2012**, *5*, 2.

(21) Akasbi, Y.; Arifi, S.; Ousadden, A.; Tizniti, S.; Amarti, A.; Ait, K.; Mesbahi, O. E. L. Cancer Science & Therapy Complete Pathologic Response in Advanced Primary Gastric Signet-Ring Cell Carcinoma : A Case Report. **2011**, *3* (4), 76–78. https://doi.org/10.4172/1948-5956.1000062.

(22) Christian, P.; Vanover, J.; Scott, T.; Tullo, G.; D'Orazio, J. A. Epidermal Pigmentation, Nucleotide Excision Repair and Risk of Skin Cancer. *J Carcinog. Mutagen. S* **2011**, *4*, 18–21.

(23) Bali, A.; Singh, M. P.; Padmavathi, K. M.; Ahmed, J. Malignant Fibrous Histiocytoma: An Unusual Transformation from Benign to Malignant. *J Cancer Sci Ther* **2010**, *2*, 53–57.

(24) Lau, G. S. K.; Chan, J. Y. W.; Wei, W. I. Role of Surgery in the Treatment of Radiation-

Induced Sarcomas of the Head and Neck. *J. Cell Sci. Ther.* **2011**.

(25) Onizuka, S.; Yonaha, T.; Tsuneyoshi, I. Local Anesthetics with High Lipophilicity Are Toxic, While Local Anesthetics with Low Pka Induce More Apoptosis in Human Leukemia Cells. *J Anesth Clin Res* **2011**, *2* (1), 1–5.

(26) Evans, S.; Moieni, M.; Subramanian, S.; Tsao, J. C. I.; Sternlieb, B.; Zeltzer, L. K. "Now I See a Brighter Day": Expectations and Perceived Benefits of an Iyengar Yoga Intervention for Young Patients with Rheumatoid Arthritis. *J. Yoga Phys. Ther.* **2011**, *1* (101).

(27) Karatepe, O.; Kokdas, S.; Kamali, S.; Aydın, T.; Kemik, A. Th e Comparison between Laparoscopic vs. Open Surgery for Trinitrobenzen e Sulfonic Acid-Induced Rat Colitis. *J Cytol Histol* **2010**, *1*, 109.

(28) Nucl, J.; Radiat, M.; Gill, R. S.; Whitlock, K.; Al-adra, D. P.; Schiller, D.; Bigam, D. L. Nuclear Medicine & Radiation Therapy Hepatic Resection for Colorectal Liver Metastases and the Role of Positron Emission Tomography Imaging. **2011**, 2–5. https://doi.org/10.4172/2155-9619.S2-001.

(29) Lu, C.; Xin, Y.; Xu, Y.; Zhao, Z.; Fu, J. Luteolin Sensitizes Fas/FasL–induced Apoptosis in HepG2 Cells through Inhibiting Akt Activation and Promoting XIAP Degradation. *J Carcinog. Mutagen.* **2011**, *2*, 121.

(30) Abdel Ghany, S. M.; El Melegy, N. T.; Mohamed-Hussein, A. A. R.; Hana, R. S. Emerging Prognostic Biomarkers in Non Small Cell Lung Cancer Patients: Impact of Treatment with Nimesulide (COX-2 Inhibitor) Combined with Chemotherapy. *J Pulm. Respir. Med S* **2011**, *5*, 2.

(31) Aljarrah, K.; Pawlickj, T.; Niemierko, A. A Clinical Study of MLC-Based IMTT Lung

Dose Calculation Accuracy on Plan Evaluation Parameters. *J Cancer Sci Ther* **2010**, *2* (3), 74.

(32) Wagner, D.; Vorwerk, H. Treatment Couch Modeling in the Treatment Planning System Eclipse. *J Cancer Sci Ther* **2011**, *3* (1), 188–193.

(33) Shaghayegh, K.; Mahdi, A.; Ali, K. Larynx Preserving Treatments in the Early and Advanced Laryngeal Cancers; a Retrospective Analysis. *J Cancer Sci Ther* **2010**, *1*, 8–10.

(34) Kamal, A.; Reddy, M. K.; Ramaiah, M. J.; Reddy, J. S.; Srikanth, Y. V. V; Dastagiri, D.; Bharathi, E. V.; Pushpavalli, S.; Sarma, P.; Pal-Bhadra, M. Synthesis and Biological Evaluation of Estradiol Linked Pyrrolo [2, 1-c][1, 4] Benzodiazepine (PBD) Conjugates as Potential Anticancer Agents. *Bioorg. Med. Chem.* **2011**, *19* (8), 2565–2581.

(35) Annor-Gyamfi, J. K.; Jarrett, J. M.; Osazee, J. O.; Bialonska, D.; Whitted, C.; Palau, V. E.; Shilabin, A. G. Synthesis and Biological Activity of Fused Tetracyclic Pyrrolo [2, 1-c][1, 4] Benzodiazepines. *Heliyon* **2018**, *4* (2), e00539.

(36) Zervosen, A.; Sauvage, E.; Frère, J.-M.; Charlier, P.; Luxen, A. Development of New Drugs for an Old Target—the Penicillin Binding Proteins. *Molecules* **2012**, *17* (11), 12478–12505.

(37) Nogrady, T.; Weaver, D. F. *Medicinal Chemistry: A Molecular and Biochemical Approach*; Oxford University Press, 2005.

(38) Lader, M.; Tylee, A.; Donoghue, J. Withdrawing Benzodiazepines in Primary Care. **2009**, *23* (1), 19–34.

(39) Wink, M. Ecological Role of Alkaloids in Modern Alkaloids: Structure, Isolation. *Synth. Biol. Wiley, Weinheim* **2008**.

(40) Chadha, S.; Paul, S.; Kapoor, K. K. Journal of Chemical and Pharmaceutical Research.

2011, *3* (2), 331–340.

(41) Grossi, G.; Di Braccio, M.; Roma, G.; Ballabeni, V.; Tognolini, M.; Calcina, F.; Barocelli, E. 1, 5-Benzodiazepines: Part XIII. Substituted 4H-[1, 2, 4] Triazolo [4, 3-a][1, 5] Benzodiazepin-5-Amines and 4H-Imidazo [1, 2-a][1, 5] Benzodiazepin-5-Amines as Analgesic, Anti-Inflammatory and/or Antipyretic Agents with Low Acute Toxicity. *Eur. J. Med. Chem.* **2002**, *37* (12), 933–944.

(42) Dourlat, J.; Liu, W.-Q.; Gresh, N.; Garbay, C. Novel 1, 4-Benzodiazepine Derivatives with Antiproliferative Properties on Tumor Cell Lines. *Bioorg. Med. Chem. Lett.* **2007**, *17* (9), 2527–2530.

(43) Hsiao, G.; Shen, M.-Y.; Chou, D.-S.; Chang, Y.; Lee, L.-W.; Lin, C.-H.; Sheu, J.-R. Mechanisms of Antiplatelet and Antithrombotic Activity of Midazolam in in Vitro and in Vivo Studies. *Eur. J. Pharmacol.* **2004**, *487* (1–3), 159–166.

(44) Xia, J.; Li, J.; Sun, H. Insights into ET A Subtype Selectivity of Benzodiazepine Endothelin Receptor Antagonists by 3D-QSAR Approaches. *J. Mol. Model.* **2012**, *18* (4), 1299–1311.

(45) Bell, S. C.; Childress, S. J. A Rearrangement of 5-Aryl-1, 3-Dihydro-2H-1, 4-Benzodiazepine-2-One 4-Oxides1. *J. Org. Chem.* **1962**, *27* (5), 1691–1695.

(46) Sternbach, L. H.; Reeder, E. Quinazolines and 1, 4-Benzodiazepines. IV. 1, 2 Transformations of 7-Chloro-2-Methylamino-5-Phenyl-3H-1, 4-Benzodiazepine 4-Oxide3. *J. Org. Chem.* **1961**, *26* (12), 4936–4941.

(47) Hurley, L. H.; Allen, C. S.; Feola, J. M.; Lubawy, W. C. In Vitro and in Vivo Stability of Anthramycin-DNA Conjugate and Its Potential Application as an Anthramycin Prodrug. *Cancer Res.* **1979**, *39* (8), 3134–3140.

(48) Siegel, R.; Ward, E.; Brawley, O.; Jemal, A. Cancer Statistics, 2011: The Impact of Eliminating Socioeconomic and Racial Disparities on Premature Cancer Deaths. *CA. Cancer J. Clin.* **2011**, *61* (4), 212–236.

(49) Rosenberg, S. A.; De_Vita, V. T.; Lawrence, T. S. *DeVita, Hellman, and Rosenberg's Cancer: Principles & Practice of Oncology*; Lippincott, Williams & Wilkins, 2015.

(50) Rice, L. B. Federal Funding for the Study of Antimicrobial Resistance in Nosocomial Pathogens: No ESKAPE. The University of Chicago Press 2008.

(51) Thurston, D. E.; Hurley, L. A Rational Basis for Development of Antitumor Agents in the Pyrrolo [1, 4] Benzodiazepine Group. *Drugs Future* **1983**, *8* (11), 957–971.

(52) Kaneko, T.; Wong, H.; Doyle, T. W.; Rose, W. C.; Bradner, W. T. Bicyclic and Tricyclic Analogs of Anthramycin. *J. Med. Chem.* **1985**, *28* (3), 388–392.

(53) Shoemaker, R. H. The NCI 60 Human Tumor Cell Line Screen: An Information-Rich Screen Informing on Mechanisms of Toxicity. In *in vitro cellular & Developmetal Biology-Animal*; Society in vitro Biology 514 Daniel Street, Ste 411, ralleigh, NC 27605 USA, 2006; Vol. 42, p 5A–5A.

(54) Abraham, E. P.; Chain, E. An Enzyme from Bacteria Able to Destroy Penicillin. *Nature* **1940**, *146* (3713), 837.

(55) Abraham, E. P.; Chain, E.; Fletcher, C. M.; Gardner, A. D.; Heatley, N. G.; Jennings, M. A.; Florey, H. W. Further Observations on Penicillin. *Lancet* **1941**, *238* (6155), 177–189.

(56) Bush, K.; Bradford, P. A. β-Lactamases: Historical Perspectives. In *Enzyme-Mediated Resistance to Antibiotics*; American Society of Microbiology, 2007; pp 67–79.

(57) Kirby, W. M. M. Extraction of a Highly Potent Penicillin Inactivator from Penicillin Resistant Staphylococci. *Science (80-.).* **1944**, *99* (2579), 452–453.

(58) Perez, F.; Endimiani, A. Hujer, MK, Bonomo, AR. *Contin. Chall. esBLs. curr opin pharmacol* **2007**, *7*, 459–469.

(59) Ambler, R. P.; Coulson, A. F.; Frere, J.-M.; Ghuysen, J.-M.; Joris, B.; Forsman, M.; Levesque, R. C.; Tiraby, G.; Waley, S. G. A Standard Numbering Scheme for the Class A Beta-Lactamases. *Biochem. J.* **1991**, *276* (Pt 1), 269.

(60) Bush, K.; Jacoby, G. A.; Medeiros, A. A. A Functional Classification Scheme for Beta-Lactamases and Its Correlation with Molecular Structure. *Antimicrob. Agents Chemother.* **1995**, *39* (6), 1211.

(61) Bush, K. Metallo-β-Lactamases: A Class Apart. *Clin. Infect. Dis.* **1998**, *27* (Supplement_1), S48–S53.

(62) Papp-Wallace, K. M.; Bethel, C. R.; Distler, A. M.; Kasuboski, C.; Taracila, M.; Bonomo, R. A. Inhibitor Resistance in the KPC-2 β-Lactamase, a Preeminent Property of This Class A β-Lactamase. *Antimicrob. Agents Chemother.* **2010**, *54* (2), 890–897.

(63) Jacoby, G. A.; Munoz-price, L. S. The New. **2005**, 380–391.

(64) Rice, L. B.; Eckstein, E. C.; DeVente, J.; Shlaes, D. M. Ceftazidime-Resistant Klebsiella Pneumoniae Isolates Recovered at the Cleveland Department of Veterans Affairs Medical Center. *Clin. Infect. Dis.* **1996**, *23* (1), 118–124.

(65) Walsh, T. R.; Toleman, M. A.; Poirel, L.; Nordmann, P. Metallo-β-Lactamases: The Quiet before the Storm? *Clin. Microbiol. Rev.* **2005**, *18* (2), 306–325.

(66) Bonomo, R. A.; Tolmasky, M. Enzyme-Mediated Resistance to Antibiotics: Mechanisms, Dissemination, and Prospects for Inhibition. *Enzym. Resist. to Antibiot. Mech. dissemination, Prospect. Inhib.* **2007**.

(67) Coleman, K. Diazabicyclooctanes (DBOs): A Potent New Class of Non-β-Lactam β-

Lactamase Inhibitors. *Curr. Opin. Microbiol.* **2011**, *14* (5), 550–555.

(68) Endimiani, A.; Choudhary, Y.; Bonomo, R. A. In Vitro Activity of NXL104 in Combination with β-Lactams against Klebsiella Pneumoniae Isolates Producing KPC Carbapenemases. *Antimicrob. Agents Chemother.* **2009**, *53* (8), 3599–3601.

(69) Stachyra, T.; Levasseur, P.; Péchereau, M.-C.; Girard, A.-M.; Claudon, M.; Miossec, C.; Black, M. T. In Vitro Activity of the β-Lactamase Inhibitor NXL104 against KPC-2 Carbapenemase and Enterobacteriaceae Expressing KPC Carbapenemases. *J. Antimicrob. Chemother.* **2009**, *64* (2), 326–329.

(70) Drawz, S. M.; Bonomo, R. A. Three Decades of β-Lactamase Inhibitors. *Clin. Microbiol. Rev.* **2010**, *23* (1), 160–201.

(71) Bebrone, C.; Lassaux, P.; Vercheval, L.; Sohier, J.-S.; Jehaes, A.; Sauvage, E.; Galleni, M. Current Challenges in Antimicrobial Chemotherapy. *Drugs* **2010**, *70* (6), 651–679.

(72) Pratt, R. F. β-Lactamase Inhibitors: Non-β-Lactams. **2012**.

(73) Pechenov, A.; Stefanova, M. E.; Nicholas, R. A.; Peddi, S.; Gutheil, W. G. Potential Transition State Analogue Inhibitors for the Penicillin-Binding Proteins. *Biochemistry* **2003**, *42* (2), 579–588.

(74) Bone, R.; Shenvi, A. B.; Kettner, C. A.; Agard, D. A. Serine Protease Mechanism: Structure of an Inhibitory Complex of. Alpha.-Lytic Protease and a Tightly Bound Peptide Boronic Acid. *Biochemistry* **1987**, *26* (24), 7609–7614.

(75) Lindquist, R. N.; Terry, C. Inhibition of Subtilisin by Boronic Acids, Potential Analogs of Tetrahedral Reaction Intermediates. *Arch. Biochem. Biophys.* **1974**, *160* (1), 135–144.

(76) Catalysis, O. F. Serine Proteases: Structure and Mechanism +949 of Catalysis. **1977**.

(77) Jungheim, L. N.; Ternansky, R. J. Non-ß-Lactam Mimics of ß-Lactam Antibiotics. In *The*

Chemistry of β-Lactams; Springer, 1992; pp 306–324.

(78) Baldwin, J. E.; Lynch, G. P.; Pitlik, J. γ-Lactam Analogues of β-Lactam Antibiotics. *J. Antibiot. (Tokyo).* **1991**, *44* (1), 1–24.

(79) Marchand-Brynaert, J.; Ghosez, L. Non β-Lactam Analogs of Penicillins and Cephalosporins. In *Recent Progress in the Chemical Synthesis of Antibiotics*; Springer, 1990; pp 727–794.

(80) Macheboeuf, P.; Contreras-Martel, C.; Job, V.; Dideberg, O.; Dessen, A. Penicillin Binding Proteins: Key Players in Bacterial Cell Cycle and Drug Resistance Processes. *FEMS Microbiol. Rev.* **2006**, *30* (5), 673–691.

(81) Lim, D.; Strynadka, N. C. J. Structural Basis for the β Lactam Resistance of PBP2a from Methicillin-Resistant Staphylococcus Aureus. *Nat. Struct. Mol. Biol.* **2002**, *9* (11), 870.

(82) Grant, E. B.; Guiadeen, D.; Baum, E. Z.; Foleno, B. D.; Jin, H.; Montenegro, D. A.; Nelson, E. A.; Bush, K.; Hlasta, D. J. The Synthesis and SAR of Rhodanines as Novel Class C β-Lactamase Inhibitors. *Bioorg. Med. Chem. Lett.* **2000**, *10* (19), 2179–2182.

(83) Miguet, L.; Zervosen, A.; Gerards, T.; Pasha, F. A.; Luxen, A.; Disteche-Nguyen, M.; Thomas, A. Discovery of New Inhibitors of Resistant Streptococcus Pneumoniae Penicillin Binding Protein (PBP) 2x by Structure-Based Virtual Screening. *J. Med. Chem.* **2009**, *52* (19), 5926–5936.

(84) Zervosen, A.; Lu, W.-P.; Chen, Z.; White, R. E.; Demuth, T. P.; Frère, J.-M. Interactions between Penicillin-Binding Proteins (PBPs) and Two Novel Classes of PBP Inhibitors, Arylalkylidene Rhodanines and Arylalkylidene Iminothiazolidin-4-Ones. *Antimicrob. Agents Chemother.* **2004**, *48* (3), 961–969.

(85) Turk, S.; Verlaine, O.; Gerards, T.; Živec, M.; Humljan, J.; Sosič, I.; Amoroso, A.;

Zervosen, A.; Luxen, A.; Joris, B. New Noncovalent Inhibitors of Penicillin-Binding Proteins from Penicillin-Resistant Bacteria. *PLoS One* **2011**, *6* (5), e19418.

(86) Phichith, D.; Bun, S.; Padiolleau-Lefevre, S.; Guellier, A.; Banh, S.; Galleni, M.; Frere, J.; Thomas, D.; Friboulet, A.; Avalle, B. Novel Peptide Inhibiting Both TEM-1 B-lactamase and Penicillin-binding Proteins. *FEBS J.* **2010**, *277* (23), 4965–4972.

(87) Shilabin, A. G.; Dzhekieva, L.; Misra, P.; Jayaram, B.; Pratt, R. F. 4-Quinolones as Noncovalent Inhibitors of High Molecular Mass Penicillin-Binding Proteins. *ACS Med. Chem. Lett.* **2012**, *3* (7), 592–595.

(88) Osazee, J. O. Molecular Docking, Synthesis and Evaluation of Pyrrolo [2, 1-c][1, 4] Benzodiazepines Derivatives as Non-β-Lactam β-Lactamases Inhibitors. **2016**.

(89) Freund, T. F.; Katona, I.; Piomelli, D. Role of Endogenous Cannabinoids in Synaptic Signaling. *Physiol. Rev.* **2003**, *83* (3), 1017–1066.

(90) Howlett, A. C.; Barth, F.; Bonner, T. I.; Cabral, G.; Casellas, P.; Devane, W. A.; Felder, C. C.; Herkenham, M.; Mackie, K.; Martin, B. R. International Union of Pharmacology. XXVII. Classification of Cannabinoid Receptors. *Pharmacol. Rev.* **2002**, *54* (2), 161–202.

(91) Mackie, K. Cannabinoid Receptors as Therapeutic Targets. *Annu. Rev. Pharmacol. Toxicol.* **2006**, *46*, 101–122.

(92) Tan, B.; Bradshaw, H. B.; Rimmerman, N.; Srinivasan, H.; Yu, Y. W.; Krey, J. F.; Monn, M. F.; Chen, J. S.-C.; Hu, S. S.-J.; Pickens, S. R. Targeted Lipidomics: Discovery of New Fatty Acyl Amides. *AAPS J.* **2006**, *8* (3), E461–E465.

(93) Alexander, S. P. H.; Kendall, D. A. The Complications of Promiscuity: Endocannabinoid Action and Metabolism. *Br. J. Pharmacol.* **2007**, *152* (5), 602–623.

(94) Basavarajappa, B. S. Critical Enzymes Involved in Endocannabinoid Metabolism. *Protein*

Pept. Lett. **2007**, *14* (3), 237–246.

(95) Okamoto, Y.; Wang, J.; Morishita, J.; Ueda, N. Biosynthetic Pathways of the Endocannabinoid Anandamide. *Chem. Biodivers.* **2007**, *4* (8), 1842–1857.

(96) Simon, G. M.; Cravatt, B. F. Endocannabinoid Biosynthesis Proceeding through Glycerophospho-N-Acyl Ethanolamine and a Role for α/β-Hydrolase 4 in This Pathway. *J. Biol. Chem.* **2006**, *281* (36), 26465–26472.

(97) Herkenham, M.; Lynn, A. B.; Johnson, M. R.; Melvin, L. S.; de Costa, B. R.; Rice, K. C. Characterization and Localization of Cannabinoid Receptors in Rat Brain: A Quantitative in Vitro Autoradiographic Study. *J. Neurosci.* **1991**, *11* (2), 563–583.

(98) Matsuda, L. A.; Lolait, S. J.; Brownstein, M. J.; Young, A. C.; Bonner, T. I. Structure of a Cannabinoid Receptor and Functional Expression of the Cloned CDNA. *Nature* **1990**, *346* (6284), 561.

(99) Munro, S.; Thomas, K. L.; Abu-Shaar, M. Molecular Characterization of a Peripheral Receptor for Cannabinoids. *Nature* **1993**, *365* (6441), 61.

(100) Pertwee, R. G. Pharmacology of Cannabinoid Receptor Ligands. *Curr. Med. Chem.* **1999**, *6*, 635–664.

(101) Di Marzo, V.; Melck, D.; Bisogno, T.; De Petrocellis, L. Endocannabinoids: Endogenous Cannabinoid Receptor Ligands with Neuromodulatory Action. *Trends Neurosci.* **1998**, *21* (12), 521–528.

(102) Pertwee, R. G. Pharmacology of Cannabinoid CB1 and CB2 Receptors. *Pharmacol. Ther.* **1997**, *74* (2), 129–180.

(103) Pertwee, R. G. Cannabinoid Receptors and Pain. *Prog. Neurobiol.* **2001**, *63* (5), 569–611.

(104) Chevaleyre, V.; Takahashi, K. A.; Castillo, P. E. Endocannabinoid-Mediated Synaptic

Plasticity in the CNS. *Annu. Rev. Neurosci.* **2006**, *29*, 37–76.

(105) Bacci, A.; Huguenard, J. R.; Prince, D. A. Long-Lasting Self-Inhibition of Neocortical Interneurons Mediated by Endocannabinoids. *Nature* **2004**, *431* (7006), 312.

(106) Mackie, K. Cannabinoid Receptors: Where They Are and What They Do. *J. Neuroendocrinol.* **2008**, *20*, 10–14.

(107) Berdyshev, E. V. Cannabinoid Receptors and the Regulation of Immune Response. *Chem. Phys. Lipids* **2000**, *108* (1–2), 169–190.

(108) Pertwee, R. G.; Ross, R. A. Cannabinoid Receptors and Their Ligands. *Prostaglandins, Leukot. Essent. Fat. Acids* **2002**, *66* (2–3), 101–121.

(109) Kamal, A.; Reddy, M. K.; Srivastava, A. K.; Srikanth, Y. V. V. Pyrrolobenzodiazepines as Sequence Selective DNA Binding Agents. In *Medicinal Chemistry and Drug Design*; IntechOpen, 2012.

(110) Annor-Gyamfi, J. K. Synthesis, Characterization and Biological Evaluation of Pyrrolo [2, 1-c][1, 4] Benzodiazepines for Cytotoxicity and Serine β-Lactamases Inhibition. **2016**.

(111) Prandi, C.; Blangetti, M.; Namdar, D.; Koltai, H. Structure-Activity Relationship of Cannabis Derived Compounds for the Treatment of Neuronal Activity-Related Diseases. *Molecules* **2018**, *23* (7), 1526.

(112) Gholipour Shilabin, A. Seven-Membered Ring Mesomeric Betaines. From Anti-Hückel Aromatics to Model Compounds of the Pyrrolobenzodiazepine Alkaloids Circumdatin A and B. 2005.

(113) Kamal, A. Enzymic Approach to the Synthesis of the Pyrrolo [1, 4] Benzodiazepine Antibiotics. *J. Org. Chem.* **1991**, *56* (6), 2237–2240.

(114) Wright Jr, W. B.; Brabander, H. J.; Greenblatt, E. N.; Day, I. P.; Hardy Jr, R. A.

Derivatives of 1, 2, 3, 11a-Tetrahydro-5H-Pyrrolo [2, 1-c][1, 4] Benzodiazepine-5, 11 (10H)-Dione as Anxiolytic Agents. *J. Med. Chem.* **1978**, *21* (10), 1087–1089.

(115) Gillard, A.; Foloppe, M.; Rault, S. Pyrrolo [2, 1-c][1, 4] Benzodiazepines. Synthesis of New Cyclic Amidines and Fused [a] Triazolo, Tetrazolo and Oxadiazolo Derivatives. *J. Heterocycl. Chem.* **1997**, *34* (2), 445–451.

(116) Shilabin, A. G.; Kasanah, N.; Wedge, D. E.; Hamann, M. T. Lysosome and HER3 (ErbB3) Selective Anticancer Agent Kahalalide F: Semisynthetic Modifications and Antifungal Lead-Exploration Studies. *J. Med. Chem.* **2007**, *50* (18), 4340–4350.

(117) Using, A.; David, A.; Data, P. P. United States Patent. **2005**, *2* (12).

(118) Shendage, D. M.; Fröhlich, R.; Haufe, G. Highly Efficient Stereoconservative Amidation and Deamidation of α-Amino Acids. *Org. Lett.* **2004**, *6* (21), 3675–3678.

(119) Anderson, E.; Carbery, D.; Coote, S.; De Meo, C.; Demchenko, A. *Science of Synthesis Knowledge Updates 2010*; Georg Thieme Verlag, 2014; Vol. 3.

APPENDICES

Appendix A1: ^{1}H NMR Spectrum for Compound **1** in DMSO-d_6

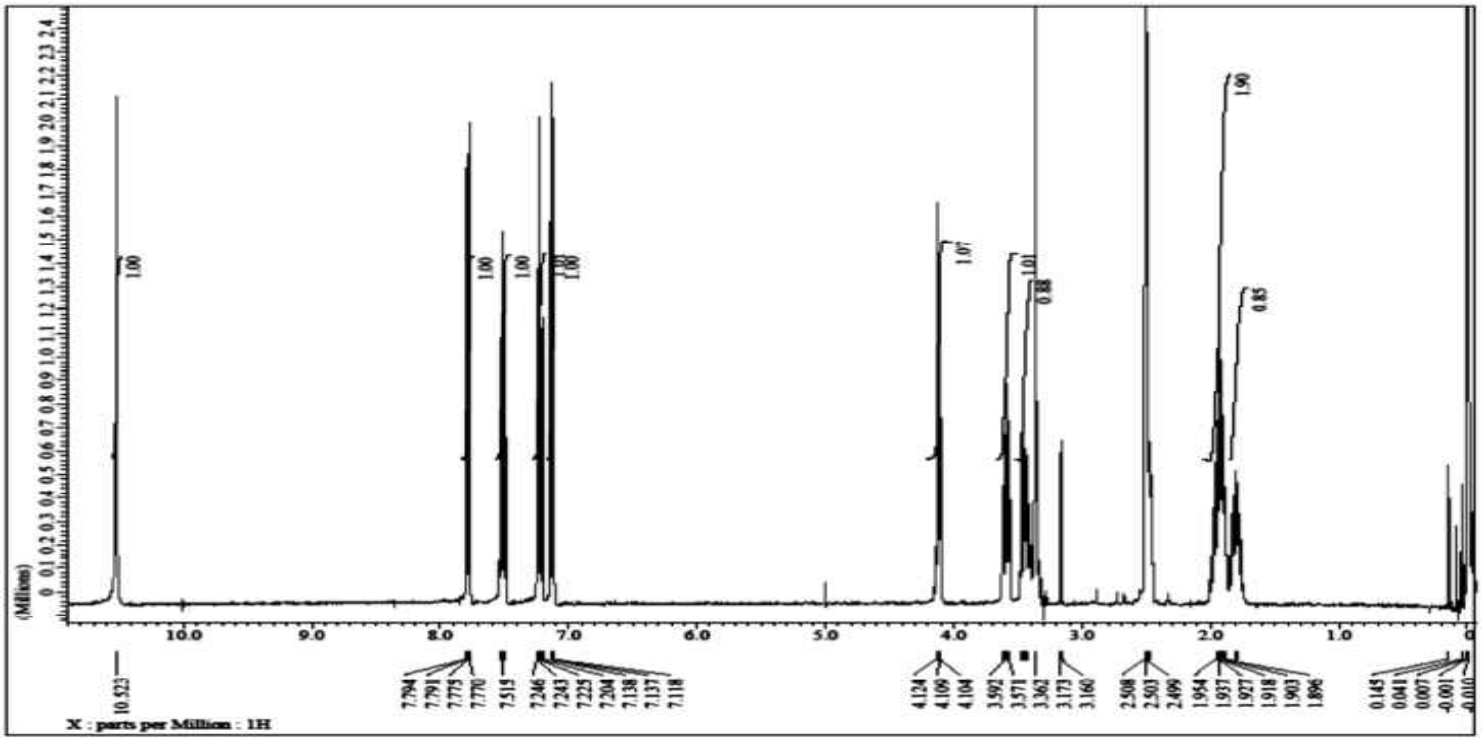

Appendix A2: ^{1}H NMR Spectrum for Compound **1** in DMSO-d_6

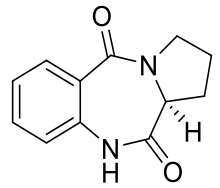

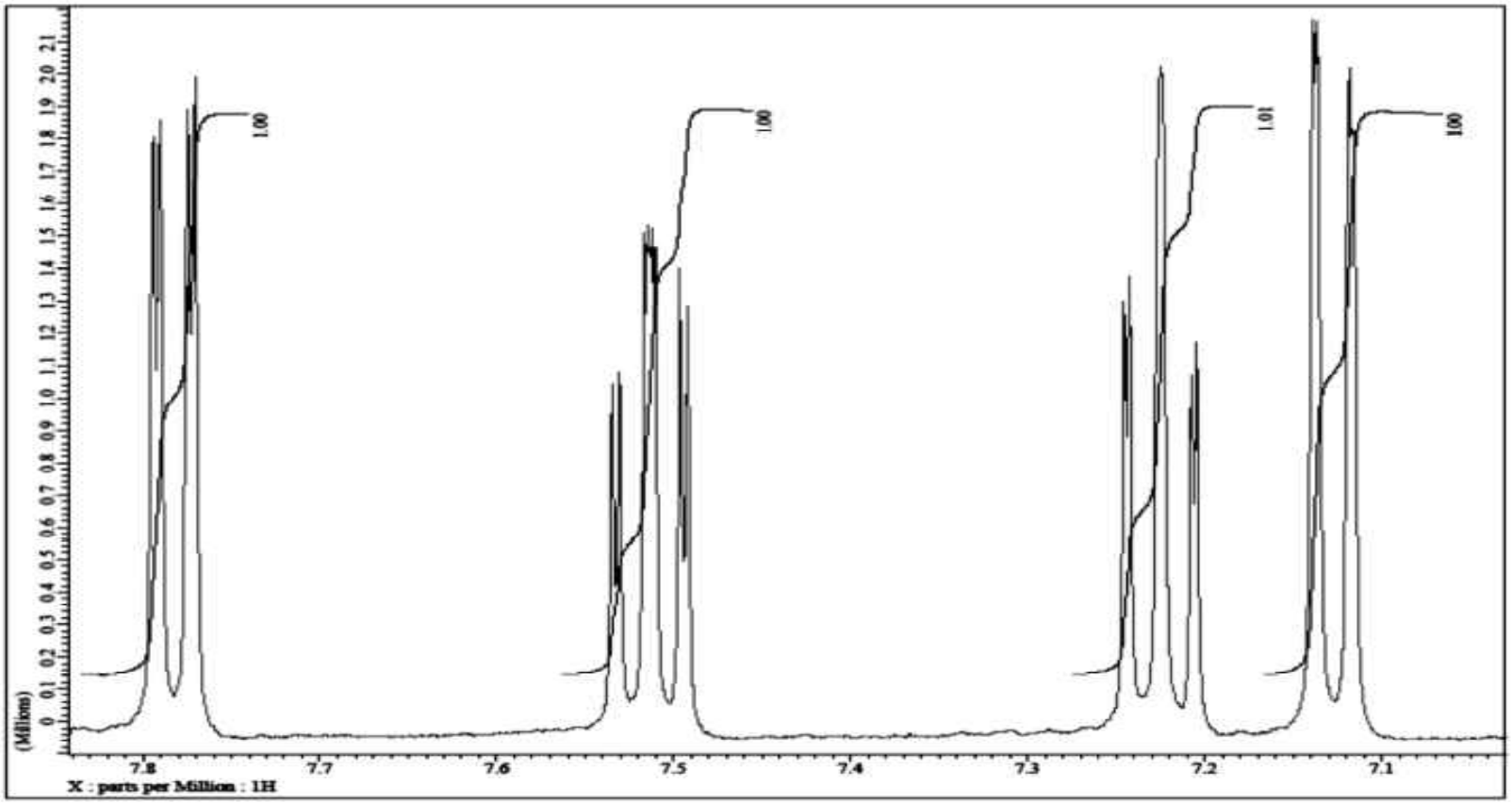

Appendix A3: ^{1}H NMR Spectrum for Compound **1** in DMSO-d_6

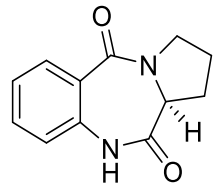

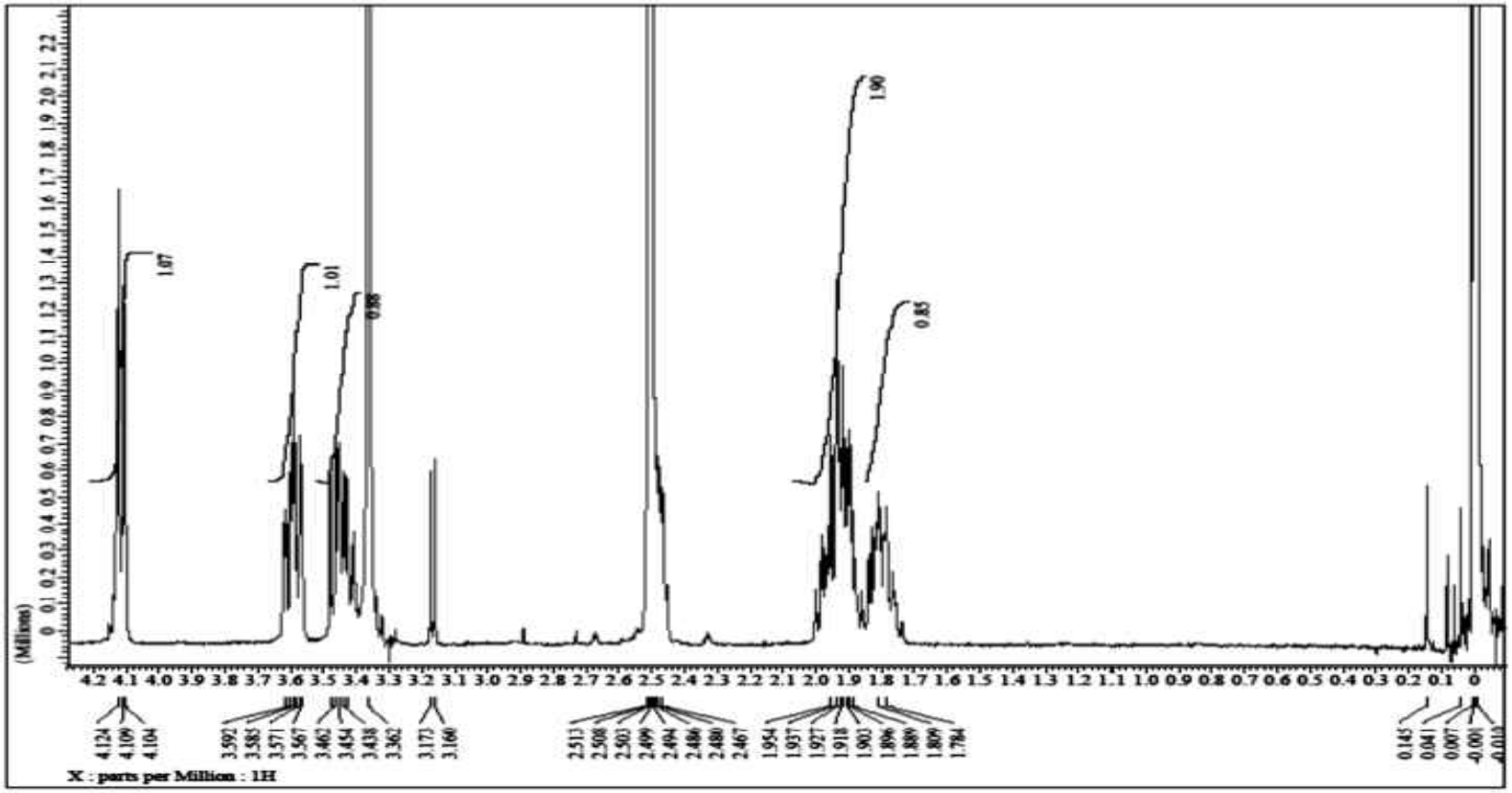

Appendix A4: ^{13}C NMR Spectrum for Compound **1** in DMSO-d_6

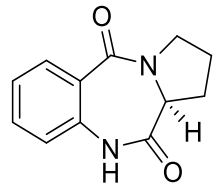

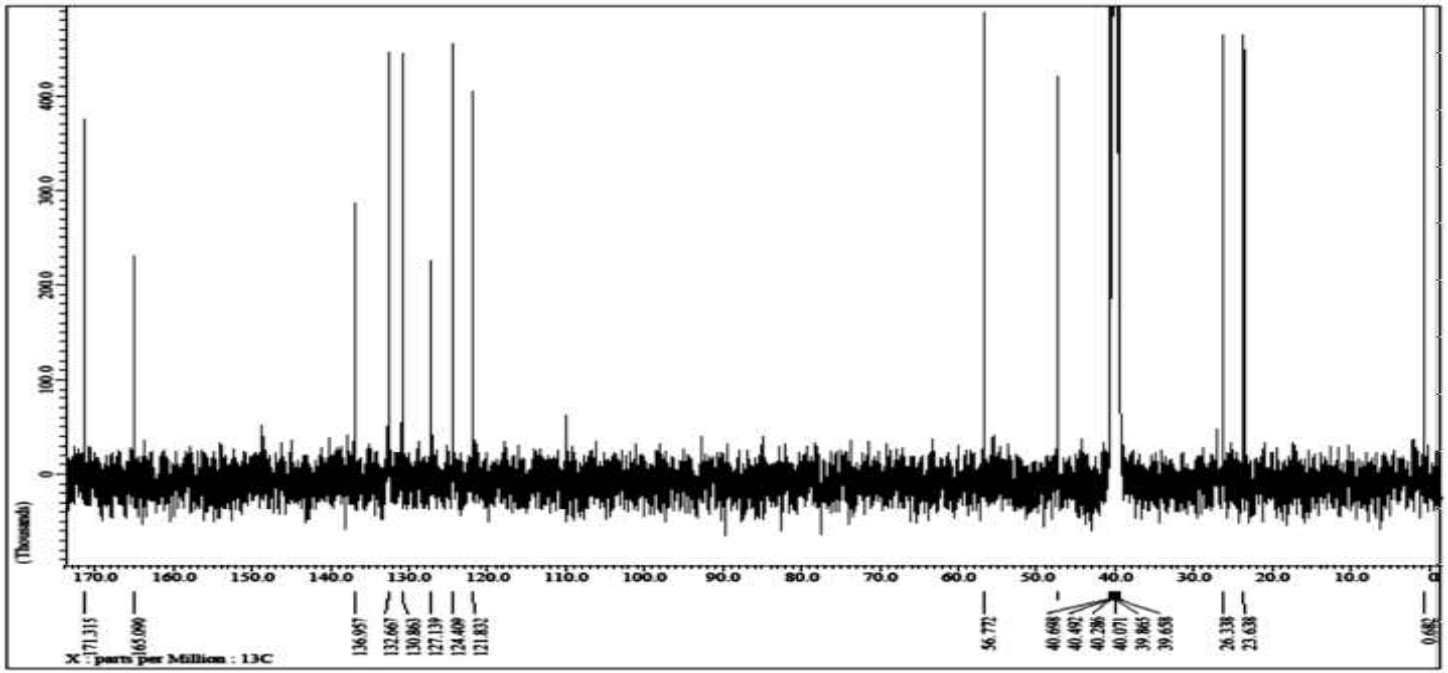

Appendix A5: C-DEPT-135 NMR Spectrum for Compound **1** in DMSO-d_6

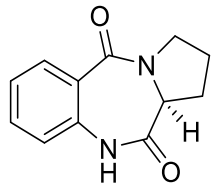

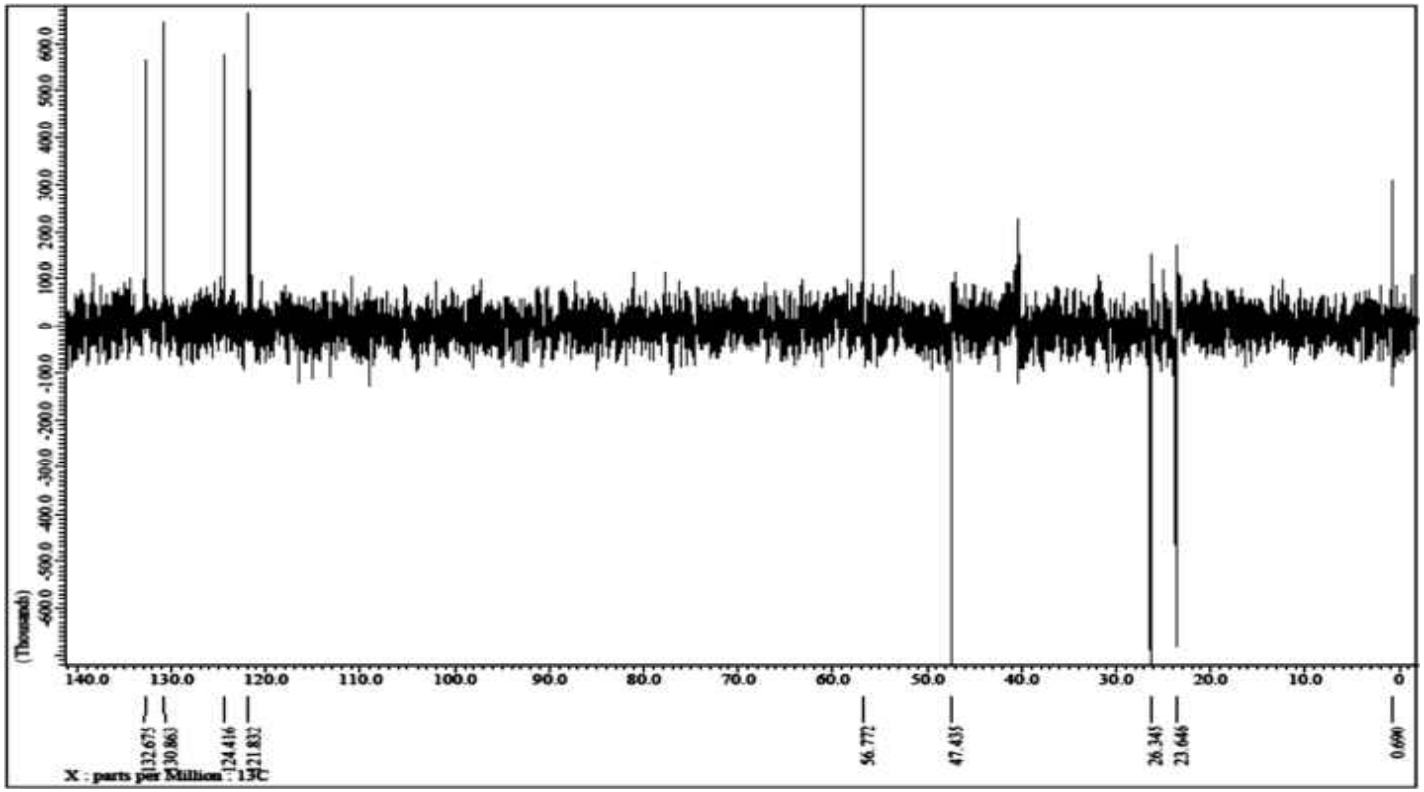

Appendix A6: GC-MS Spectrum for Compound **1**

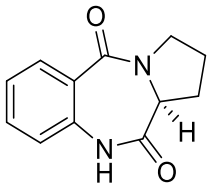

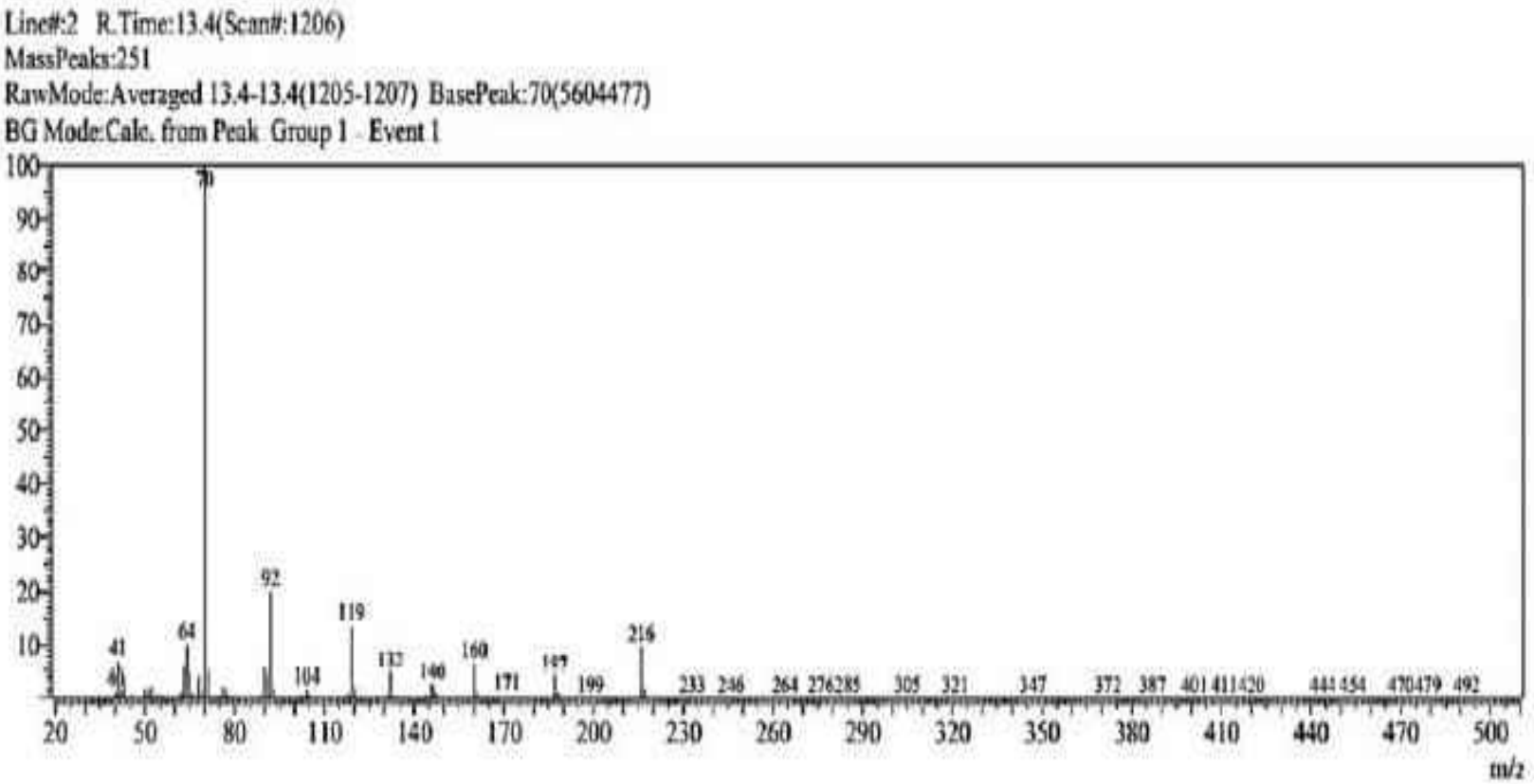

Appendix A7: IR Spectrum for Compound **1**

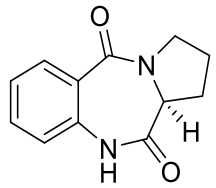

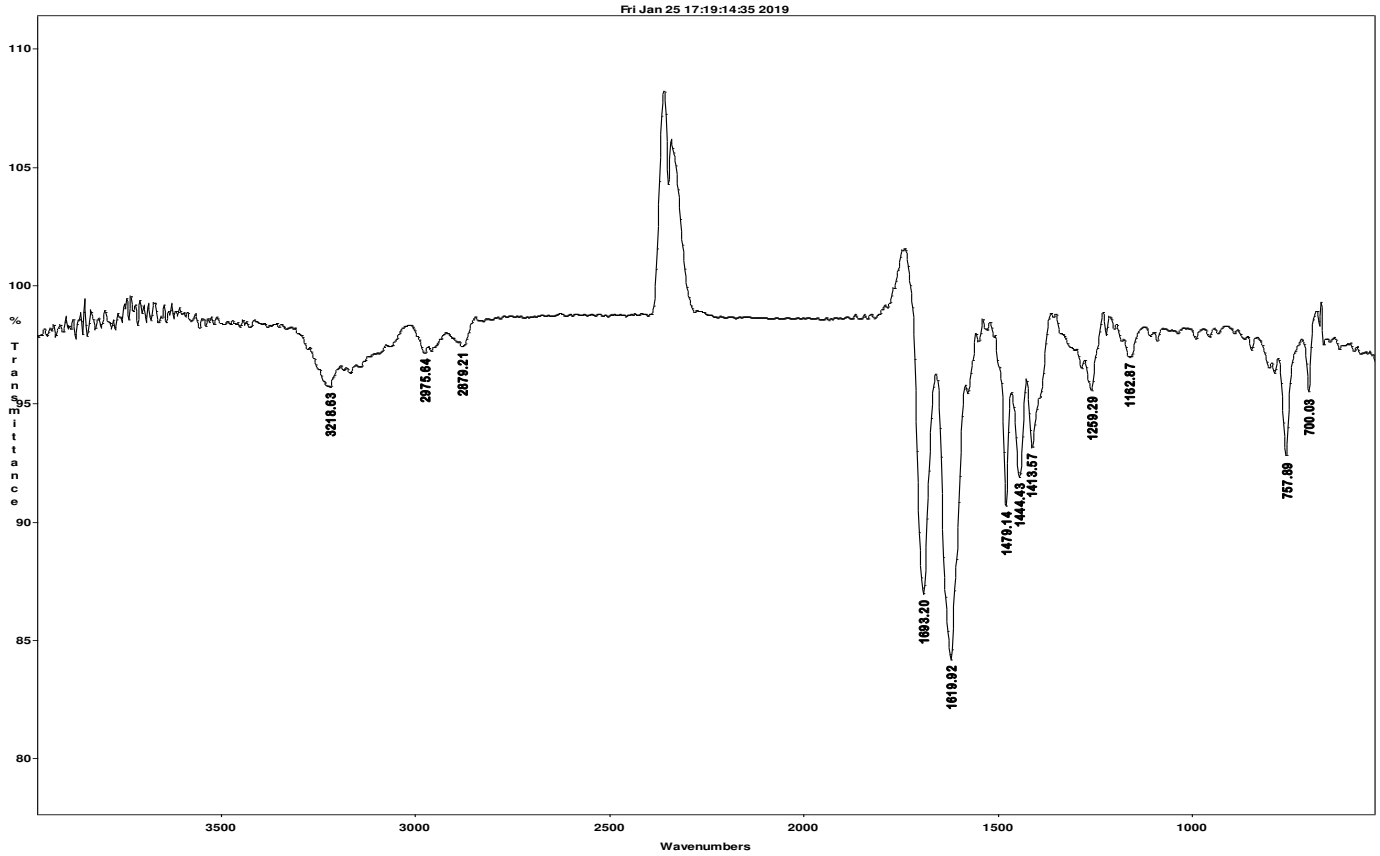

Appendix B1: ^{1}H NMR Spectrum for Compound 2 in DMSO-d_6

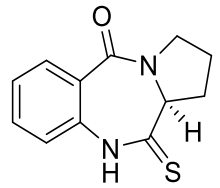

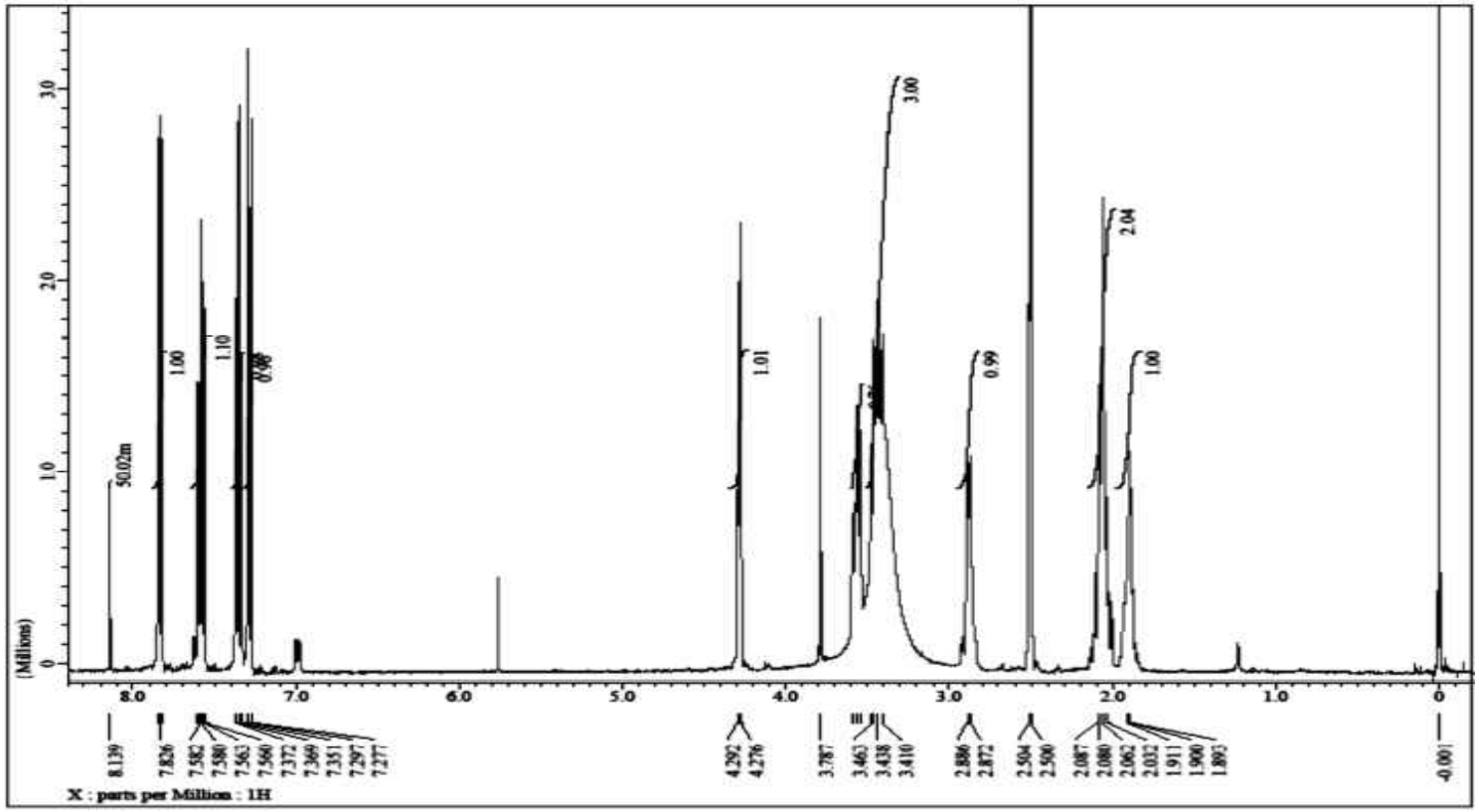

Appendix B2: ^{1}H NMR Spectrum for Compound **2** in DMSO-d_6

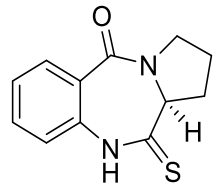

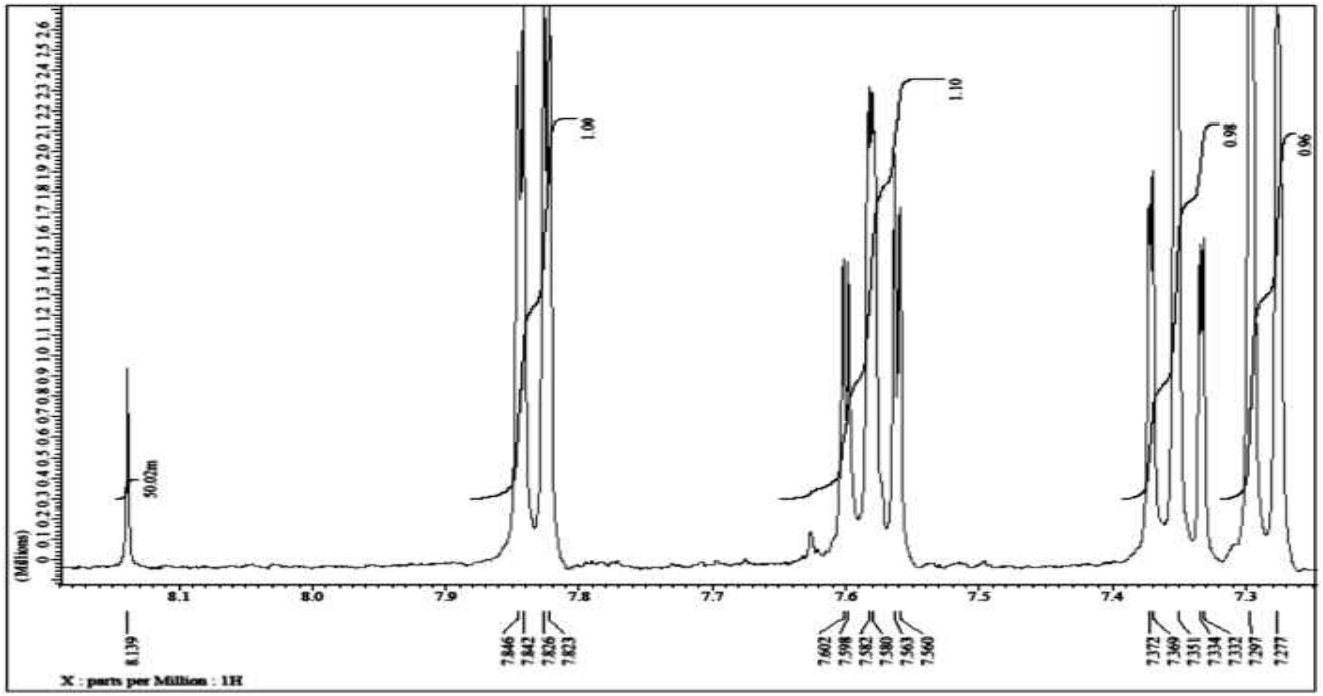

Appendix B3: ^{1}H NMR Spectrum for Compound **2** in DMSO-d_6

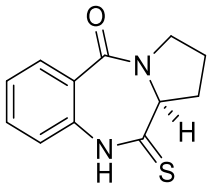

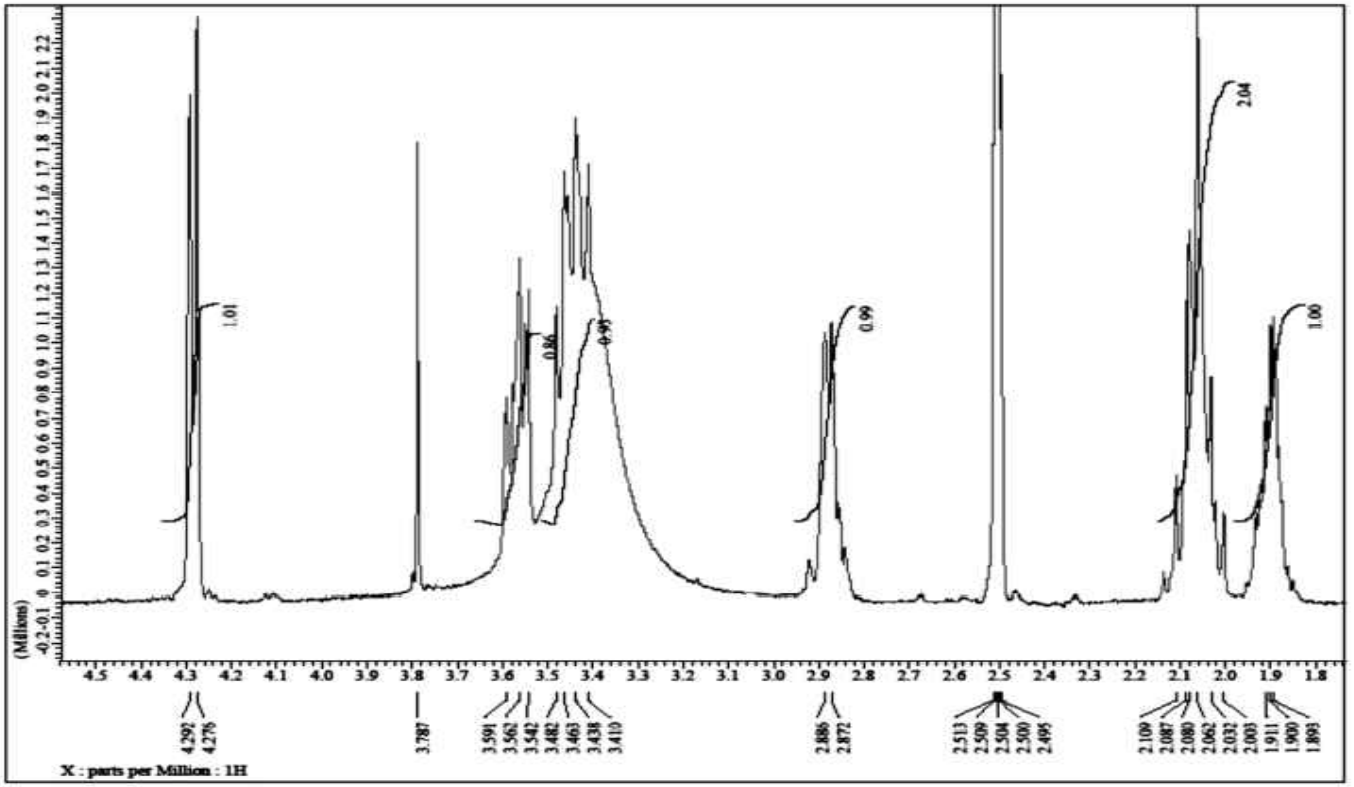

Appendix B4: ^{13}C NMR Spectrum for Compound **2** in DMSO-d_6

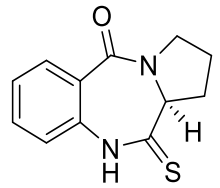

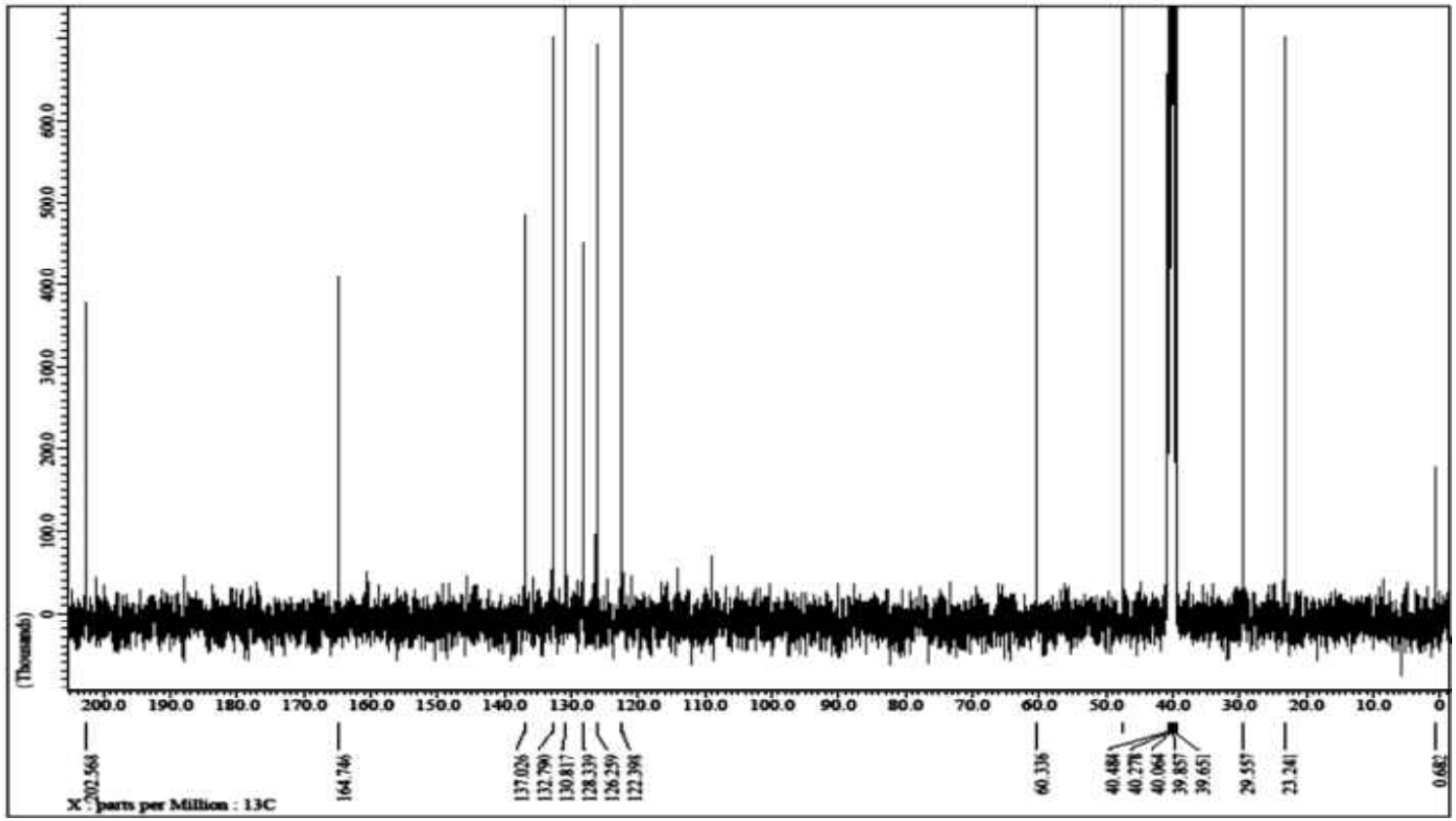

Appendix B5: C-DEPT-135 NMR Spectrum for Compound **2** in DMSO-d_6

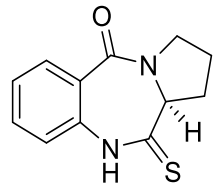

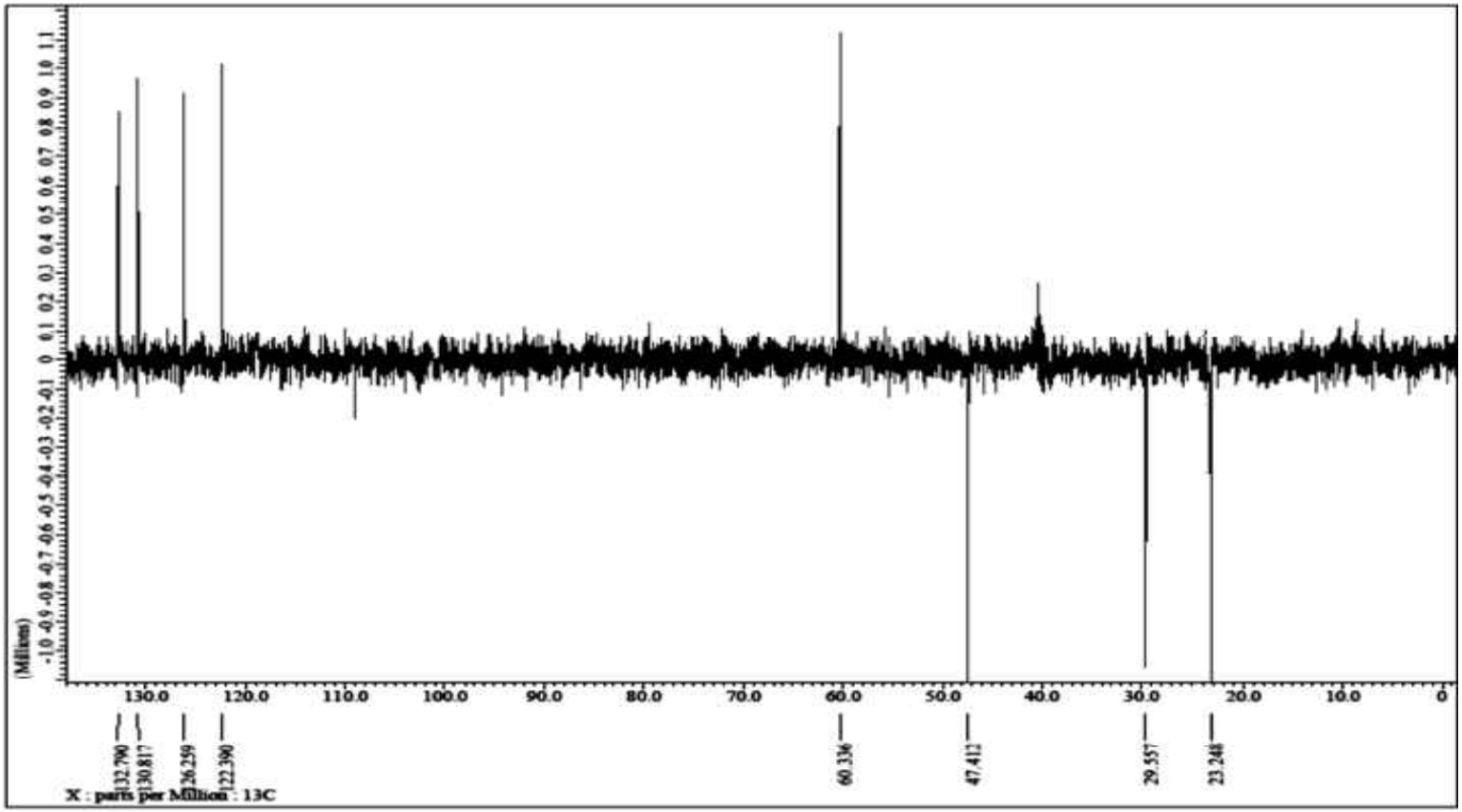

Appendix B6: GC-MS Spectrum for Compound **2**

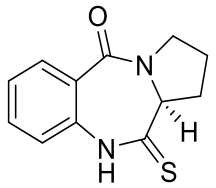

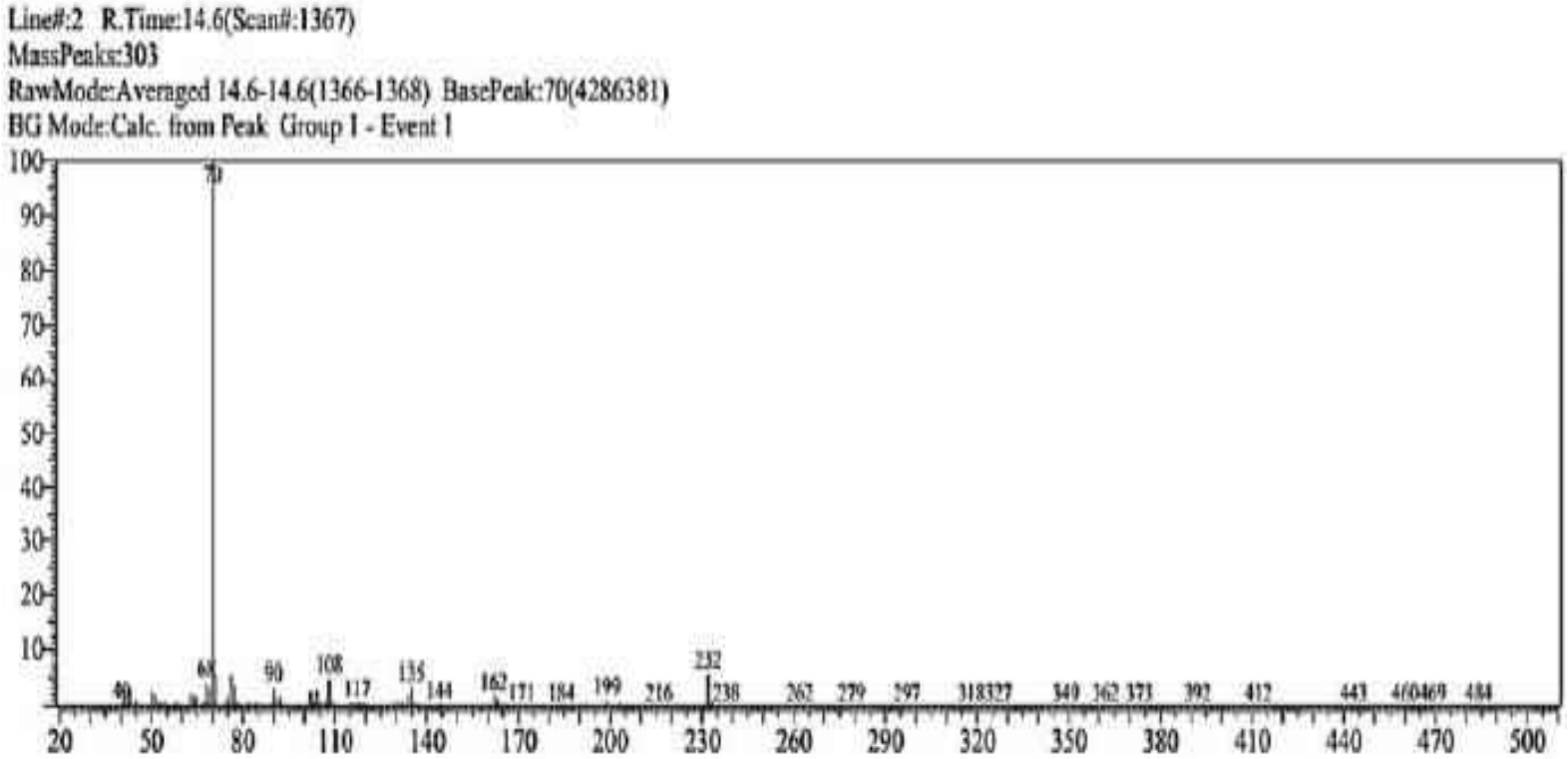

Appendix B7: IR Spectrum for Compound **2**

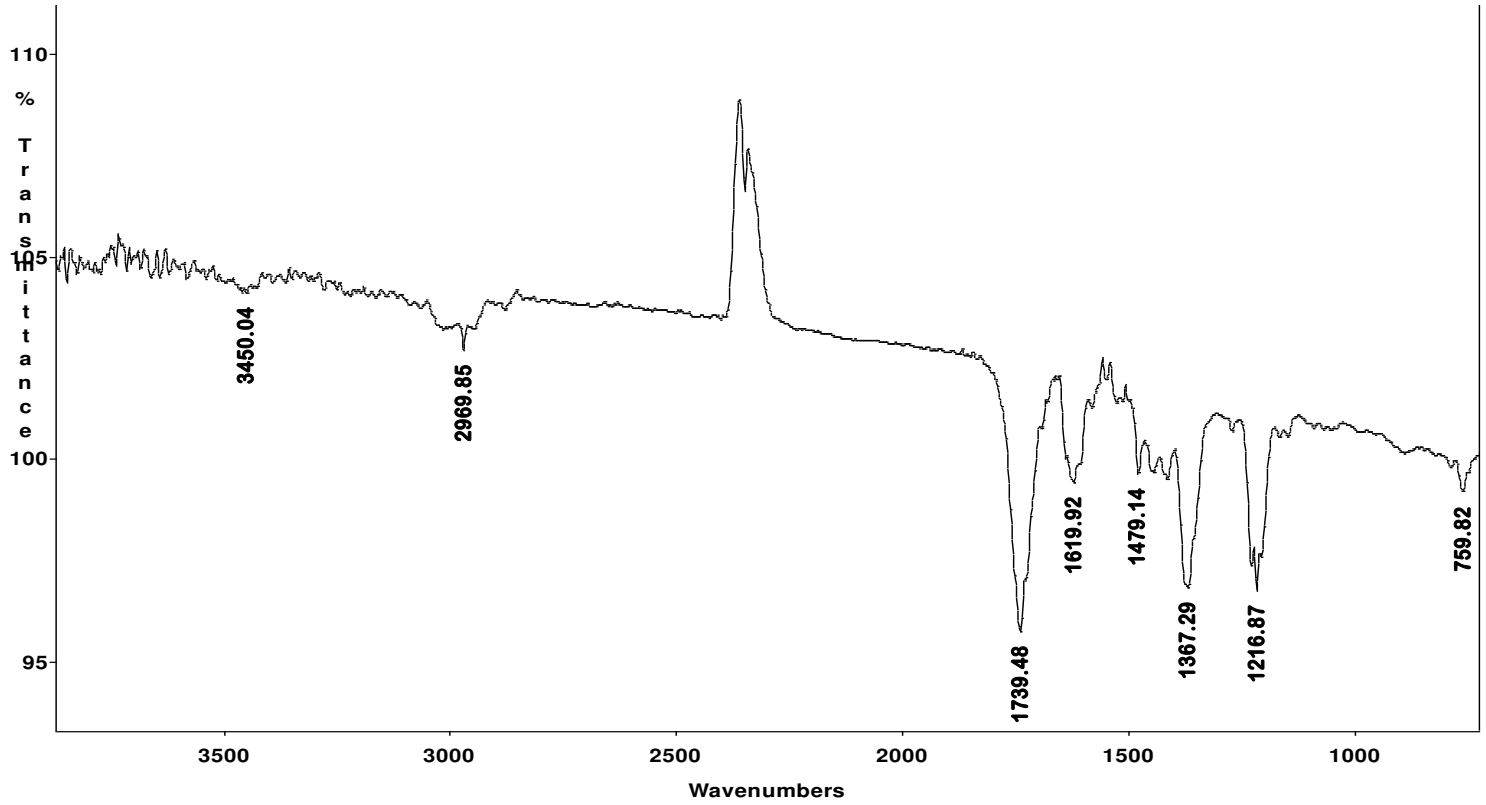

Appendix C1: ^{1}H NMR Spectrum for Compound **3** in $CDCl_3$

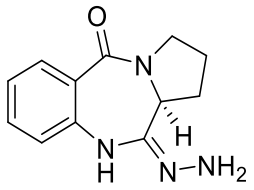

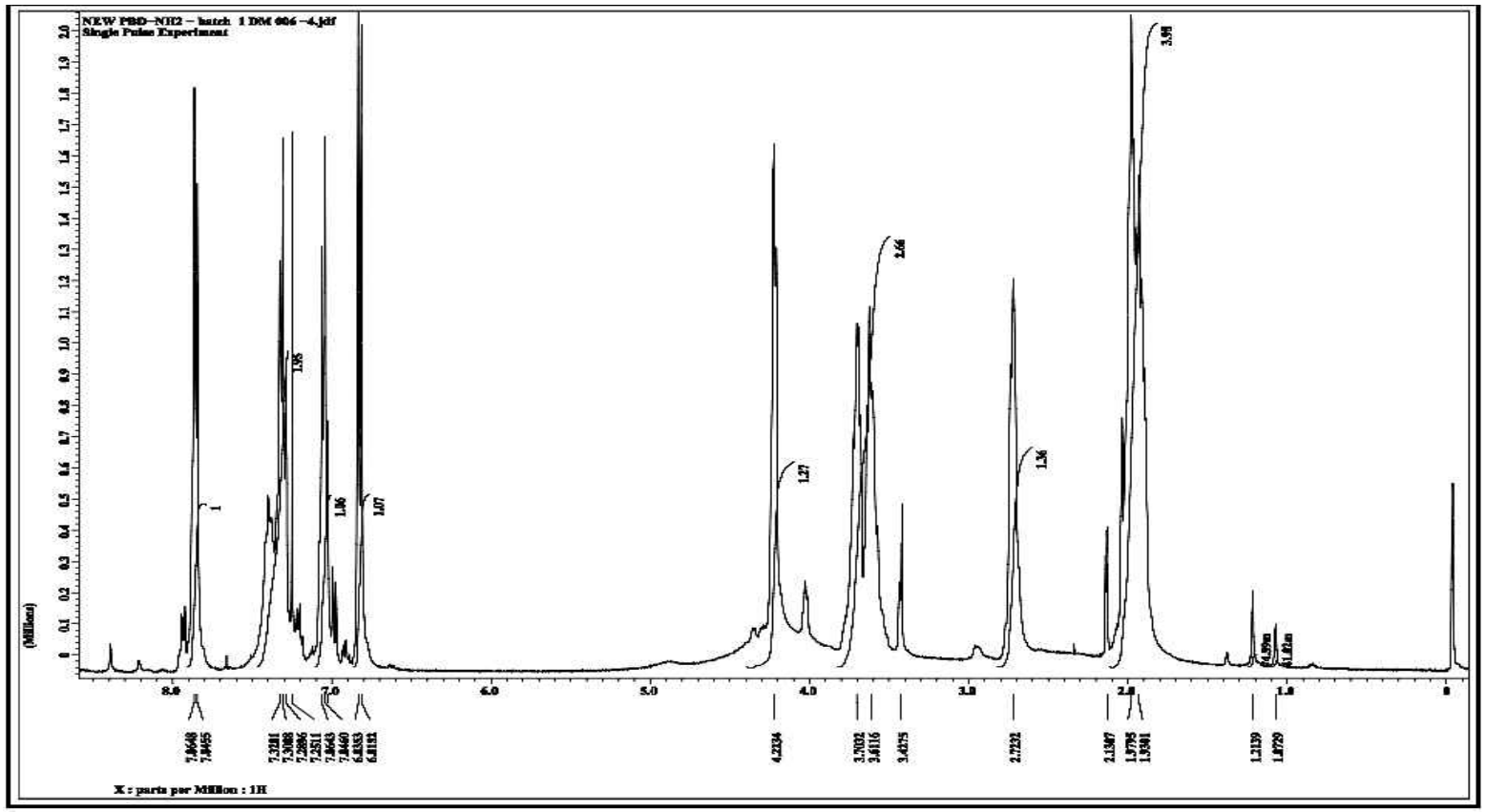

Appendix C2: ^{1}H NMR Spectrum for Compound **3** in $CDCl_3$

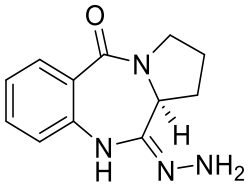

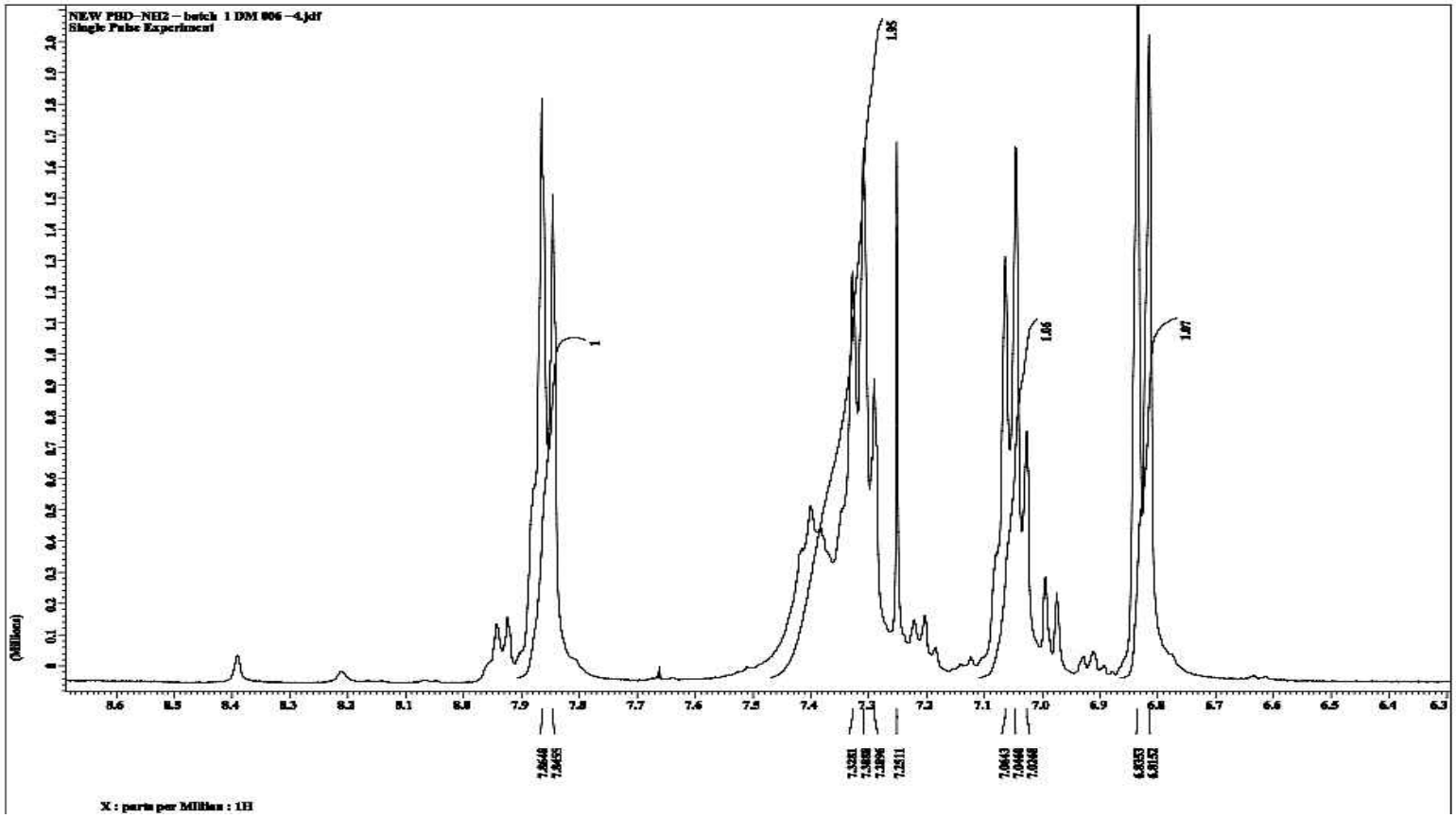

Appendix C3: ^{1}H NMR Spectrum for Compound **3** in $CDCl_3$

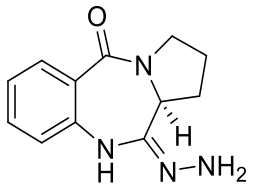

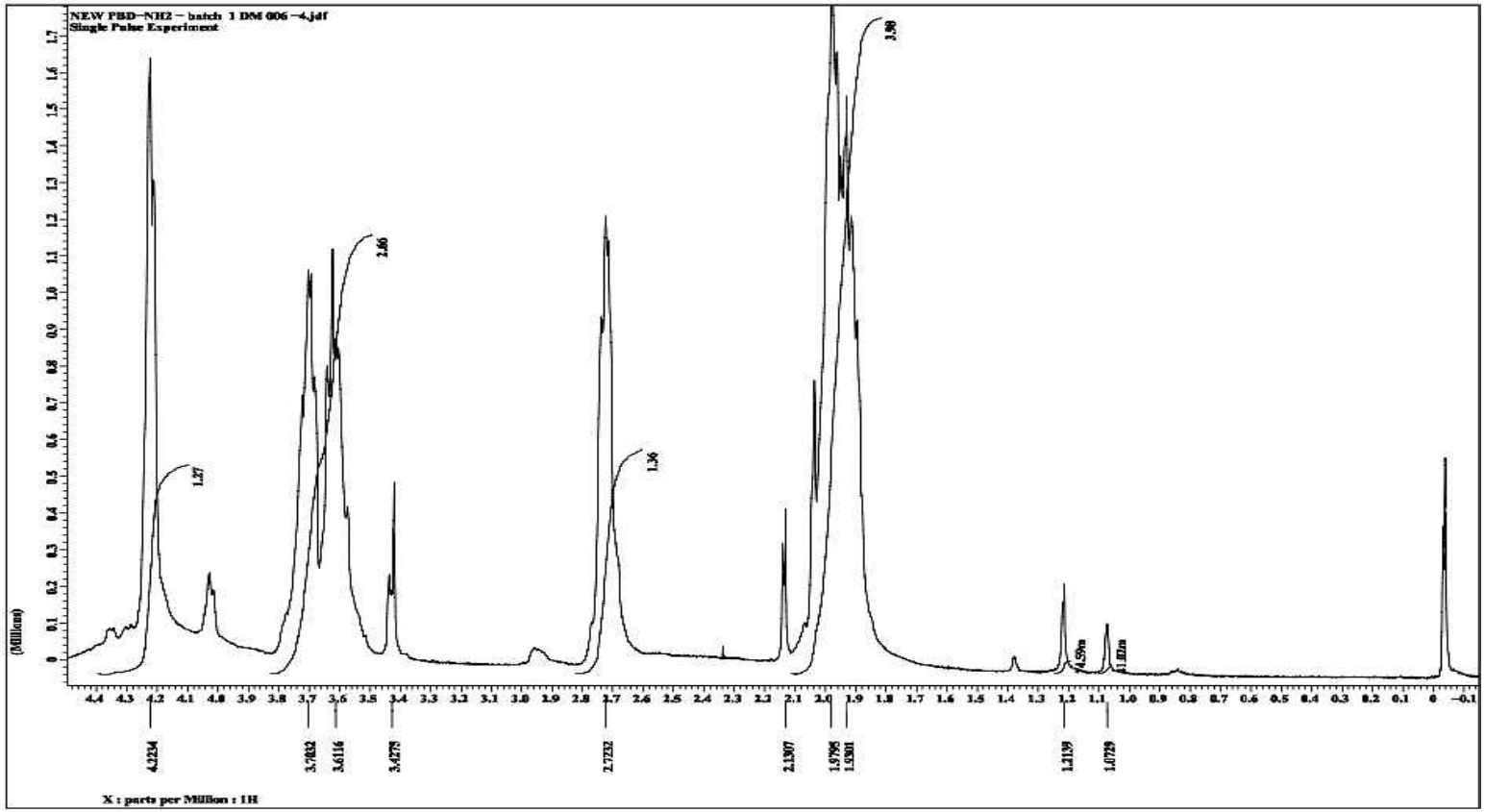

Appendix C4: ^{13} C NMR Spectrum for Compound **3** in $CDCl_3$

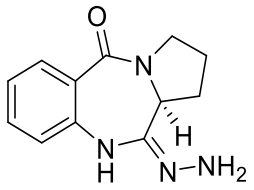

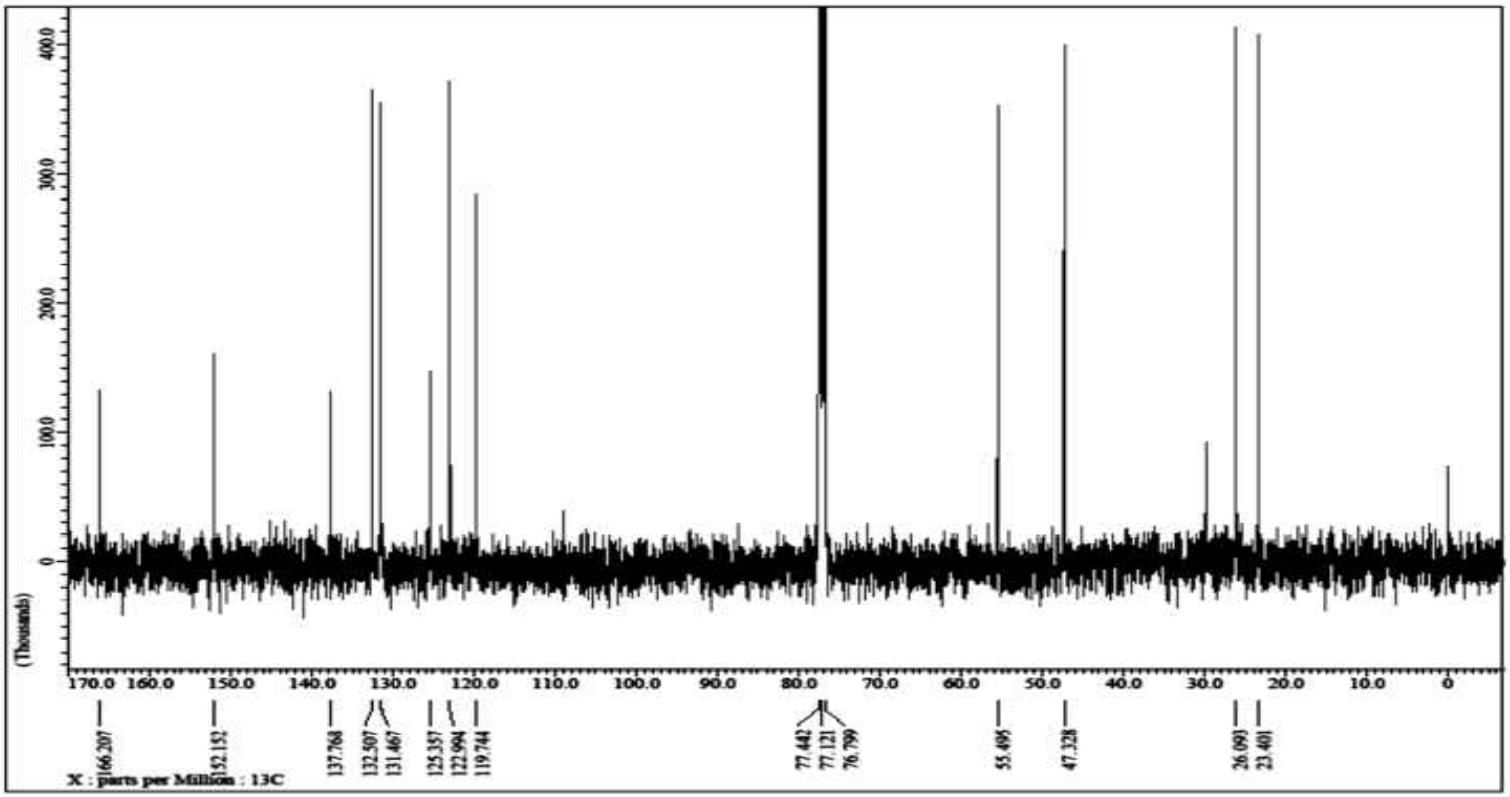

Appendix C5: IR Spectrum for Compound **3**

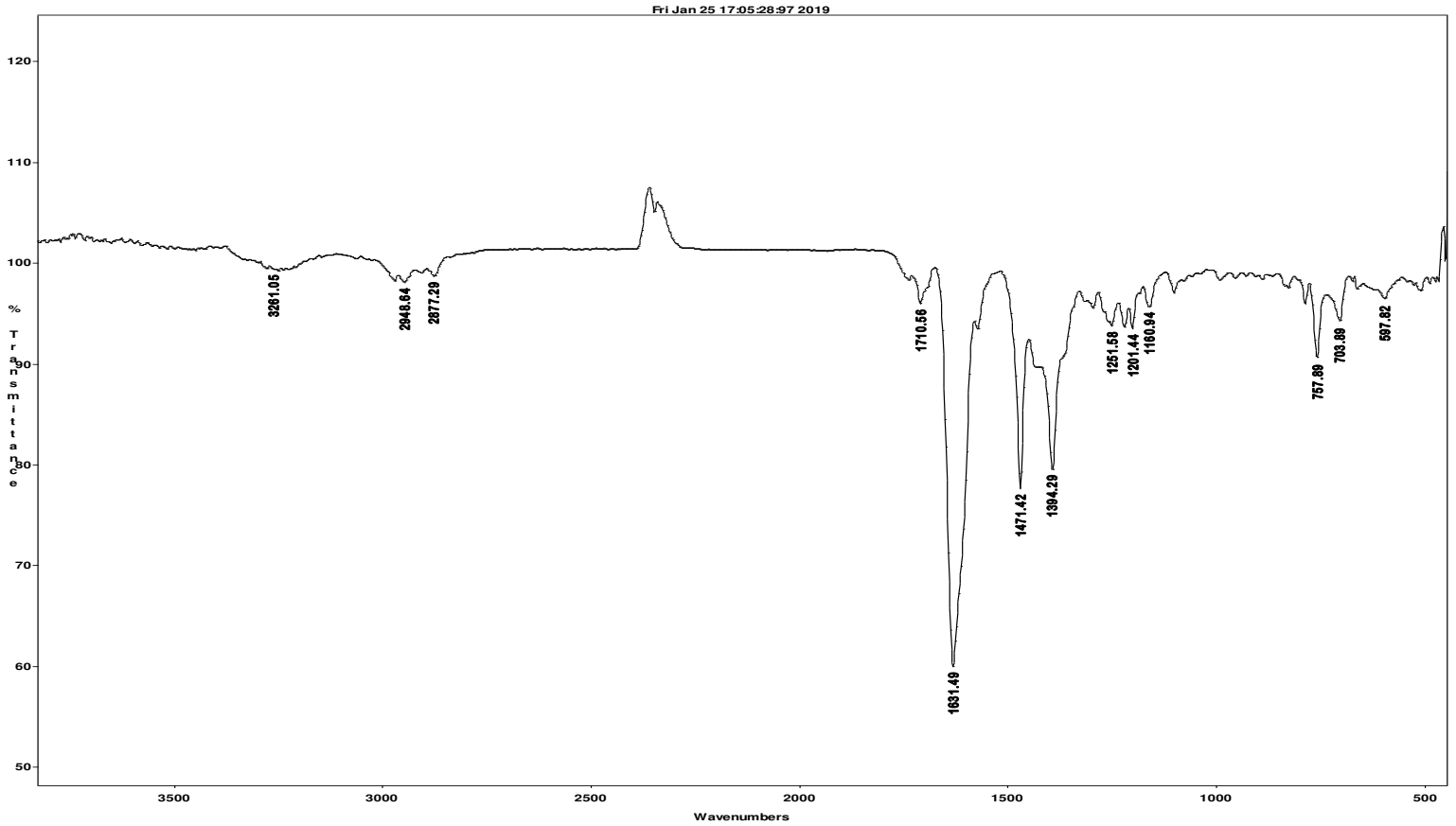

Appendix D1: ^{1}H NMR Spectrum for Compound **4a** in $CDCl_3$

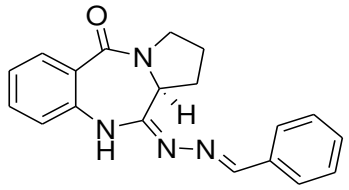

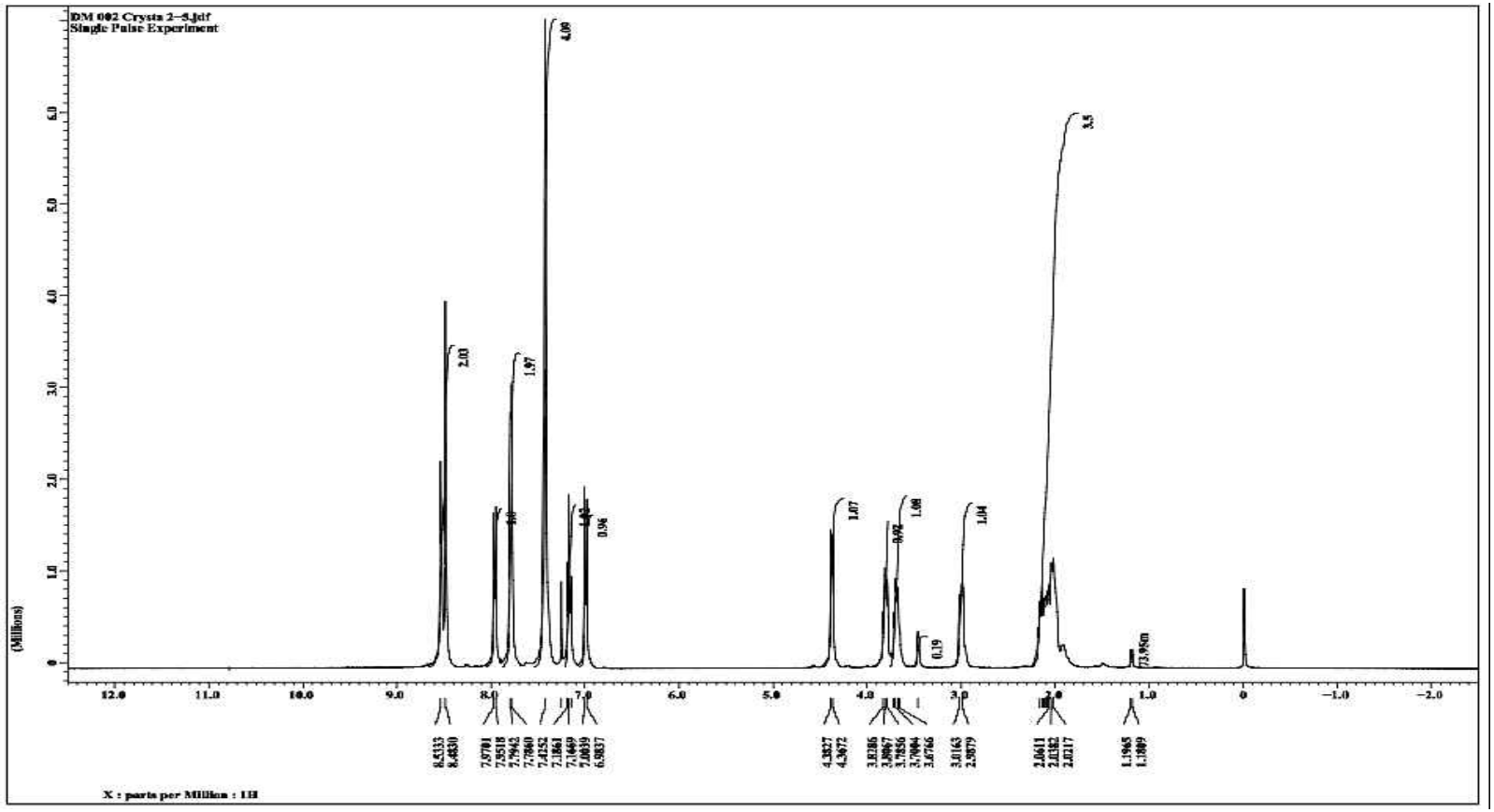

Appendix D2: ^{1}H NMR Spectrum for Compound **4a** in $CDCl_3$

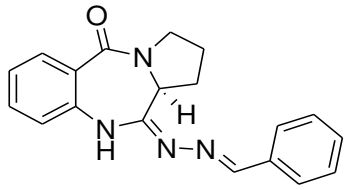

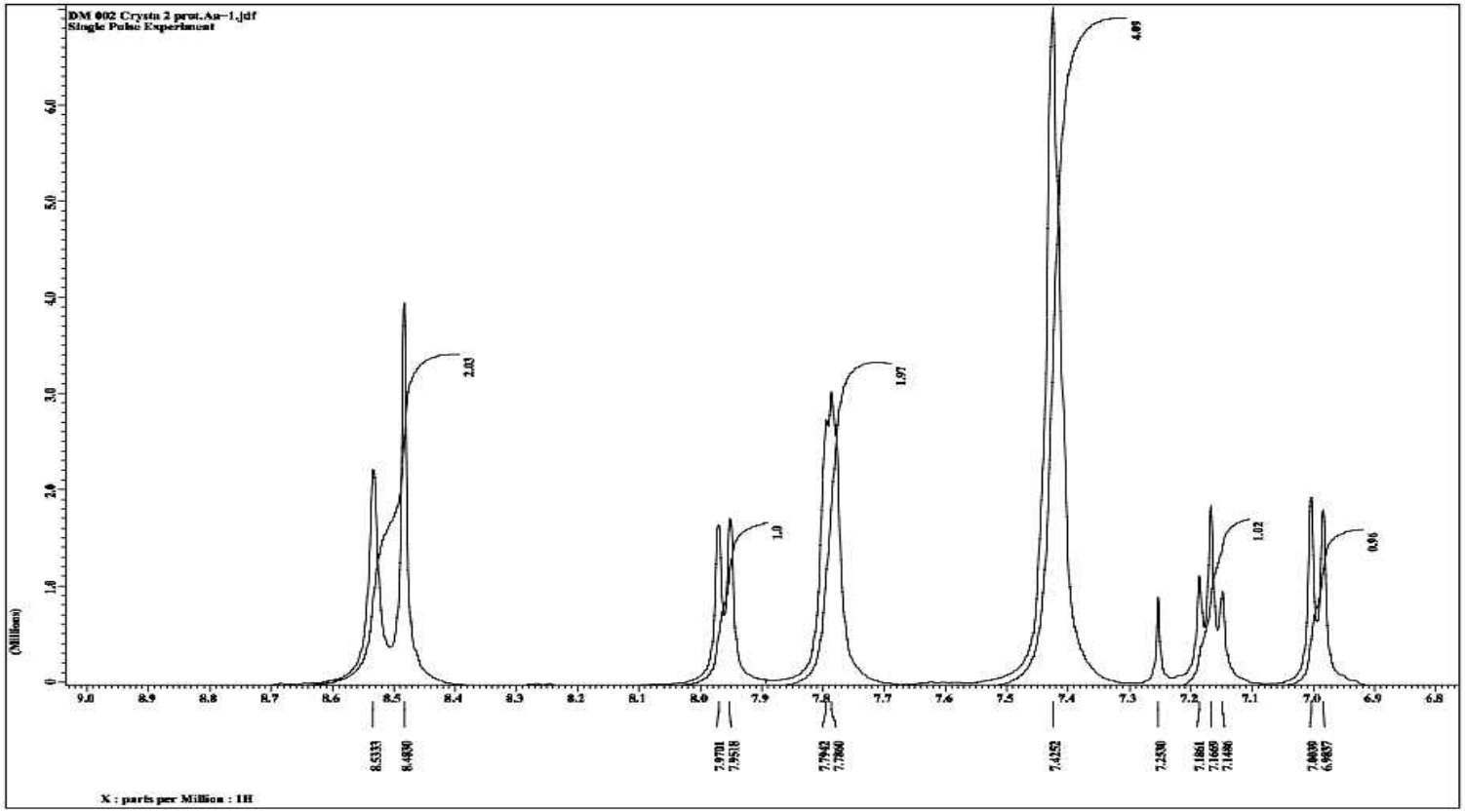

Appendix D3: ^{1}H NMR Spectrum for Compound **4a** in $CDCl_3$

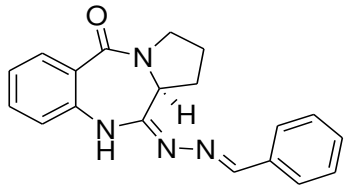

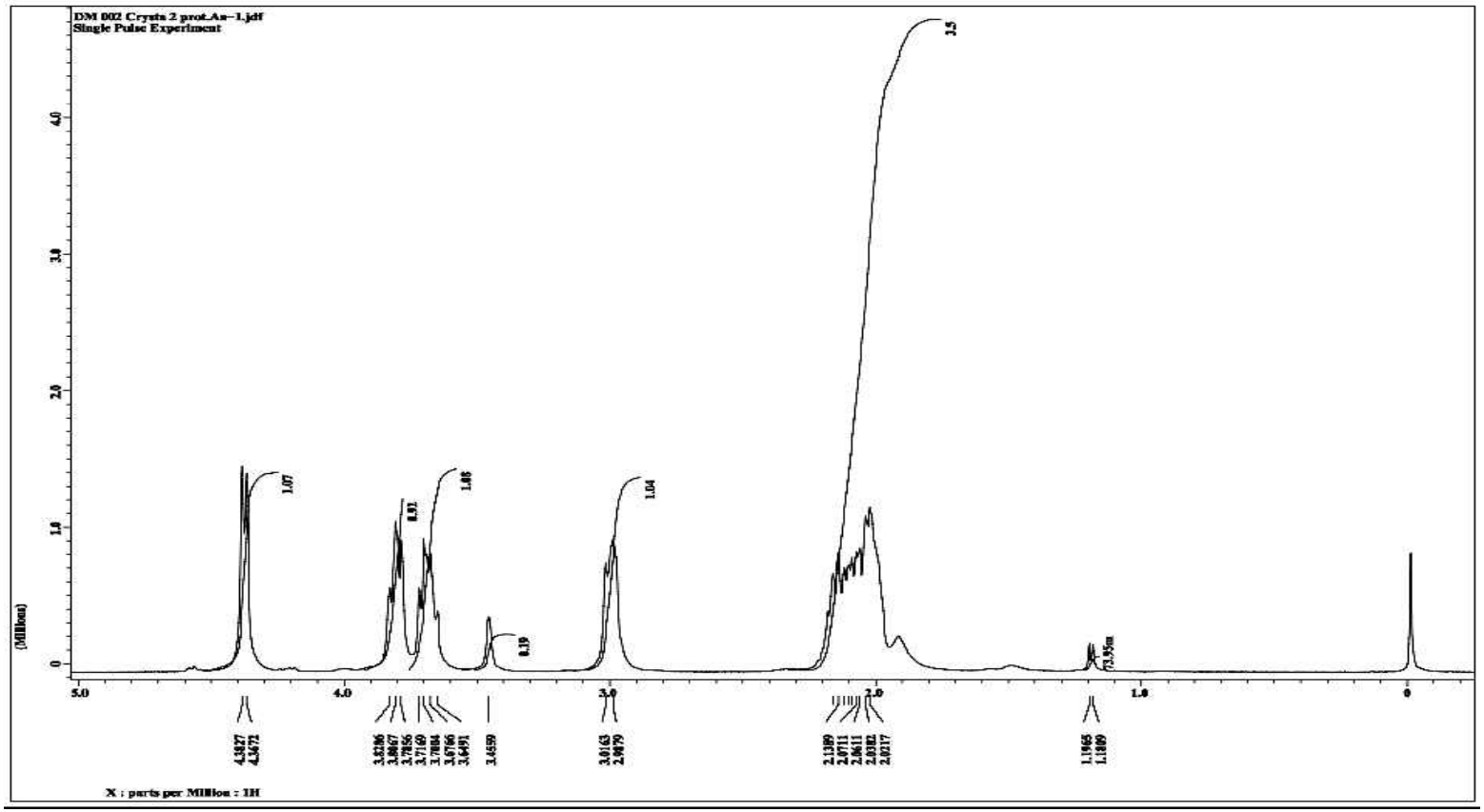

Appendix D4: ^{13} C NMR Spectrum for Compound **3** in $CDCl_3$

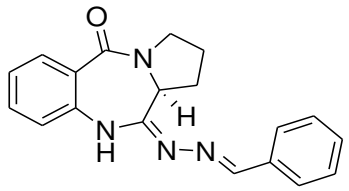

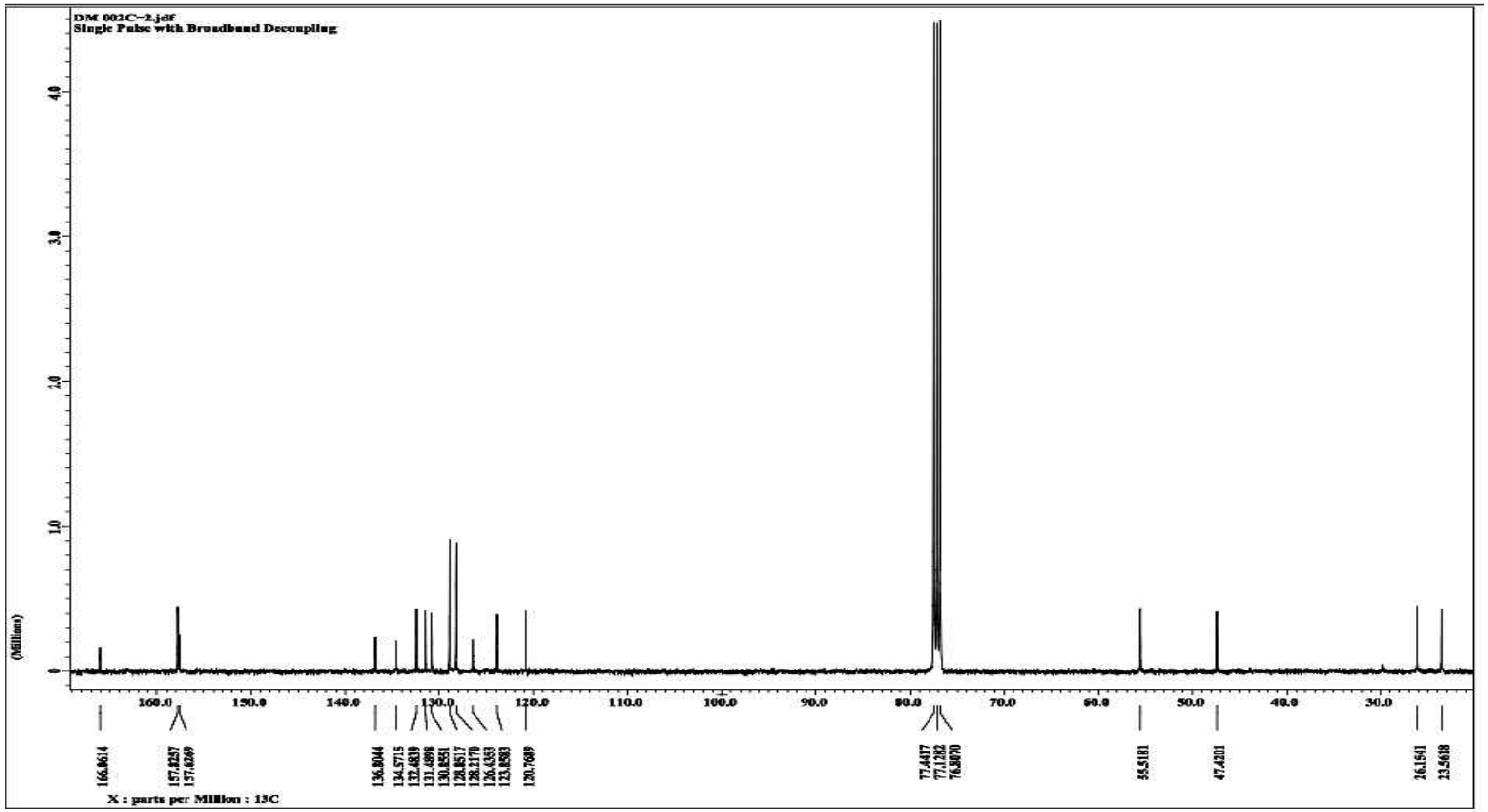

Appendix D5: ^{13} C NMR Spectrum for Compound **3** in $CDCl_3$

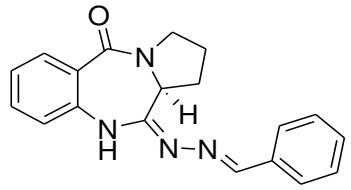

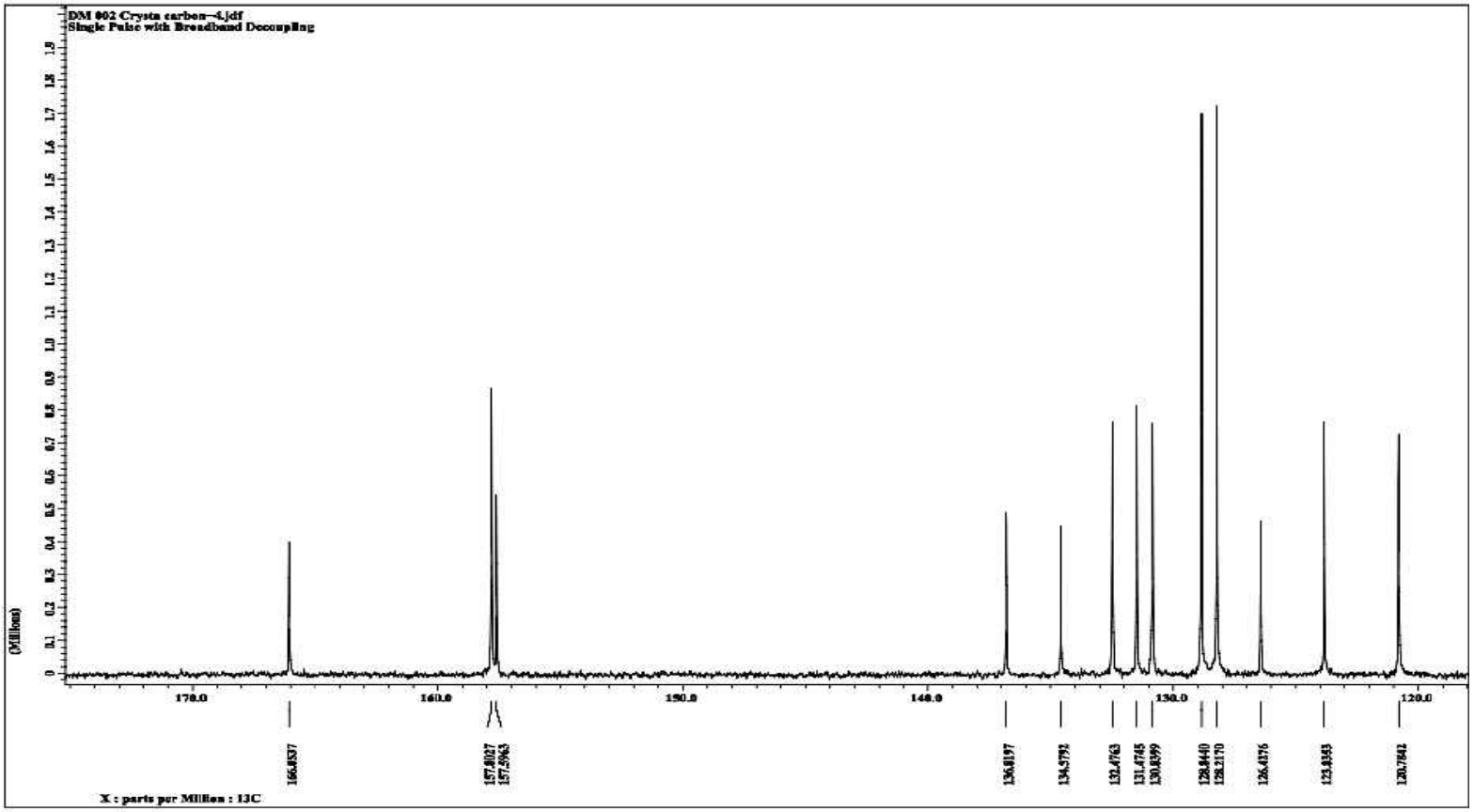

Appendix D6: C-DEPT-135 Spectrum for Compound **4a** in $CDCl_3$

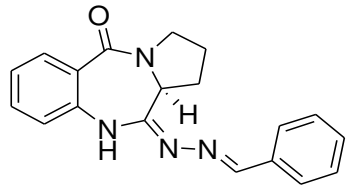

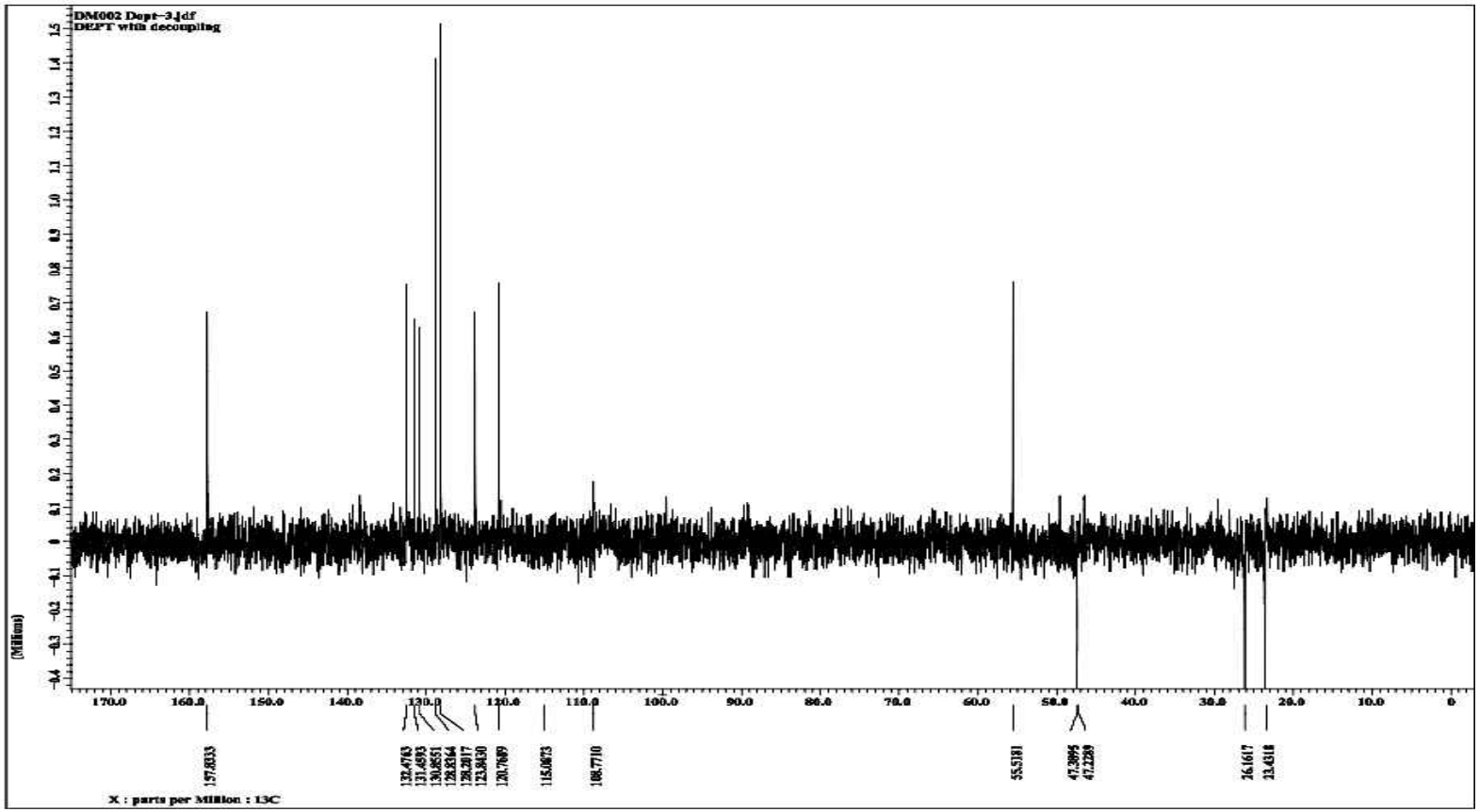

Appendix D7: IR Spectrum for Compound **4a**

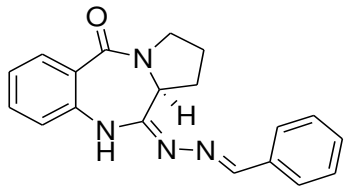

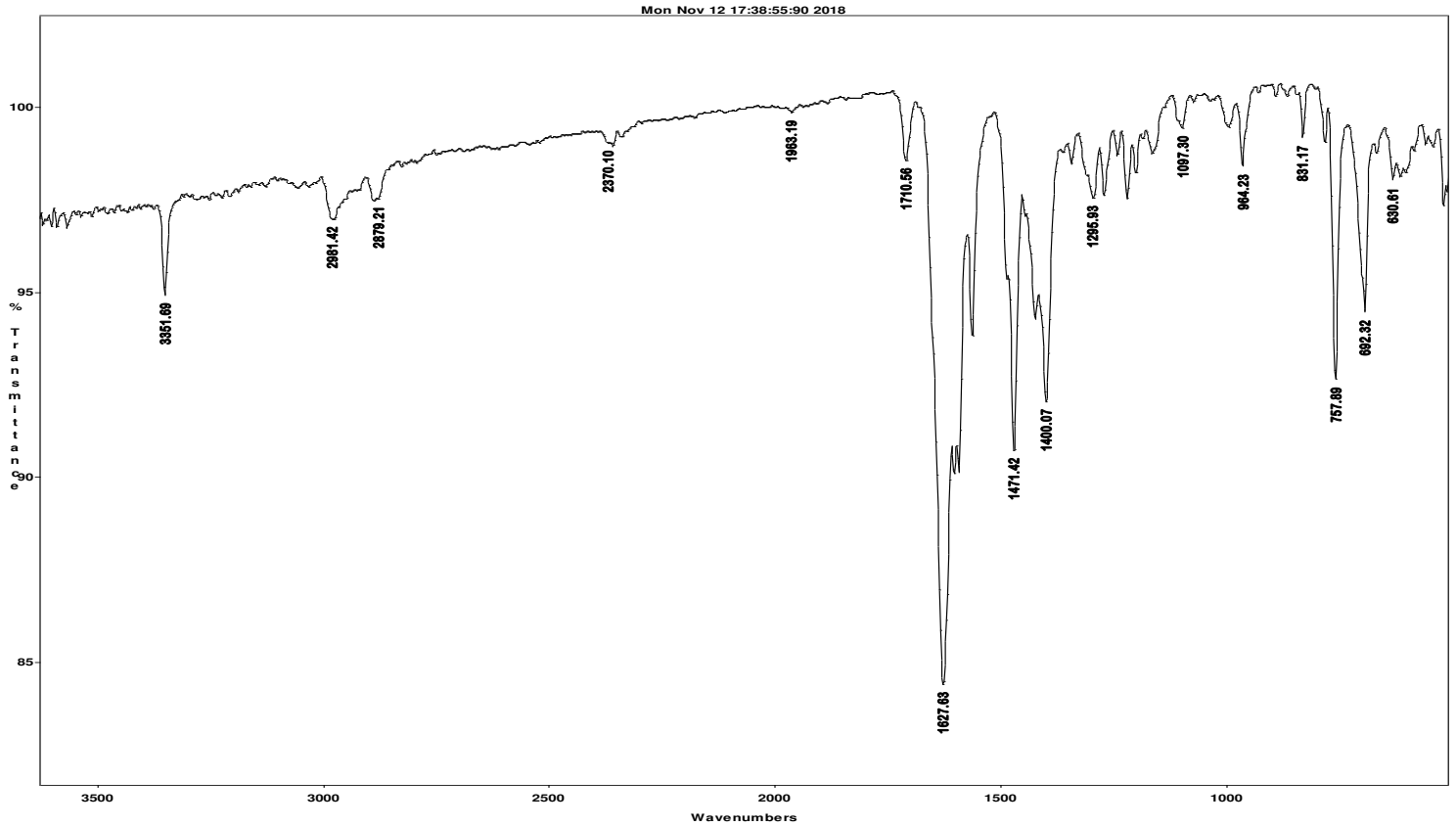

Appendix D8: UV-Vis Spectrum for Compound **4a**

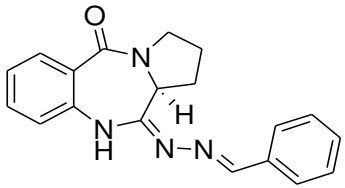

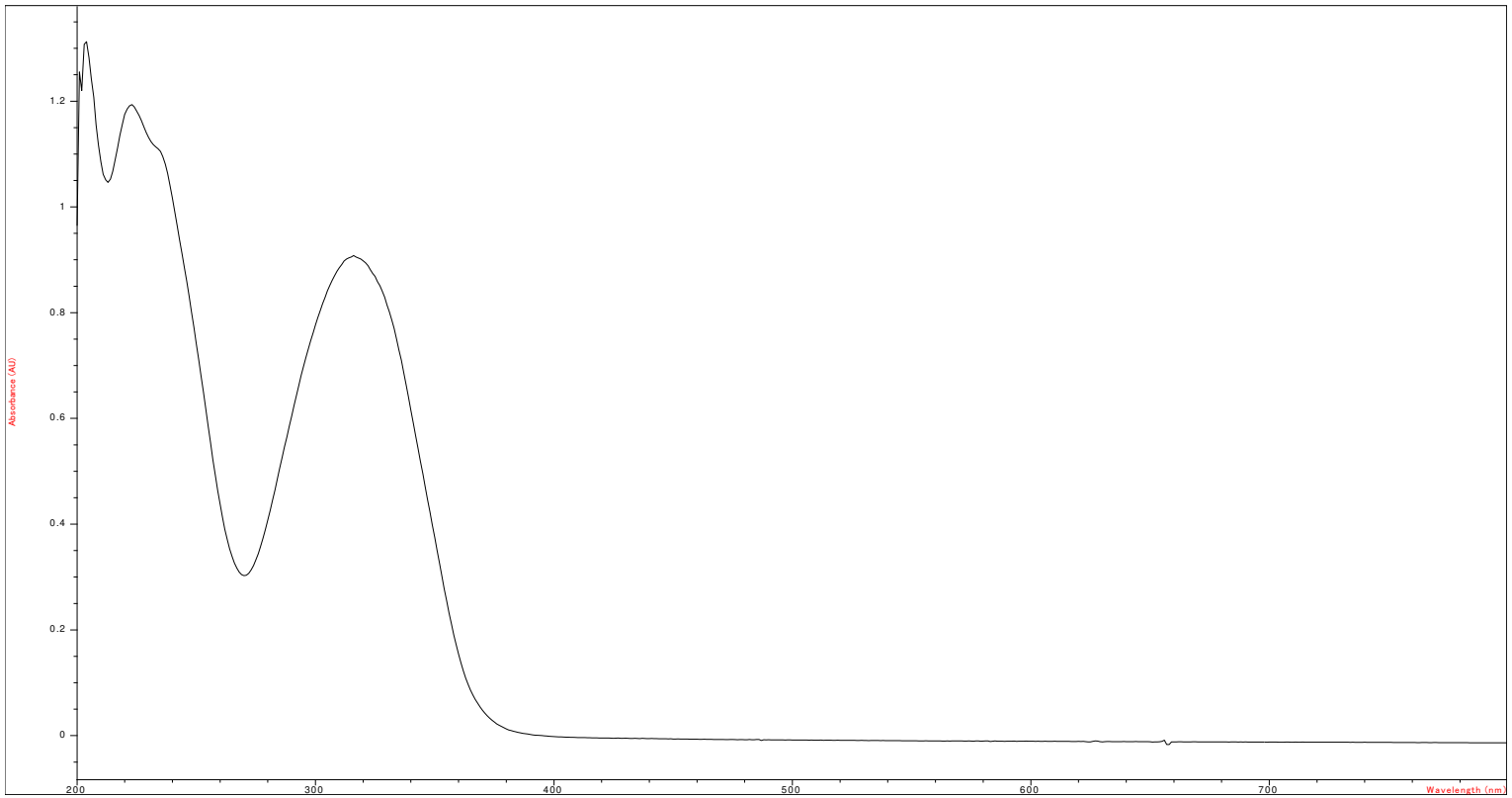

Appendix D9: GC/MS Spectrum for Compound **4a**

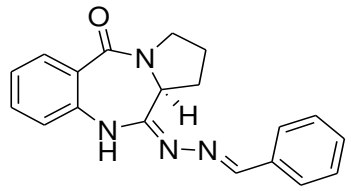

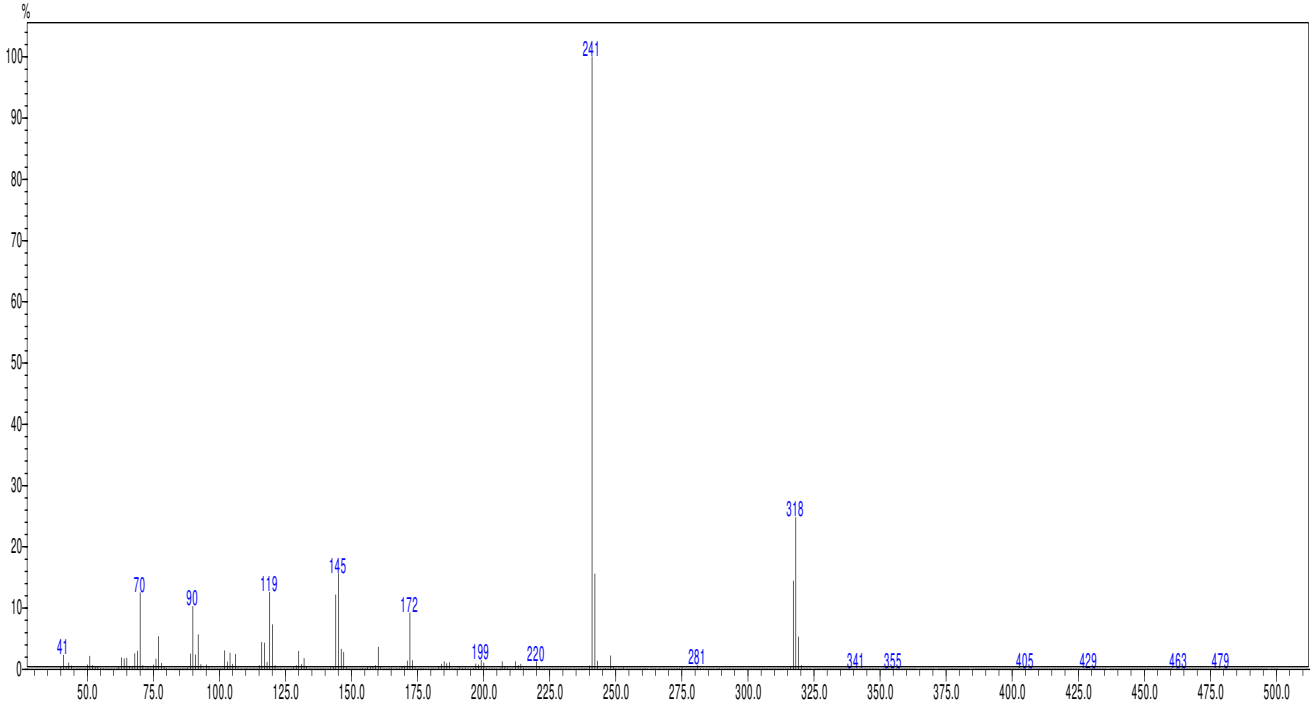

Appendix E1: ^{1}H NMR Spectrum for Compound **4b** in $CDCl_3$

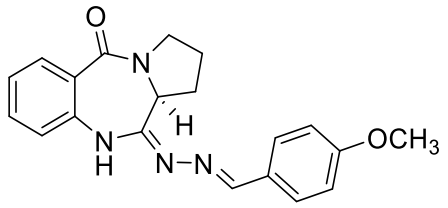

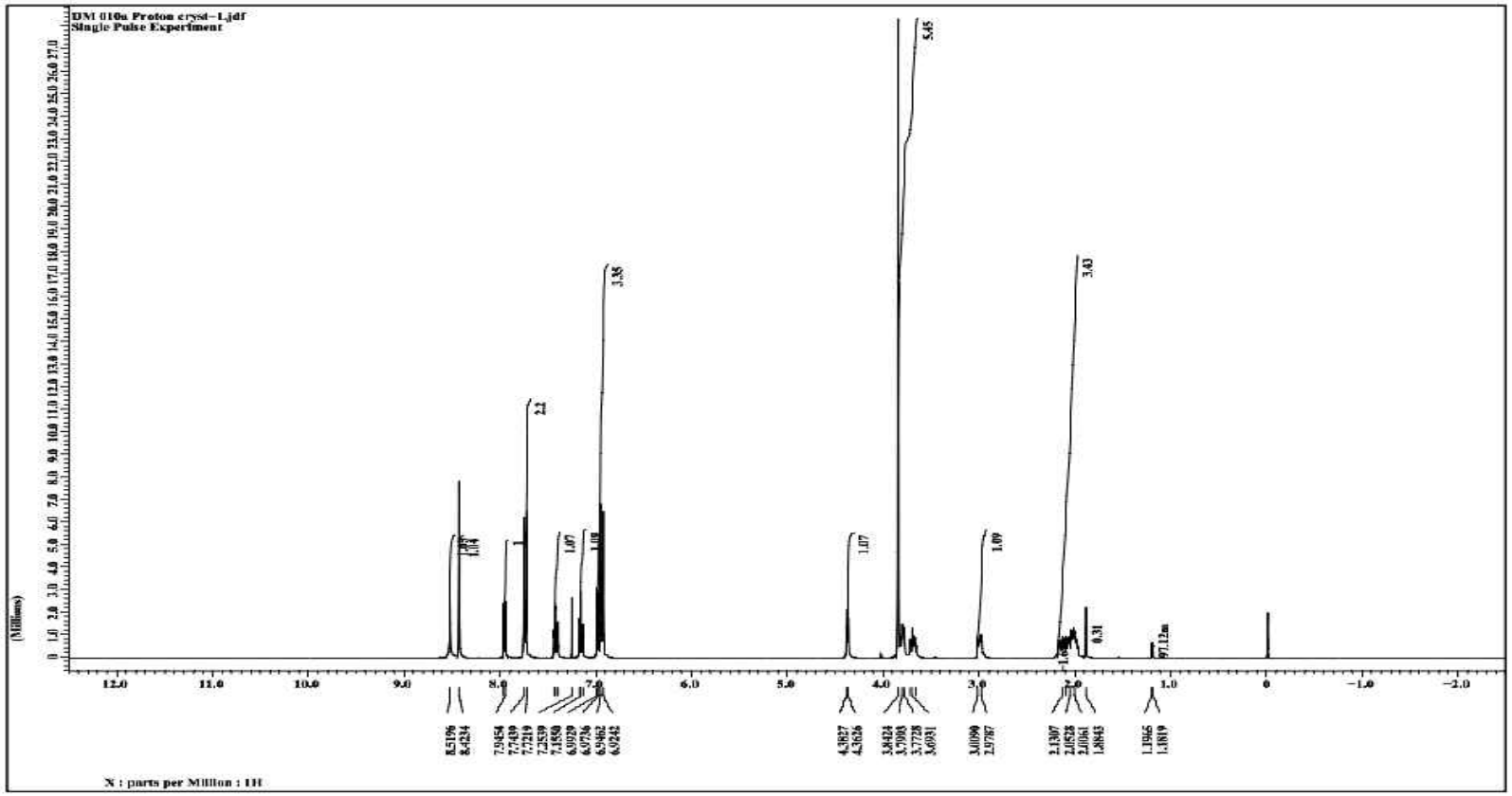

Appendix E2: ^{1}H NMR Spectrum for Compound **4b** in $CDCl_3$

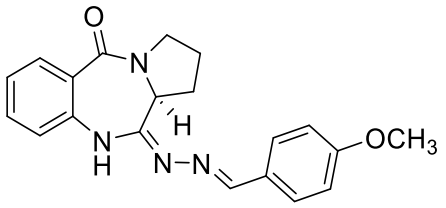

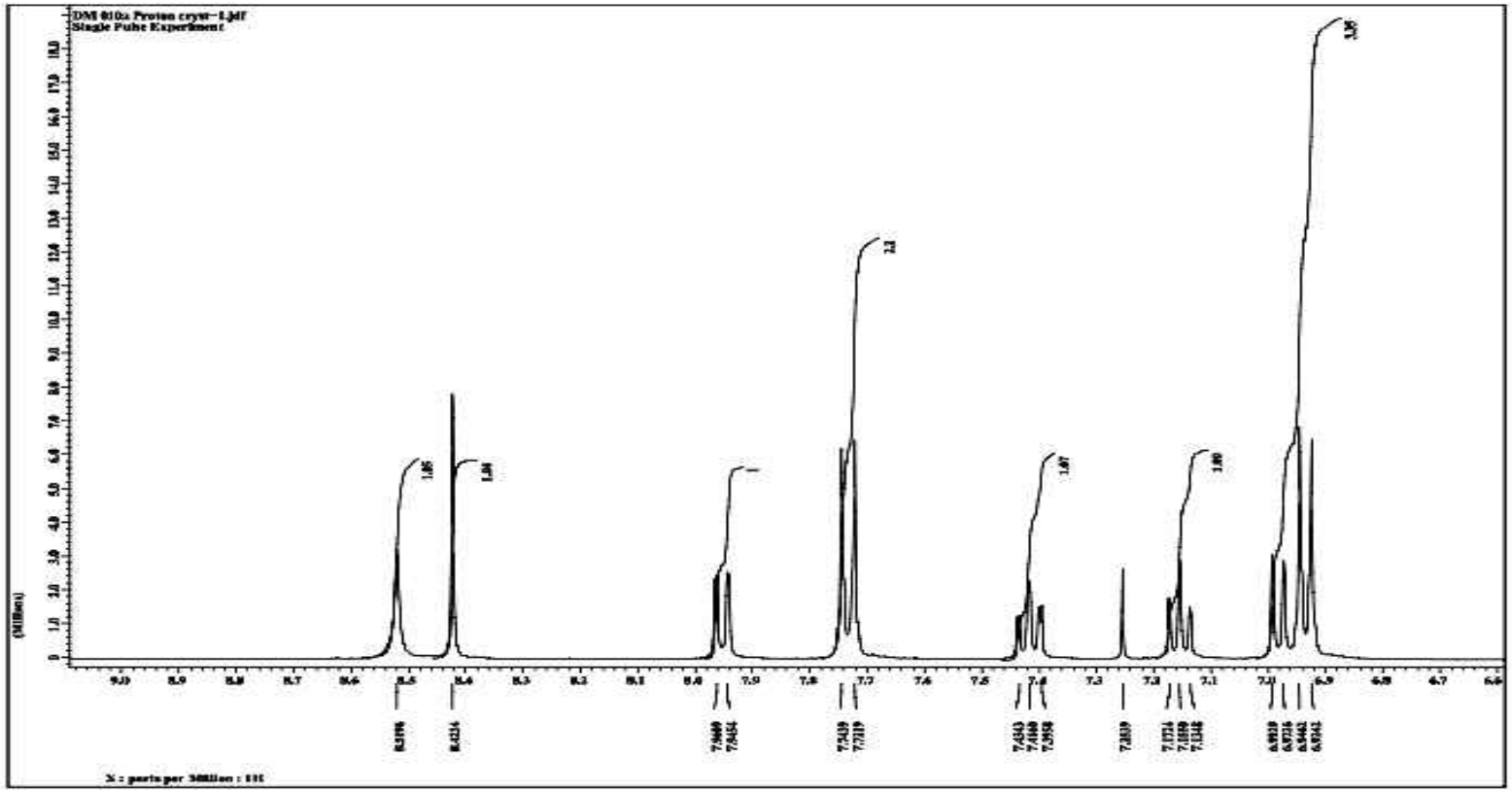

Appendix E3: ^{1}H NMR Spectrum for Compound **4b** in $CDCl_3$

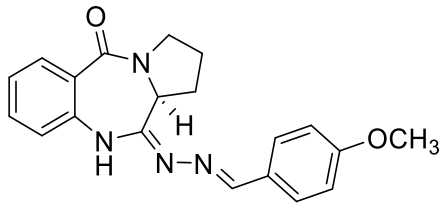

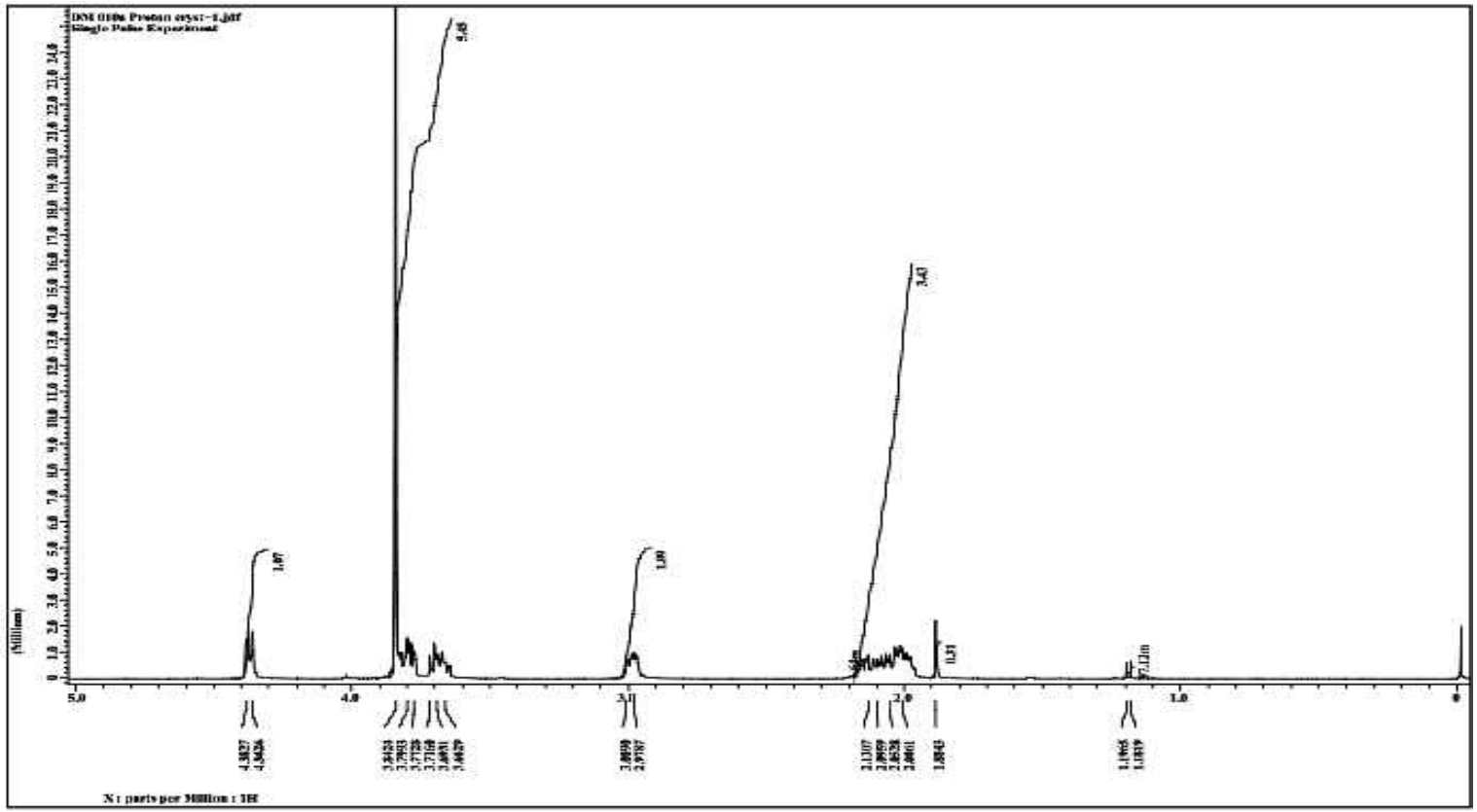

Appendix E4: ^{13} C NMR Spectrum for Compound **4b** in $CDCl_3$

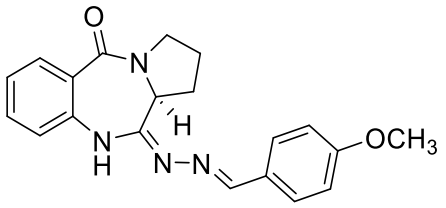

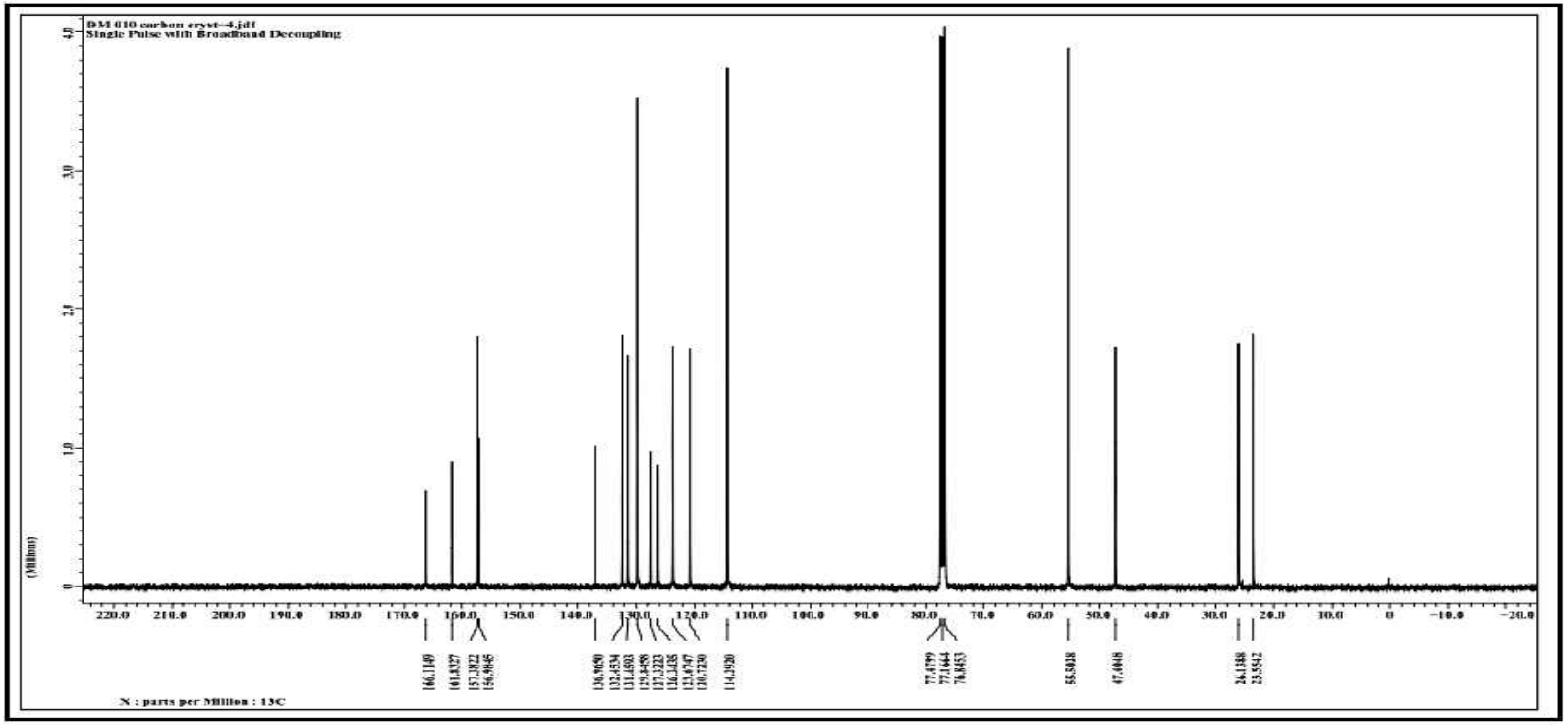

Appendix E5: C-DEPT-135 Spectrum for Compound **4b** in $CDCl_3$

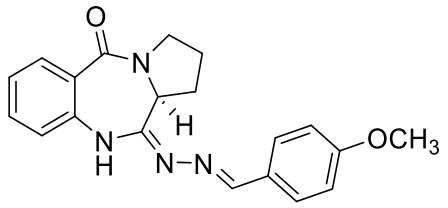

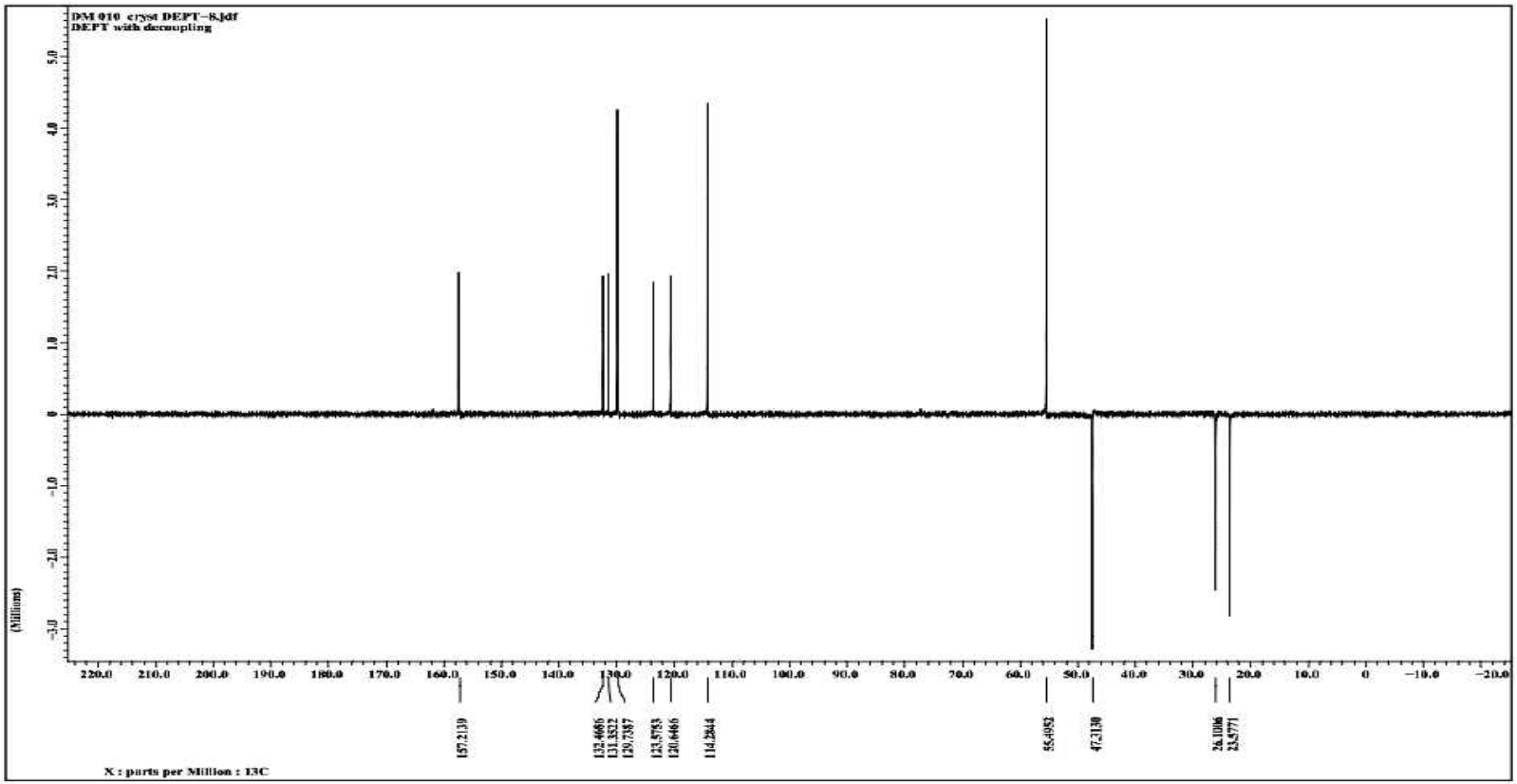

Appendix E6: IR Spectrum for Compound **4b**

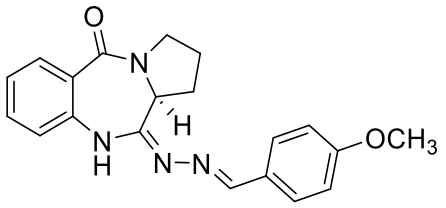

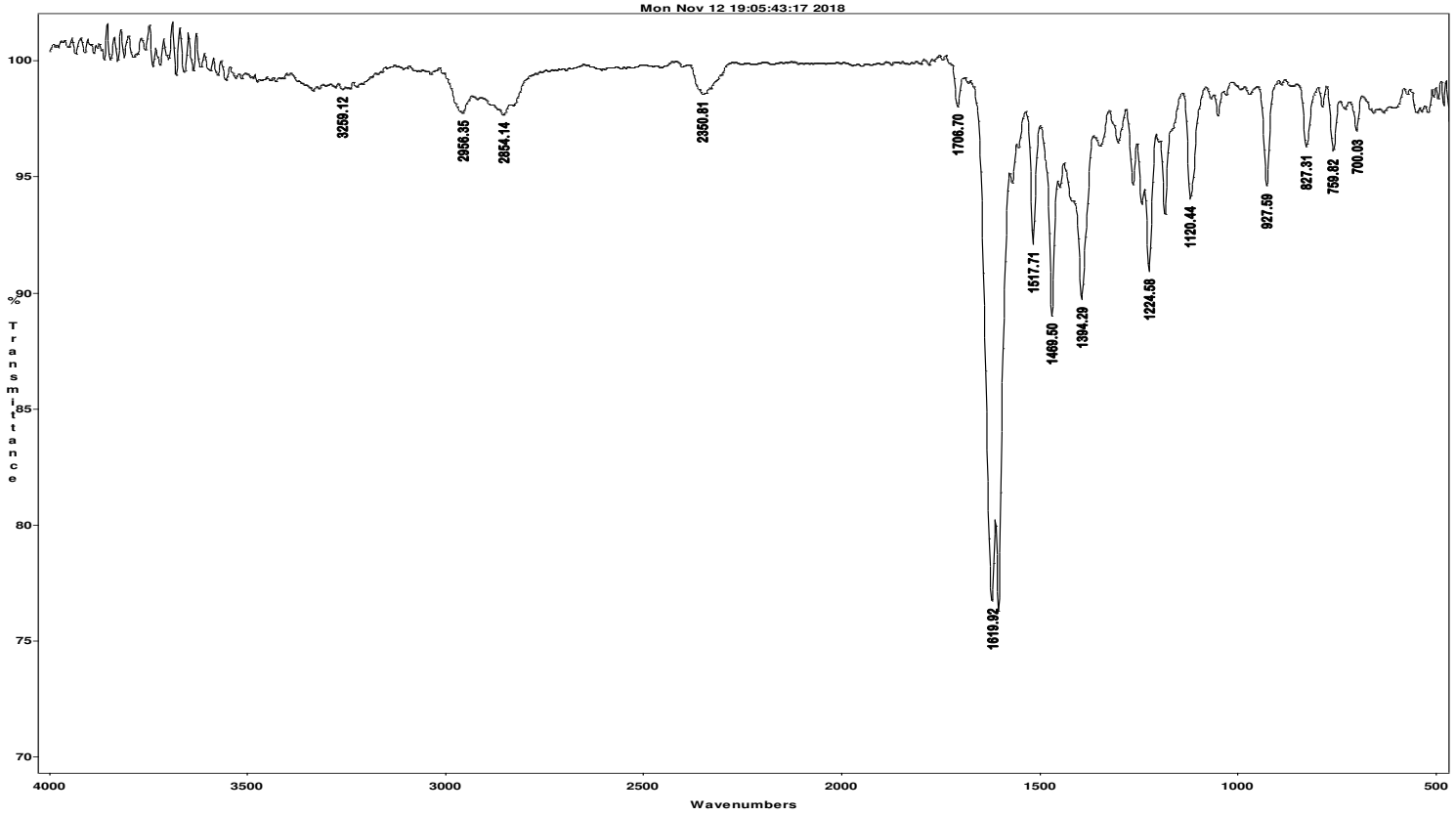

Appendix E7: UV-Vis Spectrum for Compound **4b**

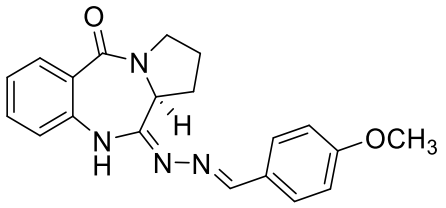

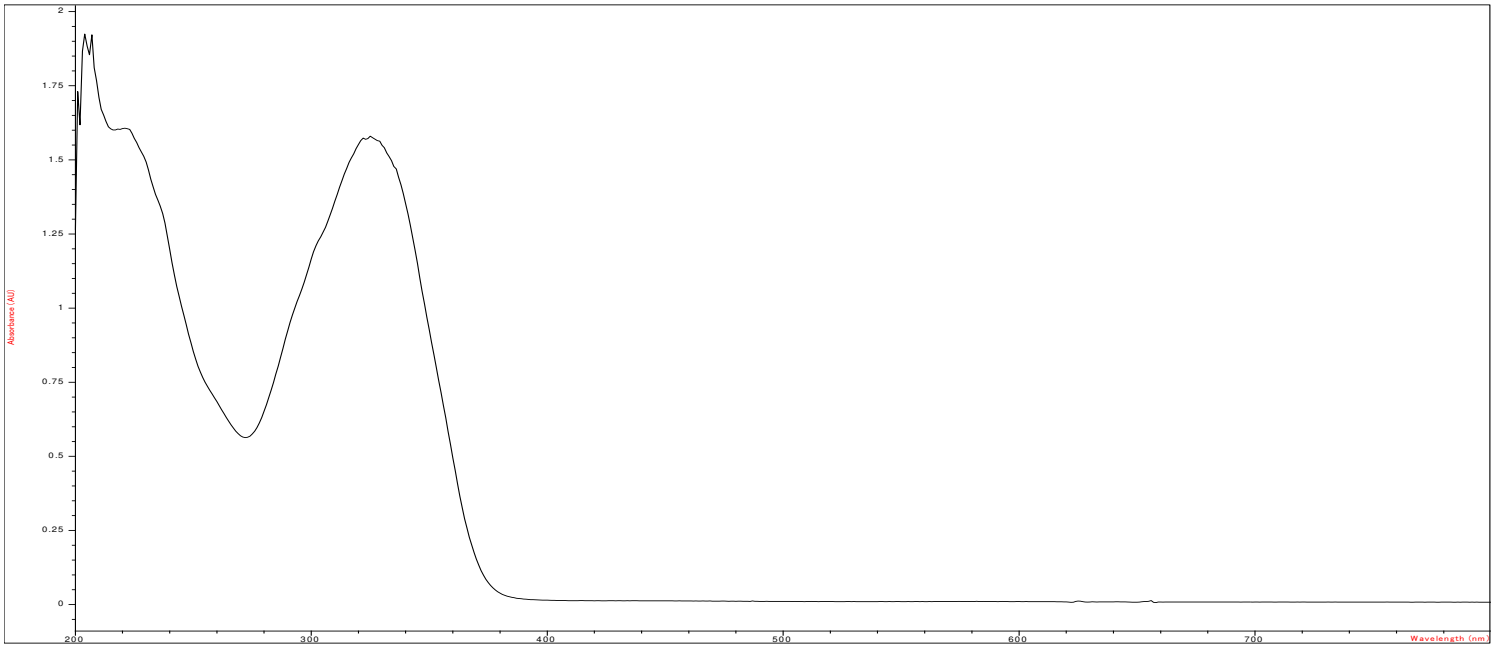

Appendix E8: GC/MS Spectrum for Compound **4b**

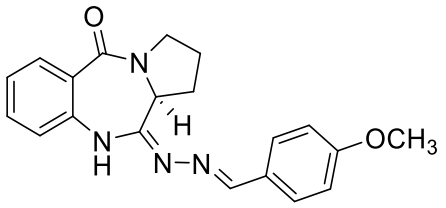

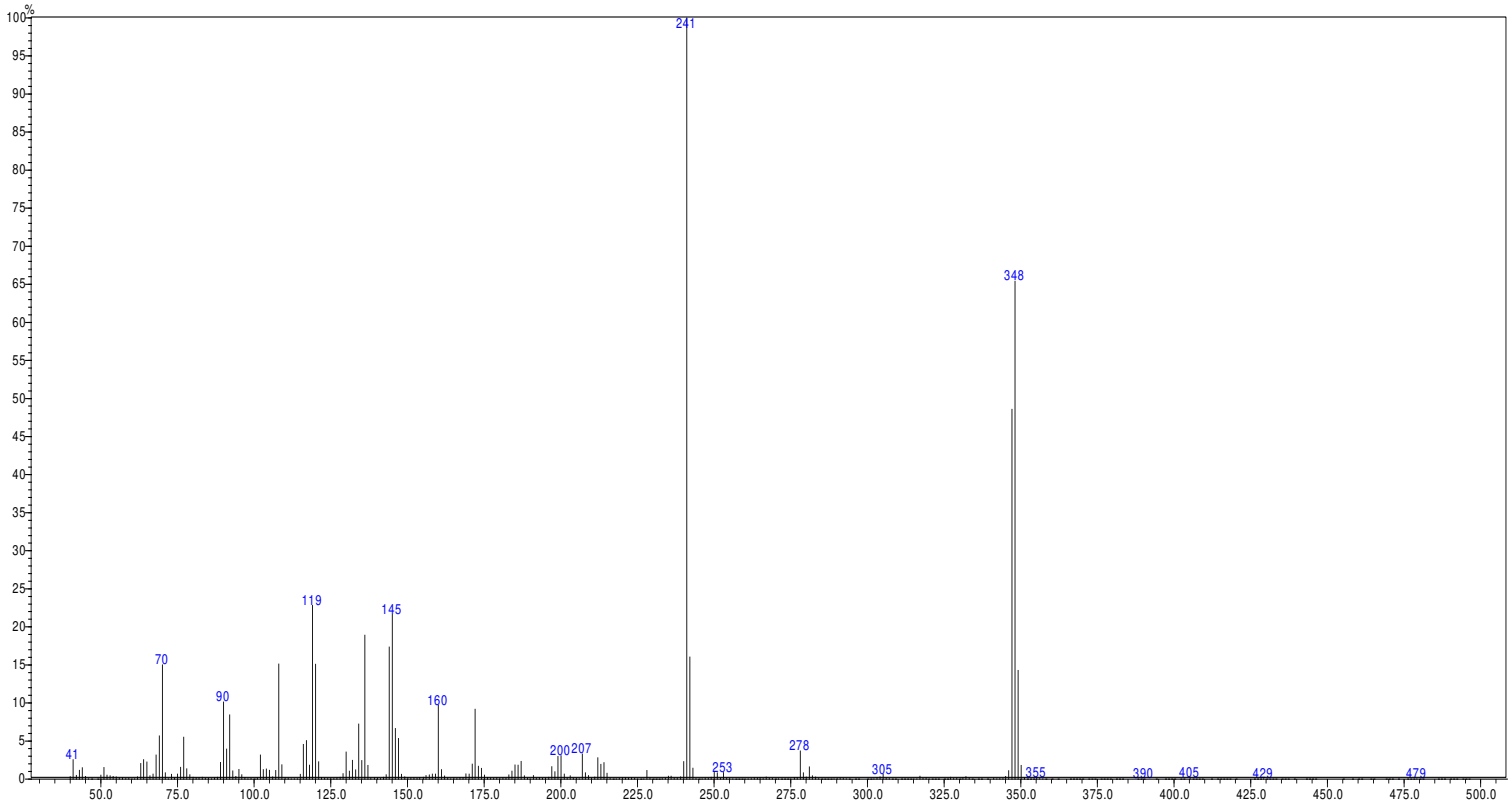

Appendix F1: ^{1}H NMR Spectrum for Compound **4c** in $CDCl_3$

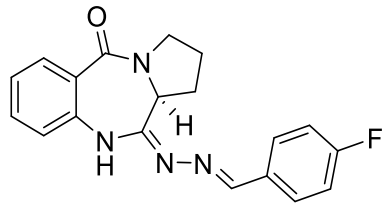

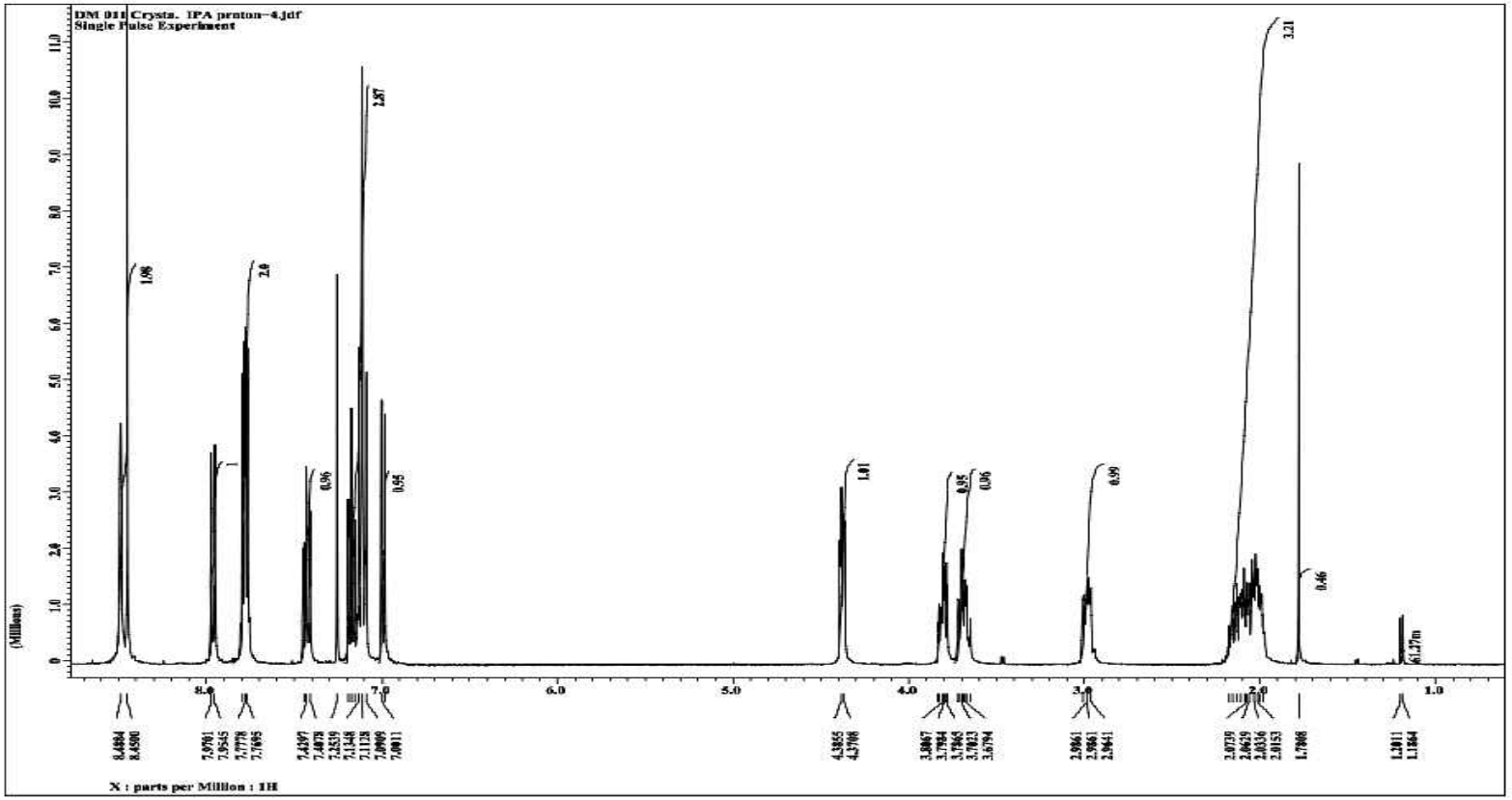

Appendix F2: ^{1}H NMR Spectrum for Compound **4c** in $CDCl_3$

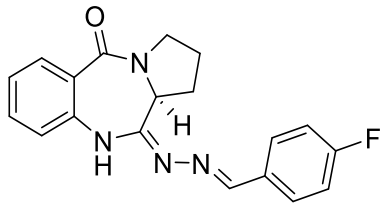

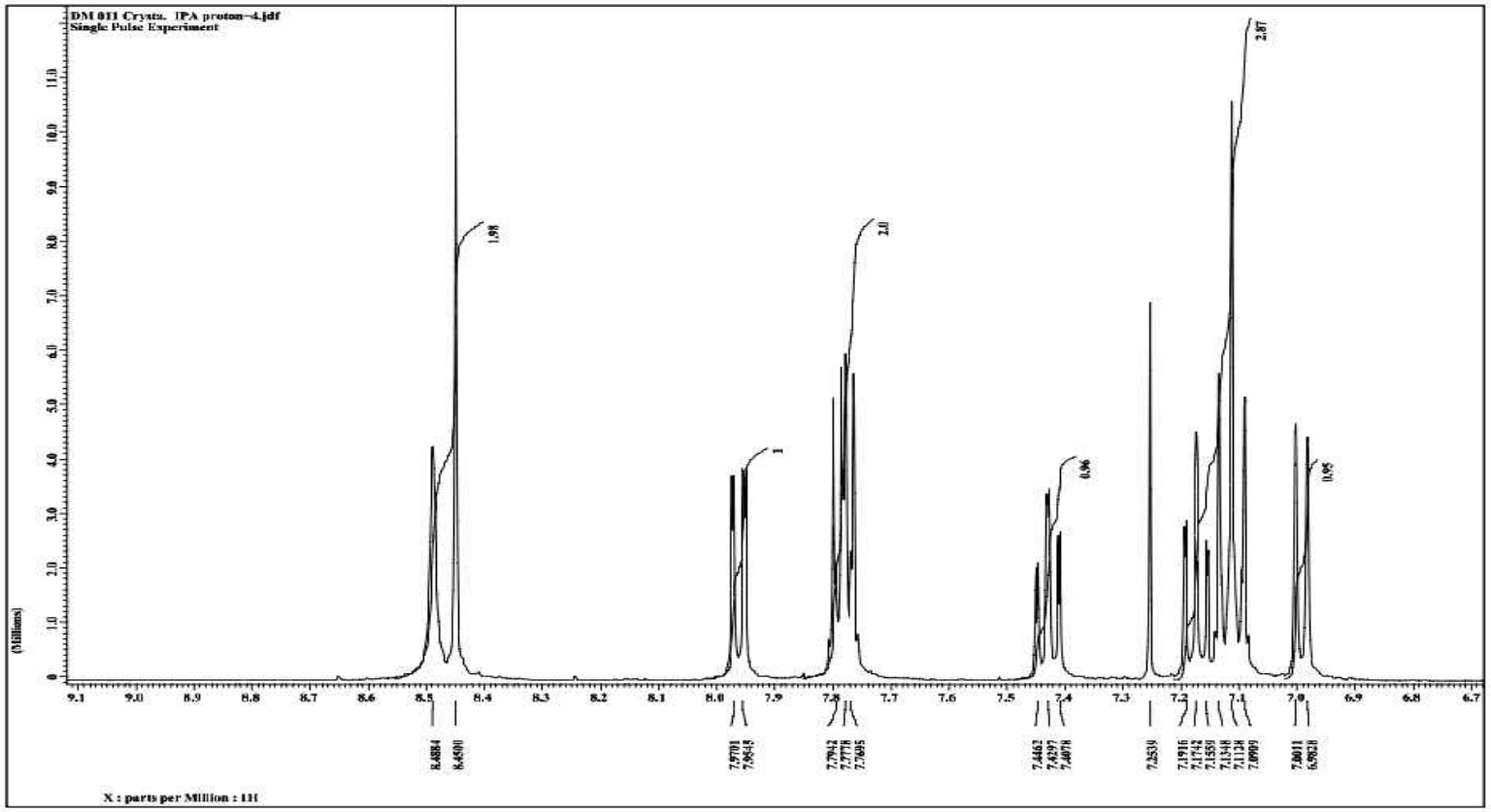

Appendix F3: ^{1}H NMR Spectrum for Compound **4c** in $CDCl_3$

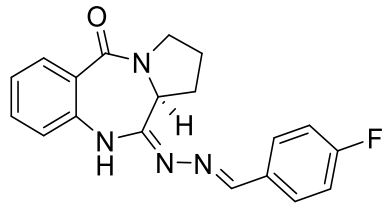

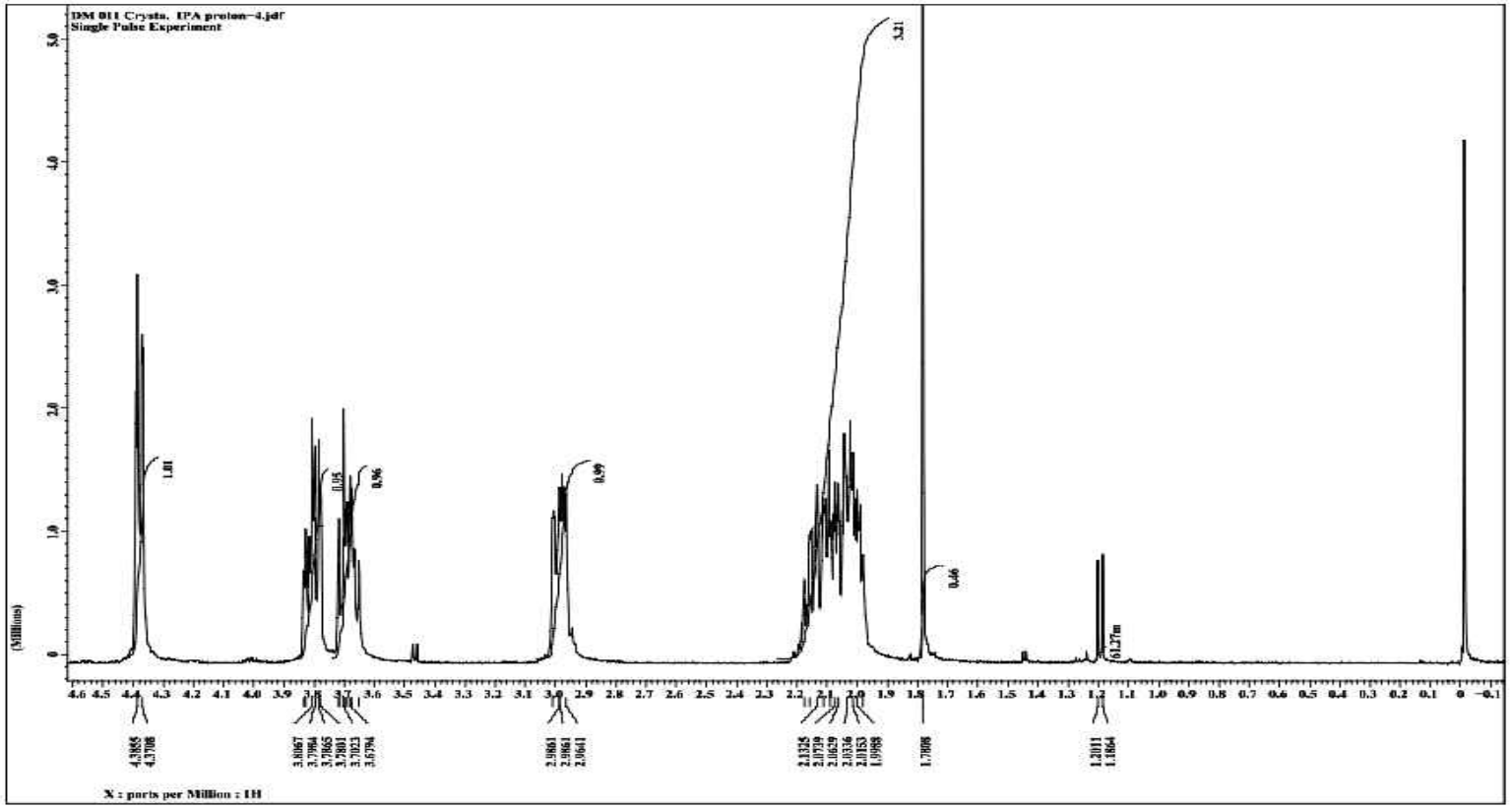

Appendix F4: ^{13} C NMR Spectrum for Compound **4c** in $CDCl_3$

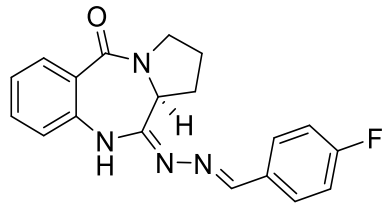

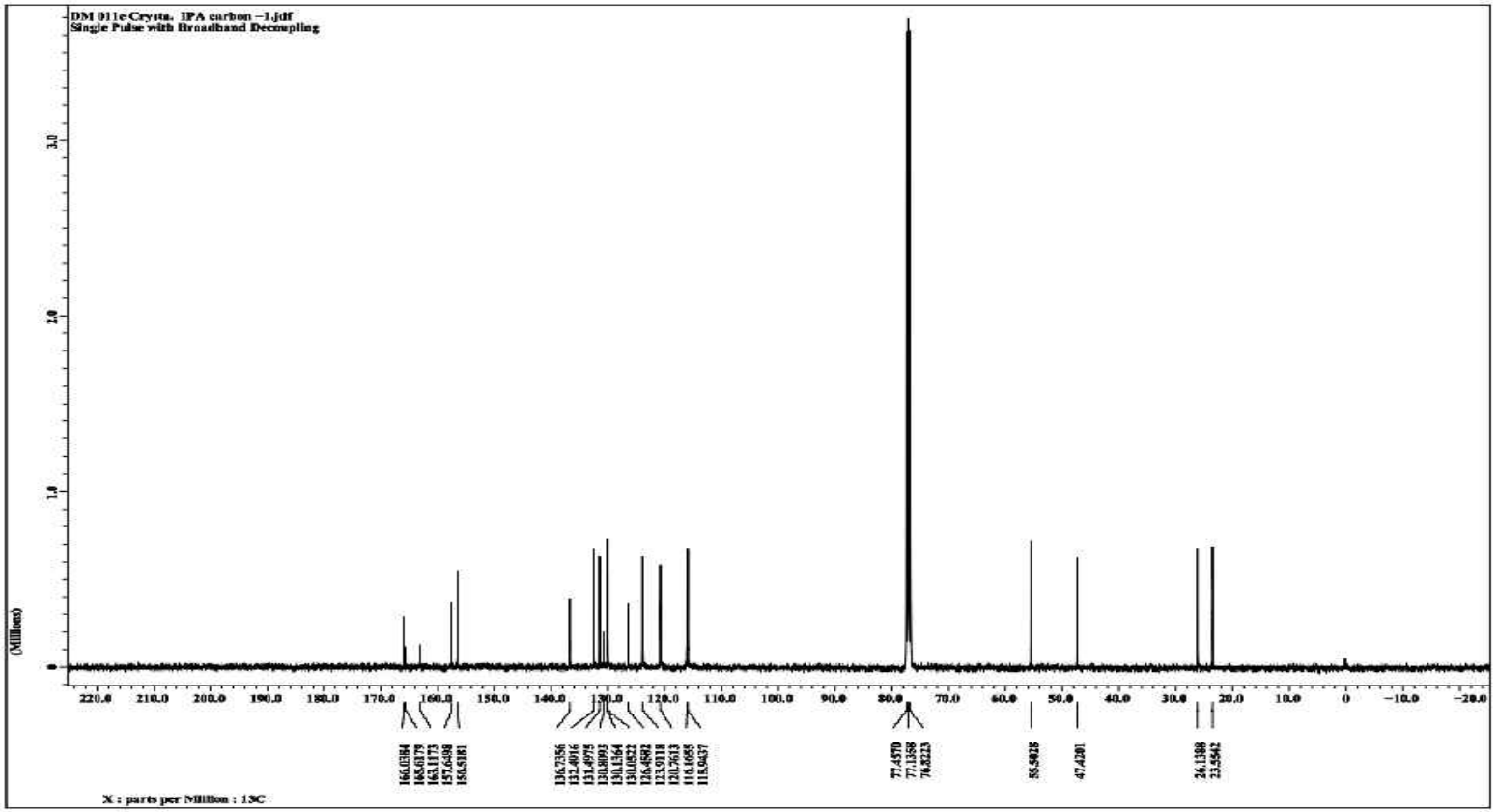

Appendix F5: ^{13} C NMR Spectrum for Compound **4c** in $CDCl_3$

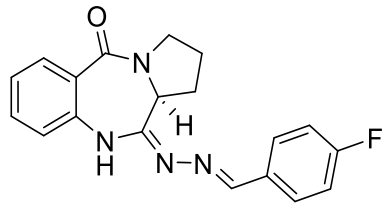

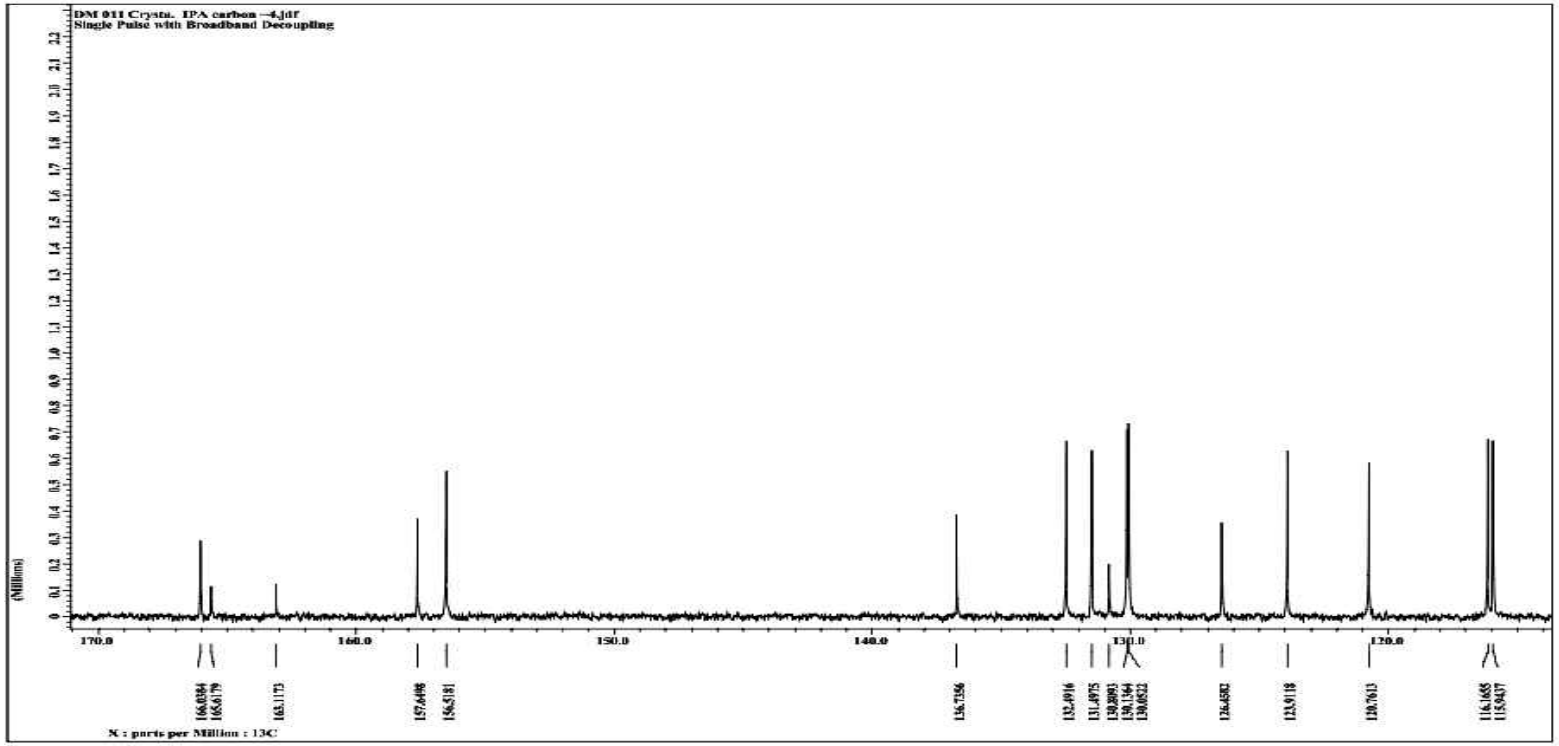

Appendix F6: C-DEPT-135 Spectrum for Compound **4c** in $CDCl_3$

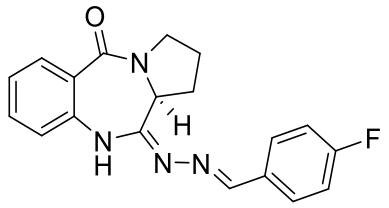

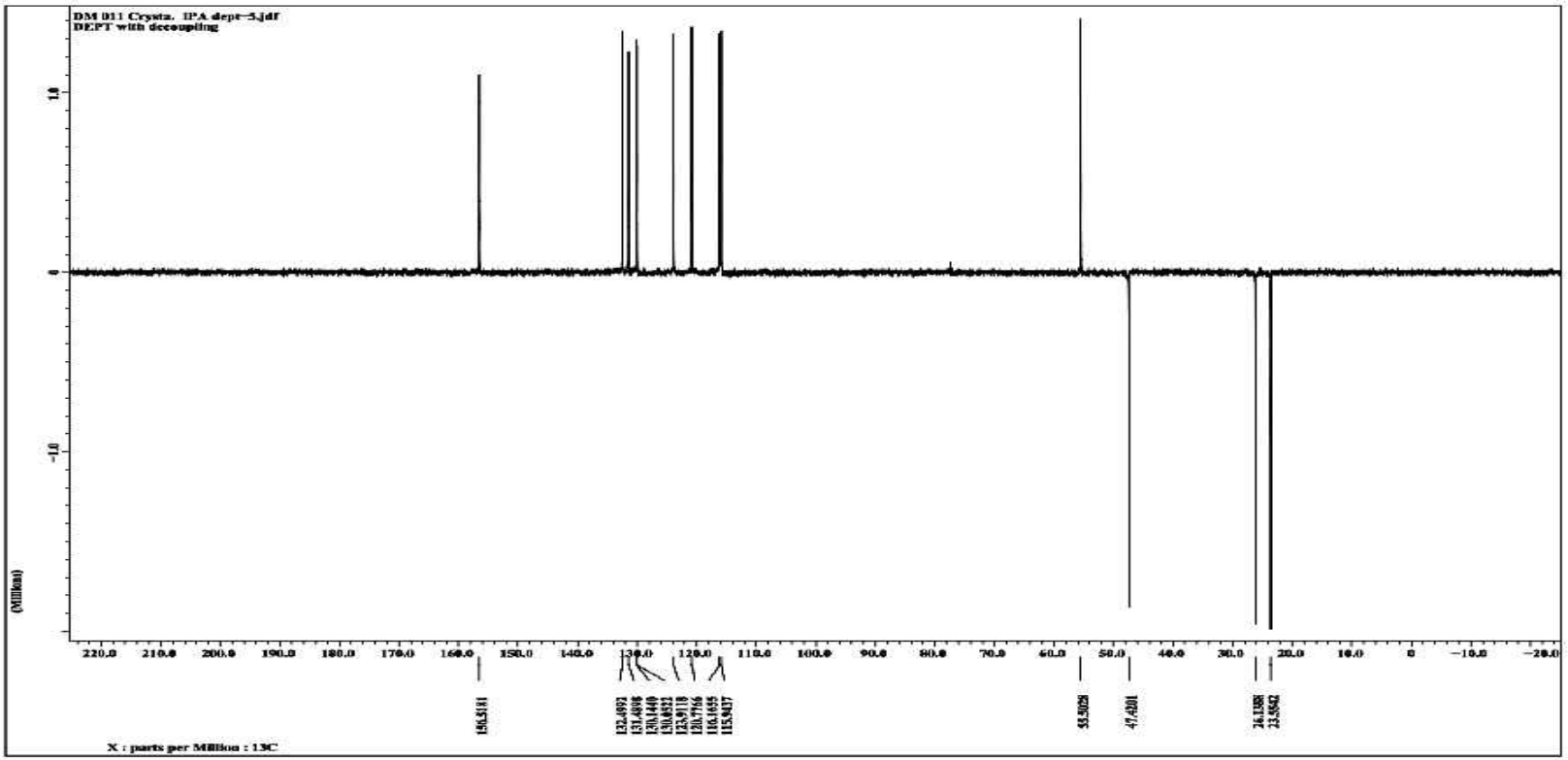

Appendix F7: IR Spectrum for Compound **4c**

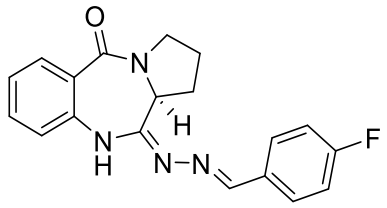

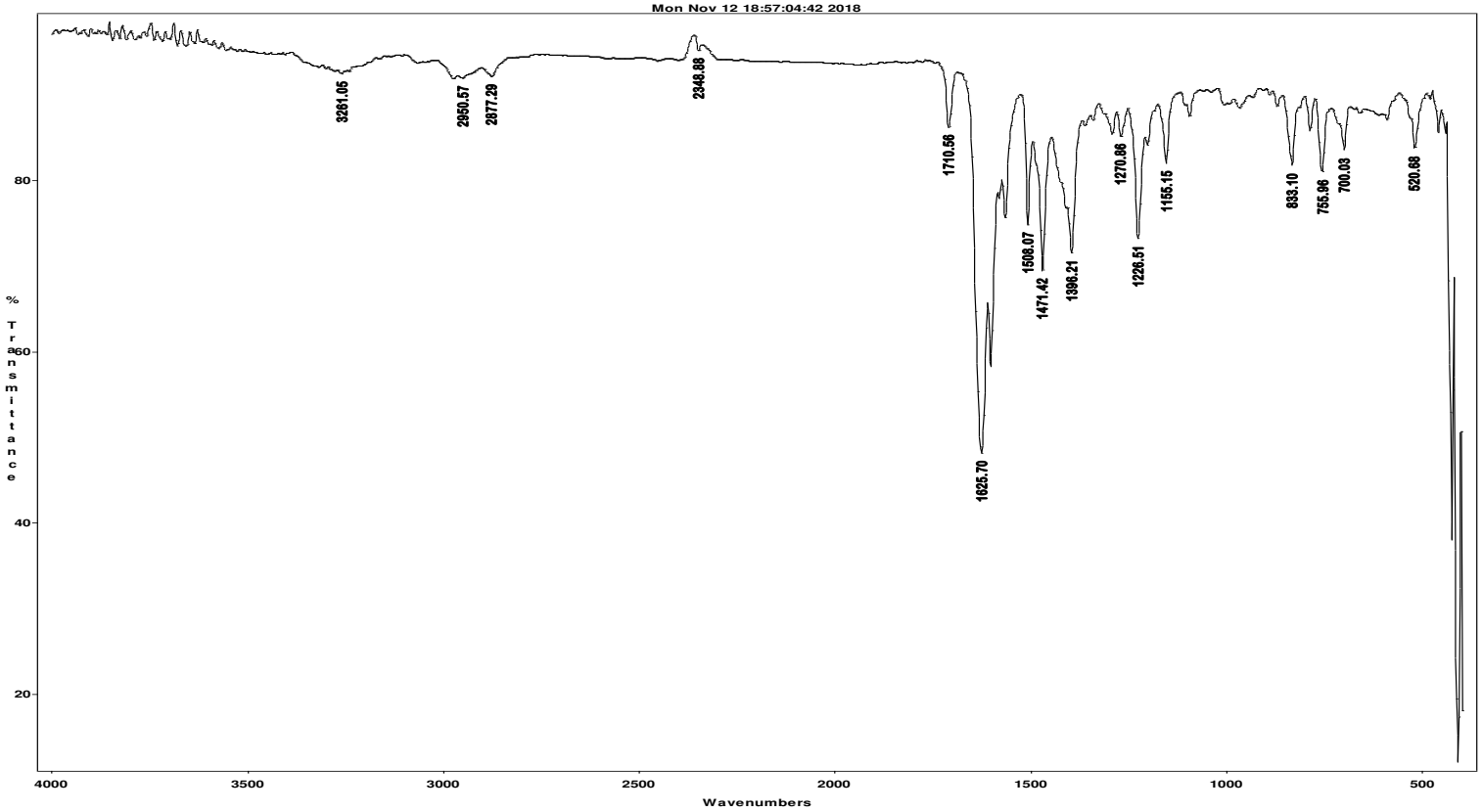

Appendix F8: UV-Vis Spectrum for Compound **4c**

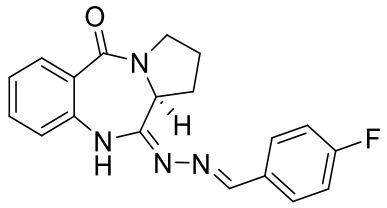

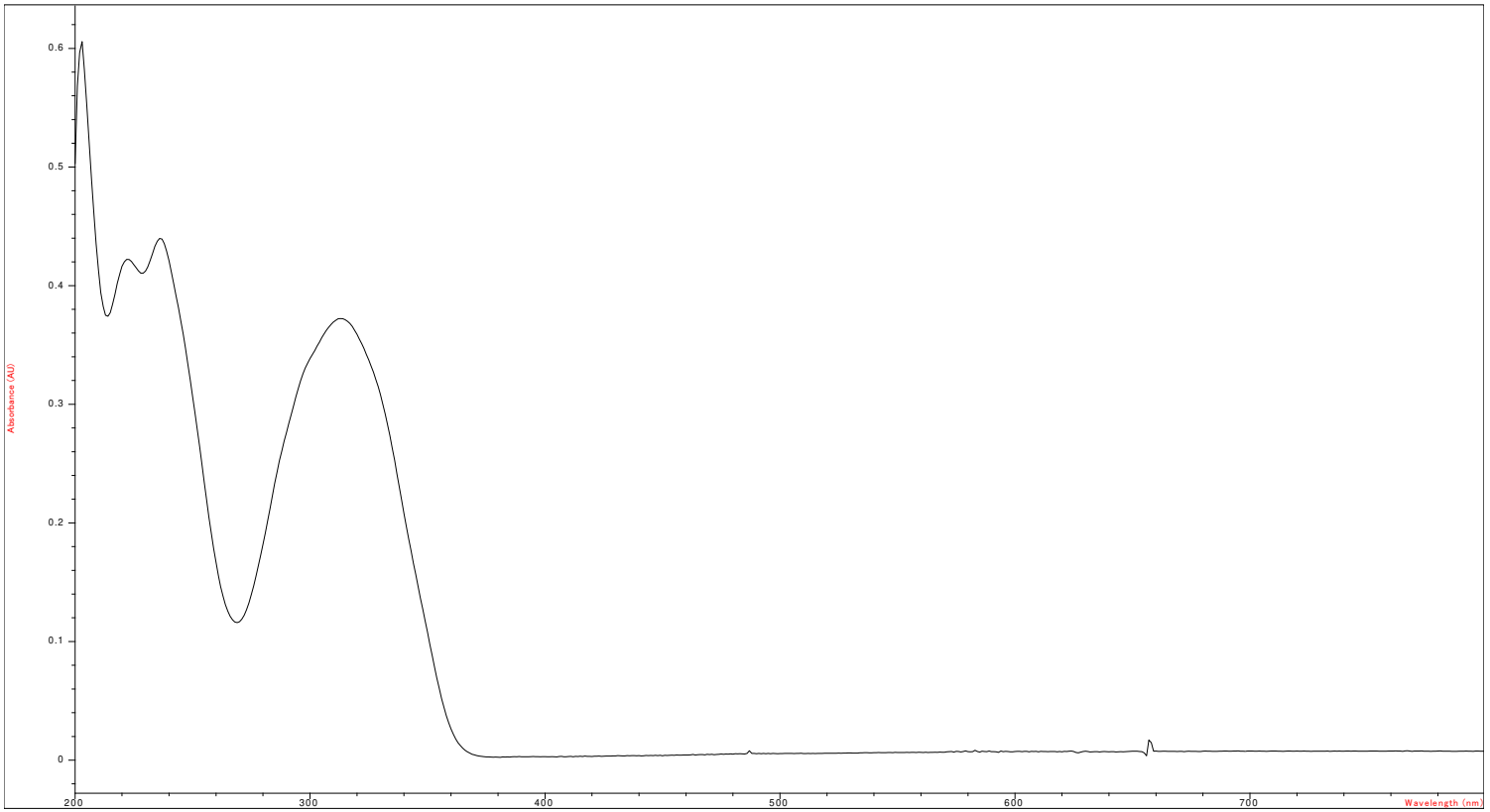

Appendix F9: GC/MS Spectrum for Compound **4c**

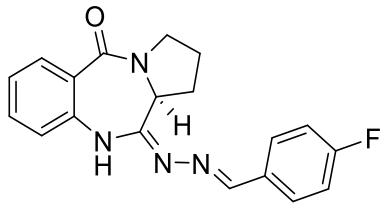

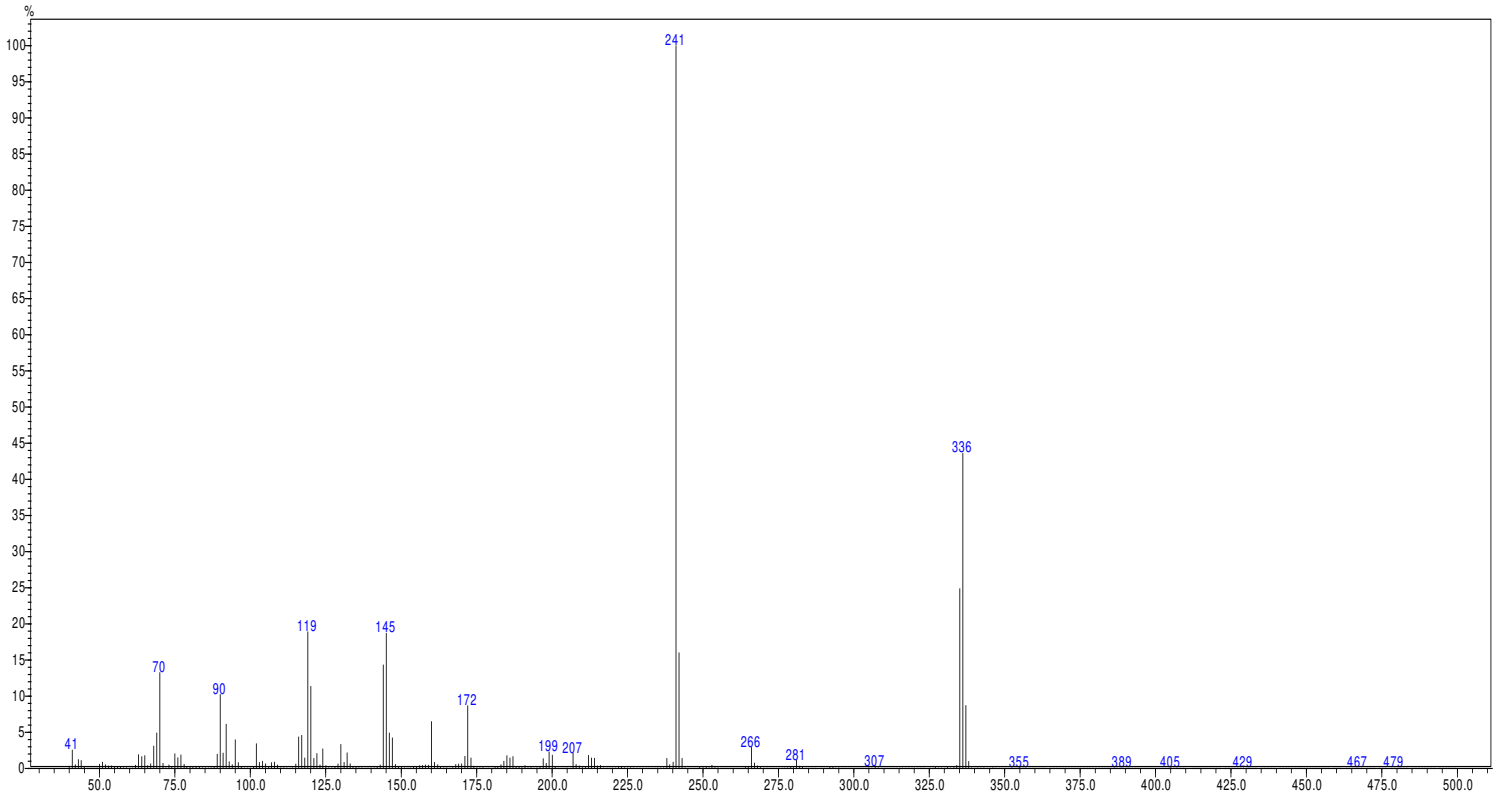

Appendix G1: ^{1}H NMR Spectrum for Compound **4d** in $CDCl_3$

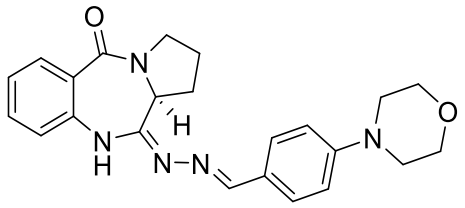

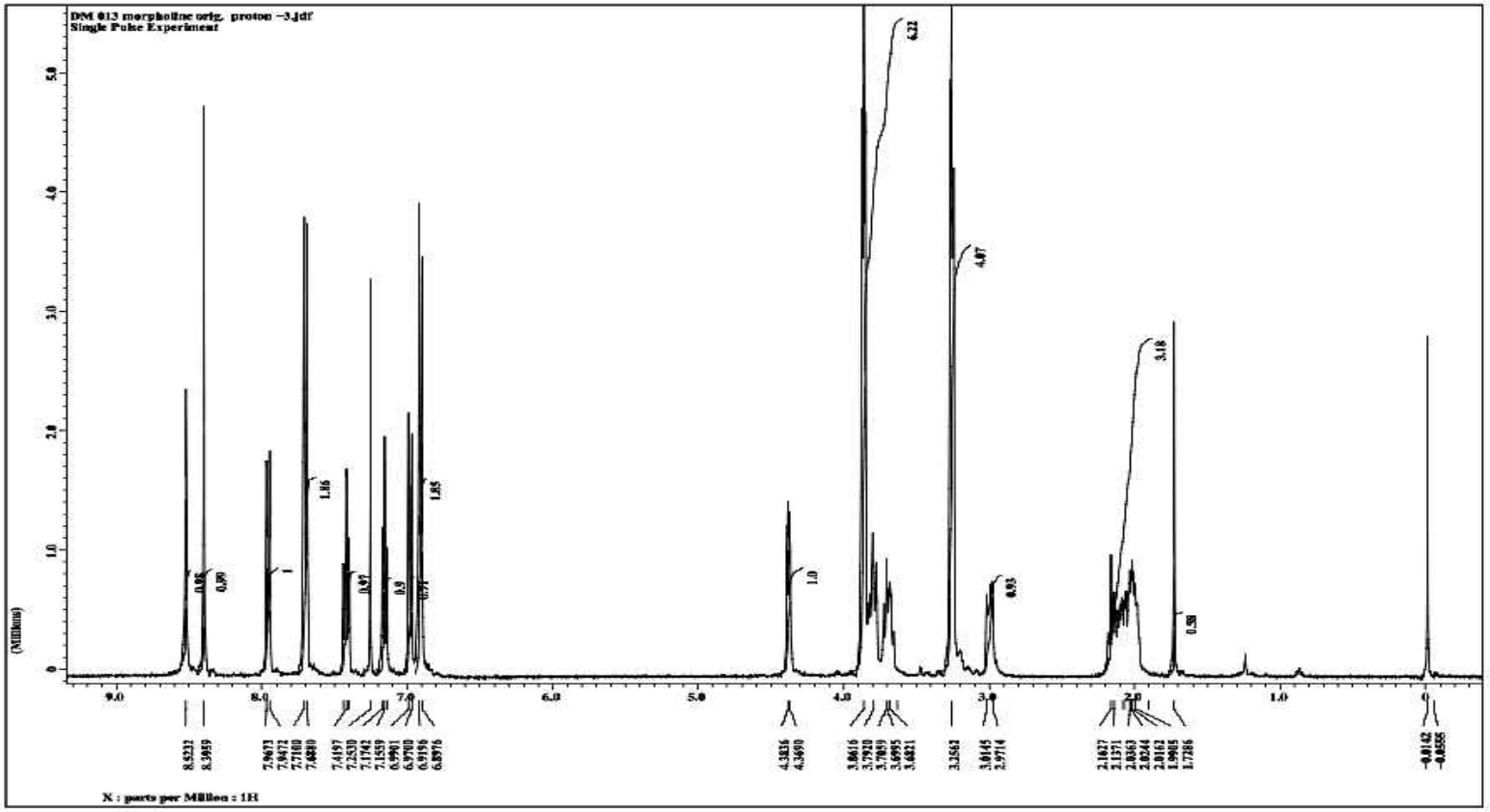

Appendix G2: ^{1}H NMR Spectrum for Compound **4d** in $CDCl_3$

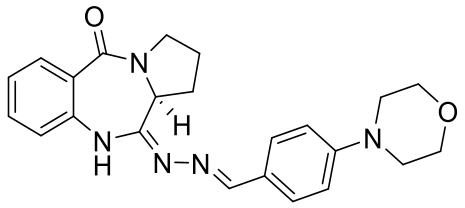

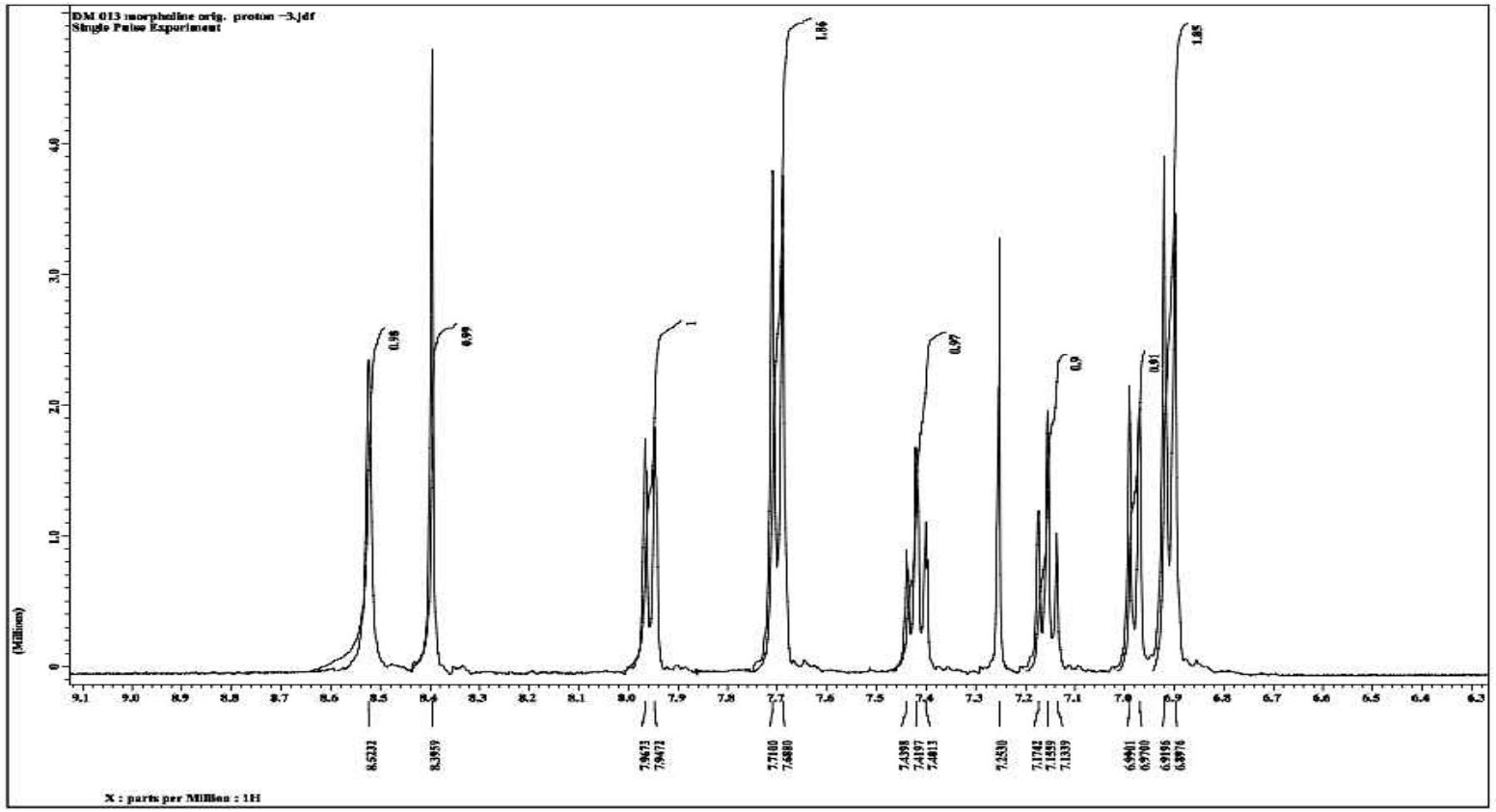

Appendix G3: ^{1}H NMR Spectrum for Compound **4d** in $CDCl_3$

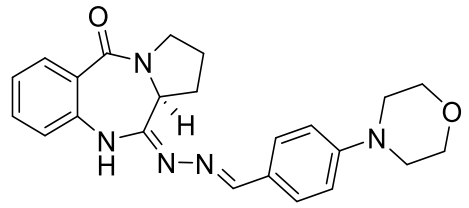

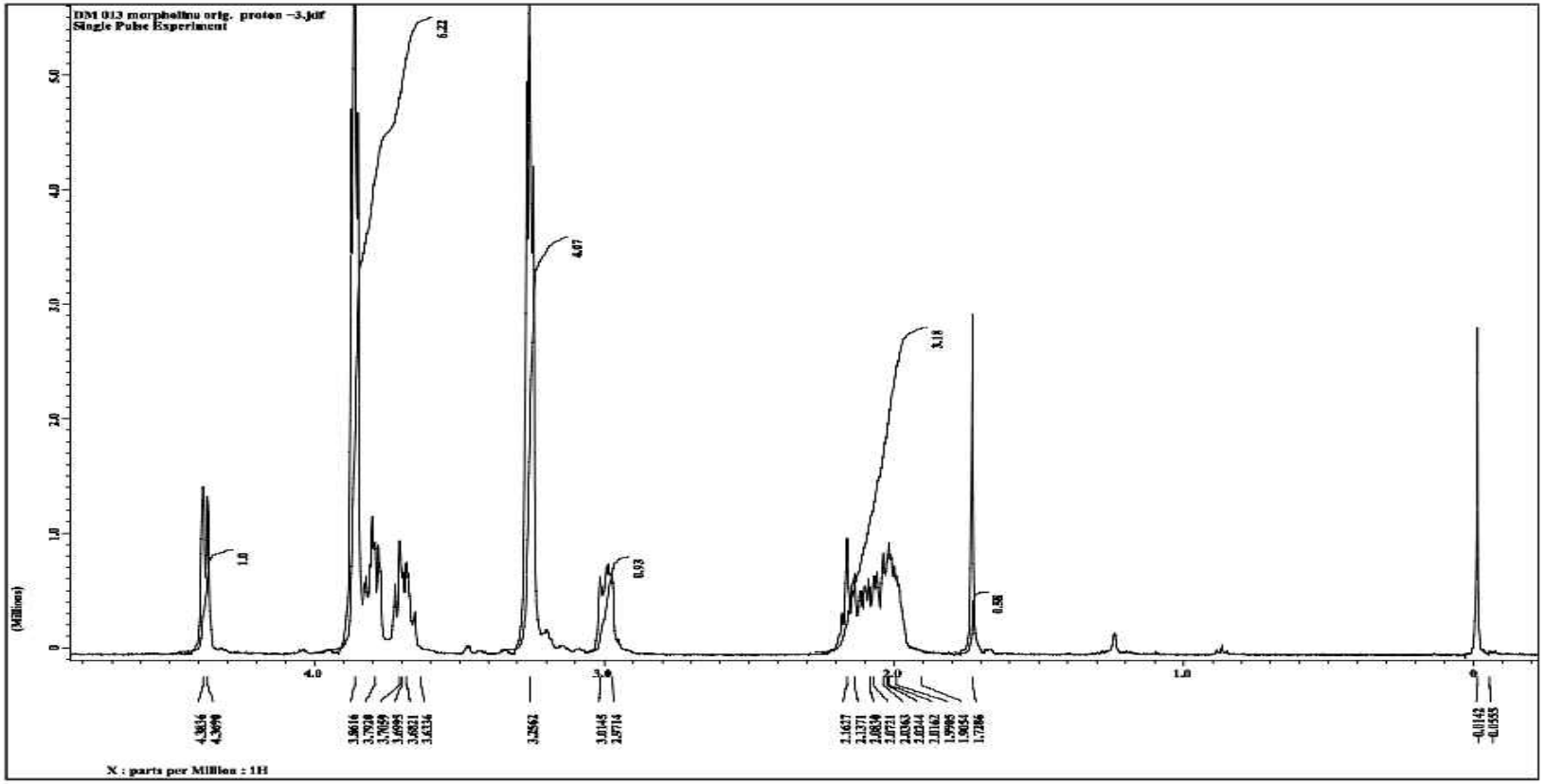

Appendix G4: ^{13} C NMR Spectrum for Compound **4d** in $CDCl_3$

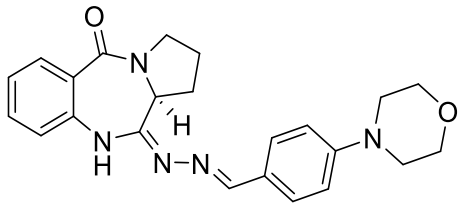

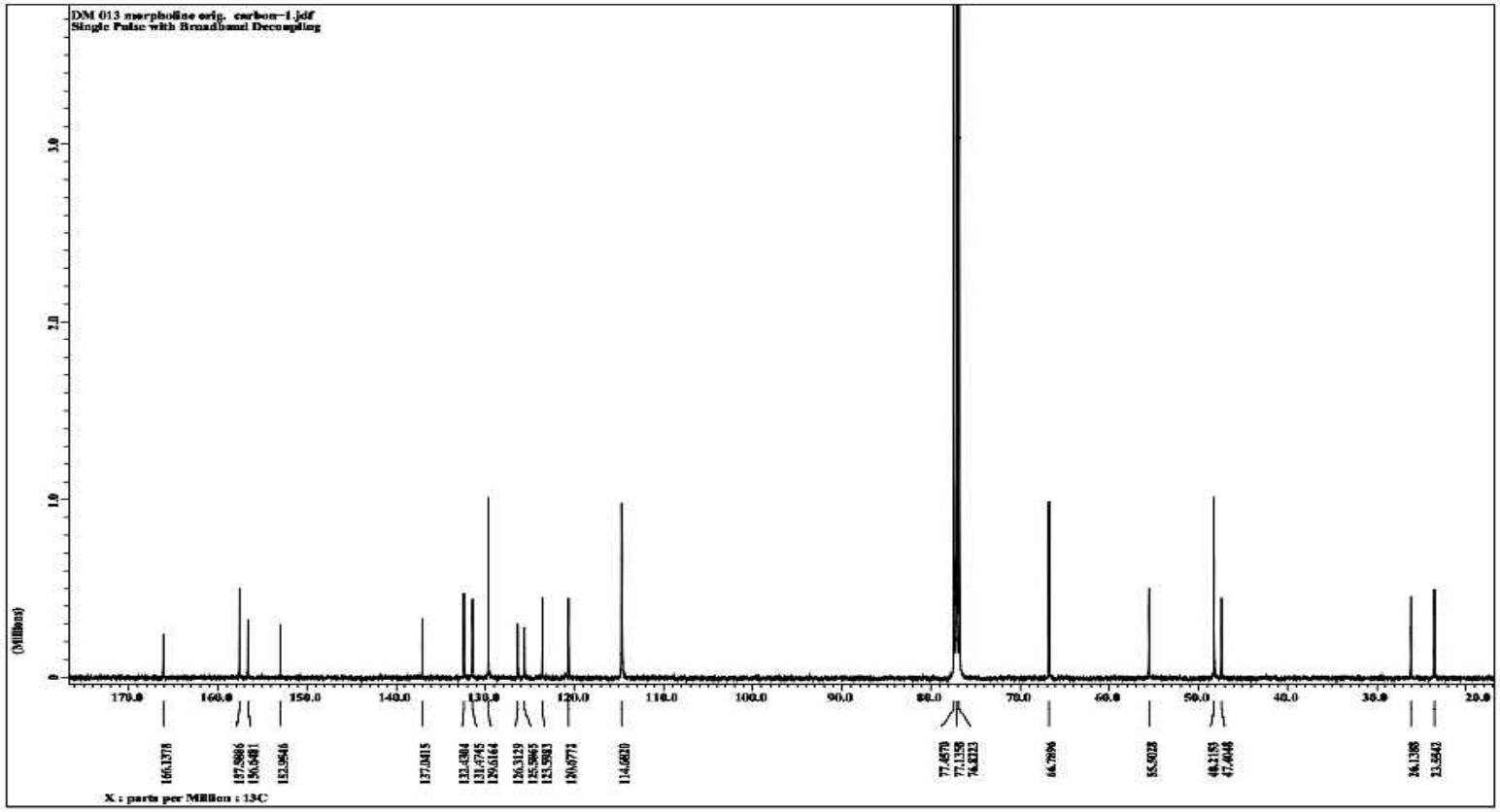

Appendix G5: ^{13} C NMR Spectrum for Compound **4d** in $CDCl_3$

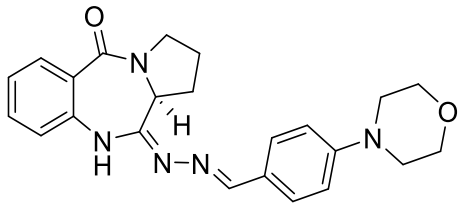

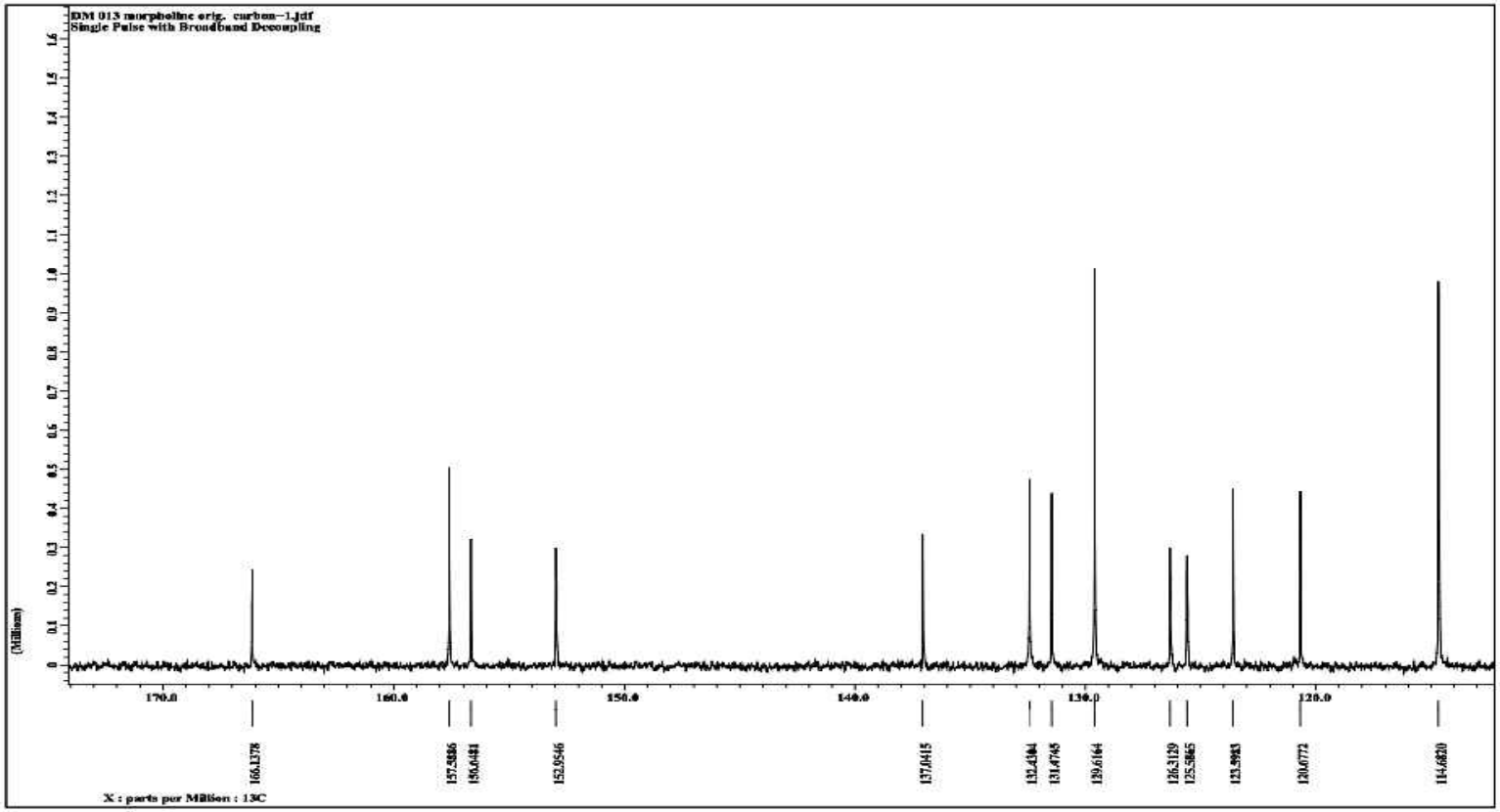

AppendixG6: C-DEPT-135 Spectrum for Compound **4d** in $CDCl_3$

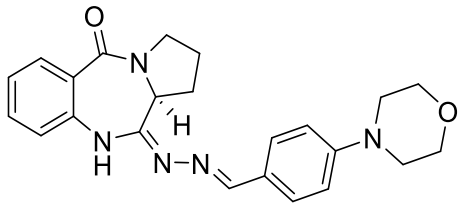

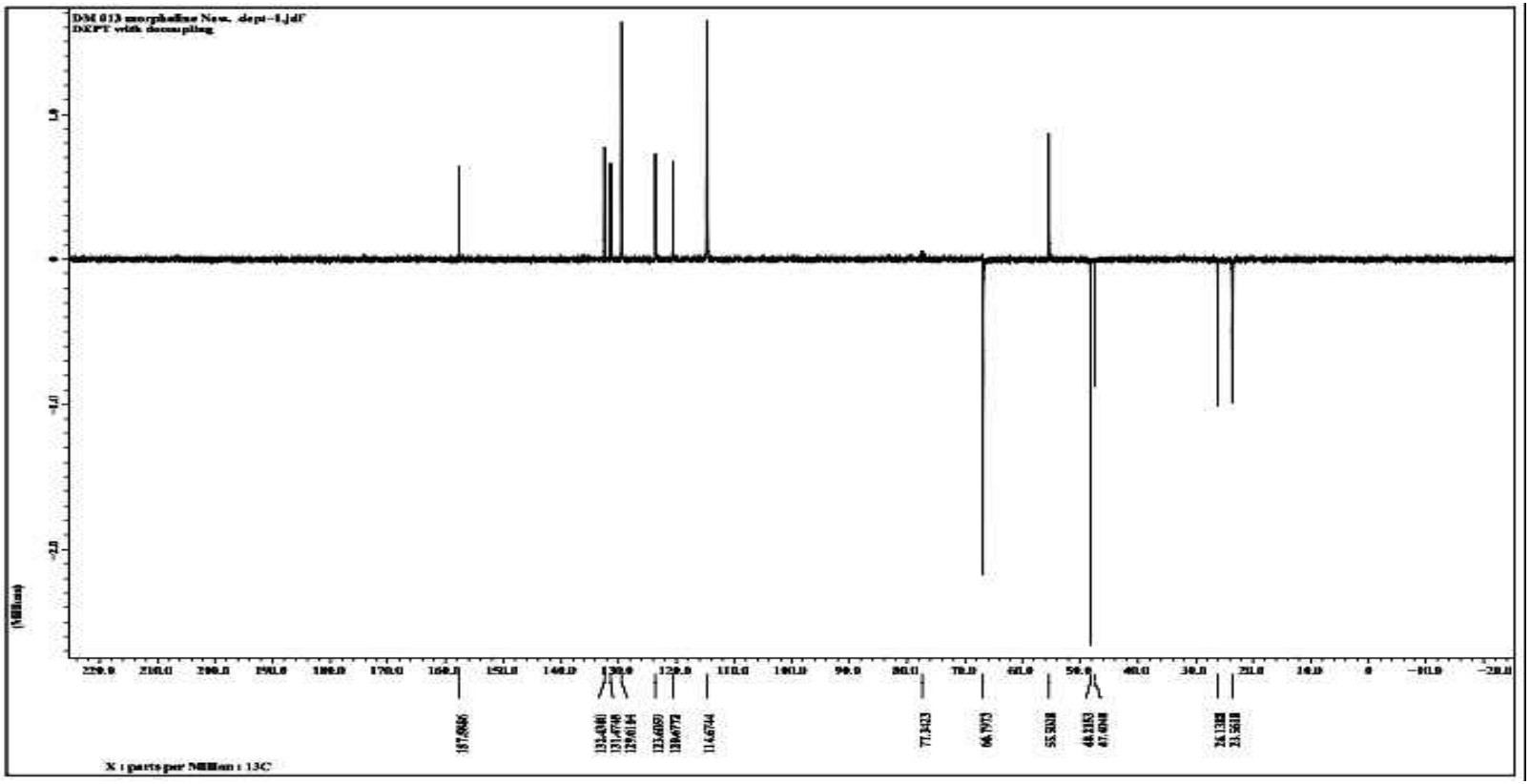

Appendix G7: IR Spectrum for Compound **4d**

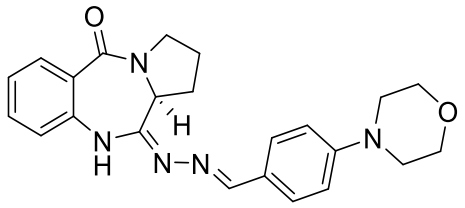

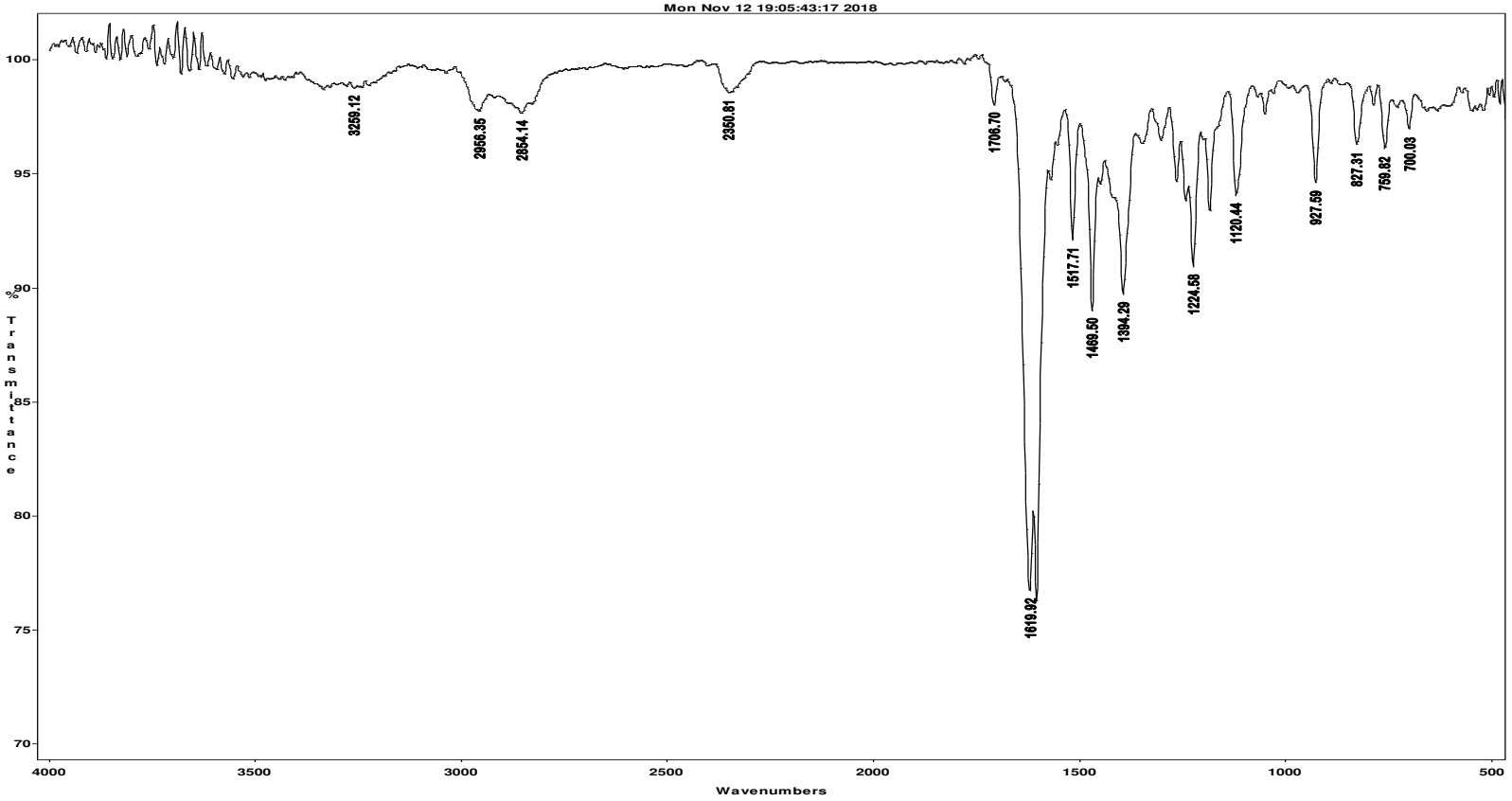

Appendix G8: GC/MS Spectrum for Compound **4d**

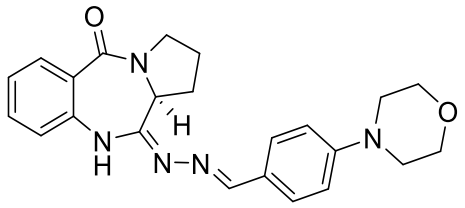

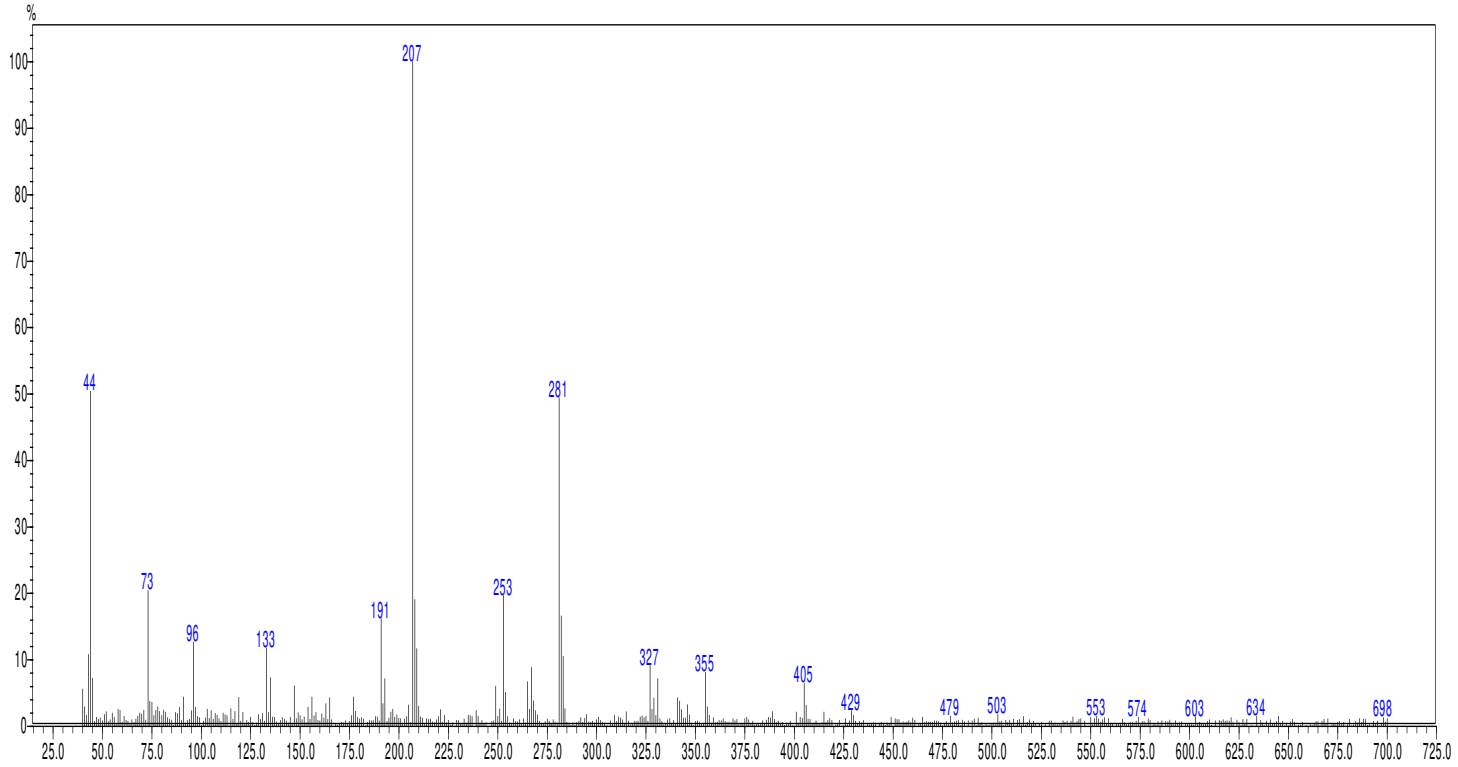

Appendix H1: ^{1}H NMR Spectrum for Compound **4e** in $CDCl_3$

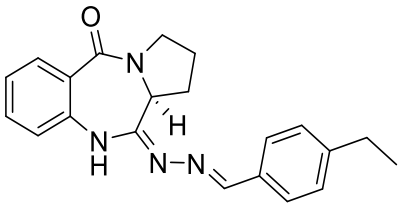

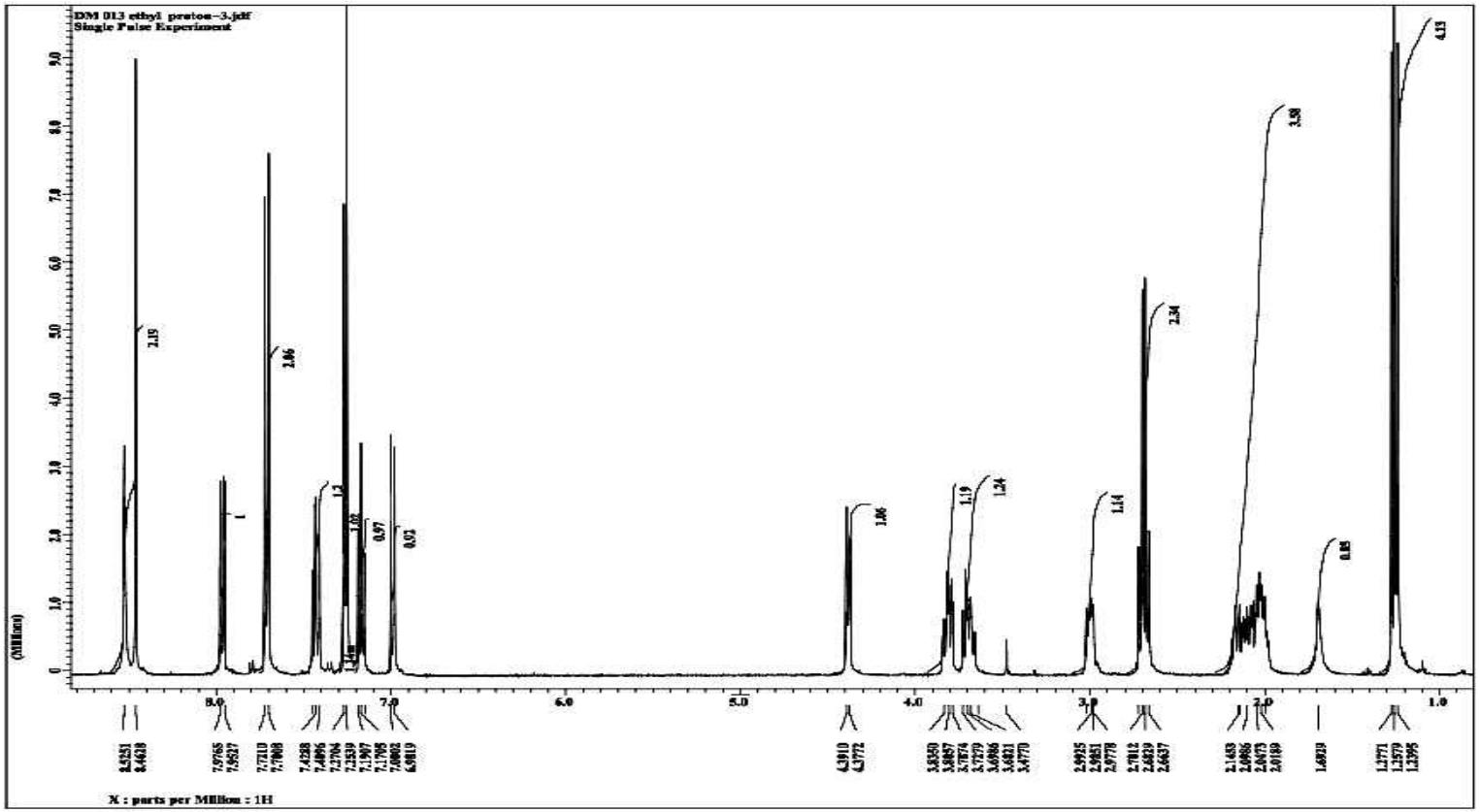

Appendix H2: ^{1}H NMR Spectrum for Compound **4e** in $CDCl_3$

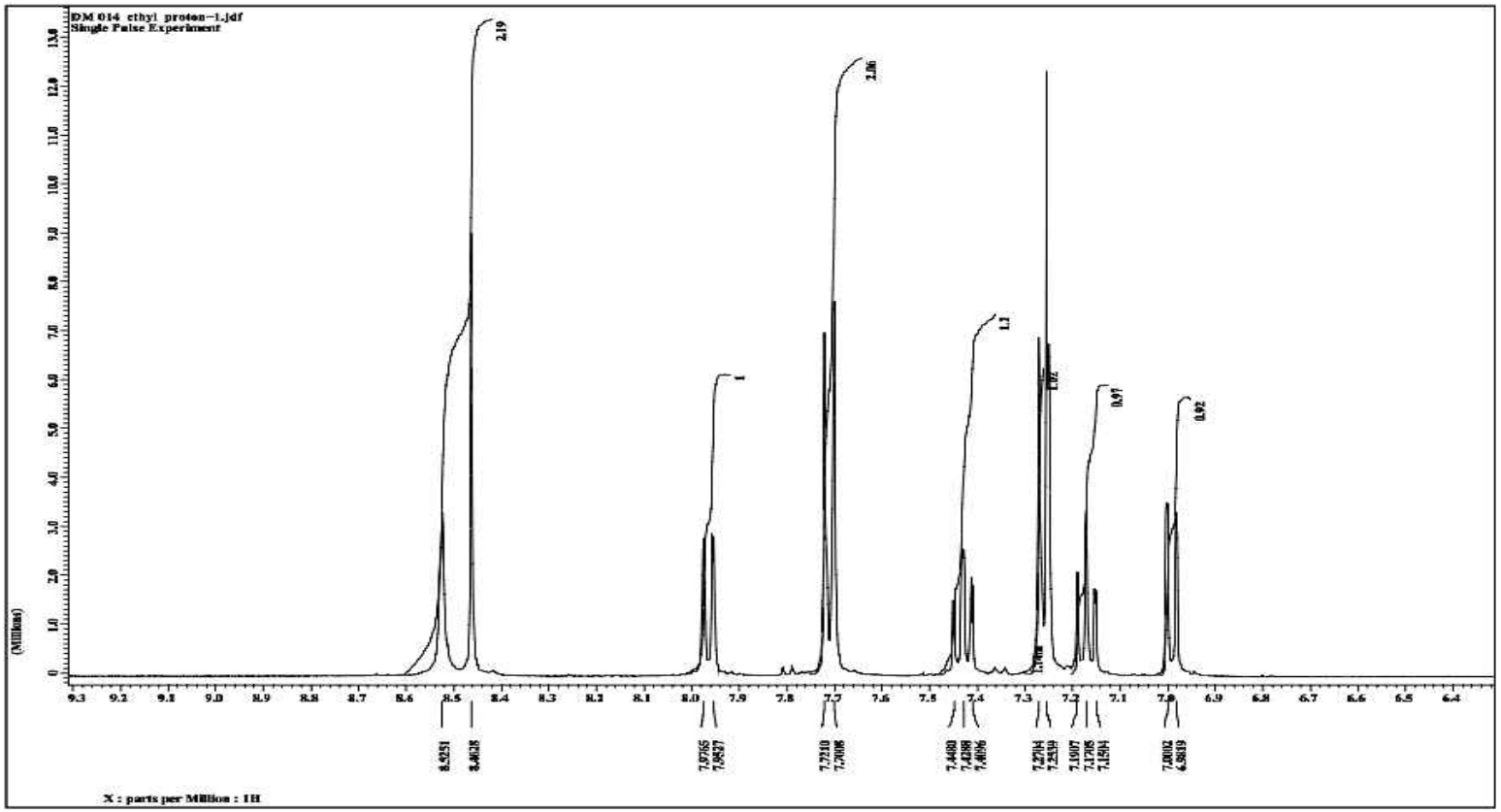

Appendix H3: ^{1}H NMR Spectrum for Compound **4e** in $CDCl_3$

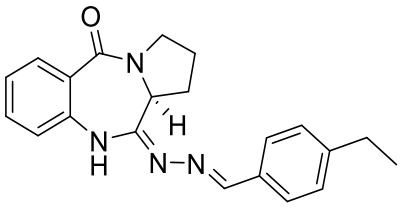

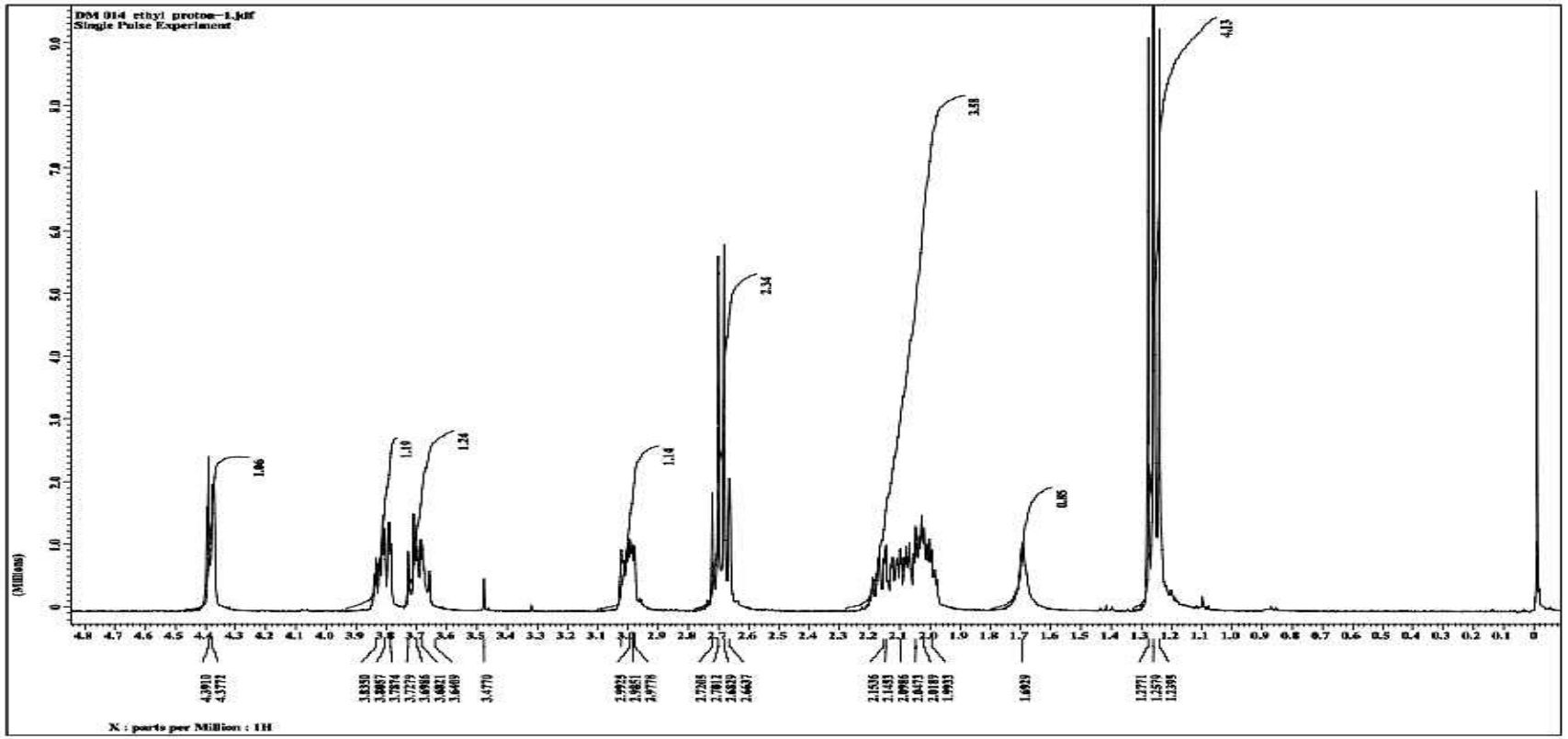

Appendix H4: ^{13} C NMR Spectrum for Compound **4e** in $CDCl_3$

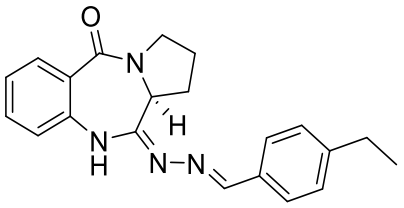

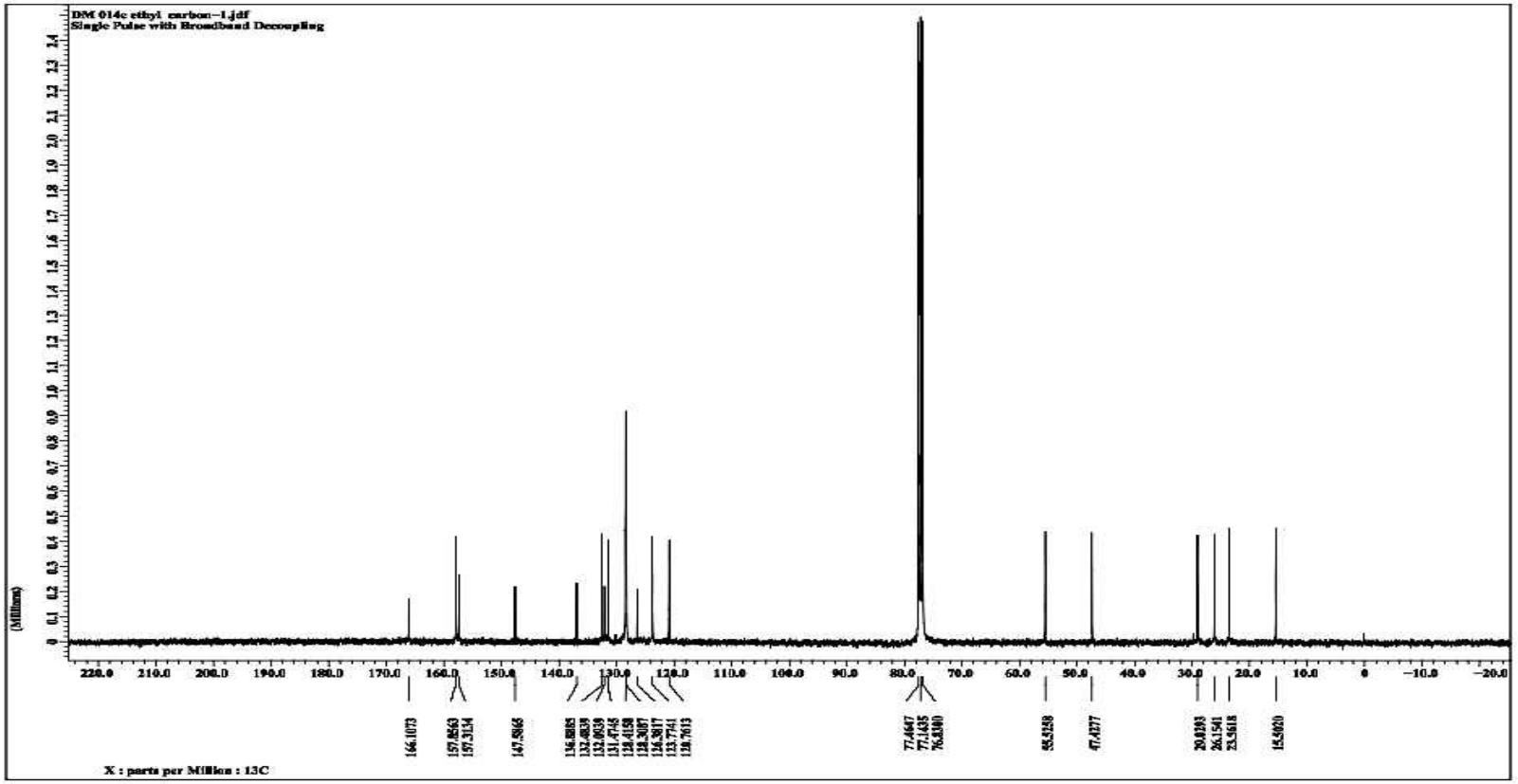

Appendix H5: ^{13} C NMR Spectrum for Compound **4e** in $CDCl_3$

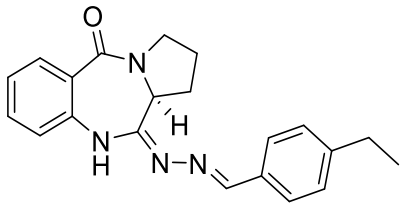

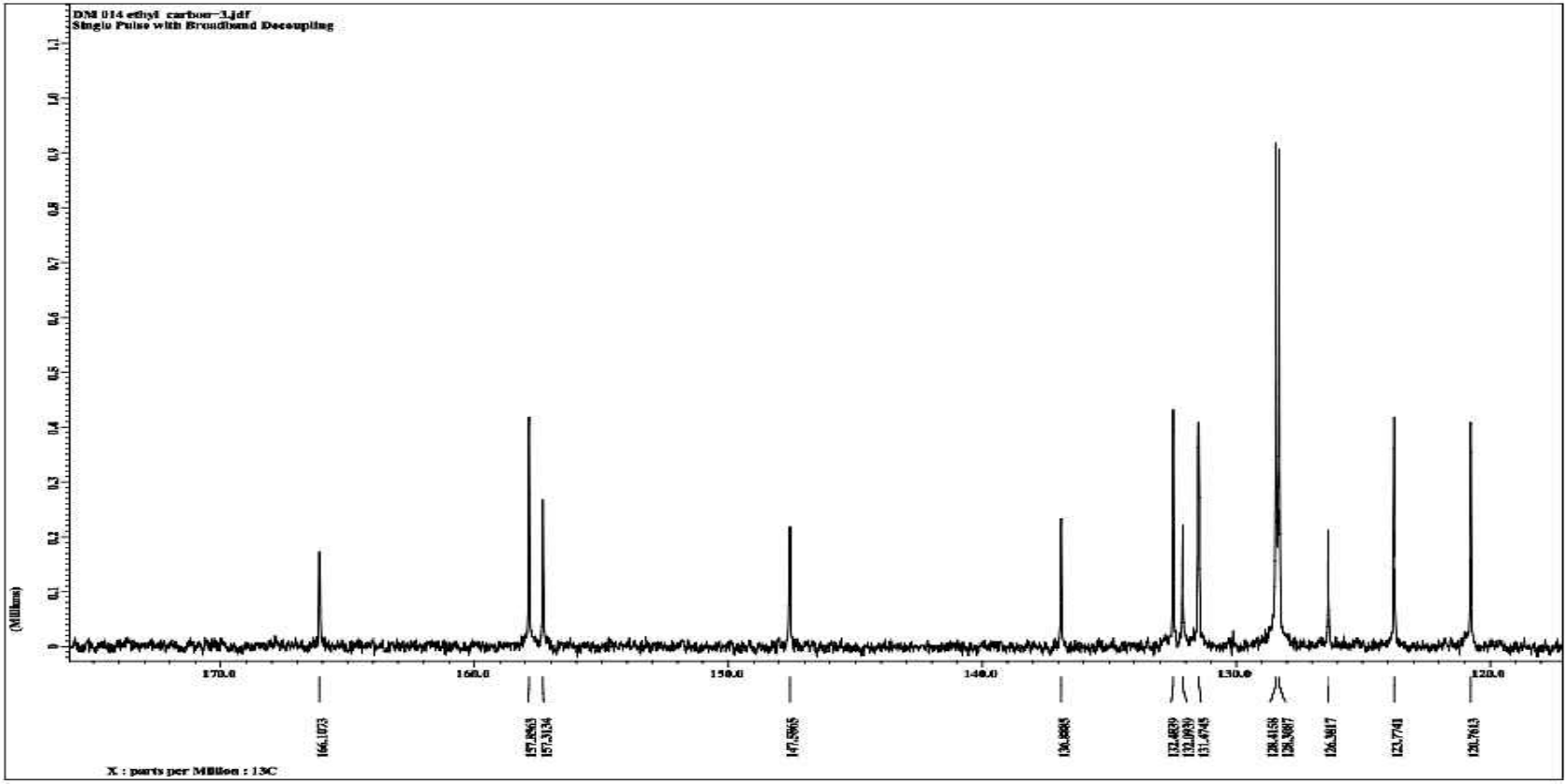

Appendix H6: C-DEPT-135 Spectrum for Compound **4e** in $CDCl_3$

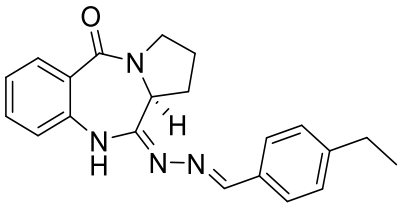

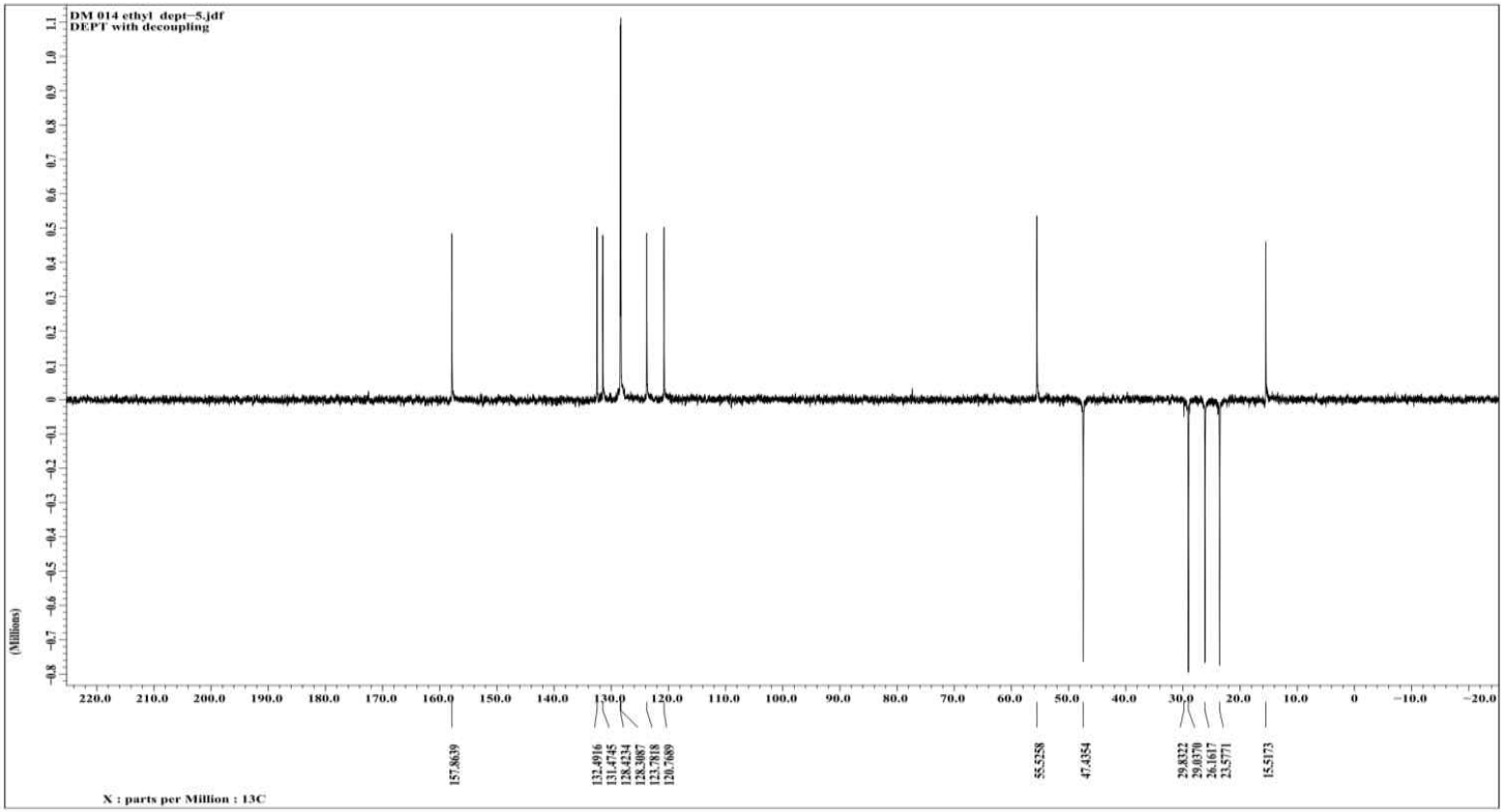

Appendix H7: IR Spectrum for Compound **4e**

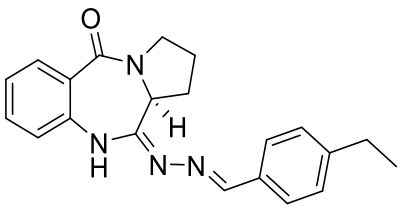

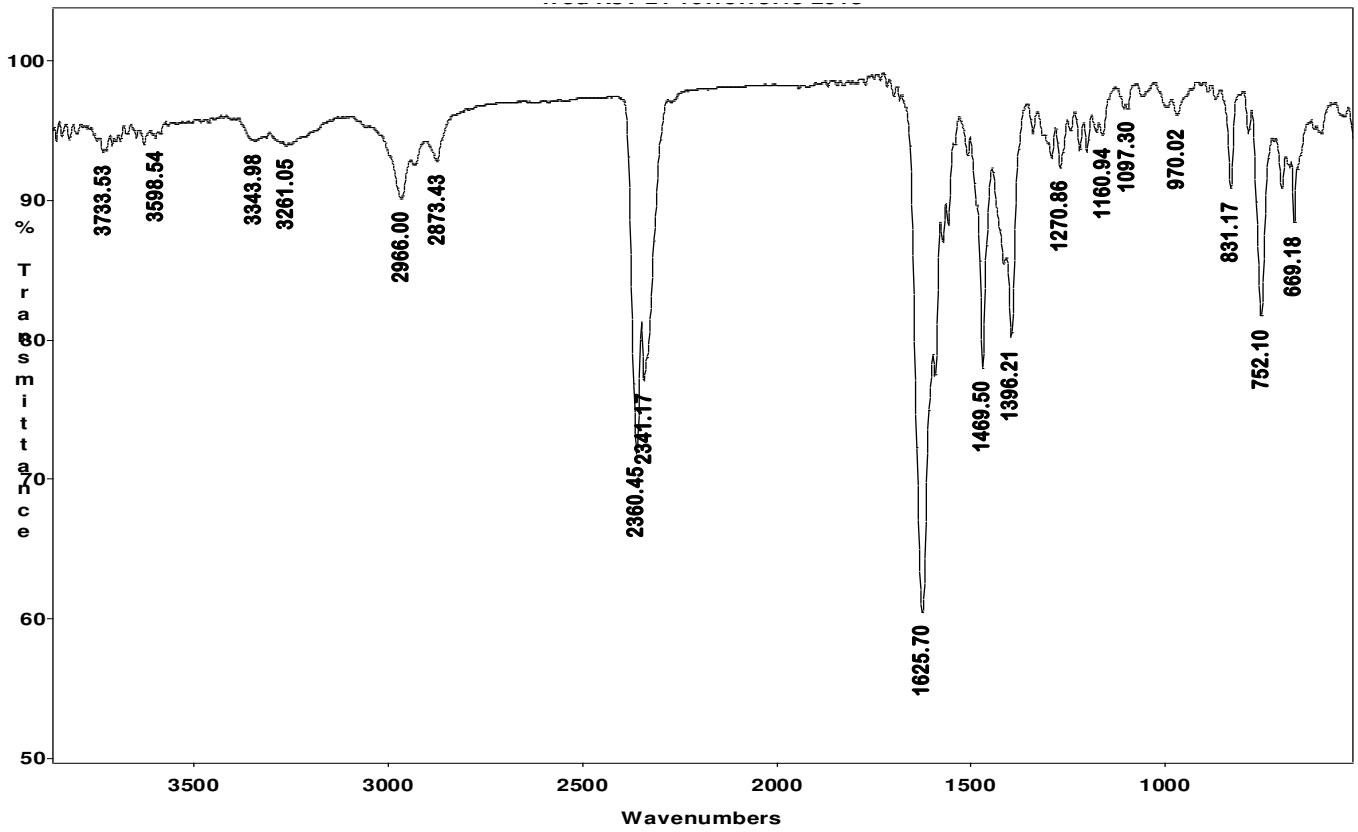

Appendix H8: GC/MS Spectrum for Compound **4e**

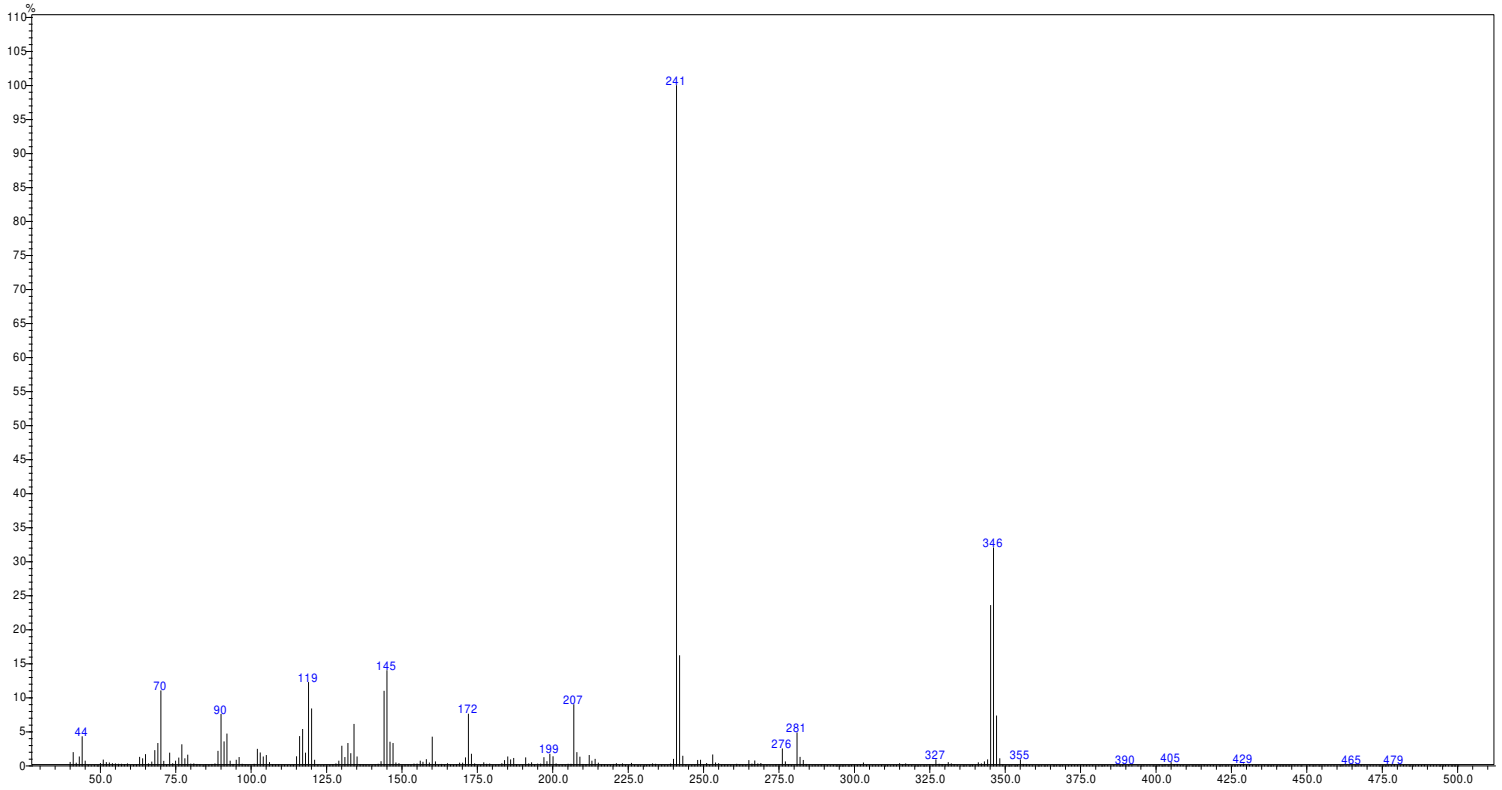

Appendix I1: ^{1}H NMR Spectrum for Compound **4f** in $CDCl_3$

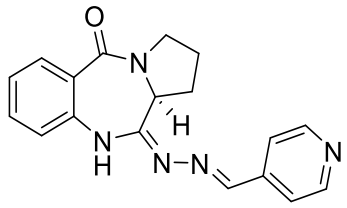

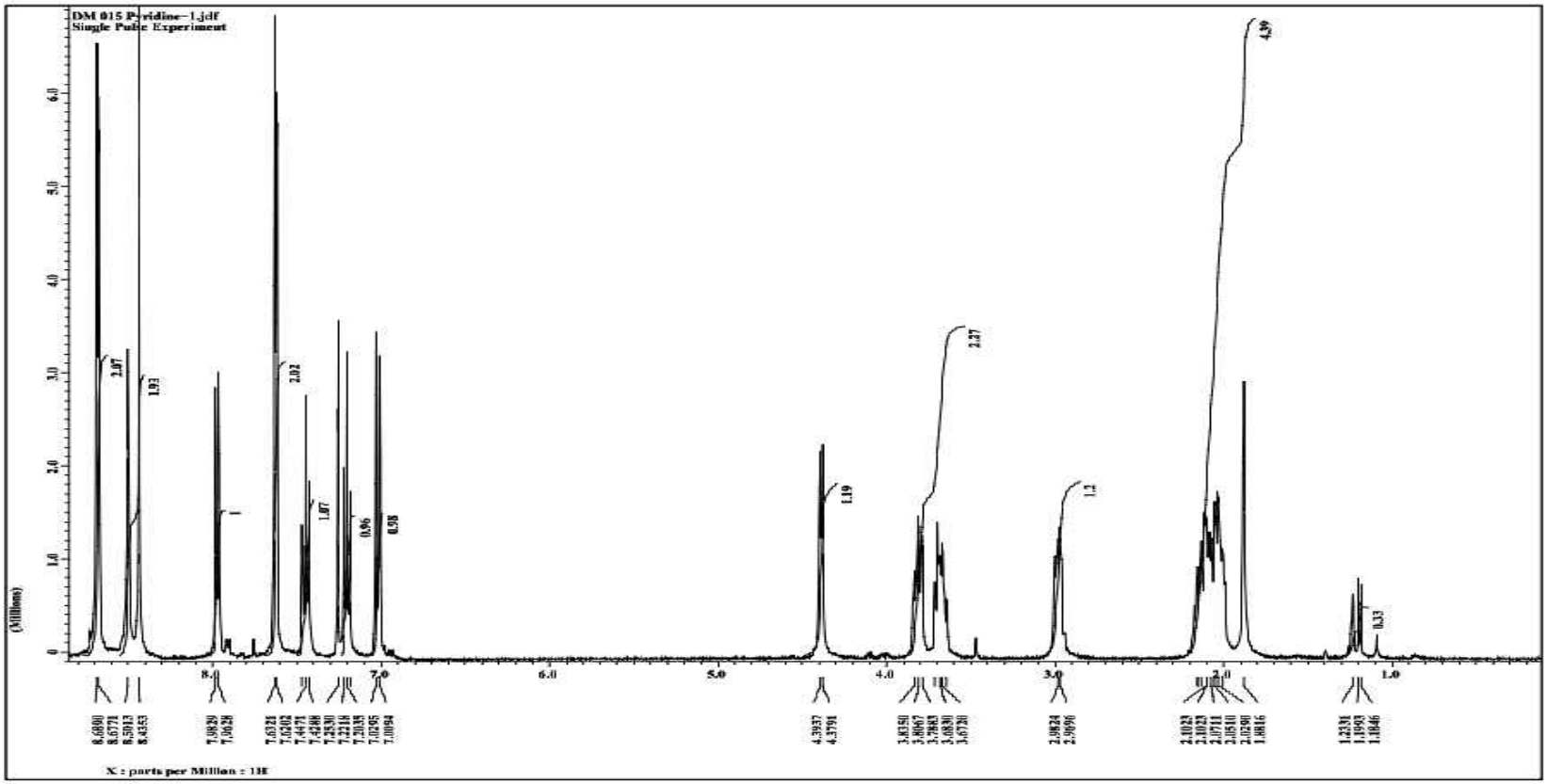

Appendix I2: ^{1}H NMR Spectrum for Compound **4f** in $CDCl_3$

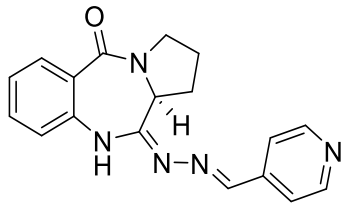

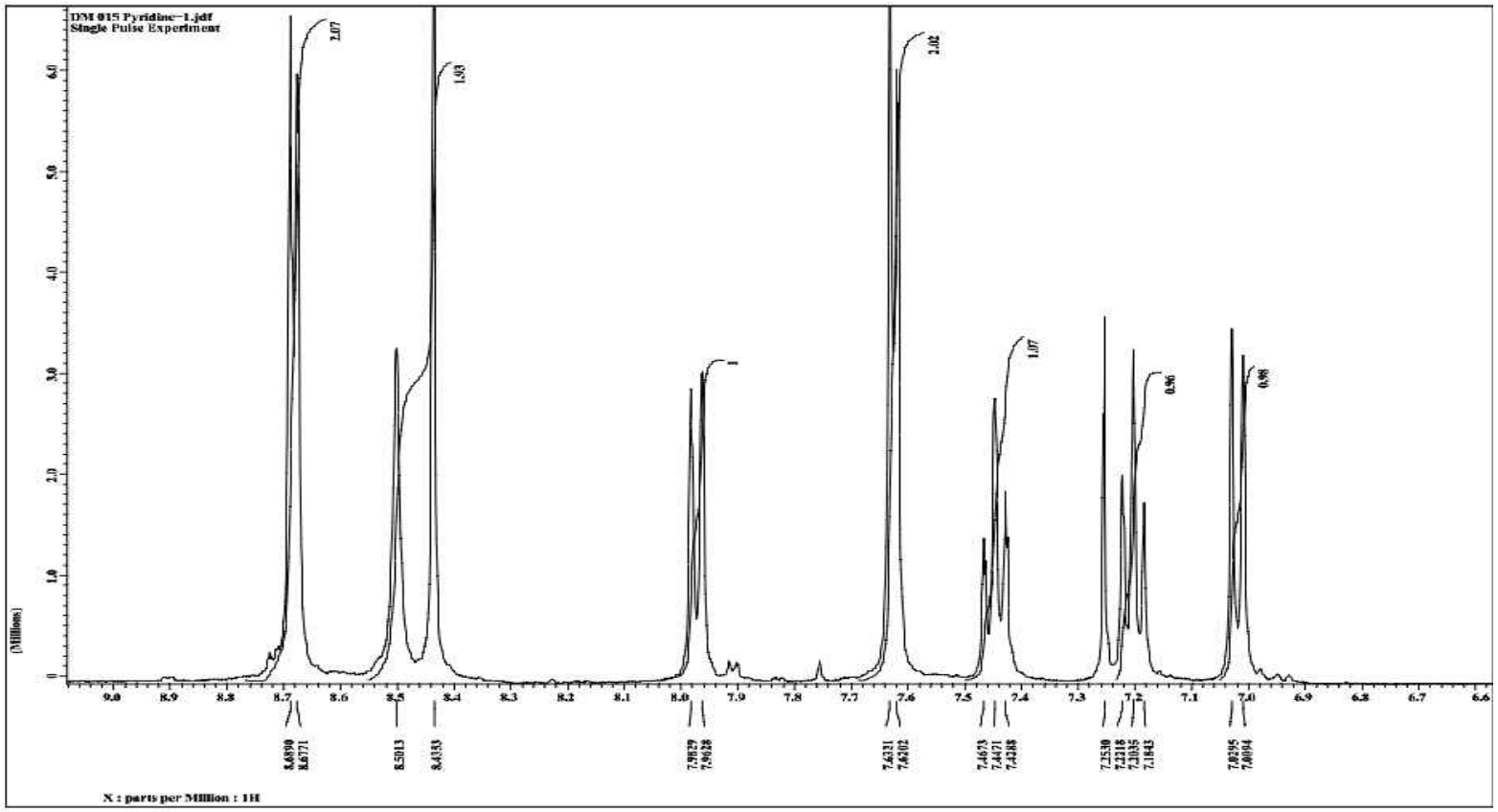

Appendix I3: ^{1}H NMR Spectrum for Compound **4f** in $CDCl_3$

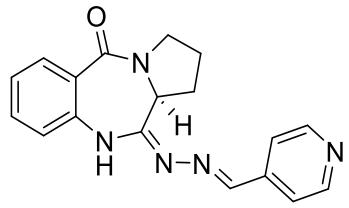

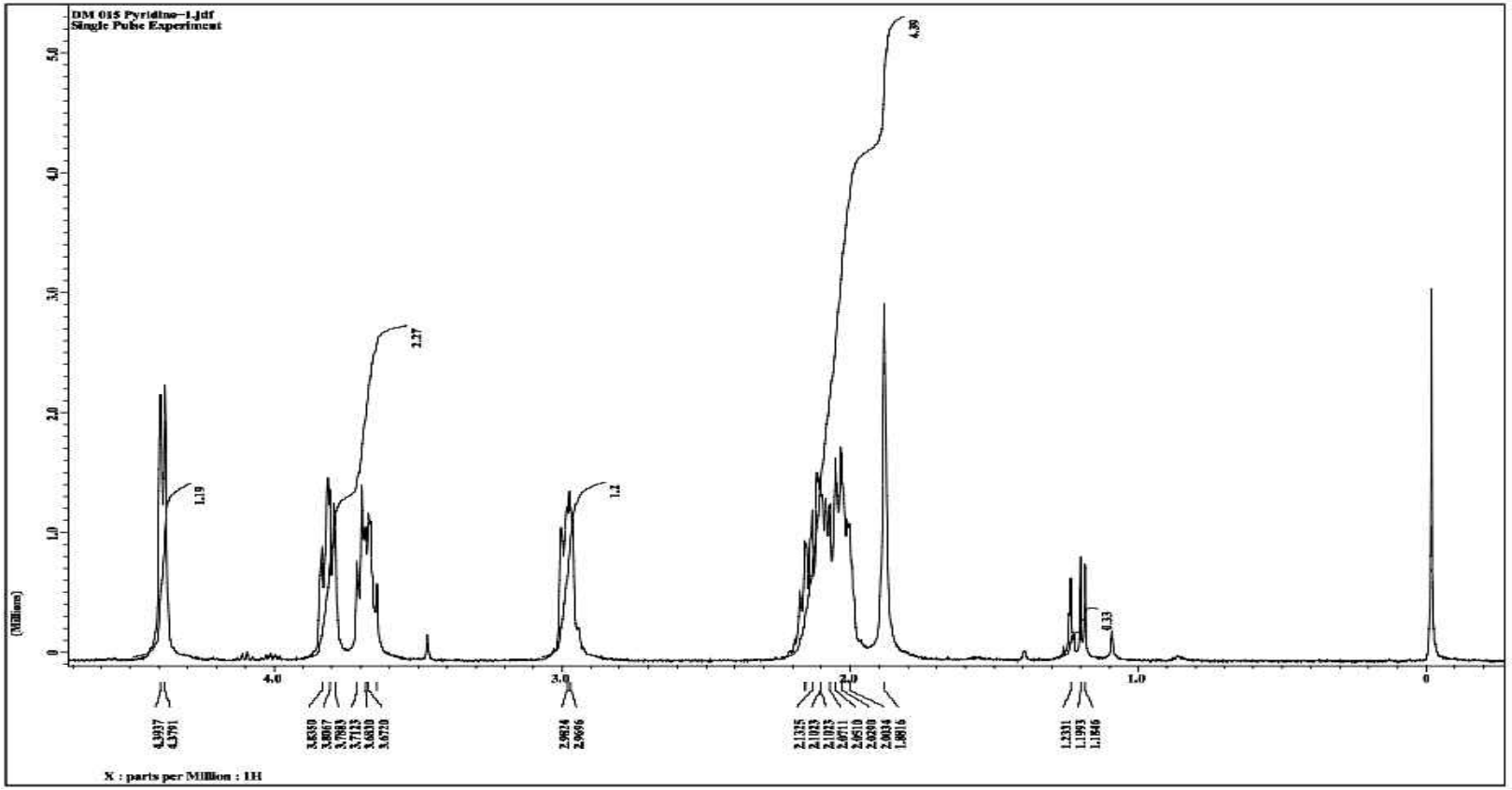

Appendix I4: ^{13} C NMR Spectrum for Compound **4f** in $CDCl_3$

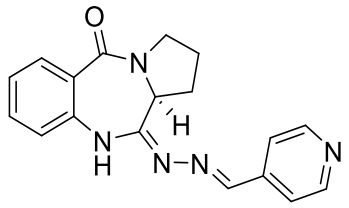

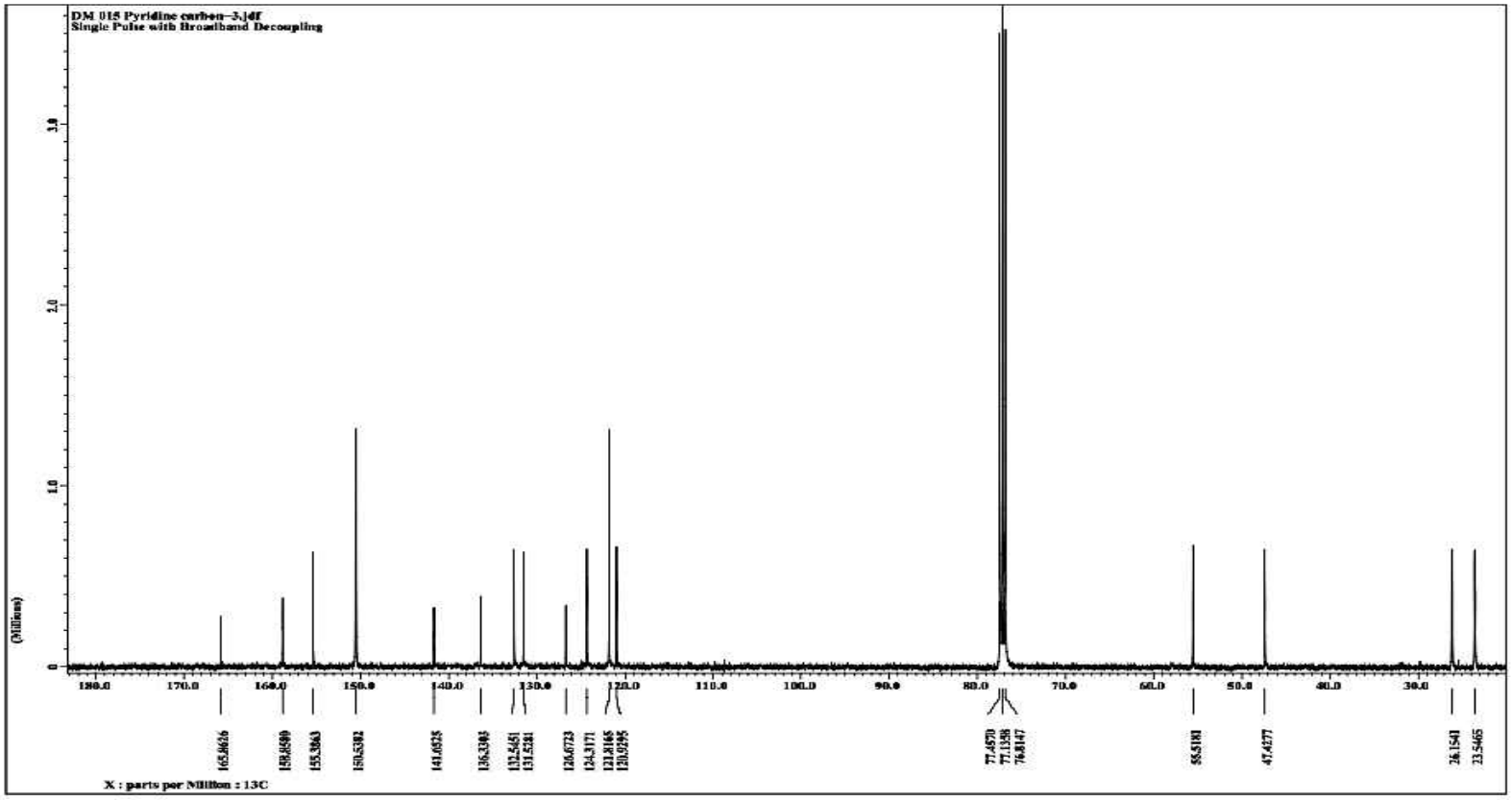

AppendixI5: C-DEPT-135 Spectrum for Compound **4f** in $CDCl_3$

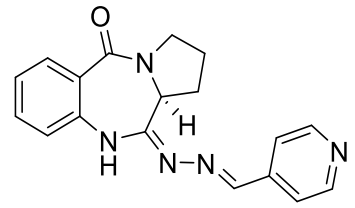

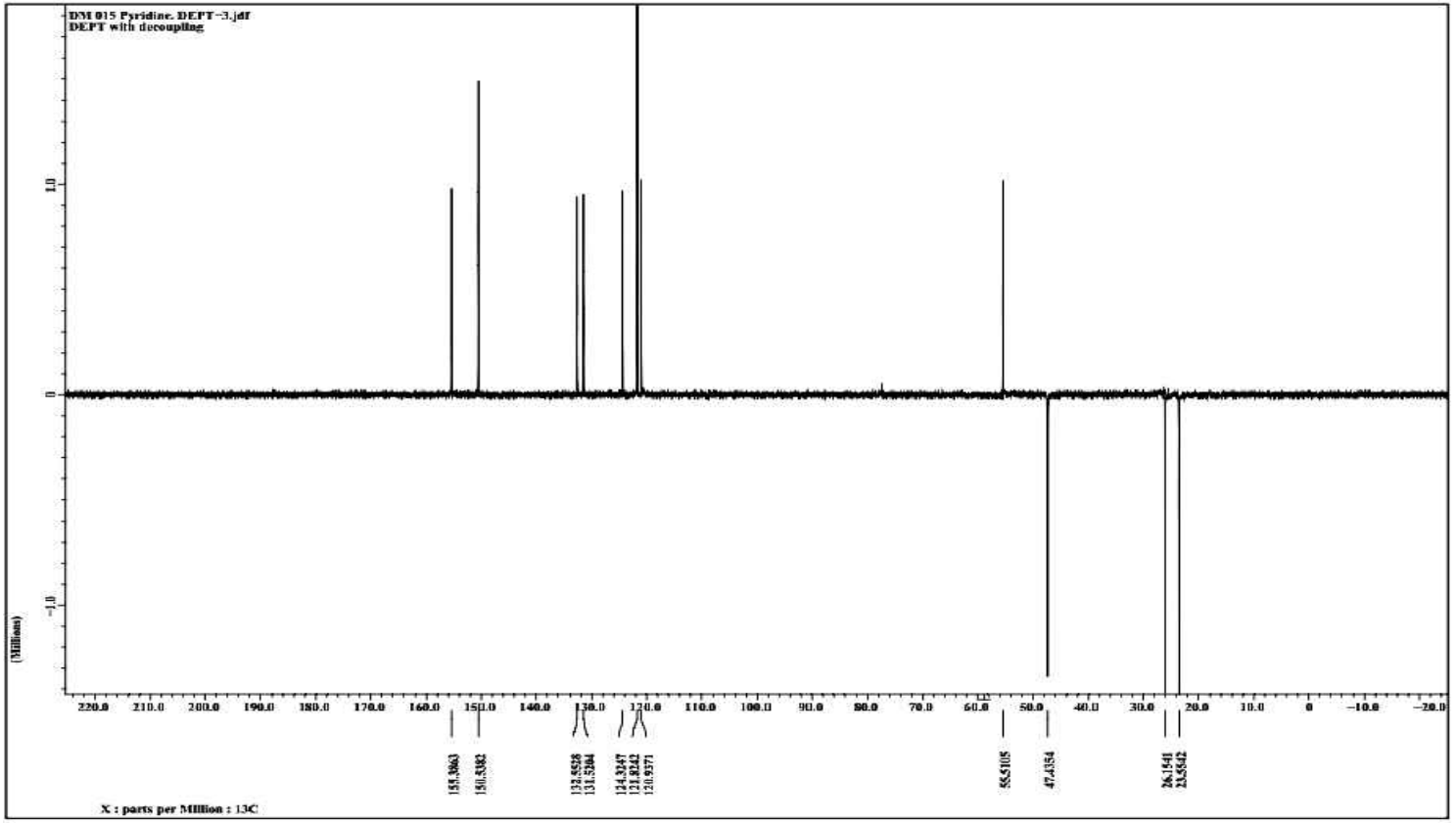

Appendix I6: IR Spectrum for Compound **4f**

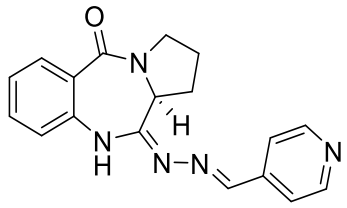

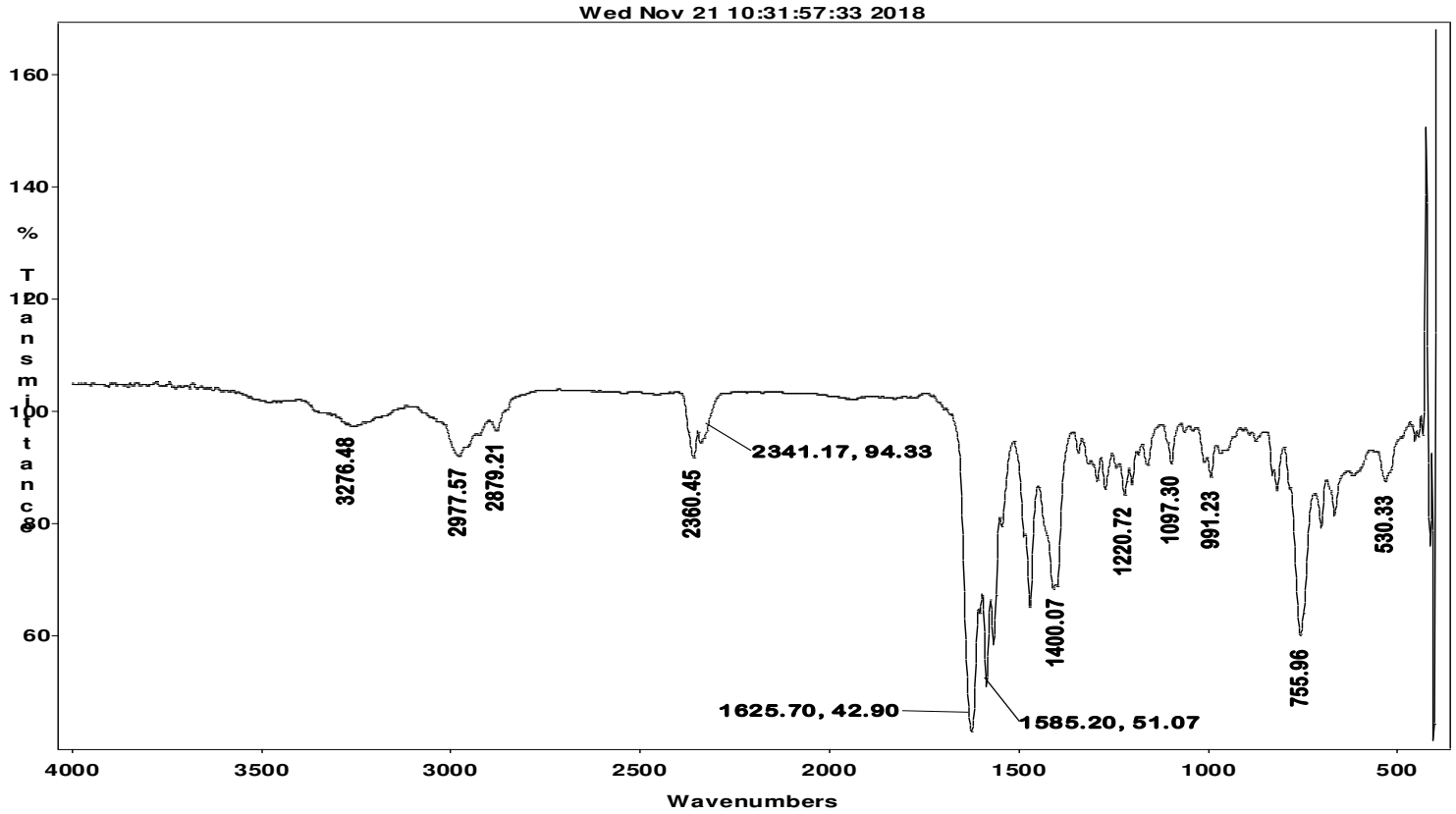

Appendix I7: UV-Vis Spectrum for Compound **4f**

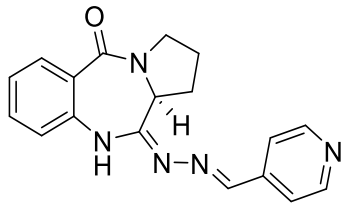

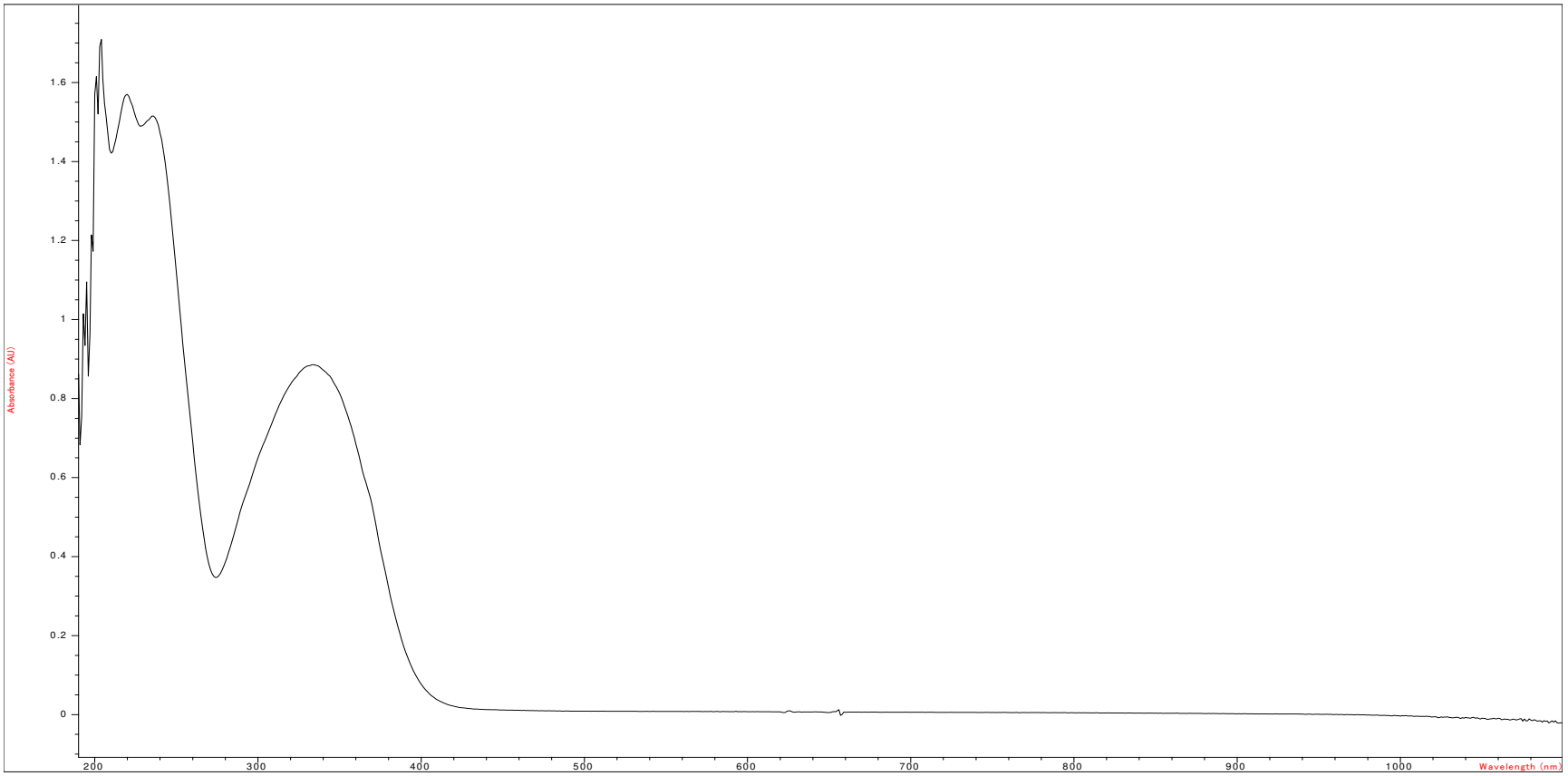

Appendix I8: GC/MS Spectrum for Compound **4f**

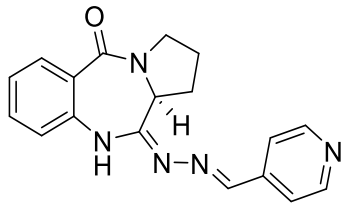

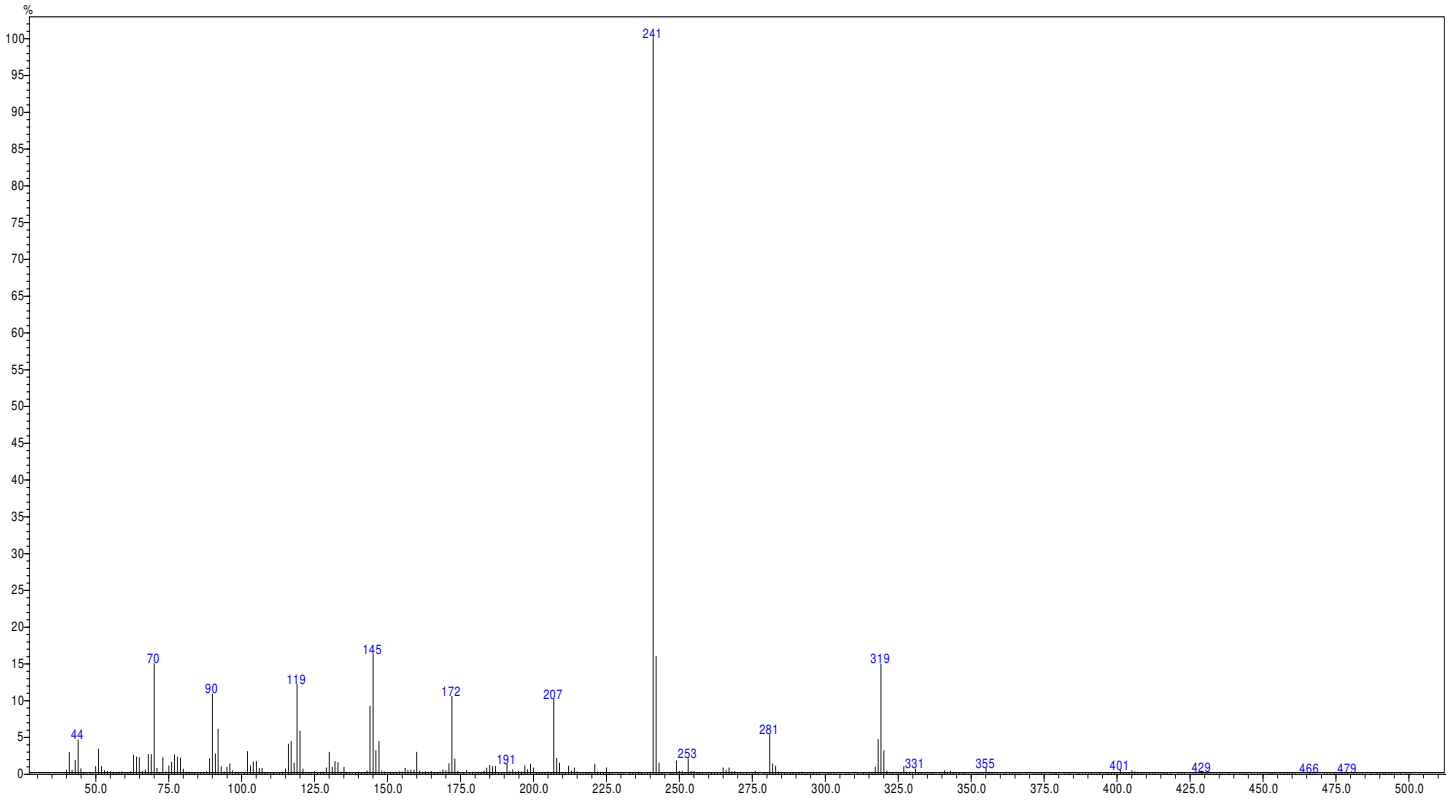

Appendix J1: ^{1}H NMR Spectrum for Compound **6** in $CDCl_3$

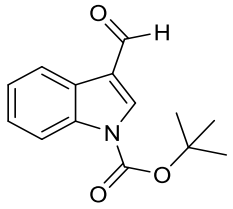

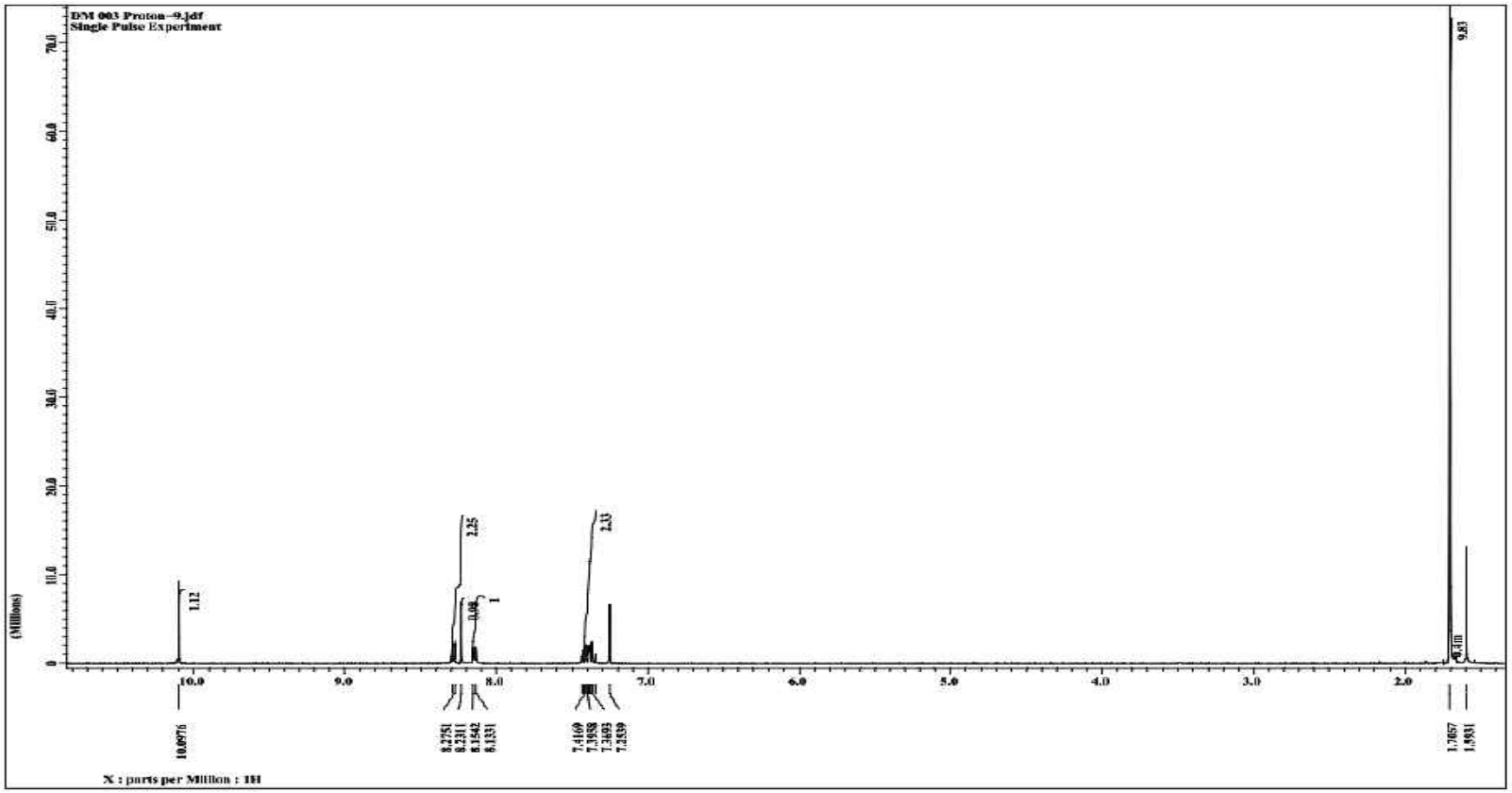

Appendix J2: ^{1}H NMR Spectrum for Compound **6** in $CDCl_3$

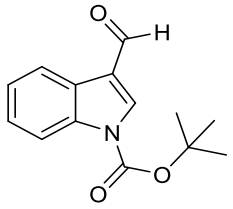

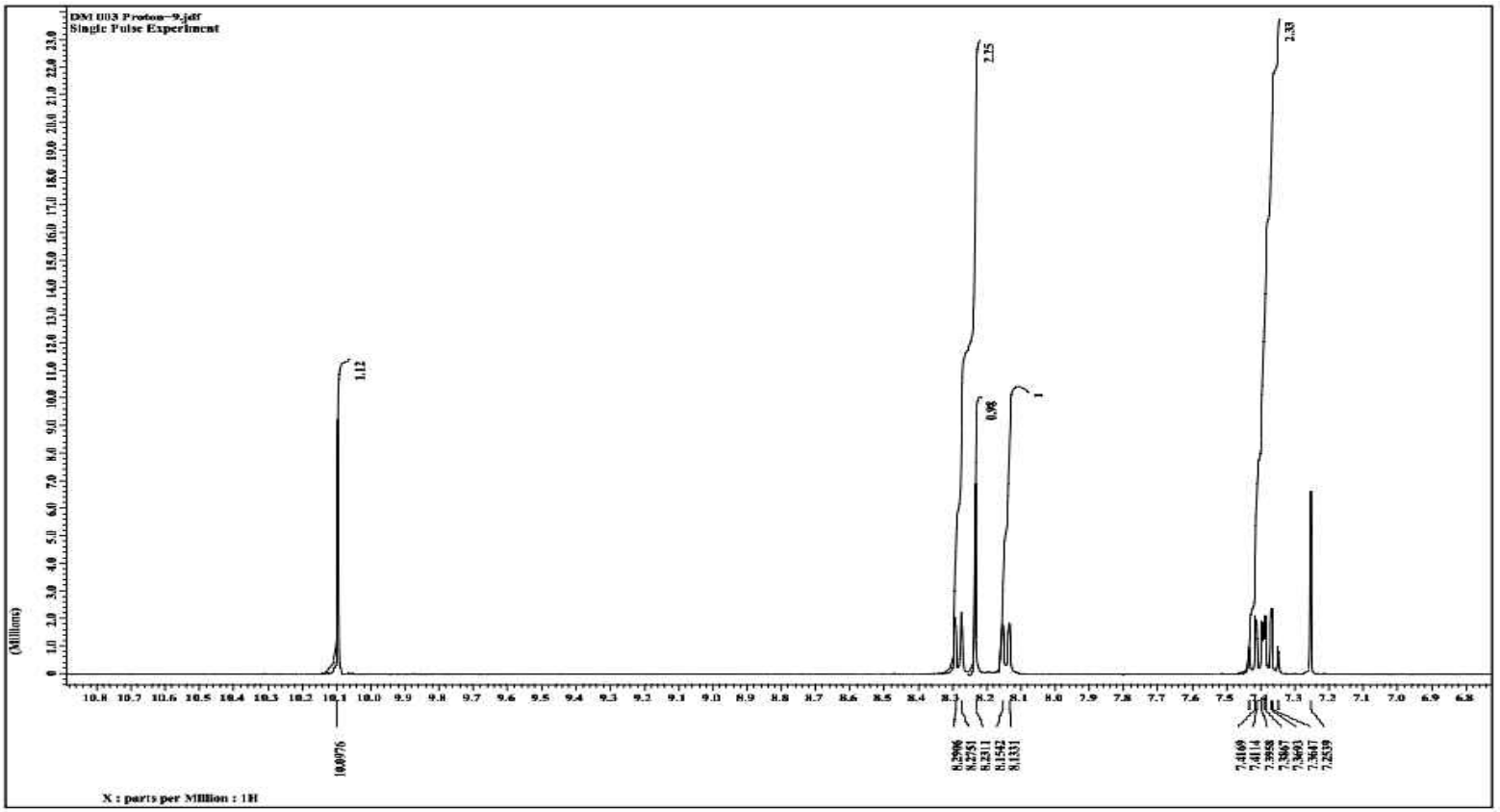

Appendix J3: ^{1}H NMR Spectrum for Compound **6** in $CDCl_3$

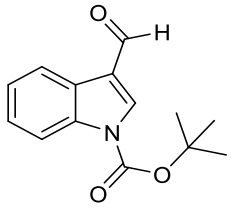

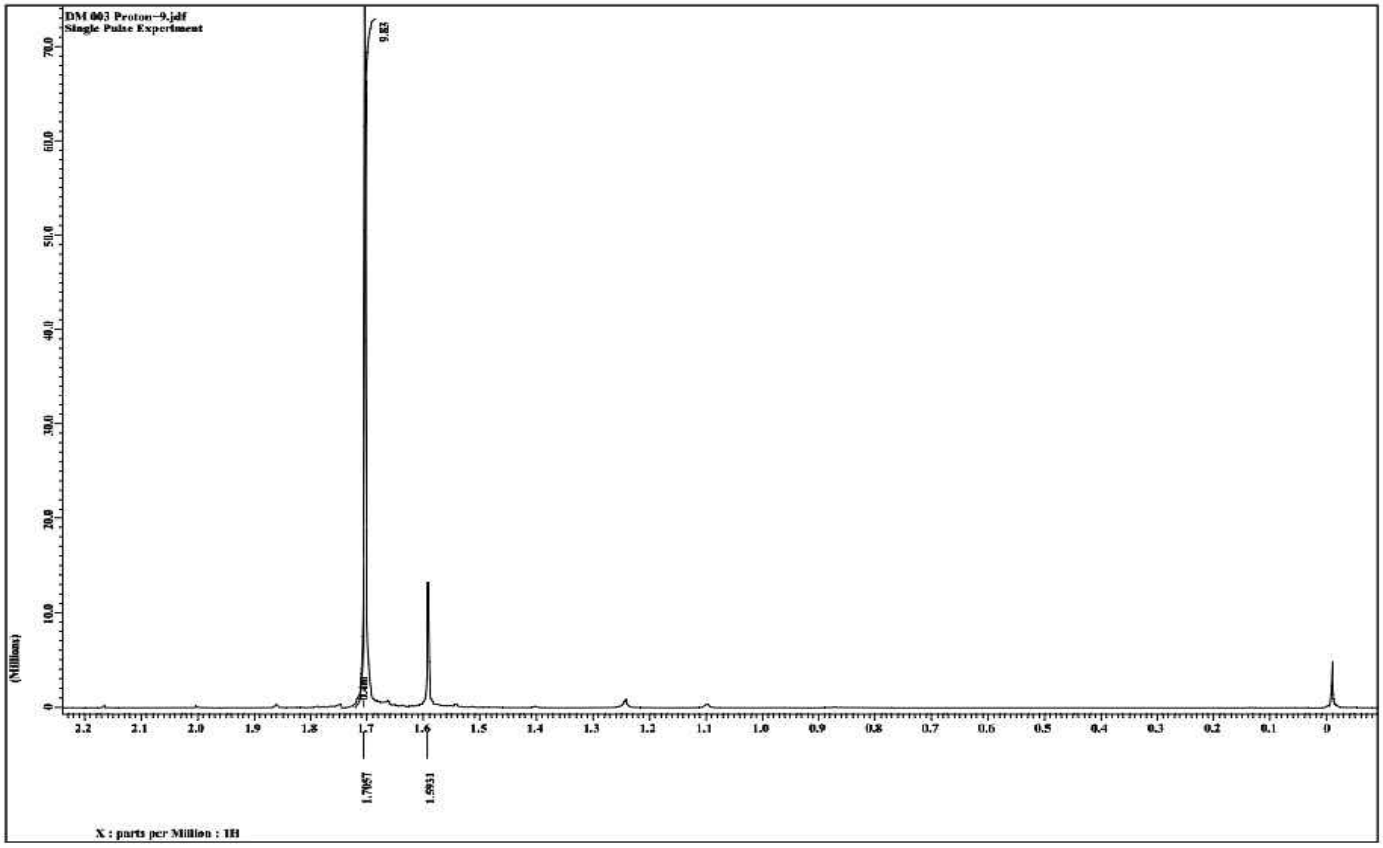

Appendix J4: ^{13} C NMR Spectrum for Compound **6** in $CDCl_3$

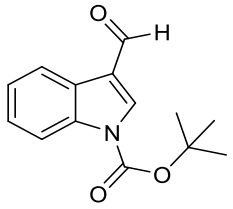

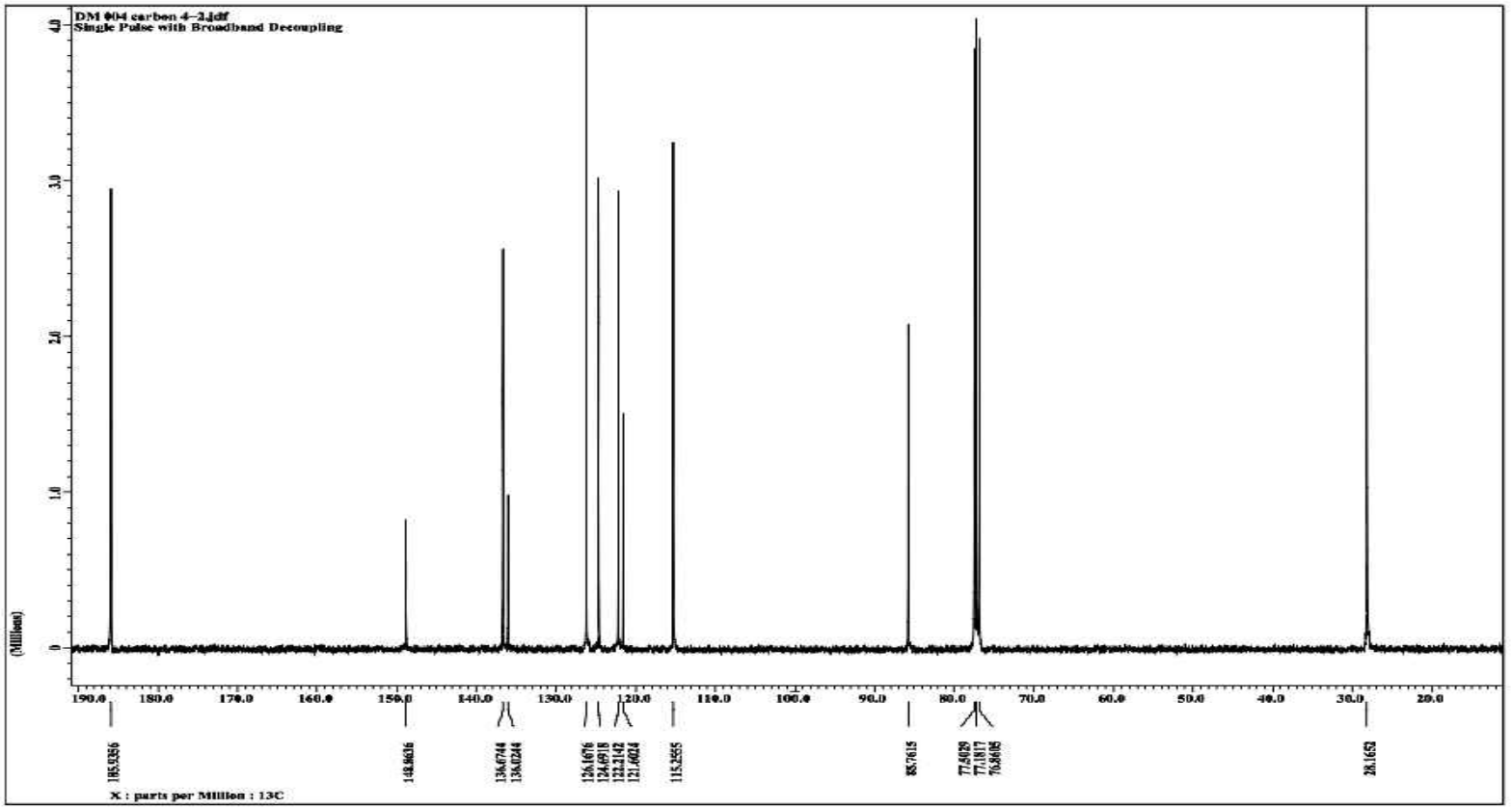

Appendix K1: ^{1}H NMR Spectrum for Compound **7** in $CDCl_3$

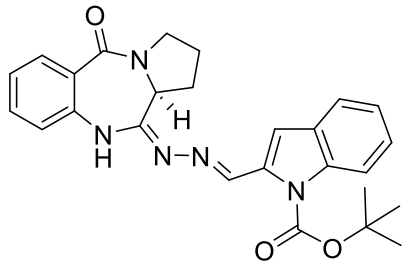

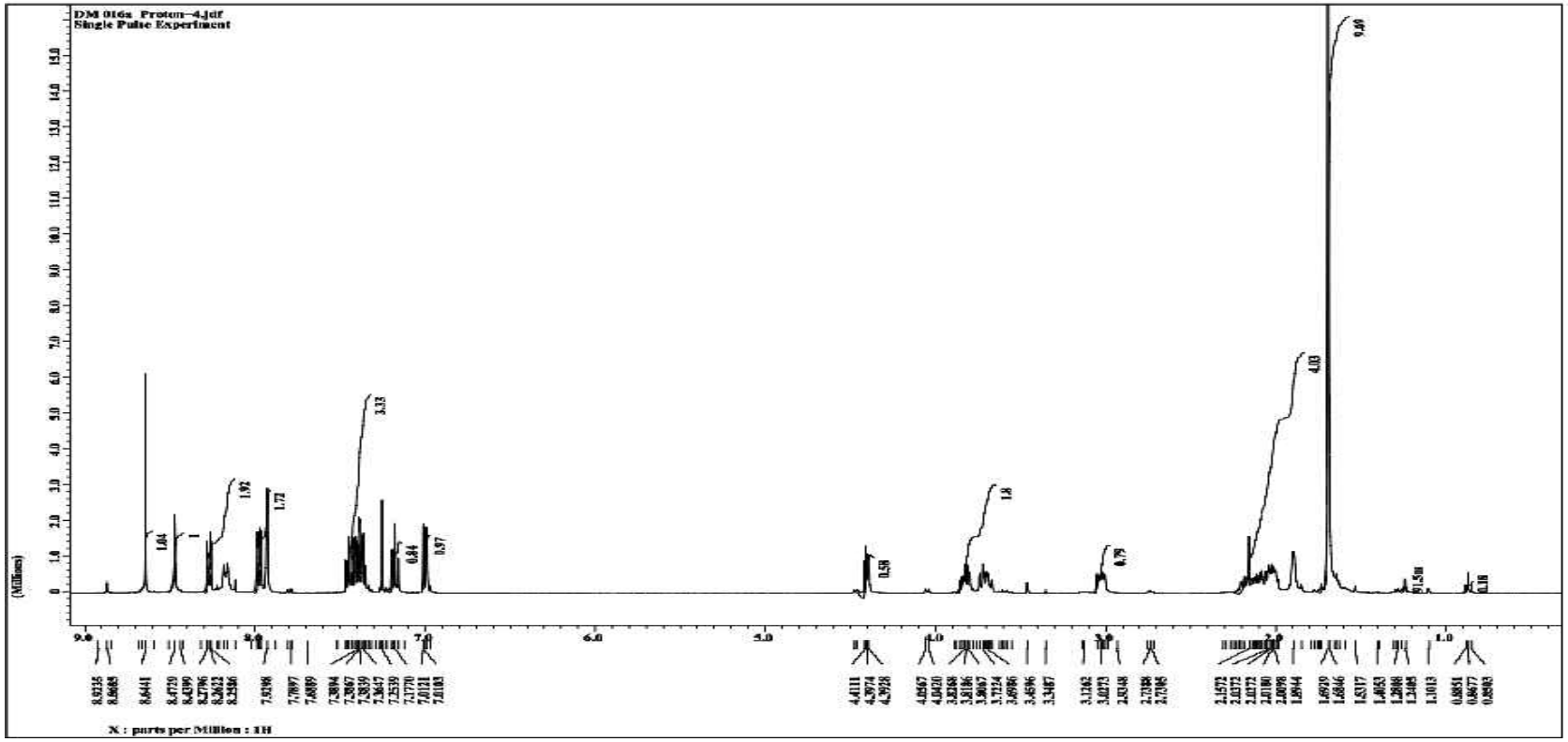

Appendix K2: ^{1}H NMR Spectrum for Compound **7** in $CDCl_3$

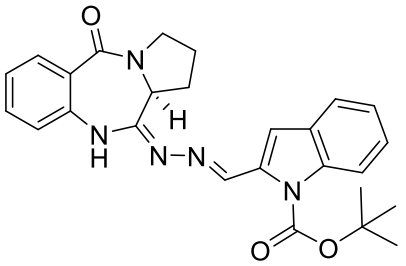

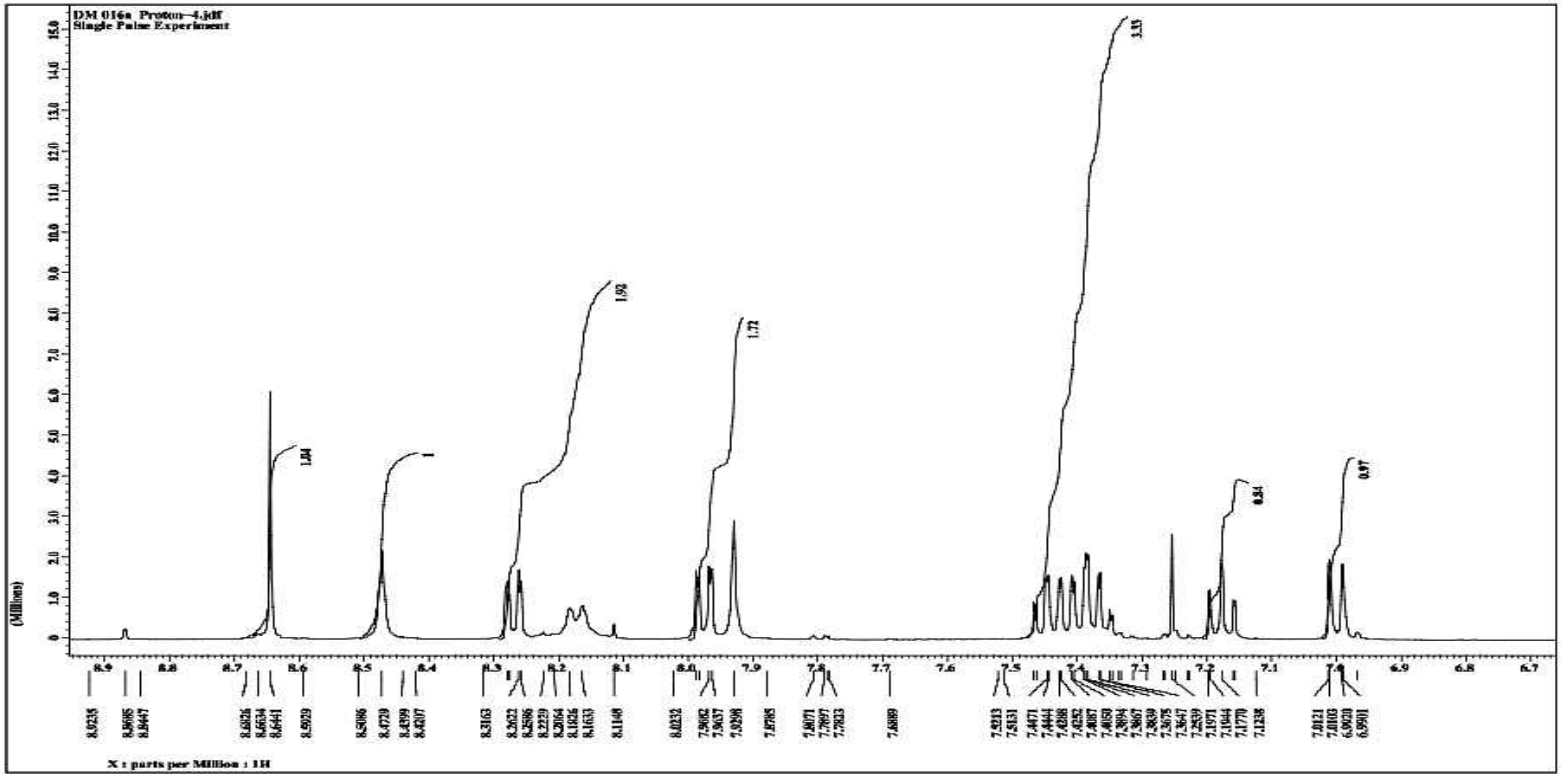

Appendix K3: ^{1}H NMR Spectrum for Compound **7** in $CDCl_3$

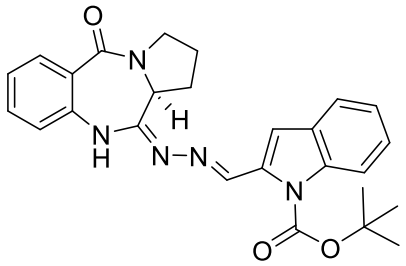

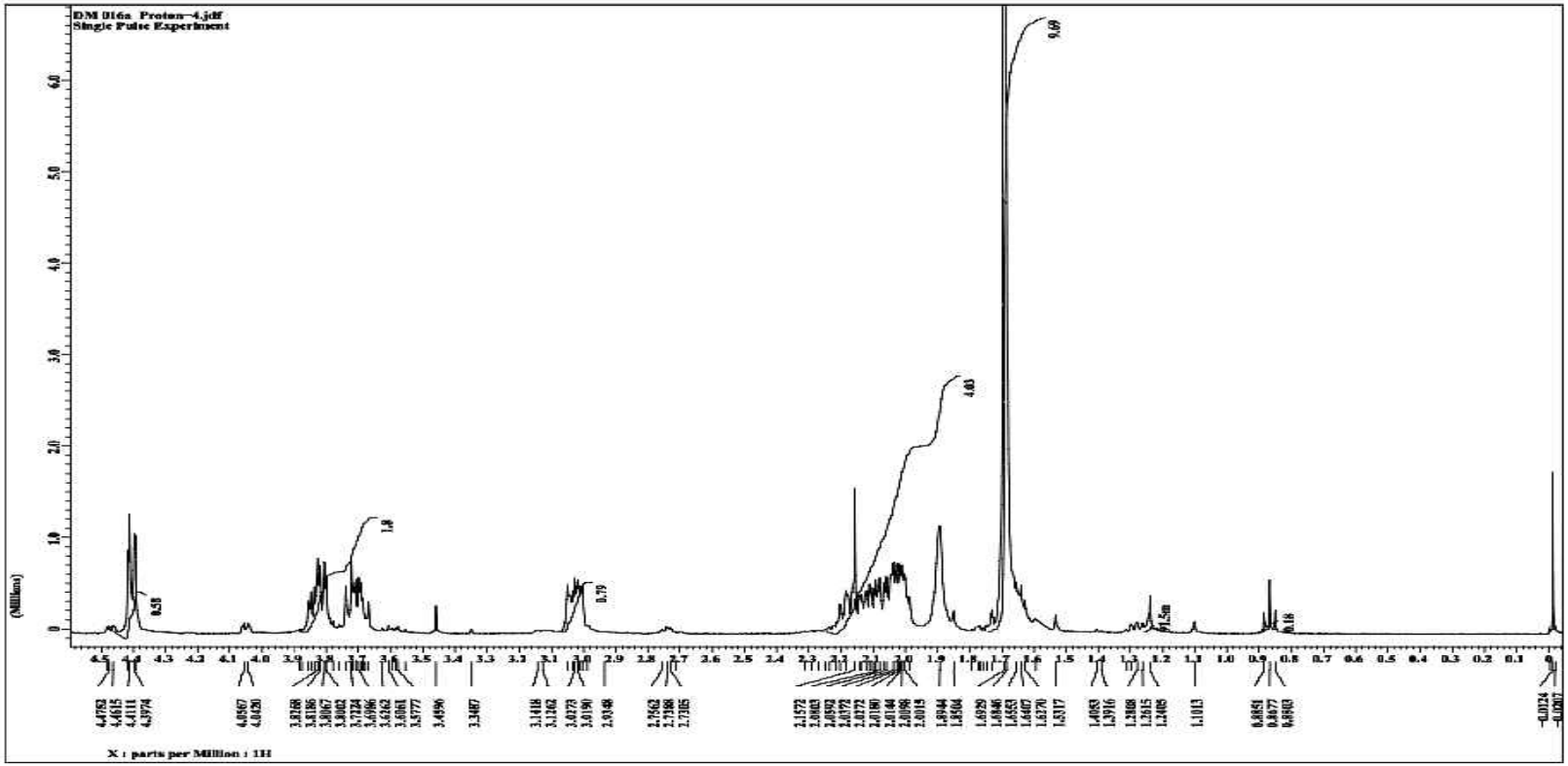
DM 016a Proton-4.jdf
Single Pulse Experiment
9.69
4.03
1.8
0.58
0.79
1.5m
0.16
(Millions)
X : parts per Million : 1H

Appendix K4: ^{13} C NMR Spectrum for Compound **7** in $CDCl_3$

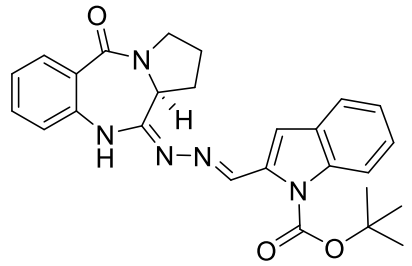

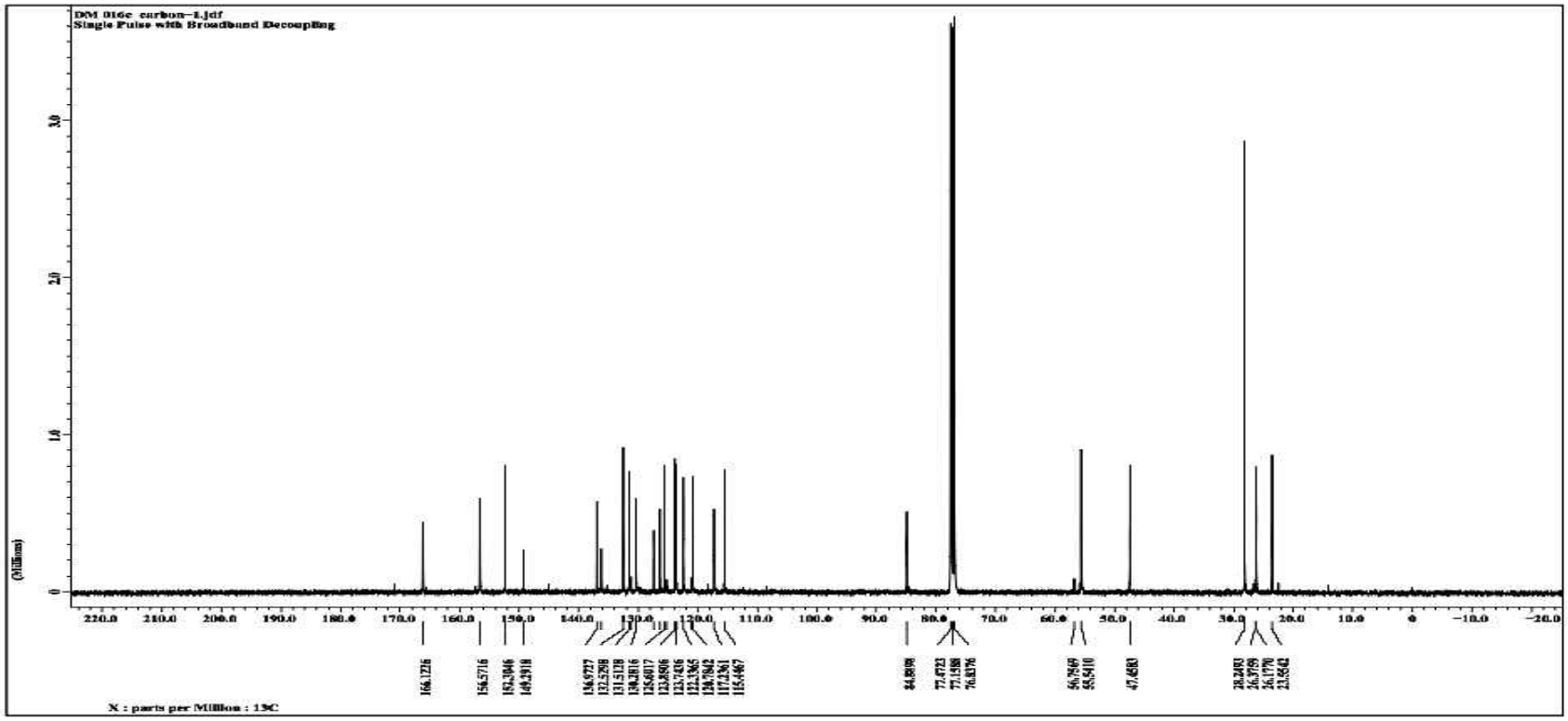

Appendix K5: ^{13} C NMR Spectrum for Compound **7** in $CDCl_3$

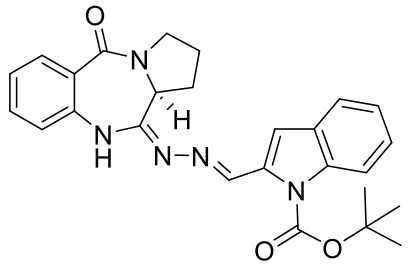

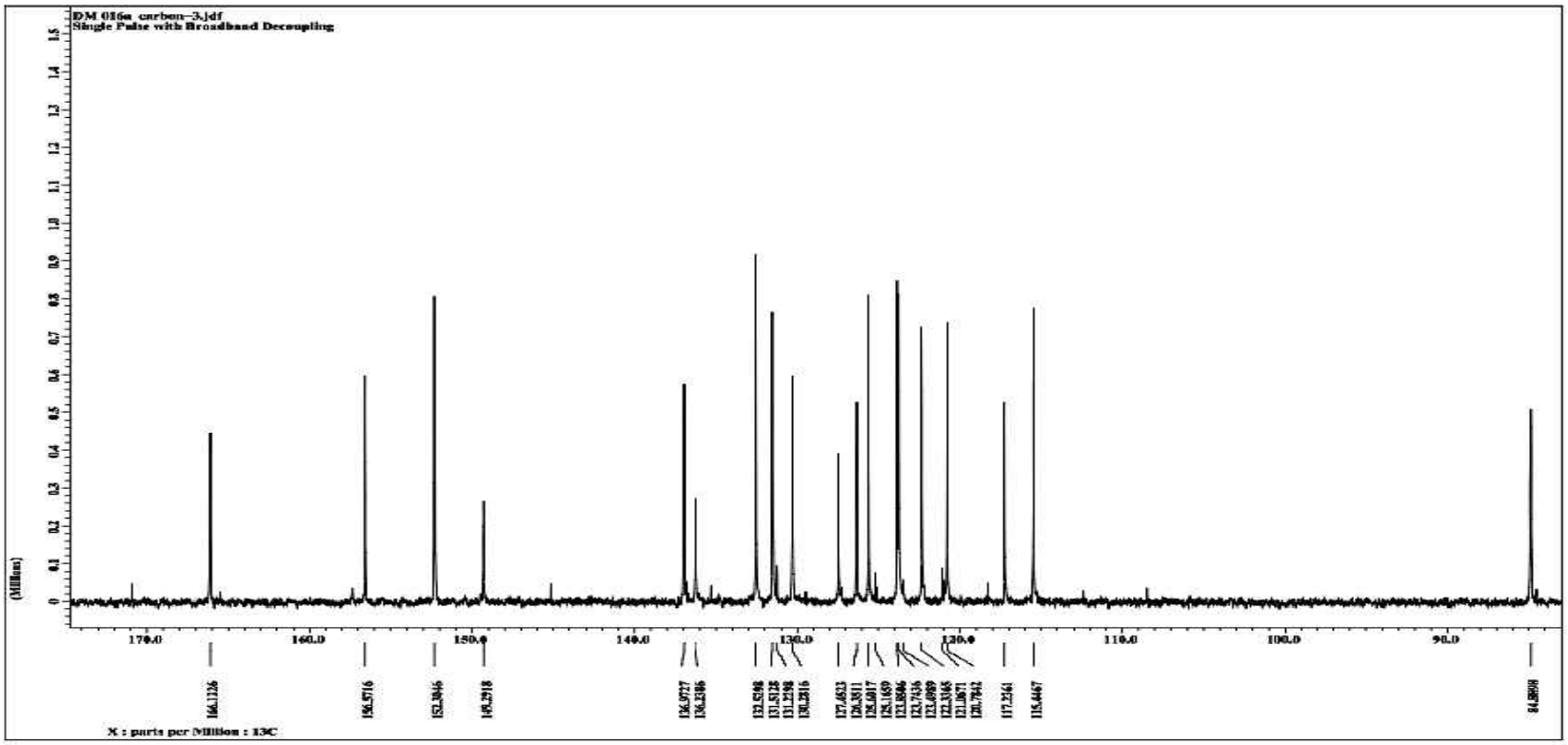

Appendix K6: C-DEPT-135 Spectrum for Compound **7** in $CDCl_3$

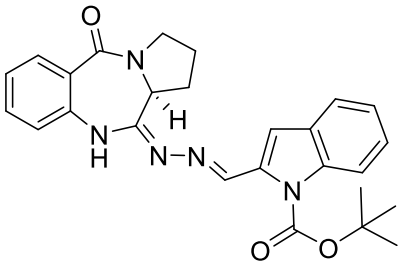

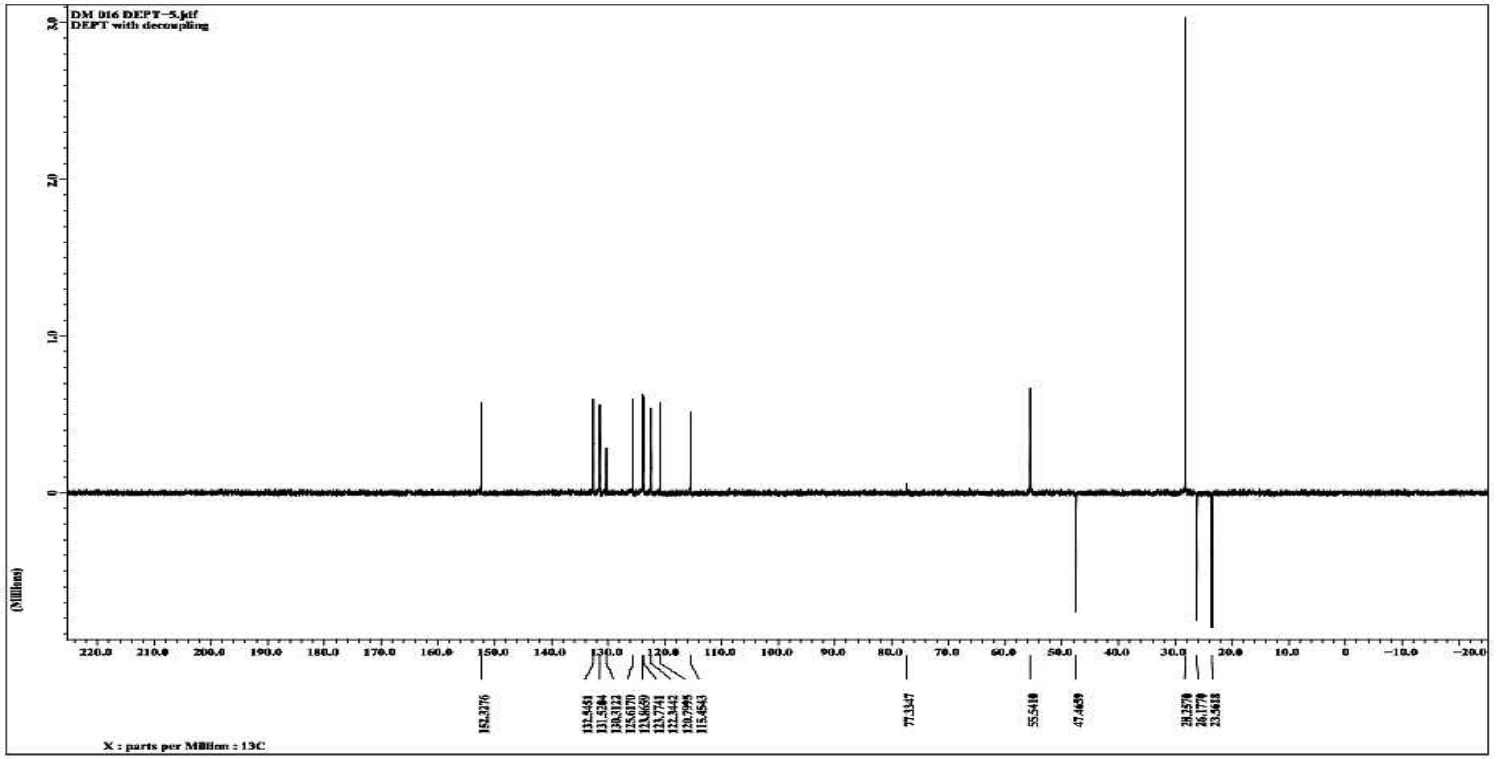

Appendix K7: IR Spectrum for Compound **7**

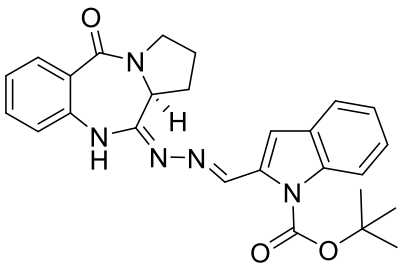

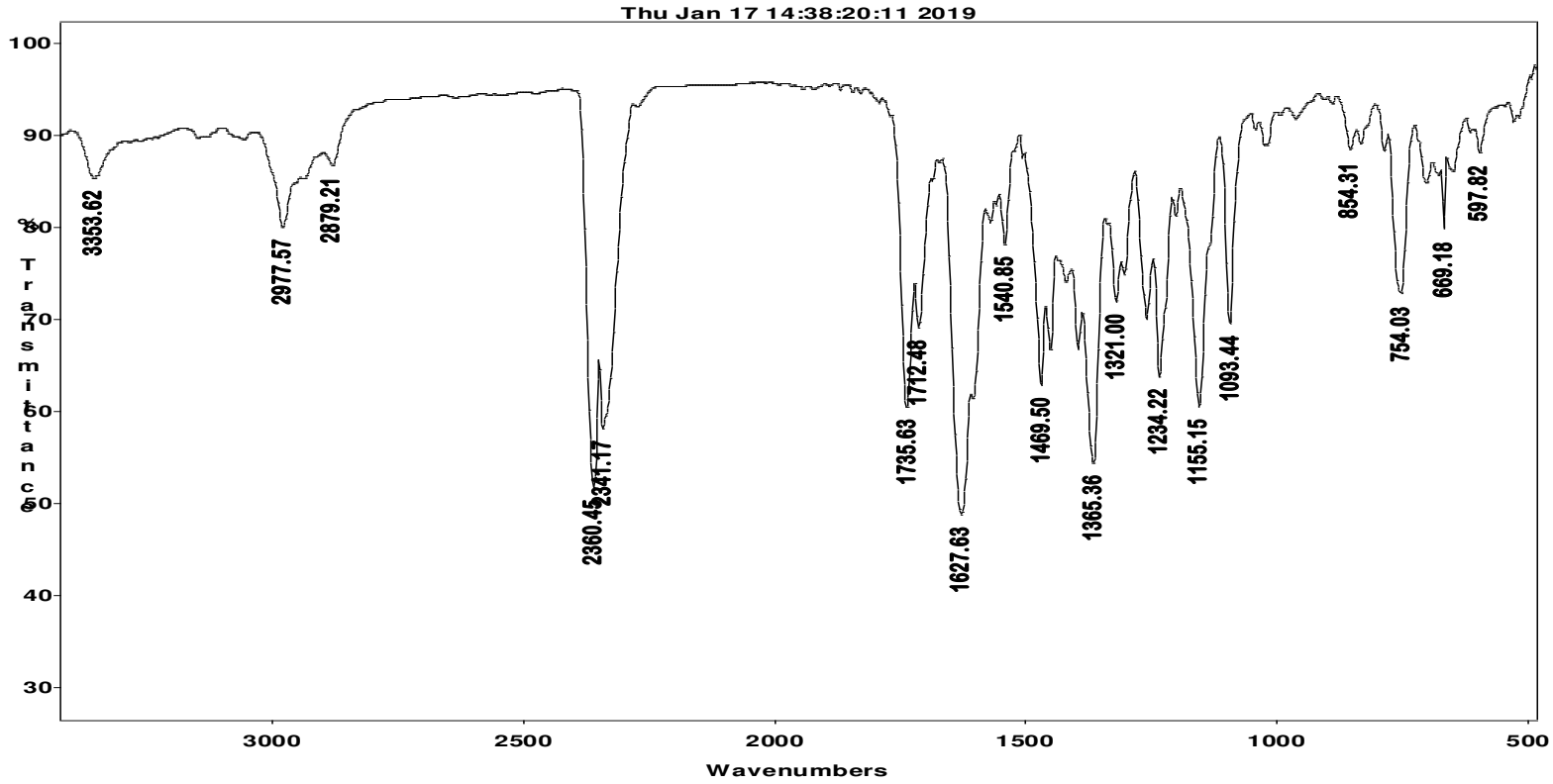

Appendix K8: GC/MS Spectrum for Compound **7**

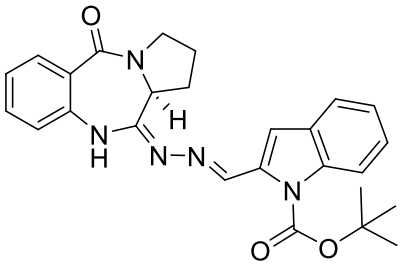

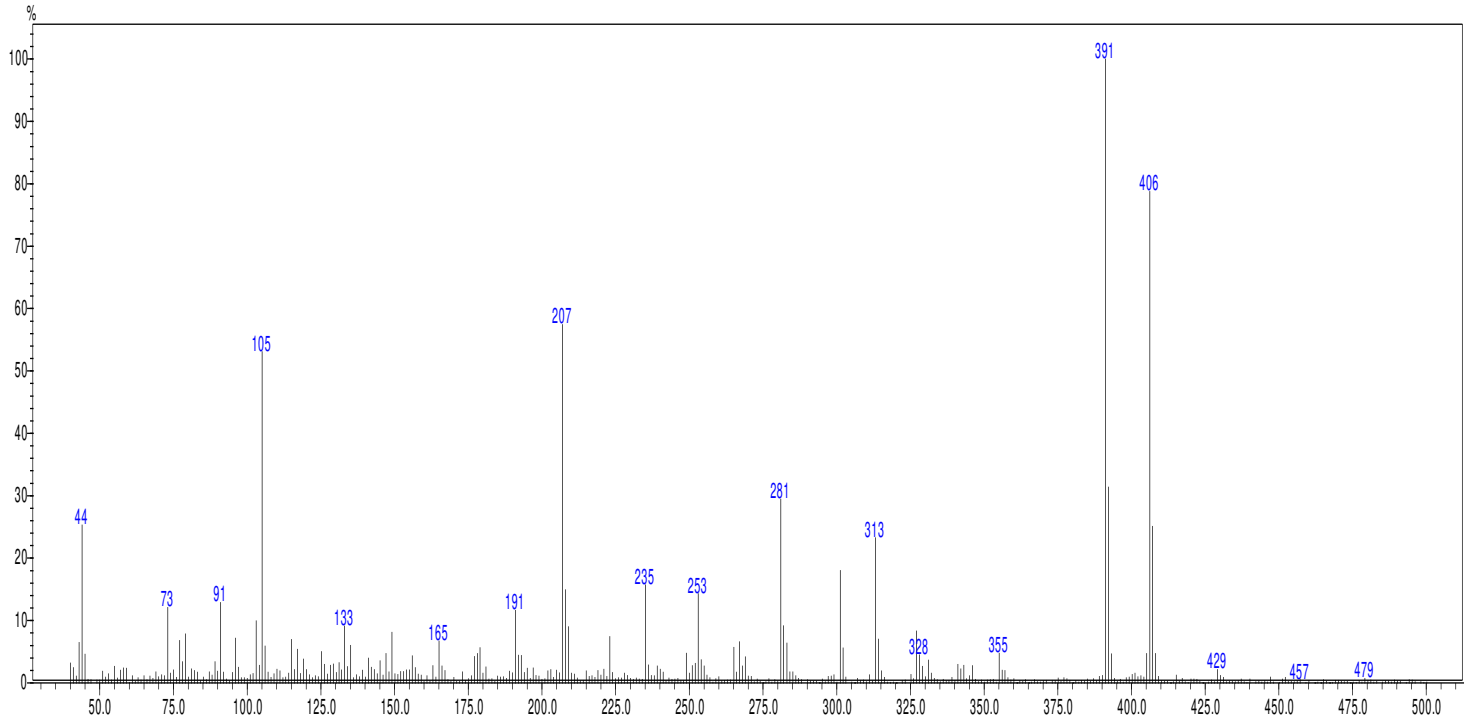

Appendix L1: ^{1}H NMR Spectrum for Compound **8** in C_2D6OS

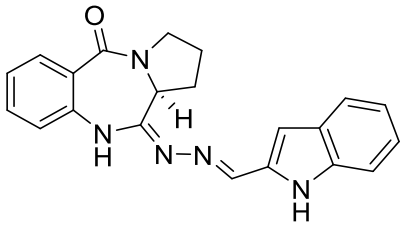

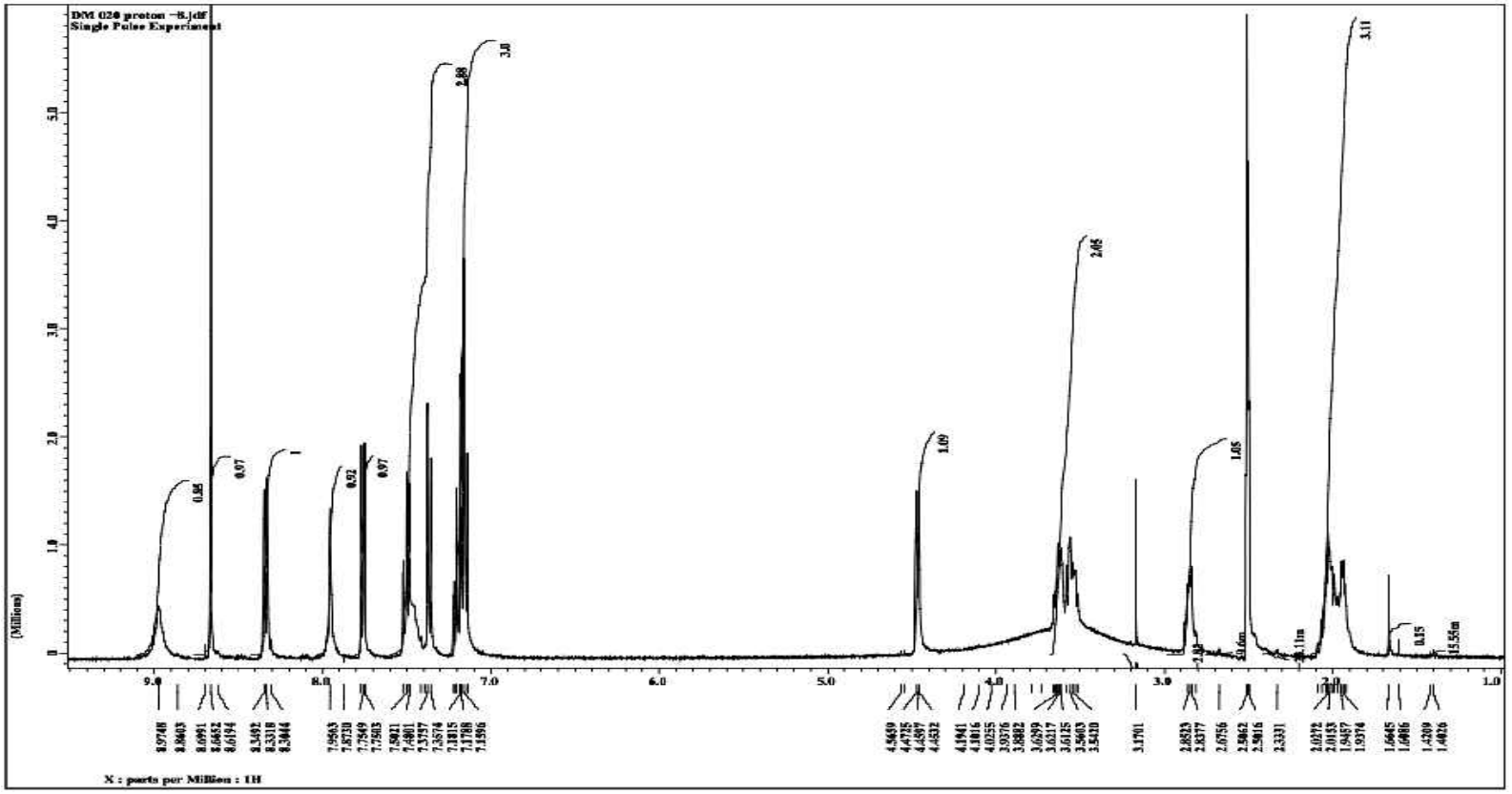

Appendix L2: ^{1}H NMR Spectrum for Compound **8** in C_2D6OS

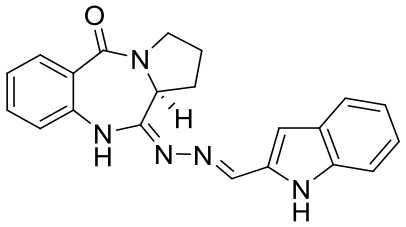

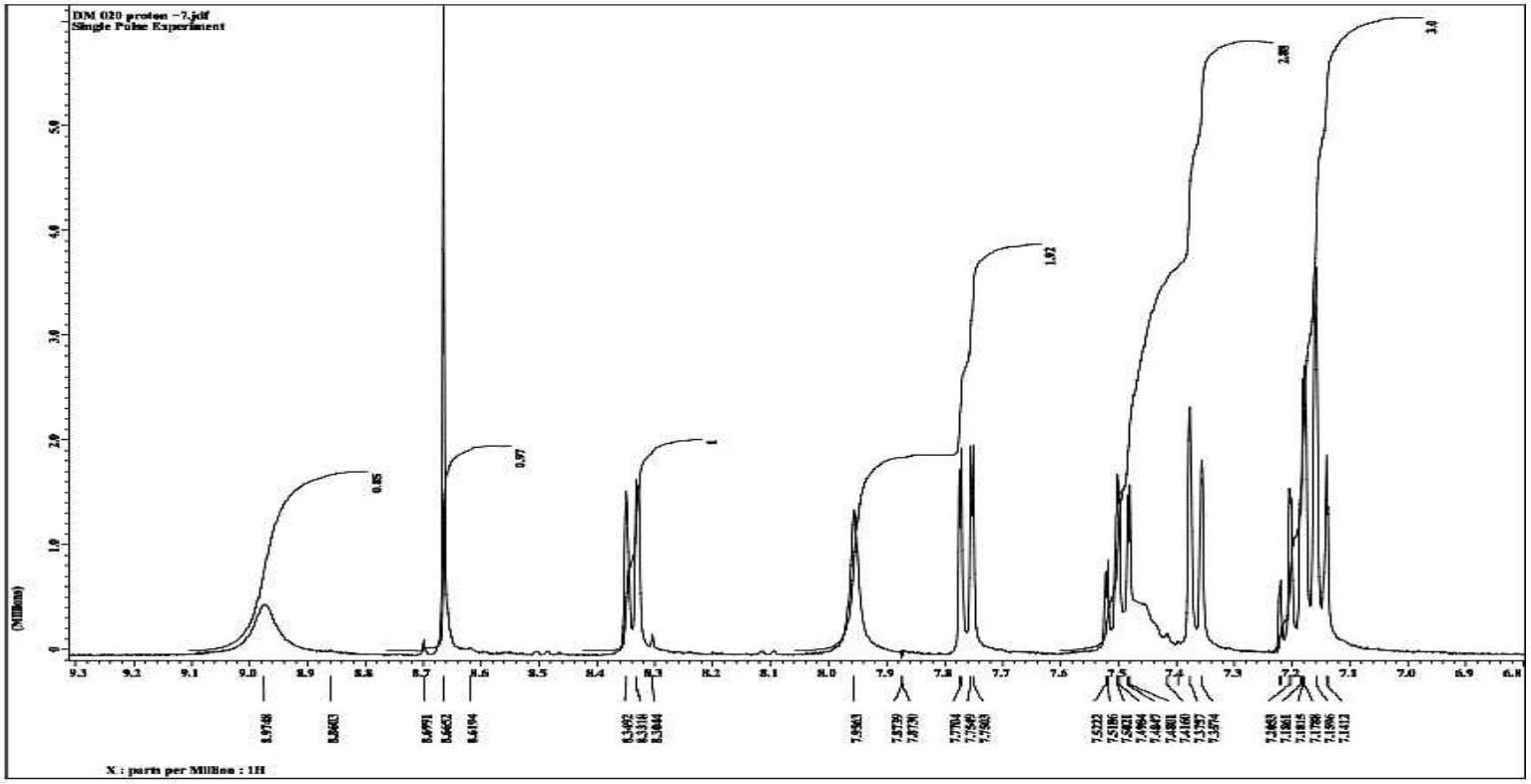

Appendix L3: ^{1}H NMR Spectrum for Compound **8** in C_2D_6OS

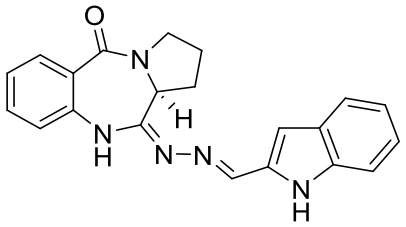

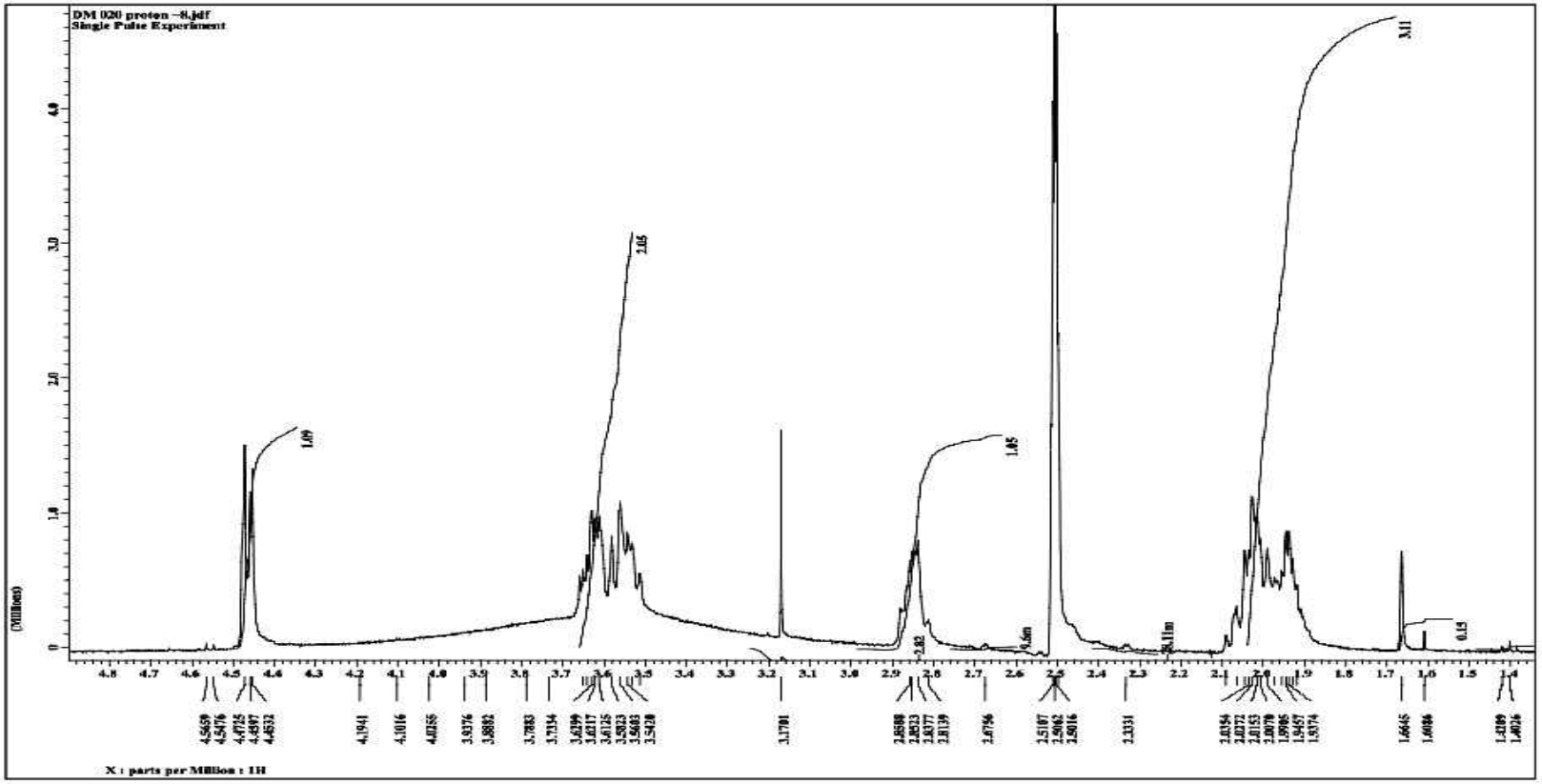

Appendix L4: ^{13} C NMR Spectrum for Compound **8** in C_2D6OS

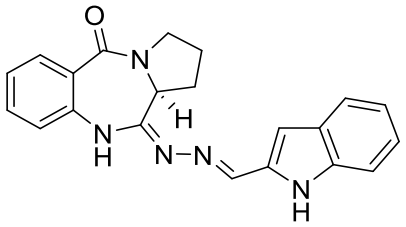

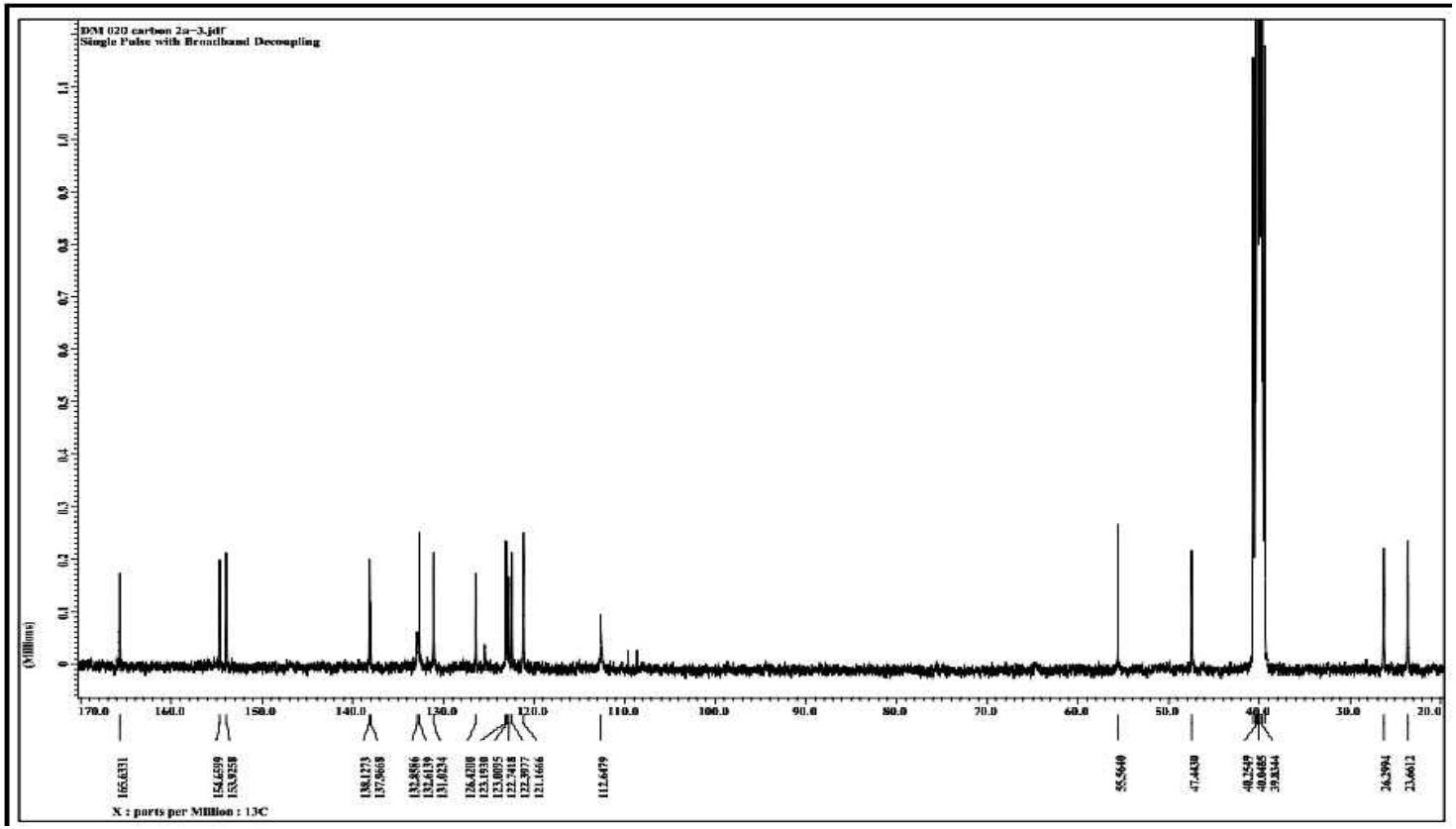

Appendix L5: ^{13} C NMR Spectrum for Compound **8** in C_2D6OS

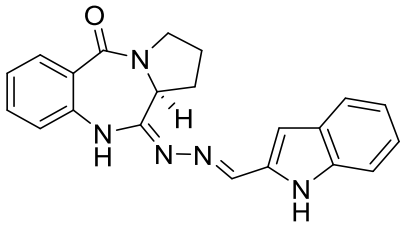

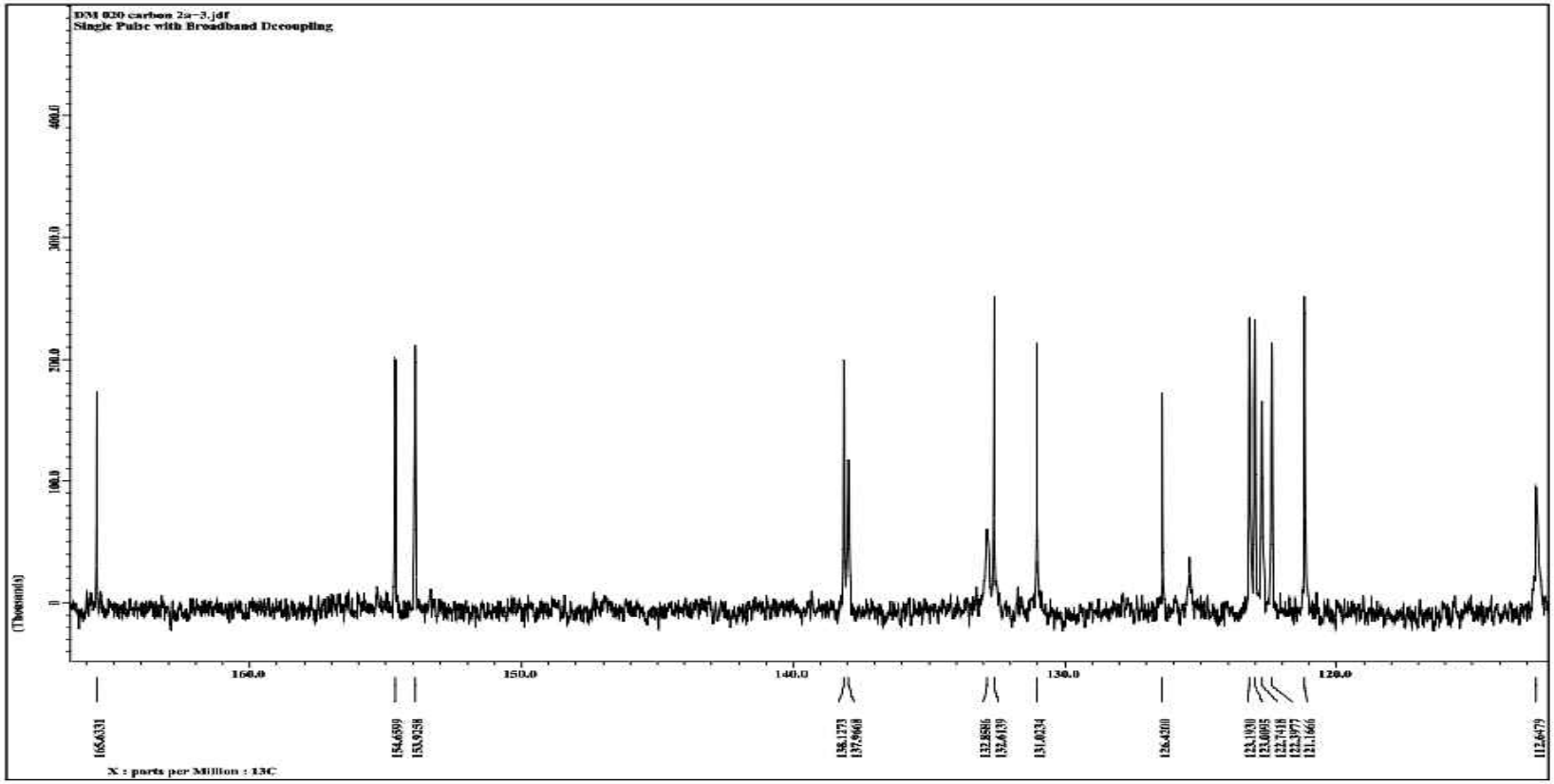

Appendix L6: C-DEPT-135 Spectrum for Compound **8** in C_2D6OS

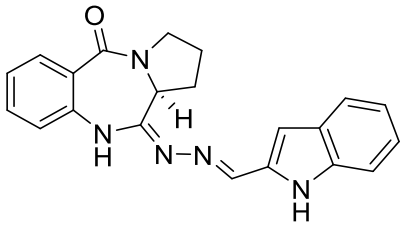

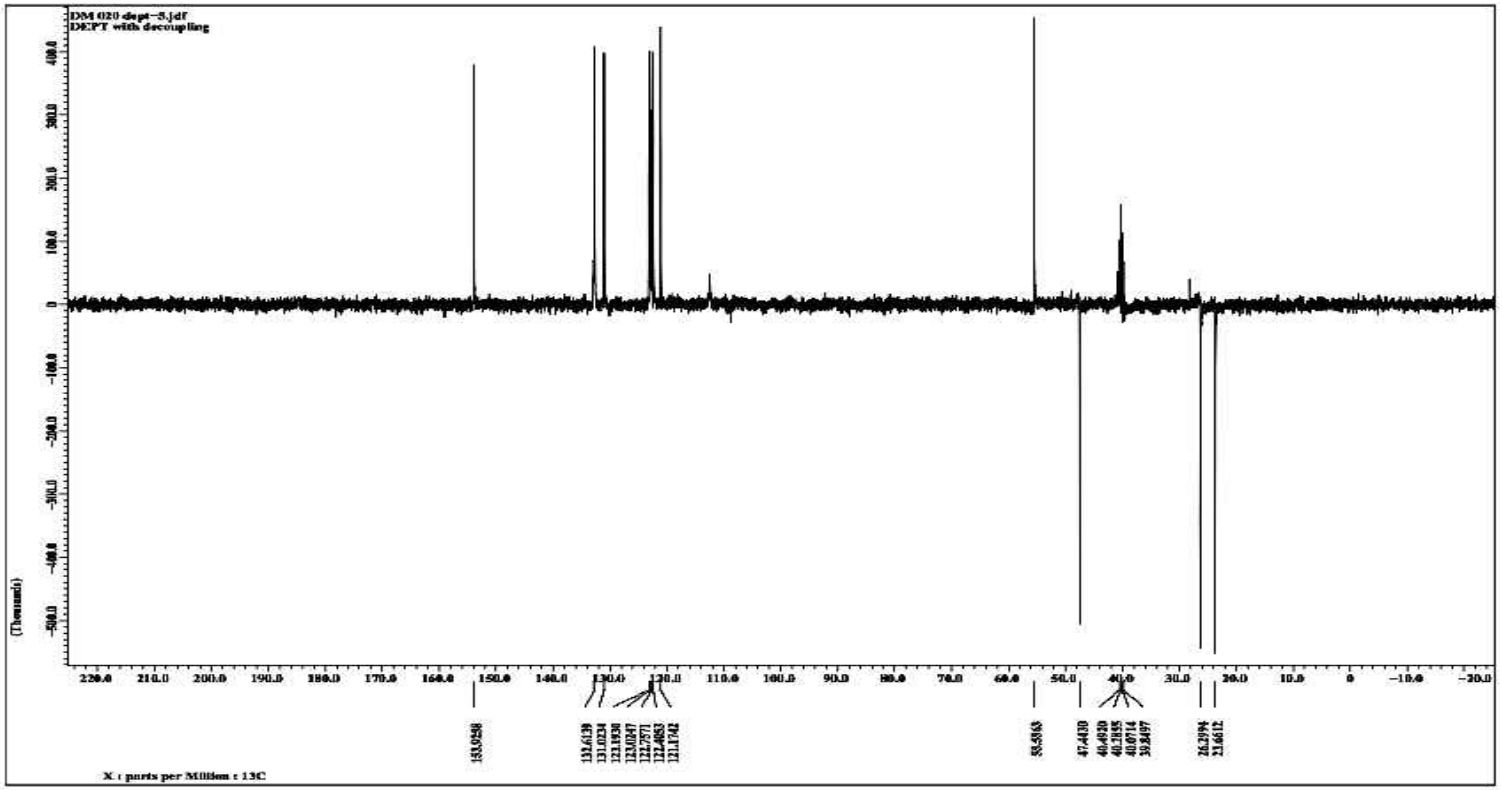

Appendix L7: IR Spectrum for Compound **8**

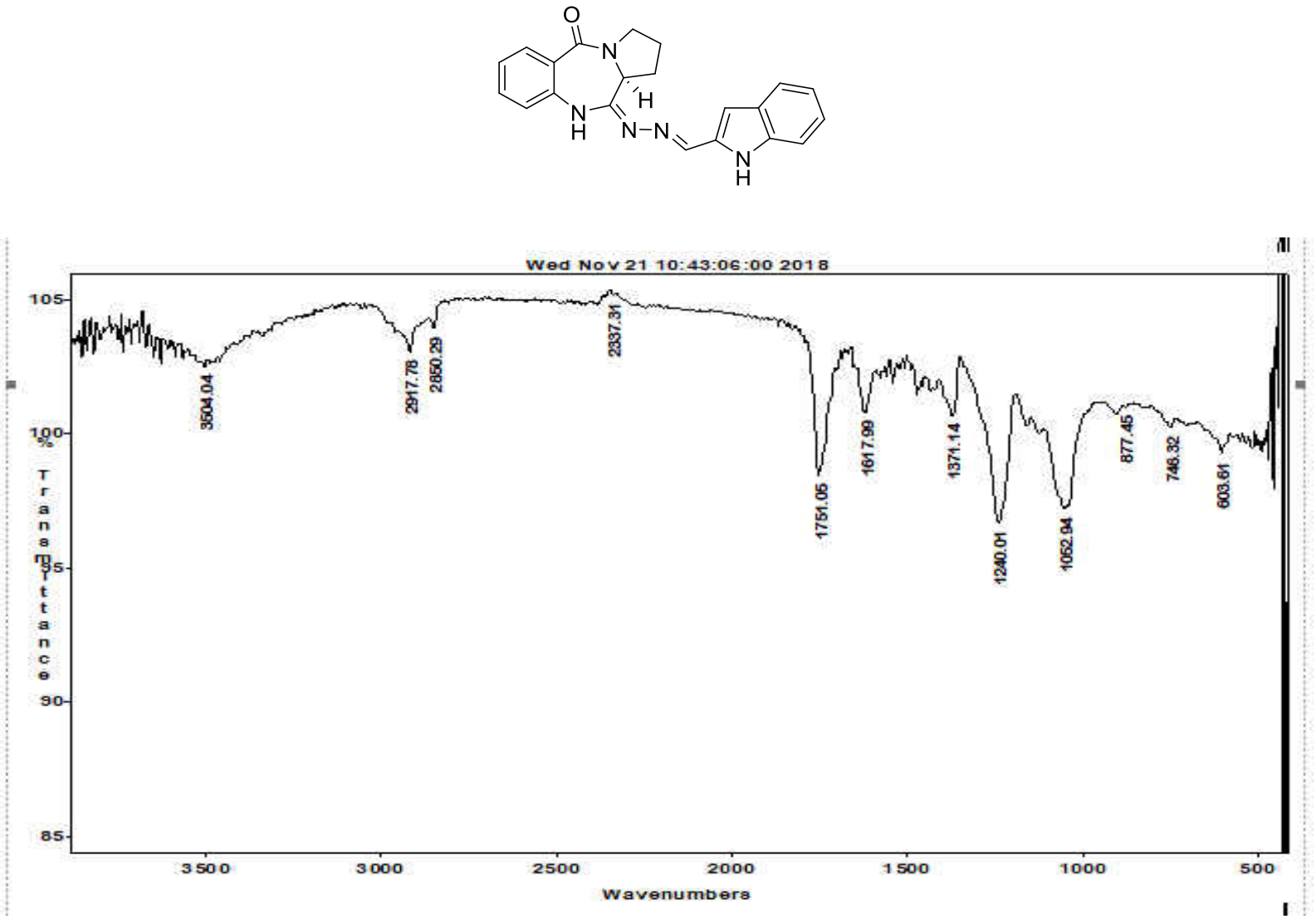

Appendix L8: UV- Vis Spectrum for Compound **8**

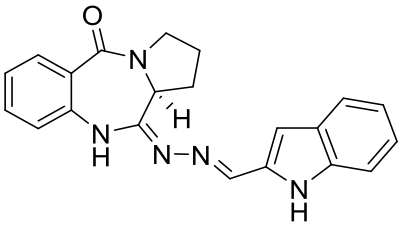

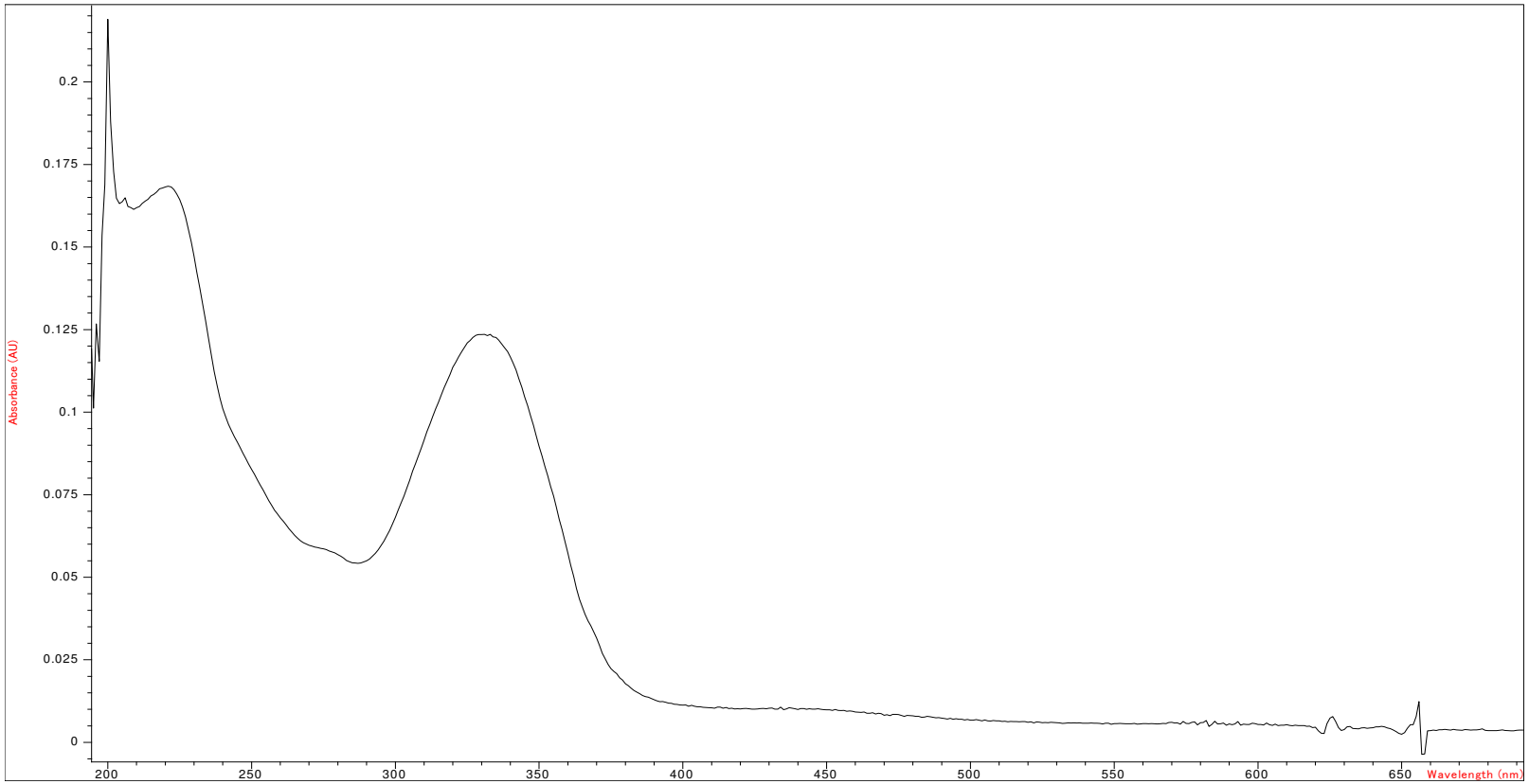

Appendix L9: GC/MS Spectrum for Compound **8**

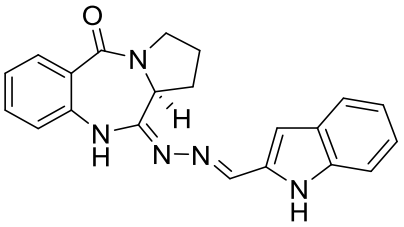

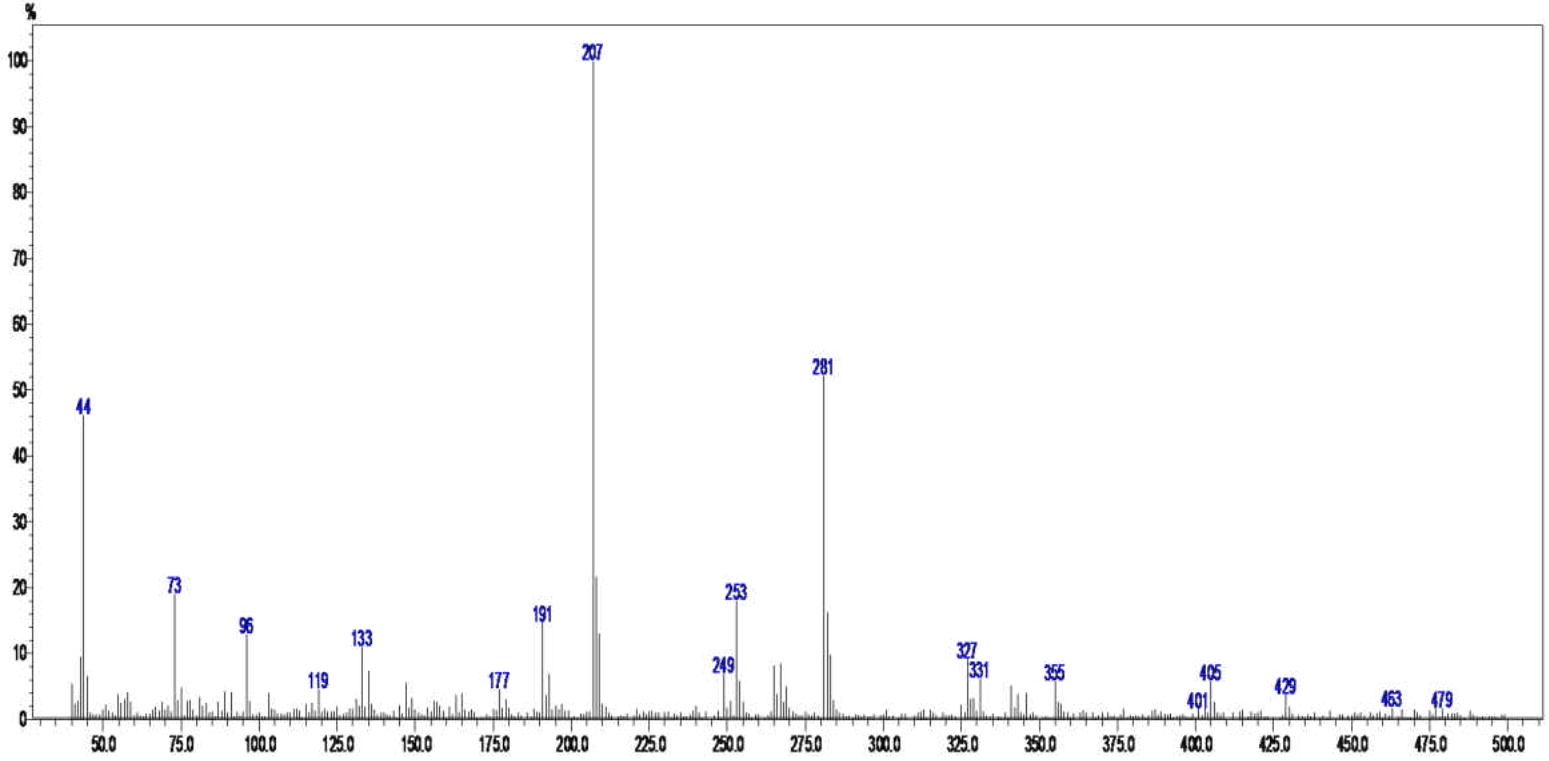

VITA

DAVID MINGLE

Education:

M.S. Chemistry, East Tennessee State University, Johnson City, Tennessee, 2019

B.Sc. Biochemistry, University for Development Studies (UDS), Ghana, 2013

Professional Experience:

Graduate Teaching Assistant, College of Arts and Sciences, East Tennessee State University, 2017-2018

Quality Control Chemist, Letap Pharmaceuticals Limited, Ghana 20114-2016

Research Assistant, Etherean Mission Herbal Pharmacy, Ghana. 2016

Chemistry Tutor, A. M.E Zion Girls Senior high school, Ghana. 2013-2014

Quality control Chemist, Phyto-Riker Pharmaceuticals Ltd, Ghana, 2012

Presentations:

David Mingle, Abbas G. Shilabin, Synthesis, Characterization And Biological Evaluation of Novel (*S,E*)-11-[2-(arylmethylene)hydrazono] pyrrolo [2,1-c] [1,4] Benzodiazepine Derivatives,

Appalachian Student Research Forum, ETSU, Johnson City, TN, April 12, 2019

David Mingle, Abbas G. Shilabin, C.T Eagle, “Synthesis, Characterization and biological evaluation of novel 11-hydrazinyl Pyrrolo [2,1-c] [1,4] Benzodiazepine derivatives as potential anti-Cancer and anti- microbial agent”, 70th Southeastern Regional Meeting of American chemical Society. Augusta, GA. Oct 3-Nov 3, 2018.

David Mingle, Abbas G. Shilabin, C.T Eagle, (2018) “Synthesis, Characterization and biological evaluation of novel 11-hydrazinyl Pyrrolo [2,1-c] [1,4] Benzodiazepine derivatives as potential anti-Cancer and anti- microbial agent” Eastman-NETSACS Student Research Symposium Oct 16, 2018.

David Mingle, Abbas G. Shilabin “Synthesis, Characterization And Biological Evaluation of novel (*S,E*)-11-[2-(arylmethylene)hydrazono] pyrrolo [2,1-c] [1,4] benzodiazepine derivatives”. Graduate Seminar, ETSU Chemistry Department, Johnson City, TN, Oct 12, 2018.

David Mingle, Abass G. Shilabin, “Synthesis of Pyrrolo[2,1-c] [1,4] Benzodiazepine 11-hydrazinyl derivatives as Potential anti- microbial agent”, Appalachian Student Research Forum, ETSU, Johnson City, TN, April 5, 2018.